

Department of Civil and Environmental Engineering

University of Strathclyde

**Decabromodiphenyl ether fate in soil system  
- Sorption in soil matrices and new  
perspective for soil remediation**

A thesis presented for the degree of Doctor of Philosophy

by

Maura Malgaretti

July 2016

## Declaration

This thesis is the result of the author's original research. It has been composed by the author; all external sources used in this study have been correctly referenced. It has not been previously submitted for examination which has led to the award of a degree.

The copyright of this thesis belongs to the author under the terms of the United Kingdom Copyright Acts as qualified by University of Strathclyde Regulation 3.50. Due acknowledgement must always be made of the use of any material contained in, or derived from, this thesis.

Signed:

Date:

We gotta do much more than believe  
if we really wanna change things  
We gotta do much more than believe  
if we wanna see the world change

Dave Matthews Band

To the people that have been on my side in these years:  
the ones that are part of me since always and always will be  
the ones with whom I shared this crazy period in Glasgow  
the ones I met here and I know since now on I will always keep with me

## Abstract

Polybrominated diphenyl ethers (PBDEs) have been used for decades as flame retardants in polymeric materials. Products containing lower brominated congeners have been banned because of concerns about their toxicity to neurological, reproductive and endocrinal systems. Restrictions on the use of the deca-BDE mixture, which contains 97% of the fully brominated congener BDE-209, have been initially delayed. Nowadays the addition of BDE-209 to the Stockholm Convention on Persistent Organic Pollutants is under evaluation. BDE-209 fate in soil, as for other hydrophobic organic compounds, is strongly related to soil organic fraction. This thesis investigates BDE-209 sorption kinetics and identifies other factors important for evaluating BDE-209 mobility, degradation and bioavailability in soil. Additionally it moves the first steps in the development of a novel bioaugmentation technique through fungi.

For this purpose, HPLC analytical methods and extraction techniques commonly used for hydrophobic organic compounds (HOC) have been tested for analysis of BDE-209 in water and soil samples. The best recoveries values were obtained by evaporation and substitution of water (WES) and by pressurised liquid extraction (PLE) of soil.

Regarding BDE-209 sorption in soil, the sorption kinetic profiles for two soil matrixes belonging to the mineral domain (kaolin) and organic matter domain (peat) were studied separately. Sorption on kaolin was much faster than in peat (4 hours compared to more than 10 days). This approach made it possible to identify other important factors influencing BDE-209 sorption and partitioning processes: clay minerals and dissolvable organic matter.

In relation to the biodegradation aspect, this thesis investigated the tolerance of *P.ostreatus* (a specie of white rot fungus with documented mycoremediation ability) to BDE-209. The fungus mycelium in co-existence with a soil bacterium demonstrated the ability to colonised straw contaminated with BDE-209 up to 1 mg/kg. The results encourage further investigation on *P. ostreatus* ability to degrade BDE-209.

# CONTENTS

<b>LIST OF FIGURES</b>	<b>XI</b>
<b>LIST OF TABLES</b>	<b>XVI</b>
<b>LIST OF ABBREVIATIONS</b>	<b>XVIII</b>
<b>1 INTRODUCTION</b>	<b>1</b>
1.1 History and use of PBDEs as flame retardant	1
1.1.1 PBDEs	1
1.1.2 Flame retardancy mechanism	2
1.1.3 Controversy on the use of flame retardants	4
1.1.4 The California Furniture Flammability Standard (TB117) case	4
1.1.5 Environmental contamination and human exposure	7
1.1.6 PBDE bans and delays in restriction on BDE-209	9
1.1.7 BDE-209 physical and chemical properties	13
1.2 Aim and objectives	15
<b>2 BDE-209 IN SOIL</b>	<b>16</b>
2.1 Sorption and mobility	16
2.2 BDE-209 biodegradation	19
2.2.1 Bacteria biodegradation	20
2.2.2 Biodegradation in the soil –plant system	21
2.2.3 White rot fungi	21
2.3 Summary and key findings	25
<b>3 EQUILIBRIUM PARTITIONING AND SORPTION MODELS</b>	<b>26</b>
3.1 Equilibrium partitioning	26
3.1.1 Partitioning coefficient $K_d$ and sorption isotherms	26
3.1.2 Parametric description of $K_d$ and $K_{om}$	27

3.1.3	The linear free energy relationship for $K_{om}$ estimate	28
3.1.4	Thermodynamic interpretation of $k_d$ : the fugacity concept	29
3.2	Models describing sorption mechanism in soil particles	31
3.2.1	Distributed reaction model (DRM)	31
3.2.2	Sorption Related Pore Diffusion model (SRPD)	34
3.2.3	Thermodynamic Potential Theory	37
3.3	Summary and key findings	40
<b>4</b>	<b>INSTRUMENTAL TECHNIQUES</b>	<b>42</b>
4.1	High pressure liquid chromatography (HPLC)	44
4.2	Pressurised Liquid Extraction (PLE)	49
4.3	Microwave assisted extraction (MAE)	51
4.4	Sample concentration and solvent substitution	52
4.5	TOC combustion analyser	54
4.6	Laser diffraction particle size detector	55
4.7	Centrifugation	56
<b>5</b>	<b>BDE-209 ANALYSIS IN AQUEOUS SAMPLES</b>	<b>58</b>
5.1	Introduction	58
5.2	Extraction methods	58
5.2.1	Liquid-liquid extraction (LLE)	58
5.2.2	Dispersive liquid-liquid micro extraction (DLLME)	59
5.2.3	Solid phase extraction (SPE)	60
5.2.4	Water evaporation and substitution (WES)	60
5.3	Experimental procedures	60
5.3.1	Materials	60
5.3.2	LLE	61
5.3.3	DLLME	61

5.3.4 SPE	61
5.3.5 WES	62
5.4 Results	63
5.4.1 LLE	63
5.4.2 DLLME	64
5.4.3 SPE	65
5.4.4 WES	66
5.5 Comparison of the techniques	67
5.6 WES tested for extraction from more complex matrix using Chrysene as internal standard	68
5.6.1 Procedure	68
5.6.2 Results	68
5.7 Conclusion	70
<b>6 BDE-209 ANALYSIS IN SOIL SAMPLES</b>	<b>71</b>
6.1 Introduction	71
6.1.1 Microwave assisted extraction (MAE)	71
6.1.2 Pressurised liquid extraction (PLE)	73
6.2 Experimental procedure	75
6.2.1 Sample preparation	75
6.2.2 MAE	75
6.2.3 PLE	76
6.3 Results and discussion	77
6.3.1 Interference from peat extraction	77
6.3.2 Quantification of the interference peak in terms of apparent BDE-209 concentration	81
6.3.3 Recovery values	84
6.3.4 Measurement uncertainty and limit of detection	85
6.4 Conclusions	86
<b>7 BDE-209 SORPTION ON PEAT AND KAOLIN</b>	<b>88</b>
7.1 Introduction	88



7.2 Methodology	88
7.2.1 Materials	88
7.2.2 Solid matrix Characterisation	89
7.2.3 Experimental setup	91
7.2.3.1 General procedures	91
7.2.3.2 Sorption kinetics of BDE-209 on peat and kaolin	94
7.2.3.3 BDE-209 sorption isotherms on peat	95
7.2.3.4 BDE-209 sorption and desorption from kaolin in non-equilibrium conditions	95
7.2.3.5 Influence of DOM on BDE-209 sorption on kaolin	96
7.3 Results and discussion	97
7.3.1 Sorption kinetics of BDE-209 on peat	97
7.3.2 BDE-209 sorption isotherm on peat	101
7.3.3 BDE-209 sorption kinetic on clay	102
7.3.4 Comparison of the two kinetics	105
7.3.5 BDE-209 sorption and desorption from kaolin in non-equilibrium conditions	107
7.3.6 Influence of dissolved organic matter (DOM) on BDE-209 sorption on kaolin	109
7.4 Conclusions	111
<b>8 PLEUROTUS OSTREATUS TOLERANCE TO BDE-209</b>	<b>113</b>
8.1 Introduction	113
8.2 Materials and method	113
8.2.1 <i>Pleurotus Ostreatus</i> spawn cultivation on straw: parameter optimisation	113
8.2.2 <i>Pleurotus ostreatus</i> BDE-209 tolerance test on straw	114
8.2.3 <i>Pleurotus ostreatus</i> isolation and cultivation on petri disks	115
8.2.4 Growing on soil	115
8.3 Results and Discussion	116
8.3.1 <i>Pleurotus Ostreatus</i> spawn cultivation on straw: parameters optimisation	116
8.3.2 <i>Pleurotus ostreatus</i> BDE-209 tolerance test on straw	117
8.3.3 <i>Pleurotus ostreatus</i> isolation and cultivation on petri disks	118
8.3.4 Growing on soil	124
8.4 Conclusions	126

<b>9 CONCLUSION AND FUTURE WORK</b>	<b>127</b>
9.1 Key findings	127
9.1.1 BDE-209 sorption on mineral and organic matter matrices	127
9.1.2 Measure of BDE-209 from environmental samples and experimental limitations	128
9.1.3 BDE-209 biodegradation	129
9.2 Future research opportunities	129
<b>REFERENCES</b>	<b>132</b>
<b>APPENDIX A</b>	<b>154</b>
<b>APPENDIX B</b>	<b>156</b>
<b>APPENDIX C</b>	<b>162</b>

## List of Figures

Figure 1.1: PBDEs structure. ....	1
Figure 1.2: Chemical structures of the most widely used halogenated flame retardant along with PBDEs (Figure 1.1) (Eljarrat and Barceló, 2004; Laoutid et al., 2009).....	3
Figure 1.3: Sources of PBDEs and their by-products in the environment and human exposure. Solid arrows indicate releases of PBDEs and movement in the environment. Dashed arrows indicate possible human exposure to PBDEs. Dotted arrows indicate the production of and possible human exposure to brominated dioxins and furans. ....	9
Figure 2.1: Possible aerobic BDE-209 biodegradation pathway by <i>P. Lindtneri JN45</i> . Dotted arrows indicate involvement of more than one step. Adapted from (Xu and Wang, 2014). 23	23
Figure 2.2: Proposed pathway for phenanthrene degradation by <i>P. ostreatus</i> . Adapted from (Bezalel & Hadar 1997). ....	24
Figure 3.1: Panel (a): the three domains (inorganic mineral, condensed SOM and amorphous SOM) identified in soil particles by the three domains DRM model. Panel (b): variation in time of the Freundlich isotherm parameters, sorption capacity ( $K_F$ ) and Freundlich coefficient ( $n$ ) reflects the variation of the predominant domain responsible for the sorption process. ....	33
Figure 3.2: Schematic representation of a soil particle as modelled in the chemisorption model. Adapted from (Wu and Gschwend, 1986). ....	36
Figure 3.3: : Schematic representation the D-A model based on the thermodynamic sorption potential concept. Adapted from (Pan and Zhang, 2014). ....	40
Figure 4.1: Schematic overview of instruments used and their applications. ....	43
Figure 4.2: HPLC Thermo Scientific Dionex Ultimate 3000. ....	44
Figure 4.3: Schematic diagram showing HPLC components and the mobile phase flow (adapted from Chromacademy.com). ....	45
Figure 4.4: Sample solvent carrier effect on sample particles distribution and peak tail. ....	46
Figure 4.5: 6 points calibration curve for BDE-209 analysis on HPLC. ....	48
Figure 4.6: Graphical evaluation of calibration curve linearity: residual distribution through the calibration range. ....	49
Figure 4.7: ASE 350 Thermo Scientific accelerator solvent extractor. ....	50
Figure 4.8: ASE Extraction process steps. ....	51

Figure 4.9: CEM MarsXpress Microwave Accelerated Reaction System and sample tubes..	52
Figure 4.10: BUCHI Syncore Polyvap and its components.....	53
Figure 4.11: Schematic diagram showing BUCHI Syncore Polyvap components and the cooling water flow (adapted from BUCHI manual).....	53
Figure 4.12: TECHNE DB-3D Dry Block .....	54
Figure 4.13: TOC Combustion Analyzer Apollo 9000 connected with 183 TOC Boat Sampler. ....	54
Figure 4.14: Calibration curve for TOC/TC measurement in solid sample. ....	55
Figure 4.15: Laser diffraction particle size detector Mastersizer 2000 and the disperser unit control Hydro 2000SM.....	56
Figure 4.16: Centrifuge Eppendorf 5804R. ....	56
Figure 5.1: Vacuum operational profile. BUCHI vacuum pump V-700 .....	63
Figure 5.2: Comparison of BDE-209 recovery from deionised water using liquid-liquid extraction (LLE), dispersive liquid-liquid micro extraction (DLLME), solid phase extraction (SPE) and water evaporation plus substitution with acetonitrile (WES). ....	67
Figure 5.3: (a) WES recovery from peat-water matrix sample for BDE-209 (5.3 µg/L) and chrysene (550 µg/L.) (b) Average recovery and standard deviation for BDE-209 and chrysene recovery.....	69
Figure 6.1: Packing of the PLE extraction cell. ....	76
Figure 6.2: Chromatograms from clean peat sample (blue colour) and standard BDE-209 solution in acetonitrile 1.4 mg/L (black colour) extracted by MAE. ....	78
Figure 6.3: Chromatograms from clean peat sample (blue colour) and standard BDE-209 solution in acetonitrile 1.4 mg/L (black colour) extracted by PLE method ASE1. ....	78
Figure 6.4: Zoomed chromatograms of BDE-209 acetonitrile standard solution 1.4 mg/L (brown line); spiked peat samples extracted with method ASE1 of PLE, concentrations 5 µg/g (pink line) 9.5 µg/g (blue line); clean peat sample extracted with method ASE1 PLE (black line).....	79
Figure 6.5: BDE-209 recovery from peat spiked at two concentrations 5 and 9.5 µg/g using different methods (a) ASE1 (b) MAE (c) ASE2 (n= number of repetition). Light grey columns indicate values calculated using the BDE-209 concentration measured as it is, values indicated by the dark grey columns are calculated after the subtraction of the interference. ....	81

Figure 6.6: Matrix interference extracted from peat with the four methods tested expressed in apparent BDE-209 concentration (n=number of repetitions). .....	83
Figure 6.7: Correlation between the interference expressed in apparent mass of BDE-209 and the mass of peat analysed. Peat extracted with ASE 3method. ....	84
Figure 6.8: Plot of the residual error between experimental data and the linear interpolation for the apparent BDE-209 peak measured from peat extracted using ASE3 method.....	84
Figure 6.9: BDE-209 recovery form peat sample spiked at 5 µg/g (dark grey columns) and interference influence (light grey column) for microwave assisted extraction (MAE) and different pressurised liquid extraction methods (ASE1, ASE2, ASE3). In sample ASE3 DE diatomaceous earth was spiked and ASE3 filter diatomaceous earth plus the glass fibre filter (n=number of repetitions). ....	85
Figure 7.1: water mixed with peat after 0.3 µm filtration; TOC 857mg/L (left) compared with pure water (right).....	90
Figure 7.2: Total Organic Carbon (TOC) measured in water (200mL) after 5 days of contact with 0, 0.04, 0.2, 0.4 g of peat. ....	91
Figure 7.3: Schematic representation of samples processing step in kinetics experiments. ....	95
Figure 7.4: Schematic representation of samples processing steps in kaolin desorption experiments. ....	96
Figure 7.5: Schematic representation of samples processing steps in experiments for DOM influence on kaolin sorption. ....	97
Figure 7.6: Panel (a): BDE-209 measured in water ( $m_w$ ) from samples (S) containing peat (full points) and water control samples (empty points). The initial mass dissolved in water is reported (dashed line). Dotted lines are the fitting profiles described in Equation 6.4 and 6.5 respectively, statistic correlation factor is reported in graph ( $R^2$ ). Panel (b): BDE-209 mass measured in water control samples plotted with the natural logarithm of time fitting the linear profile, ( $R^2$ ) statistic correlation reported. Panel (c): Natural logarithm of BDE-209 ( $m_w$ ) divided by the initial mass added in the system plotted in time fitting the linear profile, ( $R^2$ ) statistic correlation reported. ....	99
Figure 7.7: Kinetic profile obtained by plotting BDE-209 mass dissolved in water with time under the two scenarios considered: uncorrected profile (full points), profile corrected by subtraction of the mass sorbed on container surfaces in control samples (empty points).	

The dotted lines represent the fitting profiles; equations and statistic correlation ( $R^2$ ) are reported. ....	100
Figure 7.8: BDE-209 sorption isotherm for samples with initial concentration in water of 1.2, 2.3, 3.6, 6.9, 8.5 and 10.7 $\mu\text{g/L}$ . $C_w$ and $C_s$ are BDE-209 concentration in water and peat after 5 days contact time. ....	102
Figure 7.9: Panel (a): BDE-209 mass measured in water ( $m_w$ ), sorbed by container surfaces ( $m_s$ ) and the calculated sum in water control samples. Initial BDE-209 mass in water 0.36 $\mu\text{g}$ . Panel (b): BDE-209 mass measured in water ( $m_w$ ), sorbed on kaolin ( $m_s$ ) and the calculated sum in samples containing 0.1 g of kaolin. Initial BDE-209 mass in water 0.36 $\mu\text{g}$ . ....	103
Figure 7.10: BDE-209 molecule conformation when adsorbed on graphene surface modelled through density functional theory (DFT) and molecular dynamic (MD). Adapted from (Ding et al., 2014). ....	105
Figure 7.11: Sorption profile for peat (points) and kaolin (triangle) derived from the kinetic experiments discussed in Figure 6.6 and 6.9 respectively. Data are here normalised to the mass of sorbent. Dotted and dashed lines indicate the initial BDE-209 mass dissolved in water normalised to the mass of sorbent respectively for peat and kaolin. ....	106
Figure 7.12: BDE-209 mass dissolved in water after 2 minutes contact time with kaolin for decreasing kaolin/water ratio ( $n$ =number of repetitions). ....	108
Figure 7.13: BDE-209 mass measured in water ( $m_w$ ) and in kaolin ( $m_s$ ) expressed as percentage of the total mass added ( $m_T$ ) after two minutes contact time. BDE-209 desorbed from kaolin in fresh deionised water after a second period of 2 minutes contact time ( $m_d$ ) for increasing kaolin/water ratio. ....	109
Figure 7.14: BDE-209 dissolved in water ( $m_w$ ), adsorbed on kaolin ( $m_s$ ) and adsorbed on glass surface ( $m_g$ ) expressed as percentage of the total mass added ( $m_T$ ) from both experiments run with (a) DOM enriched water and (b) pure water for increasing kaolin/water ratio. ....	111
Figure 8.1: Examples for the three categories defined for evaluating the mycelia development on straw. ....	117
Figure 8.2: Fruits growing on straw in laboratory conditions. ....	117
Figure 8.3: <i>P. ostreatus</i> mycelia developed on straw containing 1000 $\mu\text{g/kg}$ of BDE-209 after 8 months from inoculation. ....	118

Figure 8.4: Filamentous microorganism developed from <i>P. ostreatus</i> spawn inoculated on N-agar enriched with antibiotic (left) or antimycotic. ....	119
Figure 8.5: Picture of <i>Bacillus mycooides</i> isolated from soil. Adapted from (Di Franco et al., 2002). ....	119
Figure 8.6: Soil bacterium development on N-agar after 4 days: slices labelled with "X" are the part in which N-agar contains BDE-209; unlabelled slices are the ones containing only methanol. ....	120
Figure 8.7: <i>P. ostreatus</i> mycelia developed on MEYA culture after 1 month from inoculation. ....	120
Figure 8.8: Fungus and bacterium colonies growing on MEYA culture enriched with antibiotic or antimycotic inoculated with a portion of <i>P. ostreatus</i> mycelia collected from straw. ....	121
Figure 8.9: Colony mutants derived from SIN96 <i>B. mycooides</i> strain on agar medium. Adapted from (Di Franco et al., 2002). ....	122
Figure 8.10: <i>P.ostreatus</i> mycelium developing after being transferred on MEYA disk sprinkled with different organic solvents (acetonitrile, methanol or acetone). ....	123
Figure 8.11: <i>P.ostreatus</i> mycelium developing after being transferred on MEYA disk sprinkled with methanol after 3 months. ....	124
Figure 8.12: <i>P. ostreatus</i> mycelia development from spawns into the two soil tested. ....	125

## List of Tables

Table 1.1: PBDEs 209 congeners grouped by number of bromine atoms .....	1
Table 1.2: Composition of commercial brominated biphenyl ethers (Chen et al., 2012; WHO, 1994) .....	2
Table 1.3: BDE-209 chemical and physical properties .....	14
Table 4.1: Retention time (RT) and peak area (mAU*min) using methanol and acetonitrile as sample solvents and mobile phase for BDE-209 concentration of 10 µg/ml. ....	46
Table 4.2: Calibration points for BDE-209 measurement by HPLC. Each calibration point has been measured three times and the peak area reported is the average of the three measurements. ....	48
Table 5.1: Procedure of extraction with Oasis HBL cartridge. ....	62
Table 5.2: Vacuum steps. BUCHI vacuum pump V-700 .....	63
Table 5.3: Operational parameters for BUCHI rack and cooling system. ....	63
Table 5.4: Recovery value for LLE extraction of BDE-209 from deionised water. Sample volume 10 mL, solvent volume 1 mL. ....	64
Table 5.5: BDE-209 recovery value for solvent substitution from hexane to acetonitrile. Hexane volume 25 mL, acetonitrile volume 1.5 mL. ....	64
Table 5.6: Recovery value for LLE extraction of BDE-209 from deionised water. Sample volume 25 mL, toluene volume 2 mL.....	64
Table 5.7: Recovery value for DLLME extraction of BDE-209 from deionised water. Different extraction solvents tested using 1.5 mL of acetonitrile as dispersive solvent. ....	65
Table 5.8: Recovery values for SPE extraction of BDE-209 from deionised water with Oasis HBL cartridge.....	65
Table 5.9: Recovery value for WES extraction of BDE-209 from deionised water (200 mL), BDE-209 concentration 5.4 µg/L.....	66
Table 5.10: Chrysene and BDE-209 spiking concentration and correspondent recovery values (%). Chrysene/BDE-209recovery ratio is calculated. Average value and standard deviation are reported.....	69
Table 6.1: Literature review on application of MAE on extraction of PBDEs form solid samples. ....	72
Table 6.2: Literature review on PLE applied on PBDEs extraction form sediments and soil samples. ....	74



Table 6.3: Extraction solvent used for PLE in the three methods tested on Dionex ASE350 extractor. All other parameters are the same: 100 °C, 1500 psi and 5 minutes static time, 3 cycles 100 % flush percentage. ....	77
Table 7.1: Peat and kaolin characterisation.....	90
Table 8.1: Properties of soil tested for <i>P. ostreatus</i> mycelia colonisation. Measure repeated in triplicate, average value reported $\pm$ standard deviation. ....	116
Table 8.2: <i>P. ostreatus</i> mycelia development after 20 days on straw for the different condition tested.....	116
Table 8.3: <i>P. ostreatus</i> mycelia development on contaminated straw. (X) indicates mould formation. ....	118

## List of abbreviations

BSEF: Bromine Science Environmental Forum  
DCM: Dichloromethane  
DE: Diatomaceous Earth  
DOC: Dissolved organic carbon  
DOM: Dissolved organic matter  
DLLME: Dispersive Liquid-Liquid Micro Extraction  
DRM: Distributed Reactive Model  
HBCD: Hexabromocyclododecane  
HFRs: Halogenated Flame Retardants  
HOCs: Hydrophobic Organic Compounds  
HPLC: High pressure Liquid Chromatography  
LLE: Liquid-Liquid Extraction  
LOD: Limit of Detection  
LOQ: Limit of Quantification  
MAE: Microwave Assisted Extraction  
MEYA: Malt Extract Yeast Agar  
PAHs: Polycyclic Aliphatic Hydrocarbons  
PBB: Polybrominated Biphenyls  
PBDEs: Polybrominated diphenyl Ethers  
PCBs: Polybrominated Diphenyl Ethers  
PLE: Pressurised Liquid Extraction  
POPs: Persistent Organic Pollutants  
PTFE: Polytetrafluoroethylene  
RoHS: Restriction of Hazardous Substances  
SRPD: Sorption Related Pore Diffusion model  
TB117: California Furniture Flammability Standard  
TBBPA: Tetrabromobisphenol A  
TBPA: Tetrabromophthalic anhydride  
THF: Tetrahydrofuran  
TOC: Total Organic Carbon  
TC: Total Carbon  
VECAP: Voluntary Emissions Control Action Programme  
WES: Water Evaporation and Substitution method

# 1 Introduction

## 1.1 History and use of PBDEs as flame retardant

### 1.1.1 PBDEs

Polybrominated biphenyl ethers (PBDEs) refer to a group of 209 compounds that differ in number and/or position of bromine atoms around the two aromatic rings (Figure 1.1). The single congener is identified by a specific number (from 1 to 209) and they are grouped in families (from mono-BDE to deca-BDE) according to the number of bromine atoms (Table 1.1).

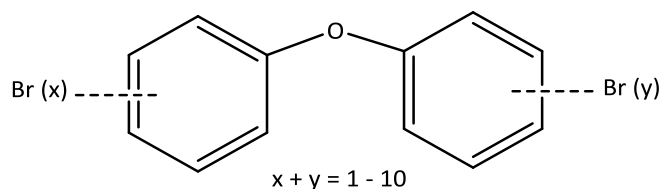


Figure 1.1: PBDEs structure.

Table 1.1: PBDEs 209 congeners grouped by number of bromine atoms

Group	Number of Congeners	Name	Molecular Mass (Da)
mono-BDE	3	BDE-1 to BDE-3	249.11
bi-BDE	12	BDE-4 to BDE-15	328.00
tri-BDE	24	BDE-16 to BDE-39	406.90
tetra-BDE	42	BDE-40 to BDE-81	485.79
penta-BDE	46	BDE-82 to BDE-127	564.69
hexa-BDE	42	BDE-128 to BDE-169	643.59
hepta-BDE	24	BDE-170 to BDE-193	722.48
octa-BDE	12	BDE-194 to BDE-205	801.38
nona-BDE	3	BDE-206 to BDE-208	880.27
deca-BDE	1	BDE-209	959.17

PBDEs have been introduced on the market in four commercial mixtures: tetra-BDE, penta-BDE, octa-BDE and deca-BDE. Each mixture is produced by the bromination of biphenyl ether and contains a mixture of tri- tetra- penta- hexa- hepta- octa- nona- and deca-

brominated congeners in various percentage (Table 1.2) (Siddiqi et al., 2003). Apart from the tetra-BDE mixture, which ceased production in 1994, the other formulations have been used for 40 years as flame retardant in paints, plastics, foam, textiles, plastics in electronic equipment, furniture, building materials, airplanes and automobiles. In some of these products, PBDE content reaches 5 to 30% by weight (BSEF, 2016; Siddiqi et al., 2003).

Table 1.2: Composition of commercial brominated biphenyl ethers (Chen et al., 2012; WHO, 1994)

Commercial Product	Components content (%)								
	bi-	tri-	tetra-	penta-	hexa-	hepta-	octa-	nona-	deca-
Tetra BDE	8		41-42	44-45	6-7				
Penta BDE		0-1	24-38	50-62	4-8				
Octa BDE					10-12	43-44	31-35	9-11	0-1
Deca BDE								0-3	97-98

### 1.1.2 Flame retardancy mechanism

Depending on their nature, flame retardants can interfere with various processes involved in polymer combustion (heating, pyrolysis, ignition, propagation of thermal degradation) by either physical (e.g. cooling, formation of a protective layer, or fuel dilution) or chemical (e.g. reacting in the condensed or gas phase) action (Laoutid et al., 2009). PBDEs belong to the family of halogenated flame retardants (HFR), which can slow down the combustion of polymers by the release of halogen radicals ( $X\cdot$ ) in the gas phase. Radicals ( $X\cdot$ ) react with highly reactive species like  $H\cdot$  or  $OH\cdot$  to form less reactive molecules, stopping the chain breaking mechanism and consequently the combustion of the polymer. As a first step, the flame retardant breaks down, forming a free radical (Eq 1.1). The halogen radical reacts to form a hydrogen halide (Eq 1.2), which interferes with the chain branching reactions (Eq 1.3 and 1.4). In this way very highly reactive radicals  $H\cdot$  and  $OH\cdot$  are removed from the combustion environment and replaced with lower energy bromine radicals (Laoutid et al., 2009).



For this purpose, it is essential that bromine radicals are released at the most favourable point of the combustion process. Brominated compounds are the most effective between halogenated flame retardants. Other halogenated chemicals, such as fluorinated compounds, result in more thermally stable polymers, so they do not release active halogen radicals in the proper temperature range. Conversely, iodinated compounds are less stable than common polymers and release radicals during the polymer processing. Chlorinated and brominated compounds present the right bonding energy between the halogen atoms and the carbon structure, so they are able to interfere in the combustion process at a more favourable point. However, brominated compounds produce the hydrogen halide in a more narrow temperature range than chlorinated compounds, which allows brominated compounds to reach higher concentrations of hydrogen halides and makes them more efficient (Laoutid et al., 2009). Finally, aromatic compounds are more temperature resistant than aliphatic compounds (Levchik, 2006). As a consequence, PBDEs and a few other aromatic or cyclic aliphatic compounds have found large success in the fire retardant marketplace. Figure 1.2 shows the structures of common fire retardant compounds.

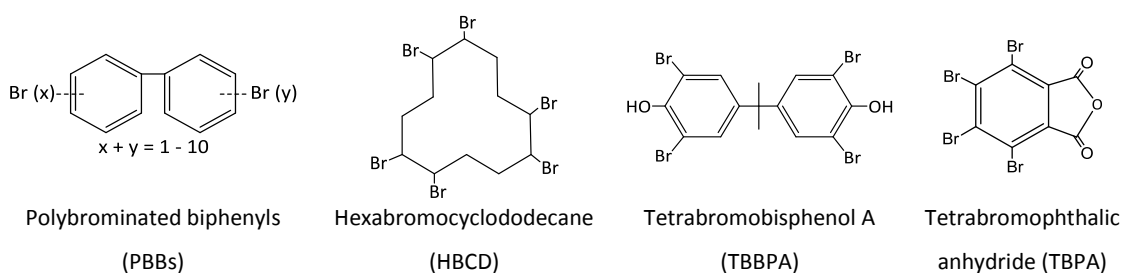


Figure 1.2: Chemical structures of the most widely used halogenated flame retardant along with PBDEs (Figure 1.1) (Eljarrat and Barceló, 2004; Laoutid et al., 2009).

PBDEs, tetrabromophthalic anhydride (TBPA), and tetrabromobisphenol A (TBBPA) are additive flame retardants. They are mixed in the polymer and not chemically bonded to the structure as it is for reactive flame retardants. For producers, the advantage is that no additional steps in polymer synthesis are required for their incorporation. On the other hand, simple mixing into the polymer makes them susceptible to migration to the material surface and release into the environment. Moreover, higher concentration are required to obtain the same product in comparison to reactive flame retardants (Laoutid et al., 2009).

### 1.1.3 Controversy on the use of flame retardants

The aim of incorporation of flame retardants in polymeric materials was to decrease the number of domestic fires and, in case of fire, reduce the number of casualties by extending the escape time. Nevertheless, it seems that at the moment of PBDEs introduction in the market, only the potential benefits of their usage have been considered and the drawbacks have been ignored (Babrauskas et al., 2011). For instance, in the United States only chemicals in foods, drugs and pesticides are regulated before their introduction in the marketplace. No health data or risk assessment are required to regulate other chemicals (Babrauskas et al., 2011). When a number of halogenated flame retardants received detailed study, they showed to have adverse effects in animals and humans, including endocrine disruption, immunotoxicity, reproductive toxicity, and diabetes, effects on foetal/child development, thyroid, neurologic function and cancer (Shaw et al., 2010). In consequence, they have been gradually phased out. Polybrominated biphenyls (PBBs) historically used in electronic equipment have been gradually phased out of market and, since 2009, banned worldwide (Stockholm Convention, 2009). Hexabromocyclododecane (HBCD) underwent severe restrictions on production and use because of evidence of its toxicity, persistency and tendency to bioaccumulate through the food chain (Babrauskas et al. 2012, Stockholm Convention 2013). TBBPA, the most widely used halogenated flame retardant, is allowed in printed circuit boards, but restrictions on its use and disposal are applied in Europe (BSEF, 2016).

The story of PBDEs is not different. After being used for 40 years, PBDEs have been found responsible for health problems such as thyroid homeostasis disruption, neurodevelopmental deficits, reproductive changes, and even cancer in animals (Abbasi et al., 2015; Chen et al., 2012; Gascon et al., 2012; Guo et al., 2015; Linares et al., 2015; Shaw et al., 2010). The production of penta- and octa-BDE commercial mixtures is now banned in all the states subscribing to the Stockholm Convention (UNEP, 2009a, 2009b) and deca-BDE annexation to the list of Persistent Organic Pollutants (POPs) is under evaluation (UNEP, 2013).

### 1.1.4 The California Furniture Flammability Standard (TB117) case

The PBDE market boom was closely related to the California Furniture Flammability Standard (TB117). The legitimacy of this statute has been subject of intense debate. TB117 introduction is an exemplar case of the role science findings and economic interests can play when important political decisions have to be taken. It is here reported to underline the importance of a fair and honest scientific debate.

TB117 required polyurethane foam in juvenile products and upholstered furniture to resist exposure to small open flame for 12 seconds (Babrauskas et al., 2011). Since its adoption, to comply with the fire safety standard in California, all products were required to contain 3-5 % by mass of flame retardant. Although California was the only state with such a standard, compliance was mandatory for all products sold in California despite their origin. Thus, for maintaining a single inventory, many national manufacturers started using flame retardants in all furniture sold across North America. Since 1975, hundreds of millions of kilograms of penta-BDE have been used to meet California TB117. In 1999, 98% of the global demand for penta-BDE was used in North America (Hale et al., 2001; Renner, 2000; Siddiqi et al., 2003). Thereafter, in 1988, a fire safety standard was introduced also in UK for all fabrics and polyurethane foams used in construction, furniture and mattress filling (Emsley et al., 2005).

While the use of flame retardants was growing to comply with the TB117 standard, experiments run by Babrauskas and Talley (Babrauskas, 1983; Babrauskas et al., 1988; Talley, 1995) investigated if material compiling TB117 standard were actually suitable for achieving either one of the two main purposes of the standard: to reduce the severity of fire and to prevent ignition from small flame sources (Babrauskas et al., 2011). In the experiments run by Babrauskas, severity of fire was evaluated by measuring the peak heat release rate (HRR). Comparing the HRR produced by furniture complying with TB117 and an identical-constructed one without fire retardant, Babrauskas concluded that: "Polyurethane foams with retardants added to meet California State requirements did not show any reduction in HRR compared to ordinary polyurethane foams" and no delay in the HRR peak was observed. The second purpose, the prevention of fire ignition, was evaluated exposing foam and foam covered with fabric to small burner flame. Results again underlined the usefulness of TB117 standard to reach the purpose. Indeed foam containing fire retardant demonstrated resistance to small open flame, but as soon the foam was covered with fabric

“TB117 foam made no significant/consistent difference in either ignition or flame spread” (Talley, 1995). Indeed, once the fabric is burning, the foam is exposed to a much greater flame than the cigarette lighter flame the foam is designed to resist. According to Babrauskas et al., (2011), these results were ignored and instead evidence in support of TB117 was obtained by “distortedly and improperly citing” results from a second experiment run in 1988 on an advanced foam. This advanced foam demonstrated a peak HRR 42 % lower than for TB117 foam and 96 % lower than for foam free from fire retardant. The study concluded that “The average available escape time was more than 15-fold greater for the fire retarded products”. The advanced foam tested is a costly material characterised by higher density and higher levels of fire retardant than required by TB117. It was not used in residential furniture and was investigated for research purposes to illustrate performance that may be achievable by state of the art technology.

Meanwhile, further concerns about safety of smoke produced by polymers containing PBDEs arose. Production of polybrominated dibenzofurans (PBDFs) and dioxins (PBDDs) was observed during combustion and smouldering of pure PBDEs mixture and flame retarded polymers (Buser, 1986; Dumler et al., 1990, 1989a, 1989b; Hutzinger et al., 1989; Sakai et al., 2001; Söderström and Marklund, 2002; Thoma et al., 1987; Thoma and Hutzinger, 1989).

In light of these considerations, queries arose about interests that led to the introduction of the TB117 standards. According to a seven part series by the Chicago Tribune in 2012, the introduction on the TB117 was solicited by major lobbies of tobacco and producers of FRs chemicals (Callahan and Hawthorne, 2012; Callahan and Roe, 2012a, 2012b, Hawthorne, 2012a, 2012b; Roe, 2012; Roe and Callahan, 2012). For fire retardant producers, the introduction of the TB117 would have meant a consistent growth of the flame retardant market. For the tobacco industry, it represented an easy escape from the pressure of producing auto-extinguishing cigarettes after cigarettes have been recognised to be one of the most frequent causes of domestic fire (Callahan and Roe, 2012c).

The scientific community in 2010 finally evaluated whether the health and environmental risk of halogenated flame retardant are justified by fire safety benefit (Shaw et al., 2010). The conclusions resulting from comprehensive literature review signed by 200 scientists



from 22 countries are here summarised. Most fire deaths and most fire injuries result from inhaling carbon monoxide, irritant gases or soot; the incorporation of HFRs can increase the yield of these toxic by-products during combustion. The current options for end-of-life disposal for products containing HFRs are problematic; therefore, the hazards deriving from the use of HFR chemicals are potentially greater than the fire risk they are supposed to prevent. Alternative policy solutions preventing fires without the potential adverse effects of HFRs are recommended. These solutions include the introduction of fire-safe cigarettes, fire-safe candles, child-resistant lighters, sprinklers, and smoke detectors along with the use of less flammable materials, safer chemicals or design changes.

### 1.1.5 Environmental contamination and human exposure

The production of flame retarded materials is in end of itself a source of PBDEs contamination for the environment. Allchin et al. (1999) analysed sediments from four rivers receiving effluents from the UK main producers and/or users of penta and octa-BDE commercial mixtures. The study showed that at least in three of the four cases, the concentrations of BDE-47 (tetra-BDE) BDE-85, BDE-99 (penta-BDE) in the main river were higher after the discharge points of treatment plants than before. Release after wastewater treatment is not the only route of contaminant release; other factors may contribute to PBDE emissions during the production of flame retarded polymers. For example, dust may escape during opening and emptying of PBDEs bags, reaching the environment during floor sweeping and through objects contaminated by PBDEs not being treated properly. Other potential emissions may occur during the disposal of dust filters and empty packaging materials (Chen et al., 2012).

Automobiles, homes and offices may be significant source of PBDEs to the environment and human exposure. Since PBDEs are additive flame retardants, they might be released not only during the manufacturing and polymer processing operations, but also throughout the product service life. Several studies detected PBDEs in the urban atmosphere and indoor dust (Hale et al., 2001). For example, in a study conducted on PBDEs atmospheric pollution in the urban area of downtown Paris, PBDEs have been found in gaseous phase and air particulate. BDE-209 proved to be the most abundant congener in ambient air (gaseous phase plus particulate) (5-175  $\text{pg}/\text{m}^3$ ). Considering the gaseous phase alone instead, pollution was dominated by BDE-47; BDE-99 and BDE-209 concentration decrease to values

between 2-25  $\text{pg}/\text{m}^3$  (Tlili et al., 2012). Focusing on PBDEs contamination in urban micro-environments like residences, offices and automobiles, Fromme et al. (2009) found that exposure to PBDEs was higher in offices and automobiles compared to residences. Again BDE-209 proved to be the dominant congener in all of the environments considered.

Wastewater treatment plants represent a point of accumulation of PBDEs. In particular, BDE-209 has been found dominating the congeners profiles in sludge, while lower brominated congeners, more water soluble, are mainly found in effluent (Vonderheide et al., 2008; Cincinelli et al., 2012). If waste sludge is then applied as fertiliser, that may increase PBDE concentrations in agricultural soil (Hale et al., 2003; Sellström et al., 2005).

Furthermore, PBDEs may be released during manipulation for articles disposal at the end of the article service life. For example, PBDE contamination has been reported in proximity of electronic waste landfill and recycling site (Allchin et al., 1999; Covaci et al., 2007; Leung et al., 2007; Li et al., 2015).

Finally, human exposure to toxic substances is enhanced by the possible release of harmful by-products during combustion processes. Production of polybrominated dibenzofurans (PBDFs) and dioxins (PBDDs) has been observed after combustion and smouldering of pure PBDE mixtures and flame retarded polymers containing PBDEs (Buser, 1986; Thoma et al., 1987; Dumler et al., 1989a, 1989b; Hutzinger et al., 1989; Dumler et al., 1990; Sakai et al., 2001; Söderström and Marklund, 2002).

As presented here, once PBDEs are incorporated in common articles as flame retardants, they are released into the environment and tend to remain in circulation long after their production and the end of articles' service lives. The presence of PBDEs in biotic and abiotic environments contributes to human exposure. Dietary intake and dust inhalation are identified as primary sources of human exposure along with occupational exposure (Vonderheide et al., 2008). Similarly to what is proposed for HBCD (Babrauskas et al., 2012), Figure 1.3 illustrates the numerous routes through which PBDEs, PBDDs, and PBDFs may contribute to human exposure to PBDEs.

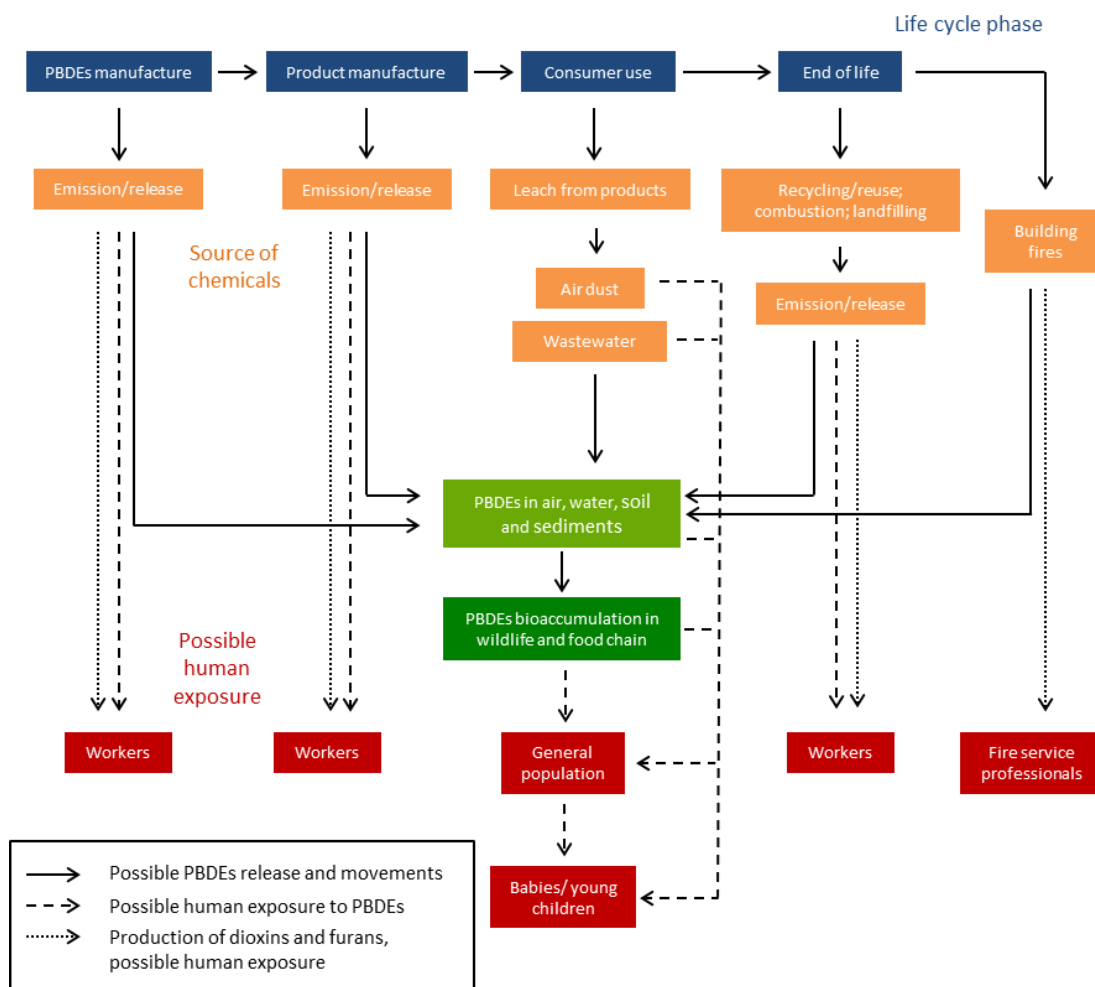


Figure 1.3: Sources of PBDEs and their by-products in the environment and human exposure. Solid arrows indicate releases of PBDEs and movement in the environment. Dashed arrows indicate possible human exposure to PBDEs. Dotted arrows indicate the production of and possible human exposure to brominated dioxins and furans.

### 1.1.6 PBDE bans and delays in restriction on BDE-209

Following increasing awareness about potential adverse effects of PBDEs on human health, the first restrictions on production and use of PBDEs arrived in Europe. Initially, only penta and octa-BDE mixtures were affected. In 2003 the European Risk Assessment Report of penta-BDE and octa-BDE mixtures ratified in the Directive 76/769/EEC a restriction on their marketing and use (PBDEs content in commercial product fixed to be < 0.1 %) (European commission, 2001, 2003). In 2006, a Restriction of Hazardous Substances (RoHS) Directive banned their use in electrical and electronic applications (BSEF, 2016; Kemmlein et al., 2009). Following that, several jurisdictions around the world spontaneously classified the components of penta- and octa-BDE mixtures as contaminants of concern or placed them on priority substances lists (BSEF, 2006; Environment Canada, 2006; European Commission,

2001, 2003; Gandhi et al., 2011; Abbasi et al., 2015). In the meanwhile, intense debate about the classification of PBDEs as Persistent Organic Pollutants in the Stockholm Convention is based on the following screening criteria: long-range transport, environmental persistence, bioaccumulation and toxicity. The distribution of PBDEs (other than BDE-209) observed in air particulates across Europe (Jaward et al., 2003) shows that at the moment of the ban there was still a large gradient between samples collected in source and remote regions. Concentrations in sample from the United Kingdom, a major producer and user of PBDEs in Europe, are about 700 times higher than lowest sample collected in Europe. However, PBDEs have been detected in abiotic samples from deep remote regions, such as Arctic and Antarctic environments; in sediments of high mountain lakes (Bartrons et al., 2011; de Wit et al., 2010; Yogui et al., 2011); and in biota from terrestrial, freshwater and marine ecosystems (de Wit, 2002). Passage of contaminants through the food chain has been observed for tri, tetra, penta and hexa-BDEs and biomagnification of PBDEs is hypothesised. Concentrations seem to increase more than one order of magnitude from gadoid fish to marine mammals in the North Sea food web (Boon et al., 2002). Several studies showed an increase in PBDEs concentration in human biological samples. PBDEs were found in human breast milk, adipose tissue, blood serum, placenta and plasma (de Wit 2002). The sum of seven tri- to hexa- brominated congeners measured in human breast milk showed an exponential increase from 1972 to 1997 in a study conducted on Swedish population (Norèn and Meironytè, 1998, 2000 cited by de Wit 2002). In Germany, concentrations of PBDEs (median sum of the same lower brominated congeners) increased from 3.1 ng/g lipid weight in 1981 to 4.7 ng/g lipid weight in 1999 (Schroter-Kermani et al., 2000 cited by de Wit 2002). In 2009, PBDEs congeners contained in penta- and octa-BDE commercial mixtures were classified as POPs and listed among amendments to the Stockholm Convention (Kemmlin et al., 2009; UNEP, 2009a, 2009b).

Strict monitoring of the production seemed to start bringing positive results: PBDE levels in serum in Californian population declined 39% from 2008-2009 to 2011-2012. Also, declines were observed in communities in Australia, European and Asian countries. Decreases in concentration of PBDEs in women breast milk have been also observed in California between 2003-2005 and 2009-2012, suggesting the efficacy of environmental policy changes (Guo et al., 2015).

Legislation related to deca-BDE commercial mixture followed a different path. A combination of factors contributed to delays in restrictions on deca-BDE production and use. Due to difficulties with the analytical method for BDE-209 (the main congener contained in deca-BDE mixture) and generally for detection of higher brominated congeners (from octa- to nona-BDE), they have been rarely measured in the first period of interest on PBDEs (Stapleton, 2006). In consequence the majority of studies on PBDEs environmental contamination, transportation, bioaccumulation and toxicity done in the first decade of 2000 concentrated on PBDEs other than BDE-209 (de Wit, 2002; Siddiqi et al., 2003; Mueller et al., 2006; Drori et al., 2008; Liu et al., 2010, 2011; Olshansky et al., 2011; W. Wang et al., 2011; S. Wang et al., 2011b; Chen et al., 2012). Fewer data are available on BDE-209 in comparison to lower brominated PBDEs congeners. That made the debate on the addition of BDE-209 in the POPs list even more complex than the one for the lower brominated congeners. BDE-209 is considered less susceptible to long range transportation and bioaccumulation and has a relatively low toxicity (Gandhi et al., 2011). In 2004, industry successfully argued that a restriction on BDE-209 was not appropriate or necessary (Vonderheide et al., 2008). As result, after the completion of the 10-year Risk Assessment Report, the EU concluded that no further restrictions BDE-209 use were required and deca-BDE mixture was exempted from the RoHS formed in 2006 (Kemmlin et al., 2009).

As analytical capabilities improve, reports of BDE-209 in environmental systems seem to be increasing. BDE-209 has been found in samples collected in remote areas like Canadian lake sediments, arctic regions, Himalayan plateau, and high Alps lake sediments (Bartrons et al., 2011; Möller et al., 2011; Wang et al., 2012; Yuan et al., 2012; Kirchgeorg et al., 2013). Furthermore, the tendency of BDE-209 to debromination under the effect of UV radiation has been observed (Watanabe and Tatsukawa, 1987; Söderström et al., 2003; Ahn et al., 2005; Ghanem and Delmani, 2012; Leal et al., 2013; Wei et al., 2013). As a result, restrictions on deca-BDE use and production have been re-considered. In 2008, the European Court of Justice annulled the European Commission decision exempting deca-BDE from the RoHS and ruled that deca-BDE can no longer be used in electronics and electrical applications in the EU market.

Meanwhile, independent initiatives for banning deca-BDE have been taken by single states like Norway and the US. Deca-BDE production started to be monitored by the Voluntary

Emission Control Action Programme (VECAP) (Kemmler et al., 2009). In the US, the Environmental Protection Agency (USEPA) started a phase-out initiative for deca-BDE according to which the major producing and importing US companies (Chemtura and Albemarle) have committed to end production, importation, and sales of deca-BDE for most uses in the United States by December 2012, and to end all uses by the end of 2013 (Hess, 2009 cited by Covaci et al., 2011; SEC, 2014; USEPA, 2016).

Because of delays in restriction on the deca-BDE commercial mixture, deca-BDE production did not follow a drop as happened for lower brominated compounds (Shih and Wang, 2009). In 1999, the total market demand of deca-BDE was 54,800 tons/year worldwide (Arias, 2001 cited by Covaci et al., 2011) and grew to 56,400 tons/year in 2003, when lower brominated congeners were banned (BSEF, 2006 cited by de Wit et al., 2010). According to a survey carried out in 2014 by VECAP based on 84% of volume sold in Europe by European Flame Retardant Association (EFRA), member companies during the period 2008-2014, production showed a constant trend (5000-7500 tons/year) with an increase in 2011 (7500-10000 tons/year) and drops in 2012 (2500-5000 tons/year) and 2014 (1000-2500 tons/year) (VECAP, 2014).

In 2013, BDE-209 (main component of deca-BDE commercial mixture) became a candidate for the Stockholm Convention POPs list (UNEP, 2013). The POPs review committee of the Stockholm Convention called for new research studies filling the gaps still existing on BDE-209 bioavailability and fate in the environment, hence the interest of this thesis in studying BDE-209 behaviour in soil. This interest that is even more justified considering that the peak of BDE-209 emission in the environment is delayed with respect to the peak in use. According to an estimate from the US market considering only existing products, BDE-209 emissions are expected to increase until 2020 (Abbasi et al., 2015). Moreover, the stock of existing products containing BDE-209 provides an on-going source of BDE-209 emissions to the environment (Abbasi et al., 2015). Furthermore, there are countries that still continue to use PBDEs as flame retardants. For example, environmental regulations and directives on PBDEs in China are still inadequate (Chen et al., 2012) and BDE-209 makes up 75 % of all PBDEs used (Chou et al., 2013). Most countries do not have regulations on PBDE content for imported finished products. Therefore, even in nations where bans and restrictions are

adopted, sources of PBDEs could come from products imported from countries where legislation is less restrictive (Abbasi et al., 2015).

### 1.1.7 BDE-209 physical and chemical properties

Due to the large number of bromine atoms and the symmetric structure of the molecule, BDE-209 is a heavy, non-polar hydrophobic molecule. The apparent similarity between chemical structures of PBDEs and polychlorinated biphenyls (PCBs) had led to presumptions that these families of compounds share similar properties. However, BDE-209 physical/chemical properties are more extreme in comparison to PCB-209, the homologous fully chlorinated congener of the PCB family. For instance PCB-209 molecular weight (498.7 g/mol) is comparable with the one of a tetra or penta brominated PBDE congener (485.8 and 564.7, respectively). Instead, BDE-209 molecular weight is more than double (959.2 g/mol). The high weight and low volatility of BDE-209 made the detection through GC-MS or LC-MS challenging rising the instrumental detection limits or forcing to use less sensitive instrument like HPLC. At the same time, BDE-209 low polarity and water solubility force to work at extremely low concentrations (in the order of few  $\mu\text{g/L}$ ). Consequently the window of available BDE-209 working concentration for experiments is narrow. Therefore sometimes values are estimated through chemical models based on BDE-209 molecular structure or elemental properties. Studies applying quantitative structure-properties or structure-activity relationship models on PBDEs are here reported: Hu et al., 2005a, 2005b; Yue and Li, 2013.

Even if there are no doubts BDE-209 is classified as an extremely hydrophobic and heavy compound, it is not easy to identify a univocal value for some of BDE-209 properties like water solubility and octanol-water partitioning coefficient. Estimates for these parameters obtained both experimentally or by modelling, vary by several orders of magnitude. Table 1.3 summarises values that have been found in literature.

Table 1.3: BDE-209 chemical and physical properties

ID		BDE-209	
Name	decabromodiphenyl ether		
Molecular mass	959.2 g/mol		
Melting point temperature			
$T_M$ in °C	Reference		
302.5	(Watanabe and Tatsukawa, 1987)		
290-306, 300-305	Cited by (Wania and Dugani, 2003)		Original source not available
290-306	(INCHEM, 1994)		
Fugacity Ratio F calculated from $T_M$	0.00179		
Vapour pressure			
$P_L$ at 25 °C in Pa	Reference		Comments
2.95E-09	Cited by (Wania and Dugani, 2003)		Extrapolated from other PBDEs data (Wong et al., 2001)
4.60E-06	(Palm et al., 2002)		Technical deca-BDE mixture
4.63E-06	(Stenzel and Markley, 1997)		Value at 20 °C
4.63E-06	(Hardy, 2002)		Value at 20 °C
2.68E-07	Cited by (Wania and Dugani, 2003)		Estimated through EPIWIN software
Water solubility			
$S_S$ at 25 °C in mol/m <sup>3</sup>	Reference		Comments
2.92E-14	(Hardy, 2002)		
2.96E-14	Cited by (Wania and Dugani, 2003)		Estimated through EPIWIN software
< 1.04E-07	(Stenzel and Markley, 1997)		
2.09E-05 - 3.13E-05	(INCHEM, 1994)		
4.17E-09	Cited by (Wania and Dugani, 2003)		Original source not available calculated from $S_L$ using F value above reported $S_S=S_L \cdot F$
3.58E-09	(Yue and Li, 2013)		
Octanol-Water partition coefficient			
Log $K_{ow}$	Reference		Comments
5.24 - 9.97	(INCHEM, 1994)		
6.265	(Hardy, 2002)		
6.265	(MacGregor and Nixon, 1997)		Generator column method
9.16 - 9.97	(Yue and Li, 2013)		
9.97	(Watanabe and Tatsukawa, 1987)		Estimated using HPLC method
9.9	(Kelly et al., 2007)		
12.8	(Langford et al., 2005)		
Octanol-Air partition coefficient			
Log $K_{OA}$ at 25 °C	Reference		Comments
13.1	(Kelly et al., 2007)		



## 1.2 Aim and objectives

The aim of this thesis is to give a contribution in the understanding of the processes characterising BDE-209 behaviour in soil. In particular the research goal is to establish some underlying understanding on factors influencing BDE-209 sorption on soil particles to allow development of methods to improve fate-predictions, bioavailability and potentially bioremediation. To achieve this aim, the following objectives have been pursued:

- 1) Testing available methods to measure BDE-209 in soil samples and develop a novel one for BDE-209 analysis in water samples .
- 2) Evaluate the sorption kinetics of BDE-209 in mineral and organic matter compartments
- 3) Investigate the role of dissolved organic matter (DOM) in sorption processes of BDE-209
- 4) Establish the tolerance of *P. ostreatus* to BDE-209, a species of white rot fungus with documented mycoremediation ability on others persistent organic pollutants in soil;

Chapters 2 and 3 introduce the reader to the topic of BDE-209 behaviour in soil. In Chapter 2, literature about BDE-209 mobility and biodegradation in soil is reviewed. In Chapter 3, models describing the partitioning of pollutants in soil and the sorption mechanisms of hydrophobic organic pollutants on soil particles are explored. The complex interaction between peat, water and BDE-209 required the development of specialist analytical techniques and method that are detailed in Chapter 4, 5 and 6. Sorption kinetics of BDE-209 and the role of DOM in the process are examined in depth in Chapter 7. Scoping work with *P. ostreatus* is presented in Chapter 8.

## 2 BDE-209 in soil

As previously described, restrictions on the production of BDE-209 are active in some countries and the addition of BDE-209 to the Stockholm convention list is now under evaluation. Although these restrictions may prevent additional production of BDE-209, a large reservoir of BDE-209 currently exists in the environment (Gandhi et al., 2011). In accordance with BDE-209 physical and chemical properties, fate models predict that soil and sediments are the main environmental reservoir for BDE-209 (Vonderheide et al. 2008). In a survey of European soils, PBDEs concentrations between 65 and 12 000 ngkg<sup>-1</sup> dry weight were observed in UK and Norwegian soils (Huang et al., 2009). The wide range reflects the gap between background contamination, in remote region far from contamination sources, and concentrations measured in correspondence of toxic contaminated sites, like PBDEs production factories, landfills or recycling plants. Unless soil has been identified as the main reservoir for PBDEs, a toxic level for BDE-209 in soil has not been established yet. In confirmation of importance of soil in the environmental fate of PBDEs, two studies using the Level III fugacity model indicate that when PBDEs are emitted simultaneously to the three media (air, water and soil), much of the substance would be expected to partition in sediment and soils; percentages in sediment and soil are 59% and 40% for penta-BDE (Environment Canada, 2006), 58.6% and 39.7% for BDE-47 (tetra-BDE) and 57.0 % and 41.8 % for BDE-209 (Palm, Cousins et al. 2002).

Despite the importance of soil in the environmental fate of BDE-209, soil is the least studied compartment in PBDEs environmental studies (Vonderheide et al., 2008). Additionally higher brominated congeners (from octa to deca-BDE) were not included in the environmental measurement of PBDEs for long time due to difficulties with analytical methods (Stapleton, 2006). The combination of these factors results in a gap of knowledge in BDE-209 distribution and behaviour in soil. Two main topics of interest have been identified: sorption and mobility of BDE-209 in soil and its biodegradation under the action of microorganism living in soil. Hereafter literature concerning these two hotspots is summarised.

### 2.1 Sorption and mobility

BDE-209 is a strongly hydrophobic organic compound (HOC) characterised by high  $\log K_{ow}$  values (6-12) and low solubility in water (<0.001-20  $\mu\text{g/L}$ ) (detailed references are provided in Table 1.3). Due to its properties, BDE-209 is expected to be sorbed by soil and sediment particles rather than remain dissolved in water. Nevertheless, there are cases in which BDE-209 showed unexpected mobility. During an experiment run over 4 years in an outdoor field lysimeter in China, consistent vertical migration of BDE-209 in the soil column was observed with an average migration rate of  $1.54 \text{ mg}\cdot\text{m}^{-2}\cdot\text{yr}^{-1}$  (Du et al., 2013). Unexpected vertical migration of PBDEs was observed also in two soil cores collected from an electronic waste polluted area in South China (Yang et al., 2010). In both cases authors inferred that the high migration rate was mainly caused by leaching with suspended particles or dissolvable organic matter eluting with rain or irrigation. Finally, in Canada, 37 PBDEs congeners were detected in groundwater samples and BDE-209 was the most commonly detected congener (Levison et al., 2012). PBDEs concentrations registered were one order of magnitude higher than typically observed in lakes or estuaries. It was hypothesised that migration happened through fractures of the rock aquifer directly connected with ground surface (classified as silty sand with minor gravel and clay-loam). How PBDE molecules could be transported to such depth (20-30 m) is not completely understood. No direct evidence of facilitated colloidal transport was collected by authors; nevertheless, it is identified as a clear area of interest for further investigation (Levison et al., 2012). More research is required to understand sorption phenomena of BDE-209 and generally PBDEs in soil (Ahn et al., 2005; Du et al., 2013; Gao et al., 2011; Levison et al., 2012) as it has major impact on their bioavailability, degradation and transport.

So far only four studies investigated PBDEs sorption and desorption kinetics and isotherms (Liu et al., 2010,2011; Olshansky et al., 2011; Liu et al., 2012). Liu and co-workers studied the sorption and desorption kinetics and equilibrium isotherms for BDE-28 and BDE-47 (tri- and tetra- brominated congeners respectively) in five soil samples (TOC 0.38 0.70 2.86 4.42 7.90 %). Kinetic profiles were fitted by a two compartments first order kinetic model of equation (Liu et al., 2010):

$$\frac{q_t}{q_e} = f_1(1 - e^{-k_1t}) + f_2(1 - e^{-k_2t}) \quad \text{Eq. 2.1}$$

Where  $k_1$  and  $k_2$  are the rate constant of fast and slow sorption compartments and  $f_1$  and  $f_2$  represent the contribution fraction of the two sorption compartments to the total sorption capacity respectively, and  $f_1+f_2=1$ . The fast compartment has been found to account for 80% of the total sorption with the first 5 hours. Authors embraced the distributed reaction model (DRM, detailed in section 3.2.1) as justification of the two compartment model, postulating the presence of different fraction of SOM with different sorption characteristics. Surprisingly, they observed an inverse correlation between the TOC content and organic carbon normalised PBDE sorbed amount at sorption equilibrium.

Sorption isotherms were well fitted by both Freundlich curves and linear distribution model (Liu et al., 2011). The narrow concentration range imposed by the analyte's low solubility in water impeded the ability to distinguish which of the two profiles better represented the sorption data. In contrast with what was observed for the equilibrium concentration reached in the kinetic experiments (Liu et al., 2010), a positive correlation between the soil organic content and the Freundlich coefficient was observed, confirming SOM was the main factor governing PBDEs sorption in natural soil.

Results from desorption experiments revealed that desorption kinetic profiles are well fitted by a two compartment first order kinetic model, again in accordance with the DRM (Liu et al., 2012). Nevertheless in desorption profiles the slow compartment dominates the process accounting for 80-100 % of the total sorption capacity. Desorption isotherms were again equally fitted by Freundlich equation and linear distribution profile. Comparing isotherms obtained for sorption (Liu et al., 2011) and desorption (Liu et al., 2012), samples with higher TOC showed Freundlich coefficient in sorption higher than in desorption while in samples with lower TOC content, the magnitude of the model coefficient were comparable. The comparison between the isotherm slopes in sorption and desorption is then used to give rough evaluation of the desorption hysteresis. The analysis showed that soil samples with lower TOC content have slightly higher propensity for hysteresis.

Olshansky and co-workers (Olshansky et al., 2011) studied sorption and desorption isotherm of BDE-15 (di-brominated congener) in three natural soil samples (TOC 0.09 0.67 1.07 %) and in a humin sample isolated from natural soil through basic and acidic washing (TOC 0.55 %). Experimental data were fitted with Freundlich equation closely matching a

linear distribution (Freundlich linearity coefficient in the range 0.9-1.1). Humins appear to be the major sorption domain for BDE-15 in soil. The humin Freundlich coefficient ( $864 \mu\text{g}/\text{kg} (\mu\text{g}/\text{L})^{-1}$ ) was higher compared to the one of natural soils (334 352 and  $33 \mu\text{g}/\text{kg} (\mu\text{g}/\text{L})^{-1}$ , data reported for soil in decreasing TOC order). When results were normalised to the organic fraction content, isotherms were well homogenised for natural soil sample, whereas humin instead maintained a distinct profile. Moreover, desorption hysteresis of BDE-15 from humin was not pronounced as it was for natural soil samples. That led authors at the conclusion that the structure and chemistry of SOM are the dominant factors influencing BDE-15 sorption and desorption in soil and the accumulation of BDE-15 in soil is mainly regulated by SOM fraction other than humin.

One of the main differences between natural soil samples and humin samples is the absence or presence of the soluble fraction of SOM. Indeed humin has been obtained from natural soil eliminating calcium carbonate and SOM soluble fractions (i.e. humic and fulvic acids) through basic and acidic washing. The influence of the dissolvable fraction of soil organic matter in the sorption and desorption process is an aspect not considered by authors and might be worthy to be investigated. Dissolved phases such as humic acids, proteins, and surfactants have been found to contribute significantly to the mass transfer of PCBs (from bi- to octa- chlorinated congeners) and PBDEs (from penta- to hepta-brominated congeners) from polymer phase to aqueous medium (Ter Laak et al., 2009). In the experiment conducted by Ter Laak and co-workers, fused silica fibres coated with polydimethylsiloxane were loaded with PCBs and PBDEs and then exposed to water solution with increasing dissolved organic carbon content (DOC) (0 2.4 11.8 47.1 and 118 mg/L). The depletion of chemicals in these five DOC solutions over two months was directly proportional to the amount of DOC in water. Additionally, Badea and co-workers (Badea et al., 2014) found that leachability of PCBs from soils samples increased with increasing pH and correlated with increases in TOC content in leachates.

## **2.2 BDE-209 biodegradation**

Despite the growing number of environmental studies on PBDEs, much is still unknown about their reactivity (Ghanem and Delmani 2012). Information on biotransformation of BDE-209 in soil and sediment are still limited at present (Shi et al., 2013). One of the major

concerns is the formation of lower brominated compounds which are more toxic, persistent, bioavailable and susceptible to long range transport (Gandhi et al., 2011; Uhnáková et al., 2009). A study on contaminated sludge incubated under aerobic and anaerobic conditions reported no significant BDE-209 degradation over 160 and 200 days respectively (Nyholm et al., 2010). This is consistent with the half-life of BDE-209 in anaerobic sludge calculated as about 700 days (Gerecke et al., 2006) and the persistence (20 years) of BDE-209 in soil amended with contaminated sewage sludge (Sellström et al., 2005). On the other hand, results produced by experimental studies designed for exploring the possibility to use biological treatment for soil remediation show that biological activity in soil might be potentially responsible for BDE-209 debromination and degradation.

### 2.2.1 Bacteria biodegradation

Studying degradation processes under optimised laboratory conditions (controlled temperature, nutrient addition, and constant media homogenisation.) allowed for the identification of several bacteria species able to debrominate highly brominated PBDE congeners in both aerobic and anaerobic conditions (Deng et al., 2011; Gerecke et al., 2005; He et al., 2006; Lee and He, 2010; Qiu et al., 2011; Rayne et al., 2003; Robrock et al., 2008; Shi et al., 2013; Tokarz et al., 2008; Yen et al., 2009). The complete mineralisation of BDE-209 involves the scission of the aromatic ring and the ether bond, both of which are considered difficult to be degraded by bacterial enzymatic reactions (White et al., 1996). Only a few studies reported proper mineralisation of BDE-209 through bacteria biodegradation. Bacteria populations isolated from environmental samples (sediments or waste treatment plant sludge) inoculated on montmorillonite produced degradation to smaller aromatic compounds when BDE-209 was the sole carbon source (Chou et al., 2013); Complete mineralisation of BDE-209 was observed in liquid culture containing *Bacillus cereus* JP12. Interestingly, the mineralisation efficiency results were sensitive to BDE-209 initial concentration. 38 % of BDE-209 was mineralised when starting from a concentration of 1 mg/L while only 13 % of BDE-209 was mineralised when starting from a concentration of 20 mg/L. The difference was possibly due to the formation of toxic intermediate by-products (Lu et al., 2013). Finally *Sphingomonas sp. PH-07* isolated from activated sludge of a wastewater treatment plant was found able to open and completely mineralise 1g/L of diphenyl ether in liquid cultures within 6 days (Kim et al., 2007).

### 2.2.2 Biodegradation in the soil –plant system

Interest is growing in the study of BDE-209 behaviour in the soil-plant system. Six different plant species proved to have effects on debromination and hydroxylation of BDE-209 in soil and an accumulation of deca-BDE and its degradation by-products in roots and shoots was observed (Huang et al., 2009). A comparative study on maize plant uptake, translocation and metabolism of PBDEs and PCBs showed that PBDEs had higher accumulation in roots and were more susceptible to be metabolised compared to PCBs (Wang et al., 2011b). BDE-209 debromination was observed in rhizobox experiment with ryegrass. Twelve and twenty-four lower brominated PBDEs were detected in soil and plant samples, respectively. Colonisation of ryegrass roots with an arbuscular mycorrhizal fungus increased the levels of lower brominated PBDEs taken up by ryegrass (S. Wang et al., 2011a).

### 2.2.3 White rot fungi

Biological treatments are attracting more and more attention due to their low cost and environmentally benign nature (Shi et al., 2013). Beside the use of bacteria, a serious interest in using fungi for bioremediation purposes started to develop in the last 20 years. This interest is justified by one peculiar characteristic of fungi: they release extracellular enzyme and use them as a strategy to degrade nutrients before their uptake and detoxify their growing environment from pollutants. Therefore recalcitrant contaminants in soil can be degraded even in case they are not used as carbon sources forming secondary metabolites (Barr and Aust, 1994).

Particular attention has been given to wood-decay fungi, which have such a strong degradation capacity that enables them to digest wood. They may be divided in three categories: Brown-rot fungi, Soft-rot fungi (which only decompose cellulose), and White-rot fungi (which are able to decompose also the complex molecule of lignin). (Tortella et al., 2005). The process of lignin degradation of white rot fungi is not totally understood. As it is currently known, the extracellular enzymes involved in lignin degradation are: laccase, lignine peroxidase (LiPs, "ligninase"), manganese peroxidase (MnPs, "Mn-dependent peroxidases") and versatile peroxidases (VPs) (Esser 2010). Thanks to action of these enzymes, some white rot fungi species like *Phanerochaete chrysosporium*, *Trametes versicolor*, *Pleurotus ostreatus*, *Coriolopsis polyzona*, *Pleurotus pulmonarius* have

demonstrated the ability to degrade or oxidize a variety of recalcitrant pollutants like munitions waste (2,4,6 trinitrotoluene and several dinitrotoluenes), organochlorine pesticides (DDT, PCBs), Polycyclic aromatic hydrocarbons, synthetic polymers (PVC, PVA, nylon, wood preservatives (creosote and pentachlorophenol (Bumpust and Austt, 2008; Durán and Esposito, 2000; Field et al., 1992; Machado et al., 2005; Pallerla and Chambers, 1998; Pointing, 2001; Stahl and Aust, 1995; Vitali et al., 2006).

The few studies investigating the feasibility of BDE-209 degradation through white rot fungi are here reported. A fungus belonging to the white rot fungi family, species not better specified, has been tested in liquid culture. The effects of two solubilising agents (Tweed 80 and  $\beta$ -cyclodextrine) on mycelia growth and BDE-209 transformation were investigated. In absence of solubilising agents, the amount of BDE-209 decreased by 42%, passing from 1.6 mg/L to 0.92 mg/L in 10 days. In the presence of Tweed 80, the degradation increased to 96 % and no traces of BDE-209 were found after 12 days.  $\beta$ -cyclodextrine enhancing capability on BDE-209 degradation was less than Tweed 80, but, differently from Tweed 80, it promoted mycelia growth (Zhou et al., 2007). More recently, *Phlebia lindtneri* degradation of BDE-209 was investigated under the influence of glucose and heavy metals (Cd, Cu or Pb) that are potent inhibitors of enzyme reactions. The fungus degraded BDE-209 in liquid cultures through debromination, hydroxylation and ring-opening reaction following the biodegradation pathway suggested in Figure 2.1. In the absence of heavy metals, 77.3% BDE-209 was degraded within 30 days from a starting concentration of 20 mg/L BDE-209.



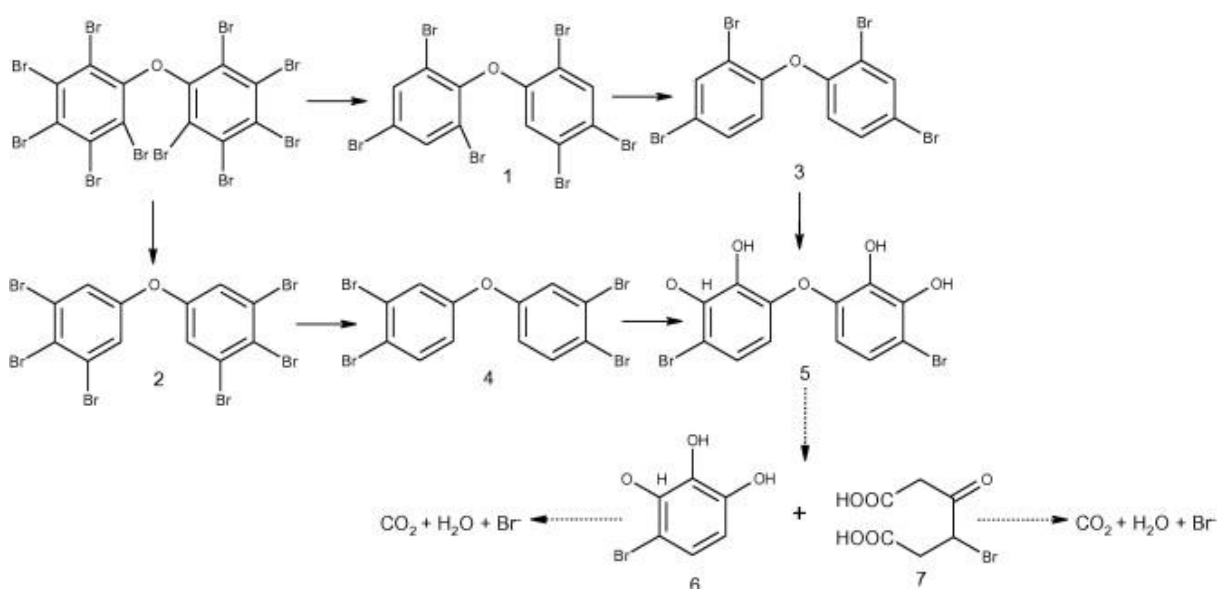


Figure 2.1: Possible aerobic BDE-209 biodegradation pathway by *P. Lindtneri* JN45. Dotted arrows indicate involvement of more than one step. Adapted from (Xu and Wang, 2014).

The main enzyme involved in BDE-209 degradation is laccase, a nonspecific polyphenol oxidase able to oxidise a variety of substrates including polyphenols, methoxy-substituted phenols and diamines (Baldrian & Gabriel 2002). The influence of heavy metals on biological activity is important considering that PBDE contamination in e-waste recycling regions is usually accompanied by the presence of high concentrations of heavy metals (Xu and Wang, 2014). The presence of Cd and Pb did not inhibit the extracellular laccase activity at concentration below 2 mg/L; Cu concentration below 5 mg/L increased laccase activity and no adverse effects were noticed up to 10 mg/L. With the addition of glucose, a 2.2-fold increase in laccase activity was noticed.

Within the family of white rot fungi, *Pleurotus ostreatus* is commercially cultivated and its fruiting bodies are grown and sold as oyster mushrooms for human consumption (Hestbjerg et al., 2003). From this production, a large amount of refuse substrate colonised by fungus mycelia known as SMC (spent mushroom compost) is available (Hestbjerg et al., 2003). In the mushroom industry, about 5 kg of refuse SMC is generated for the production of 1 kg of mushroom (Lau et al., 2003). The use of *P. ostreatus* SMC for bioaugmentation purposes in contaminated soil showed promising potential. After nine weeks, concentrations of 3-, 4-, 5-, 6-ring PAHs in soil were reduced by 78, 41 and 4 %, respectively, in coal tar-contaminated soil amended with SMC in field conditions (Hestbjerg et al., 2003). Creosote

contaminated soil mixed with SMC and fish oil incubated for 7 weeks at ambient temperature resulted in the following PAH removal: 89% 3- rings PAHs, 87% 4- rings PAHs, 48% 5-rings PAHs (Eggen, 1999). A study comparing the degradation ability of different white rot fungi (*Phanerochaete chrysosporium*, *Trametes versicolor* and *Pleurotus ostreatus*) found that only *P. ostreatus* was able to degrade low chlorinated polychlorinated biphenyl (commercial mixture Delor 103) in soil. In two months, about 40 % of Delor 103 was removed (Kubátová et al., 2001). Moreover, *P. ostreatus* has been successfully tested in field-scale studies for the remediation of soil contaminated by pentachlorophenol (99.9 % degradation), 2,4,6 trinitrotoluene (98% degradation), polychlorinated dibenzodioxins and dibenzofurans (69% reduction in the toxic equivalent) (Steffen and Tuomela, 2010).

There are no studies investigating *P. ostreatus* degradation of BDE-209 either in liquid cultures or field test. Nevertheless *P. ostreatus* lignin degradation mechanism relies on the action of laccase the same enzyme responsible for BDE-209 degradation by *Phlebia lindtneri* (Bezalel et al., 1996) and the enzymatic mechanism involved in phenanthrene mineralisation by *P. ostreatus* (Figure 2.2). BDE-209 degradation by *Phlebia lindtneri* present strong similarities (Figure 2.1).

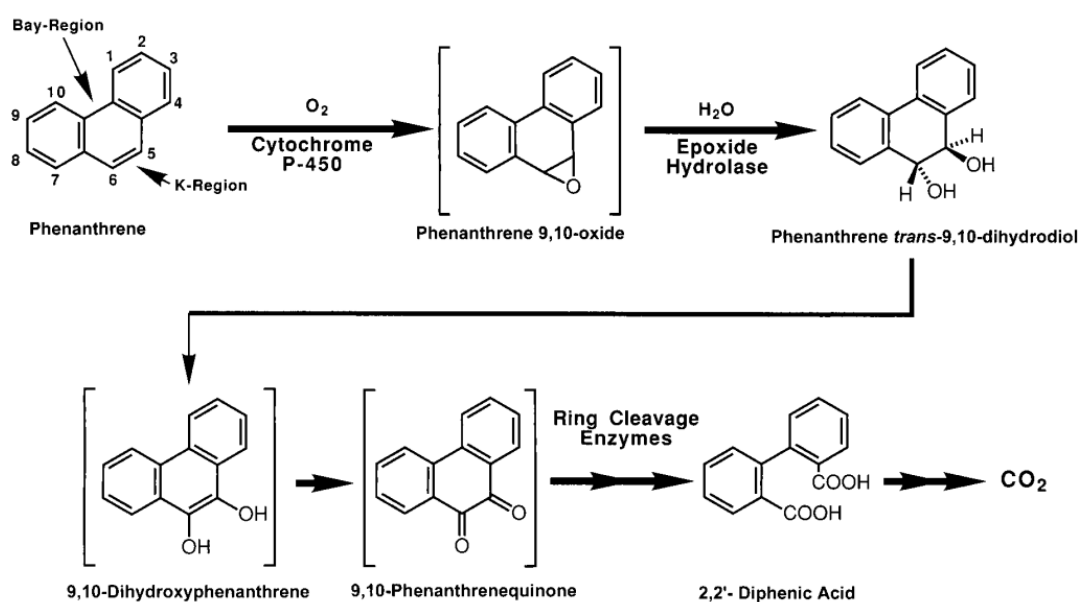


FIG. 4. Proposed pathway for phenanthrene degradation by *P. ostreatus*.

Figure 2.2: Proposed pathway for phenanthrene degradation by *P. ostreatus*. Adapted from (Bezalel & Hadar 1997).

### 2.3 Summary and key findings

So far no experimental data have been produced for studying BDE-209 sorption and desorption processes in soil. Literature available for lower brominated PBDEs shows that SOM is the main factor influencing sorption processes. Changing of SOM structure and properties results in different PBDE sorption kinetics and desorption hysteresis. A possible reason is the different diffusion rates that PBDEs might undergo in soil organic matter with different densities. Recently the presence of dissolved organic carbon in water started to be considered as another important factor affecting partitioning and sorption processes of hydrophobic organic compounds. Investigating these aspects with respect to BDE-209 sorption processes would help in gaining a better understanding of environmental fate of BDE-209, its mobility and bioavailability.

According to the literature on BDE-209 here reported, BDE-209 might be affected by the biological activity in soil. Bacteria as well fungi are potentially able to debrominate and in some cases degrade and mineralise BDE-209. Deeper knowledge of BDE-biodegradation is essential for evaluating BDE-209 fate in soil and the possible secondary emission of lower brominated PBDEs. An important application regarding the implementation of bioaugmentation techniques for remediation of PBDE polluted soil. From this perspective, *P. ostreatus* is particularly interesting and the large amount of spent mushroom compost produced for commercial cultivation of *P. ostreatus* would provide a cheap substrate to be employed in bioaugmentation.

### 3 Equilibrium partitioning and sorption models

Adsorption and absorption of chemicals on soil particles are complex phenomena which include diffusion (e.g. in the bulk water, pore water and soil organic matter) and partitioning (e.g. between solid surfaces and the surrounding water). In this chapter concepts behind the partitioning and sorption mechanisms and models developed for describing sorption of chemicals in soil particles are resumed. The aim is to provide the necessary background for better understanding discussion on BDE-209 sorption in soil addressed in chapter 2 and 7.

#### 3.1 Equilibrium partitioning

##### 3.1.1 Partitioning coefficient $K_d$ and sorption isotherms

In the soil-water bi-phase system, the ratio of a chemical's concentrations in soil and water phase at equilibrium is defined as partitioning coefficient  $K_d$ :

$$K_d = \frac{q_e}{c_e} \quad \text{Eq. 3.1}$$

where  $q_e$  is the total sorbate concentration in soil ( $\text{mol}\cdot\text{kg}^{-1}$ ) and  $c_e$  is the total chemical concentration in water ( $\text{mol}\cdot\text{L}^{-1}$ ). Fixed soil type and chemical,  $K_d$  still depends on several system parameters (e.g. temperature, water salinity etc.). When all these parameters are constant,  $K_d$  might still vary with the overall chemical concentration in the system. The relationship between concentration in soil and water is therefore generally described by a curve which is referred to as sorption isotherm (Schwarzenbach, 1993). Experimentally isotherm curves are commonly fitted with Freundlich isotherm equation:

$$q_e = K_F c_e^n \quad \text{Eq. 3.2}$$

where  $K_F$  is the Freundlich constant or sorption capacity and  $n$  is the Freundlich linearity coefficient. Inserting  $K_d$  Equation 3.1 in Equation 3.2 it yields to a new  $K_d$  expression

$$K_d = K_F c_e^{n-1} \quad \text{Eq. 3.3}$$

$K_d$  is constant when Freundlich isotherms present a linear profile ( $n=1$  in Eq. 3.3) or when the relative concentration variation  $dc_e/c_e$  is so small that the relative  $K_d$  variation  $dK_d/K_d$  is also small (Eq. 3.4).

$$\frac{dK_d}{K_d} = (n - 1) \frac{dc_e}{c_e} \quad \text{Eq. 3.4}$$

An alternative model used to fit sorption isotherms is the Langmuir isotherm.

$$q_e = \frac{Q_L b c_e}{1 + Q_L c_e} \quad \text{Eq. 3.5}$$

where  $Q_L$  and  $b$  are the monolayer adsorption capacity and equilibrium constant, respectively. Langmuir isotherm is a constant energy limited surface model initially developed for gas phase sorption based on the assumption of monolayer coverage of the adsorption surface and equivalence and independence of sorption sites. Coherently with these hypotheses, linear isotherms are not contemplated in the Langmuir model.

### 3.1.2 Parametric description of $K_d$ and $K_{om}$

The parametric description of  $K_d$  better capture the heterogeneous nature of soil and therefore the complex nature of  $K_d$  that is generically described as the combined contribution of different factors representing different soil matrixes and different analyte forms:

$$K_d = \frac{C_{om} f_{om} + C_{min} \cdot A + C_{ie} \cdot \sigma_{ie} \cdot A}{C_{w,neut} + C_{w,ion}} \quad \text{Eq. 3.6}$$

where  $C_{om}$  is the concentration of sorbate associated with the natural organic matter ( $\text{mol} \cdot \text{kg}^{-1}$ ),  $f_{om}$  is the weight fraction of solid which is natural organic matter ( $\text{kg om} \cdot \text{kg}^{-1}$  solid),  $C_{min}$  is the concentration of sorbate associated with the mineral surface ( $\text{mol} \cdot \text{m}^{-2}$ ),  $A$  is the area of mineral surface per mass of solid ( $\text{m}^2 \cdot \text{kg}^{-1}$ ),  $C_{ie}$  is the concentration of ionised sorbate drawn toward positions of opposite charge on solid surface ( $\text{mol} \cdot \text{mol}^{-1}$ ),  $\sigma_{ie}$  is the net concentration of suitably charged sites on the solid surface ( $\text{mol surface charges} \cdot \text{m}^{-2}$ ),  $C_{w,neut}$  is the concentration of uncharged chemical in solution ( $\text{mol} \cdot \text{L}^{-1}$ ) and  $C_{w,ion}$  is the concentration of the charged chemical in solution ( $\text{mol} \cdot \text{L}^{-1}$ ). Depending on analyte and soil

composition, it is possible that some terms deserve further subdivisions (e.g. several mineral surfaces can be involved) and other terms might not be relevant (e.g. ionised term for not ionisable compounds). In regards to HOC, they tend to interact much more easily with soil organic matter that provides a relatively non polar environment rather than with the polar mineral particles. Therefore, as long as  $f_{om}$  is “significant”, the partitioning coefficient composite formulation can be approximated with Equation 3.7.

$$K_d = \frac{C_{om} \cdot f_{om}}{c_e} \quad \text{Eq. 3.7}$$

Defining the organic matter-water partitioning coefficient ( $K_{om}$ ) as the ration between the sorbate concentration in the SOM ( $C_{om}$ ) and water ( $C_e$ )

$$K_{om} = \frac{C_{om}}{c_e} \quad \text{Eq.3.8}$$

A new expression for the soil-water distribution ratio is obtained

$$K_d = f_{om} \cdot K_{om} \quad \text{Eq.3.9}$$

It is difficult to quantify which is the “significant” value for  $f_{om}$  at which the contribution of the soil matrixes other than organic matter is negligible and this approximation is sensible. Indeed it depends on both analyte and soil properties. Nevertheless normalising  $K_d$  to the organic matter content in soil is particularly useful for comparing  $K_d$  measured for the same analyte in soil with different  $f_{om}$

### 3.1.3 The linear free energy relationship for $K_{om}$ estimate

To relate the partitioning constants for the same chemical in different systems, considerably efforts have been done for estimating partition constants from the chemical structure and property of the analyte (structure-property relationship). These relationships are known under the name of Linear Free Energy Relationships (LFERs). In first approximation, simple LFERs depending on few well known analyte properties might be considered. In particular, under the assumption that for HOC variations in chemical activity in water ( $\gamma_w$ ) are much greater than in the organic matter ( $\gamma_{om}$ ), variations in  $K_{om}$ , from

chemical to chemical, principally arise from differences in chemical activity in water ( $\gamma_w$ ) which is directly related to chemical solubility. Therefore water solubility seems to be a useful property for estimation of  $K_{om}$  for HOC. The LFER derived for various set of chemicals has this form (Schwarzenbach et al., 1993a)

$$\log K_{om} = -a \cdot \log(c_{sat}) + b \quad \text{Eq. 3.10}$$

Where  $C_{sat}$  is saturation concentration,  $a$  and  $b$  are constants. Since a correlation has been found between  $K_{om}$  and  $C_{sat}$ , then any other chemical property which is related to  $C_{sat}$  could be related directly to  $K_{om}$ . For example  $K_{ow}$  (octanol-water partitioning coefficient), which also is inversely related to  $C_{sat}$  (Equation 3.11), is directly related to  $K_{om}$  as shown in Equation 3.12.

$$\log K_{ow} = -a \cdot \log(c_{sat}) + b \quad \text{Eq.3.11}$$

$$\log K_{om} = c \cdot \log K_{ow} + d \quad \text{Eq. 3.12}$$

Where  $c$  and  $d$  are constants. That provided a useful tool for  $K_{om}$  estimation from more standardised chemical properties like water solubility of octanol-water partitioning coefficient. In the last 20 years, the LFERs theory evolved and recently, more complex and accurate formulations for LFERs are considered. For example a polyparameters linear free relationships (pp-LFERs), which capture much better the complexity of the sorption phenomenon, have been used to predict octanol-water partitioning coefficient ( $K_{ow}$ ) for 40 flame retardant chemicals. The pp-LFERs proposed considers instead of the single water solubility the following sorbent and sorbate parameters: hexane/air partitioning coefficient, polarizability, H-bond donor properties, H-bond acceptor properties and molar volume (Stenzel et al., 2013).

### 3.1.4 Thermodynamic interpretation of $k_d$ : the fugacity concept

In single phase systems, mass diffuses according to the gradient concentration. The equilibrium condition is reached when the entropy of the system is maximised which corresponds to a homogeneous distribution of analyte in the system. The mass flow generated to reach the equilibrium condition ( $J_x$ ) is usually expressed by Fick's law, which in one dimension has the following formulation

$$J_x = -\frac{\partial C}{\partial x} \quad \text{Eq.3.13}$$

In multiphase systems at equilibrium analyte concentration in different phases are different and the partitioning coefficient previously discussed is nothing else than a measure of the concentrations when equilibrium is reached. The transfer of mass from different phases is ruled by the same thermodynamic principle of maximisation of entropy. That corresponds to the equalisation of the chemical potential, which in a real multiphase system is reached when fugacity values in all the phases are equalised. Therefore the mass flow will be guided by fugacity gradient rather than by differences in chemical concentration (Mackay, 1979).

The fugacity of a chemical ( $f$ , in units of Pascal) for a given phase is related linearly to its molar concentration ( $C$  in  $\text{mol}\cdot\text{m}^{-3}$ ) by the fugacity capacity ( $Z$ ,  $\text{mol}\cdot\text{m}^{-3}\cdot\text{Pa}^{-1}$ ) of the phase in which the chemical is solubilised.

$$f = C/Z \quad \text{Eq. 3.14}$$

In a multiphase system at equilibrium, since fugacity values in all phases are the same, the concentration in each phase will be inversely proportional to the fugacity capacity for the sorbate for each phase. Therefore, knowing the fugacity capacity of sorbate in each phase, it is possible to predict the sorbate concentration in each phase at equilibrium (Mackay, 1979). In ideal conditions, following from ideal gas law, the fugacity capacity in air for all compounds is equal to

$$Z_A = \frac{C}{f} = \frac{n}{VP} = \frac{1}{RT} \quad \text{Eq.3.15}$$

where  $n$  is mol,  $V$  is volume in  $\text{m}^3$ ,  $P$  is pressure in Pa,  $R$  is the gas constant and  $T$  is temperature in Kelvin (Mackay, 1979). In water, fugacity capacity ( $Z_w$ ) is inversely proportional to the chemical's Henry's law constant

$$Z_w = C/f = C/HC = 1/H \quad \text{Eq.3.16}$$

where  $H$  is the Henry's law constant in  $\text{Pa}\cdot\text{m}^3\cdot\text{mol}^{-1}$  (Mackay, 1979). For a sorbed phase, the fugacity capacity ( $Z_s$ ) is calculated as a product of sorption partitioning coefficient  $K_d$  and  $Z_w$



$$Z_S = 10^{-6} \cdot K_d \cdot \rho_S \cdot Z_W = 10^{-6} \cdot K_d \cdot \rho_S / H \quad \text{Eq.3.17}$$

where  $K_d$  is the partitioning coefficient in  $(\text{g}\cdot\text{Mg}^{-1})\cdot(\text{g}\cdot\text{m}^{-3})^{-1}$  and  $\rho_S$  is the sorbent density in  $\text{g}\cdot\text{m}^{-3}$  (Mackay, 1979).

## 3.2 Models describing sorption mechanism in soil particles

Many models have been developed to represent sorption of HOC to suspended sediment and soil particles. While some of them are mainly empirical, some others are based on physical/chemical processes. The most general of models rely on thermodynamic description of the system. Here are summarised three of the most used ones explaining the principles behind them.

### 3.2.1 Distributed reaction model (DRM)

The simplest model of HOC sorption in soil is the one box model that considers sorbent particles as a homogenous box characterised by a single kinetic profile driving the sorption reaction and resulting in a single equilibrium partitioning coefficient ( $K_d$ ). (Wu and Gschwend, 1986). The Distributed Reaction Model (DRM) developed by Weber, Pignatello, Young, Xing and LeBeouf and co-workers (Huang et al., 1996; McGinley et al., 1993; Weber et al., 1992) can be considered a sort of multi-box model. Its principal assumption is that soil consists of areas with different sorption reactivity and therefore, soil particles can be represented as a multi-compartment sorbent. The overall sorption reaction is a combination of the single sorption phenomena in the different compartments. The model is formulated as a series of linear and nonlinear adsorption reactions (Equation 3.18).

$$q_{e,T} = \sum_{i=1}^k (q_{e,L})_i + \sum_{i=1}^m (q_{e,NL})_i = \sum_{i=1}^k x_{Li} K_{D_i} C_e + \sum_{i=1}^m x_{NLi} K_{F_i} C_e^{n_i} \quad \text{Eq. 3.18}$$

where  $q_{e,T}$ ,  $q_{e,L}$ , and  $q_{e,NL}$  refer to the total, linear contribution and nonlinear contribution solid-phase concentrations respectively;  $k$  is the number of distinguishable linear components;  $x_{Li}$  is the mass fraction of the  $i$ th linearly sorbing component;  $m$  is the number of distinguishable nonlinear components (typically be only 1 or 2);  $x_{NLi}$  is the mass fraction of the  $i$ th nonlinearly sorbing component;  $K_{D_i}$  is the partitioning coefficient for

reaction  $i$  expressed per mass of component  $i$ ;  $K_{F_i}$  and  $n_i$  are the Freundlich capacity factor and the Freundlich exponent for the  $i$ th component, respectively; and  $C_e$  is the residual solution-phase concentration of solute at equilibrium.

For describing the nonlinear reactions Freundlich model has been used for two reasons: (1) because of the heterogeneous characteristic of soil, Langmuir behaviour is rarely observed even in the most homogenous of soils and (2) a linear combination of Langmuir isotherms yields a composite Freundlich isotherm. Therefore, when multiple Langmuir reactions happen simultaneously, even if individually distinguishable, they globally result in a Freundlich like isotherm (Weber et al., 1992).

The DRM model demonstrates to be a valid alternative to Freundlich isotherms in fitting experimental HOC sorption isotherms (Weber et al., 1992); Using the DRM approach in combination with Ideal Adsorption Solution Theory (IAST), mixed-solutes competitive effects have been predicted from single-solute sorption isotherms (McGinley et al., 1993). Additionally as prove of the multi-compartmental character of the sorption phenomena, it has been found that expanded and condensed organic matter (corresponding to different degree of diagenetic alteration) shows different sorption isotherms profiles. This proves that organic matter composition varies and does not have the same capacity and affinity for a particular HOC, thus the sorption energy for the same compound can change regarding the SOM structure and the solid-phase loading level. That represents a possible explanation even for the variations registered in the normalized organic carbon partition coefficient, which is not justifiable by single compartment models (Young and Weber, 1995). Finally they extended the DRM to non-equilibrium conditions, studying phenanthrene sorption isotherms at different reaction time (from 1 minute to 14 days). They observed that Freundlich parameters show dependence on time: after a short initiation stage, the Freundlich capacity factor increase with a logarithmic profile and similarly the Freundlich coefficient decreases (Figure 3.1b). This dependence of the sorption parameters on time suggested changes in dominant sorption mechanisms over time, confirming the multi-compartmental approach of DRM.

Based on geochemistry and soil science observation along with previous finds about variation of SOM affinity to HOC with SOM structure and diagenetic degradation, the authors finally simplified the general multi-compartment DRM model postulating a three-

domain model composed by the exposed inorganic mineral surface (domain I), the amorphous SOM (domain II) and a condensed SOM (domain III) (Figure 3.1). Sorbate molecules migrating through the amorphous SOM phase penetrate faster following Fick's law presenting a diffusion coefficient ( $D$ ) concentration-independent and a mass transfer symmetrical with respect to forward and direct direction (no hysteresis in sorption-desorption cycles). Whereas when sorbate molecules meet the glassy phase slower nonlinear isotherms, concentration dependent- $D$  and sorption-desorption hysteresis are expected (Pignatello and Xing, 1995).

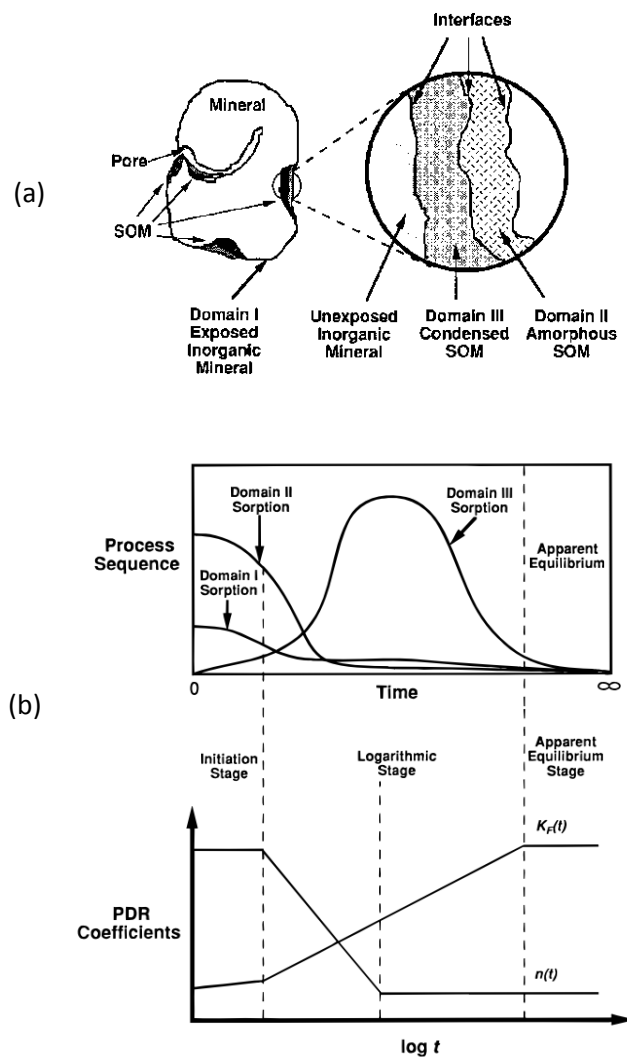


Figure 3.1: Panel (a): the three domains (inorganic mineral, condensed SOM and amorphous SOM) identified in soil particles by the three domains DRM model. Panel (b): variation in time of the Freundlich isotherm parameters, sorption capacity ( $K_f$ ) and Freundlich coefficient ( $n$ ) reflects the variation of the predominant domain responsible for the sorption process.

The ultimate argument in support of the DRM model is the existence of a glass transition temperature ( $T_g$ ) for SOM constituents. For polymers the  $T_g$  is defined as the temperature region where the polymer transitions from a hard, glassy material to a soft, rubbery material. The existence of  $T_g$  for SOM justifies the existence of two SOM fractions: one condensed characterised by slow sorption and one amorphous with soft-rubbery characteristics and faster sorption profiles. That create an important analogy between the organic matter and polymer; analogy which is well reflected in the similarity between the DRM model and the model proposed by polymer scientists (Equation 3.19) for describing the combined rubbery and glassy sorption behaviour of chemically homogenous polymers (LeBoeuf and Weber, 1997).

$$q_{e,T} = q_{e,L} + q_{e,NL} = K_{D,C}C_e + \frac{Q_a^0 b C_e}{1 + b C_e} \quad \text{Eq.3.19}$$

where  $q_{e,T}$ ,  $q_{e,L}$ , and  $q_{e,NL}$  refer to the total, linear contribution and nonlinear contribution solid-phase concentrations respectively;  $K_{D,C}$  is the distribution coefficient of the linear component;  $Q_a^0$  is the saturation concentration of the adsorbed phase of a homogenous site-limited sorption domain;  $b$  is a coefficient related to the enthalpy of sorption in that domain; and  $C_e$  is the residual solution-phase concentration of solute at equilibrium.

The polymer model features two simplifications of the more general DRM. Firstly, the mineral domain is assumed negligible so that a single partitioning reaction for the rubbery domain accounts for all of the linear components. Secondly, the nonlinear sorption reaction by glassy SOM domain is assumed to be a single Langmuir type partitioning with site-limited and relatively constant energy processes. In contrast, the DRM represents both mineral and rubbery SOM domains as linear components as well as multiple reactions involving different sites at different energies with Freundlich profiles that result from sums of series of Langmuir profiles. Under this perspective, the polymer model in Equation 3.19 suits the description of soil and sediment particles when only domain II and II are considered. This simplified version of the DRM has been named Dual Reactive Domain Model (DRDM) (LeBoeuf and Weber, 1997).

### 3.2.2 Sorption Related Pore Diffusion model (SRPD)

The diffusion model approaches the sorption kinetics of HOC into soil particles from a different perspective. The Sorption Related Pore diffusion (SRPD) model described the sorption phenomena by a radial diffusive penetration model modified by a retardation factor that reflects micro-scale partitioning of sorbate between intra-aggregate pore fluids and the solids making of the aggregate grains (Wu and Gschwend, 1986). Similarly to DRM, the sorption reactions are considered a mass transfer limited process rather than a chemisorption process (Schwarzenbach et al., 1993b). In contrast to DRM, which has an empirical origin, the diffusion model describes the sorption phenomena based on known physical and chemical processes (Wu and Gschwend, 1986). The model identifies the molecular diffusion into pore water, retarded by a chromatographic-like local sorption on pore walls as the main limiting factor.

The time required for a molecule to reach the sorptive sites can be conceptualised as a sequence of three steps: (i) the time ( $\tau_1$ ) required for the sorbate particles to diffuse through the thin layer of stagnant solution surrounding the soil aggregate or loose particles, (ii) the time ( $\tau_2$ ) required for migration into the open pores within the soil aggregate (inter particles pores), and (iii) the time ( $\tau_3$ ) required to penetrate the intra particles pores (e.g. inter-layer space of clay minerals, dead-end pores of mineral particles or SOM).  $\tau_1$  is usually in the order of seconds. For instance, considering a layer thickness (L) of 200  $\mu\text{m}$ , BDE-209 molecular volume (V) of 427.5  $\text{cm}^3 \cdot \text{mol}^{-1}$  (Yue and Li, 2013), the time  $\tau_1$  can be calculated with Equation 3.20, where  $D_w$  is the molecular diffusion coefficient in water calculated with Equation 3.21 (Schwarzenbach et al., 1993b)

$$\tau = \frac{L^2}{2D_w} \quad \text{Eq. 3.20}$$

$$D_w = \frac{2.3 \cdot 10^{-4}}{V^{0.71}} \quad \text{Eq. 3.21}$$

The resulting  $\tau_1$  for BDE-209 particles therefore is equal to 64 seconds, which is negligible considering the time required for approaching the sorption equilibrium for BDE-209 into clay or peat is in the order of magnitude of hours or days. Time  $\tau_2$  is important when unperturbed soil is considered and soil structure is maintained intact, but it becomes irrelevant under conditions of batch tests where soil particles and aggregates are suspended in the water solution. Therefore, time  $\tau_3$  (related to the time required for

sorbate molecules to penetrate in soil aggregate and reach the active sorptive site) plays the major role in the overall process. The physical model is developed to describe the retarded diffusion into intra-particle pore water assuming that the entire surface area is available for mass flux and the pore length of diffusive transfer is equal to the particle radius  $r$  and soil particle is schematised as shown in Figure 3.2. Under these initial assumption the physical model as the form shown in equation 3.22 (Schwarzenbach et al. 1993, Wu & Gschwend 1986).

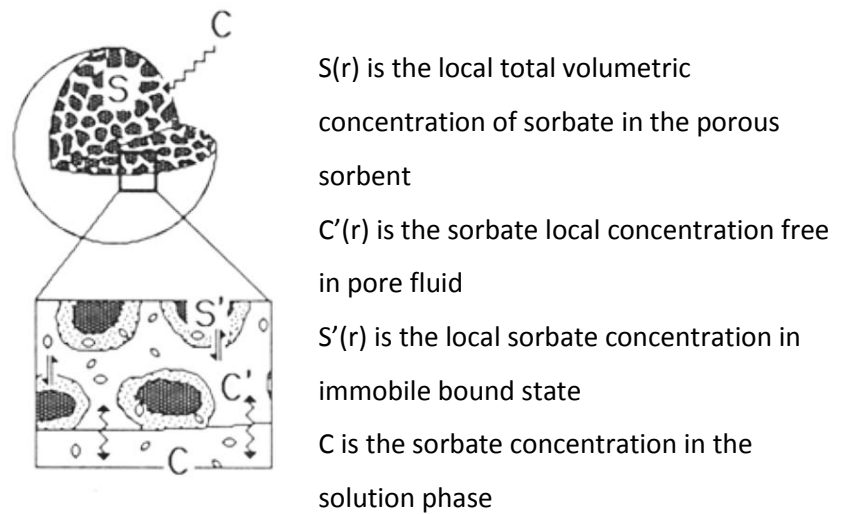


Figure 3.2: Schematic representation of a soil particle as modelled in the chemisorption model. Adapted from (Wu and Gschwend, 1986).

$$\frac{\partial S(r)}{\partial t} = D_w n f \left[ \frac{\partial^2 C'(r)}{\partial r^2} + \frac{2}{r} \frac{\partial C'(r)}{\partial r} \right] \quad \text{Eq. 3.22}$$

where  $S(r)$  is the local total volumetric concentration of sorbate in the porous sorbent,  $C'(r)$  is the sorbate local concentration free in pore fluid,  $r$  is particles radius,  $n$  is the particle porosity,  $D_w$  is analyte molecular diffusivity in water and  $f$  is a tortuosity factor. Indeed diffusion of analyte particles in the pore water will result delayed in reason of the irregularity of pores obstructing analyte diffusion.

When local equilibrium is reached,  $S'(r)$  can be expressed in function of  $C'(r)$  through the equilibrium partitioning coefficient  $K_p$ :

$$S'(r) = K_p C'(r) \quad \text{Eq. 3.23}$$

By definition,  $S(r)$  is a combination of the sorbate bound to the immobile state and sorbate in solution:

$$S(r) = (1 - n)\rho_s S'(r) + nC'(r) \quad \text{Eq. 3.24}$$

where  $n$  and  $\rho_s$  are the porosity and specific gravity of the sorbent. Substituting Equation 2.23 into Equation 3.24, the variation of  $S(r)$  in function of the sorbent properties and  $C'(r)$  is obtained:

$$S(r) = C'(r)[(1 - n)\rho_s K_p + n] \quad \text{Eq. 3.25}$$

Incorporating Equation 3.25 in Equation 3.22, intra-particle diffusion kinetics can be expressed in function of  $S$  only:

$$\frac{\partial S(r)}{\partial t} = \frac{D_w n f}{(1-n)\rho_s K_p + n} \left[ \frac{\partial^2 S(r)}{\partial r^2} + \frac{2}{r} \frac{\partial S(r)}{\partial r} \right] \quad \text{Eq. 3.26}$$

$$D_{eff} = \frac{D_w n f}{(1-n)\rho_s K_p + n} \quad \text{Eq. 3.27}$$

Where  $D_{eff}$  is the effective intra-particle diffusivity ( $\text{cm}^2/\text{s}$ ) that, when  $K_p$  is large (true for hydrophobic compounds) can be approximated as:

$$D_{eff} = \frac{D_w n f}{(1-n)\rho_s K_p} \quad \text{Eq. 3.28}$$

Knowing the compound properties (diffusivity in solution and hydrophobicity) and those of the natural sorbents (organic content, particle size, density and porosity), the model has been found suitable for predicting sorption kinetic for various chemical and/or site of interest (Wu and Gschwend, 1986).

### 3.2.3 Thermodynamic Potential Theory

Another approach used to describe sorption of chemicals into soil recalls the thermodynamic potential theory. The concept of adsorption potential ( $\epsilon$ , cal/mol) developed by Polanyi (1914) is defined as the work done by the adsorption forces in the

transference of an adsorbate molecule from the bulk gas to a point in the surface phase. Since the forces of attraction decrease with distance from the surface, it is possible to construct equipotential surfaces around a solid (Aveyard and Haydon, 1973). Each equipotential surface together with the solid surface encloses a volume  $v(\epsilon)$ . Plotting  $v(\epsilon)$  against  $\epsilon$  will form a sorbate characteristic adsorption curve, which are temperature independent and determined by the structure of the adsorbent, if non-specifically interacting sorbate are considered.

Initially Polanyi gave a formulation for the adsorption potential for sorbate in gas phase and hypothesised that adsorption from liquid-phase would be analogous to gas-phase one with precipitation solid taking the place of liquefaction of gas near the adsorption surface. Under this hypothesis Polanyi expressed the adsorption potential for liquids ( $\epsilon_s$ ) in the same form used for gases substituting the vapour pressure and the pressure at equilibrium with saturated ( $C_w$ ) and equilibrium concentration ( $C_e$ ) respectively (Manes and Hofer, 1969)

$$\epsilon_s = RT \ln \left( \frac{C_w}{C_e} \right) \quad \text{Eq. 3.29}$$

where  $C_w$  and  $C_e$  are the solubility and equilibrium concentrations of the solute at temperature  $T$  (K), respectively, and  $R$  is the ideal gas constant. Nevertheless there is a critical difference between adsorption phenomena in vapour and liquid phases: in the case of the aqueous solution, the adsorbate has to replace an equal volume of water to be adsorbed on the solid surface (Manes and Hofer, 1969). The effective adsorption potential ( $\epsilon_{sw}$ ) of solutes therefore is expressed by the Polanyi-Manes model (PMM):

$$RT \ln \left( \frac{C_w}{C_e} \right) \equiv \epsilon_{sw} = \epsilon_s - \epsilon_w (V_s/V_w) \quad \text{Eq 3.30}$$

where  $V_s$  and  $V_w$  are the molar volumes of solute and water ( $\text{cm}^3/\text{mol}$ ), and  $\epsilon_s$  and  $\epsilon_w$  are the adsorption potentials (cal/mol) of solute and water.

Polanyi theory included no equation linking the adsorbed volume to the equilibrium adsorption potential. Subsequently, Dubinin (1960) observed that plotting the adsorbed volume against equilibrium adsorption potential density (adsorption potential normalised



to the sorbate molar volume) yields to single “correlation curve”, temperature independent and specific for each adsorbate-adsorbent system. This concept was applied to describe adsorption on activated carbons (Crittenden et al., 1999) and an empirical formulation for the correlation curve was proposed:

$$\log(q_e) = \log(Q_0) + a (\epsilon_{sw}/V_s)^b \quad \text{Eq. 3.31}$$

where  $q_e$  is the adsorbed solute volume per unit mass of sorbent ( $\text{cm}^3/\text{kg}$ ),  $Q_0$  is the adsorption volume capacity at saturation ( $\text{cm}^3/\text{kg}$ ), and  $a$  and  $b$  are fitting parameters.

Xia and Ball (1999) included the adsorption equation derived from the Polanyi-Manes model (Eq.3.31) in an overall adsorption-partitioning model (Equation 3.32) successfully tested for describing adsorption of nonpolar organic compounds (e.g. polycyclic aromatic hydrocarbons and chlorinated benzenes) on natural geosorbents in both single solute and competitive systems (Xia and Ball, 1999, 2000).

$$q_e = Q_0 \times 10^{a(\epsilon_{sw}/V_s)^b} \times \rho + K_p C_e \quad \text{Eq. 3.32}$$

where  $\rho$  is the sorbate molecular density ( $\text{g}/\text{cm}^3$ ) and  $K_p$  is the partitioning coefficient.

So far only nonspecific interaction forces were taken into account in the adsorption, limiting the application of the model to physisorption phenomena. Interaction forces were approximated by the molecular polarizability which is proportional to the molecular molar volume ( $V_s$ ) in the liquid form (Dubinin, 1960). Pan and Zhang (Pan and Zhang, 2012, 2014) observed that when specific interactions are also responsible for adsorption (e.g. chemisorption), molar volume ( $V_s$ ) is not sufficient to represent all adsorption forces. Therefore they proposed an enhanced version of the PMM model able to consider other interaction types which could participate in the adsorption process, like hydrophobic interactions or H-bonding. The normalising factor introduced instead of the molar volume it has been proposed again by Dubinin and Astakhov (1971): the adsorption energy  $E_o$ , which for a given solute takes into account all the interaction forces involved in adsorption. The new Dubinin– Astakhov (D–A) model to describe adsorption isotherms is

$$\log(q_e) = \log(Q_o) - (\epsilon_o/E_o)^b \quad \text{Eq. 3.33}$$

where  $q_e$  and  $Q_o$  are the equilibrium and maximum adsorption capacity, respectively  $E_o$  is the characteristic energy,  $\epsilon_o$  is the equilibrium adsorption potential,  $b$  is the D-A model heterogeneity parameter. The new formulation was then extended for describing isotherms adsorption in different phases: gas-phase water-phase and n-hexadecane-phase. Figure 2.3 illustrates a schematic representation of the general formulation for the D-A model.

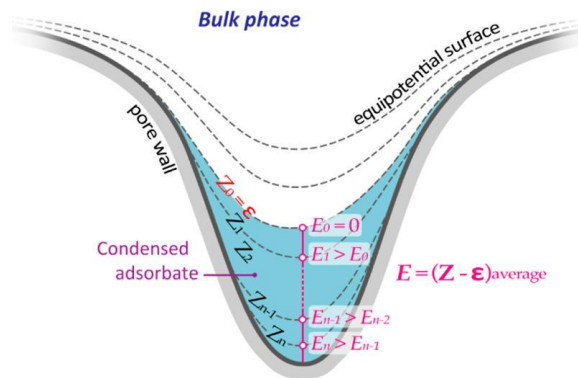


Figure 3.3: : Schematic representation the D-A model based on the thermodynamic sorption potential concept. Adapted from (Pan and Zhang, 2014).

where ( $Z$ ) is the adsorption potential value that varies with the distance from the adsorbent surface. At any point within the adsorption volume,  $Z$  should be greater than or equal to equilibrium adsorption potential ( $\epsilon$ ) representing the energy required condensing the molecule from the bulk phase (e.g., aqueous phase, HD phase, or gas phase). The excess of energy ( $Z - \epsilon$ ) then varies with location in the adsorption volume. The characteristic energy ( $E$ ) is defined as the average value of all ( $Z - \epsilon$ ) over the adsorption space and it varies with equilibrium concentration.

### 3.3 Summary and key findings

All the models here presented for description of the sorption mechanism from the most descriptive to the most mechanistic one all include water solubility as a variable. Water solubility appears implicitly (Equation 3.18, 3.23) or explicitly (Equation 3.29) in their formulations. Indeed the first two models rely on the concept of partitioning ( $k_d$ ) and the third one on the chemical potential, all variables which have been shown to be strongly related to analyte activity in water or its solubility. That means that any variation in the

liquid phase properties that changes the analyte solubility or the fugacity capacity of the liquid phase, it could potentially affect the overall partitioning and the sorption process. DOM released by SOM in water is one of the factors that could change the liquid phase properties resulting in an apparent enhancement of HOC solubility. Few results on the influence of DOM in the calculation of the partitioning coefficient of HOC confirm this hypothesis (Lee et al., 2003; Wang et al., 2011). Nevertheless, so far consequences of DOM on kinetic profiles has not been considered in the interpretation of slow kinetic profiles measured for HOC sorption on organic matter.

## 4 Instrumental techniques

As anticipated in previous chapters, the main goal of this study is to investigate BDE-209 sorption kinetic on different soil matrixes, with the scope of filling part of the gap existing on knowledge of BDE-209 fate in the environment. Usually, measurement in batch experiment are taken in the liquid phase, and the fraction sorbed by soil is calculated using the mass balance equation. The high hydrophobicity of BDE-209 and its consequent adsorption on containers surfaces make the application of the mass balance equation not univocally applicable. Therefore is preferable to measure BDE-209 mass also in the soil phase using the mass balance equation as double check. The experimental evaluation of available methods for extracting BDE-209 from water and soil samples is described separately in chapter 5 and 6. In this chapter the instruments used for samples preparation and analysis are described along with the operation principles and procedures followed. A schematic overview of these instruments and their applications in experiments steps is provided in Figure 4.1.

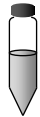











Kind of sample	Kaolin  Peat 
Separation water & soil	 Centrifuge  Vacuum filtration
Soil particles extraction	 Re-suspended in THF: water solution  ASE- Pressurised Liquid Extraction  MAE- Microwave Assisted Extraction
Water extraction and solvent substitution	 BUCHI- Rotovapor  Nitrogen flow evaporator
Analysis	 HPLC- UV Liquid Chromatography
Soil particle size & soil and water organic matter content	 Laser diffraction particle size detector  TOC Analyser

Figure 4.1: Schematic overview of instruments used and their applications.

## 4.1 High pressure liquid chromatography (HPLC)

The high-pressure liquid chromatography (HPLC) instrument used in this study is the Thermo Scientific Dionex UltiMate 3000 Series composed as shown in Figure 4.2.

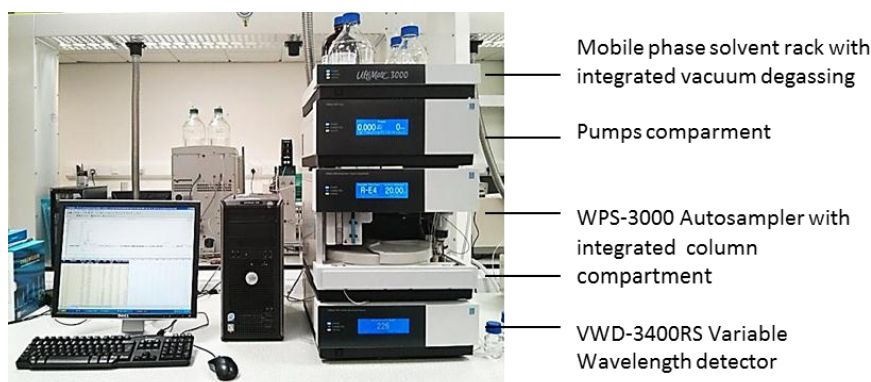


Figure 4.2: HPLC Thermo Scientific Dionex UltiMate 3000.

The diagram in Figure 4.3 reproduces schematically the HPLC components and mobile phase flow line. A reservoir holds solvents used as mobile phase and for the washing cycle. Proper degassing and filtration of all solvents is essential in order to avoid the introduction of particles into the system that can plug tubes and creation of air bubbles that cause problems in the pumping system and increase baseline noise in the chromatogram. It is possible to use sonication for degassing the mobile phase. It has the advantage that it helps in dissolution of buffer salts if present; however, it is the least effective method of degassing and it quickly heats up the mobile phase causing a drift in the baseline if solvent enters in the system before cooling down. Instead, vacuum filtration optimally degasses and filters solvents in a single step.

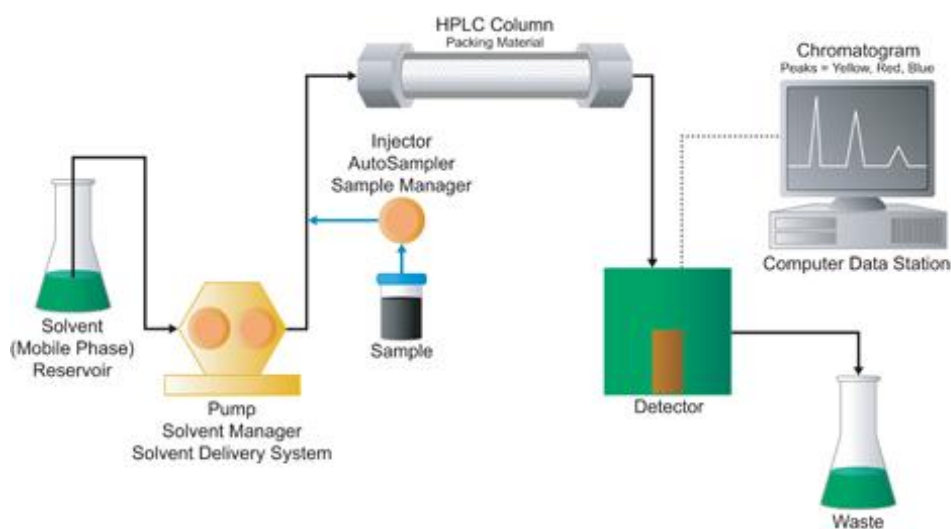


Figure 4.3: Schematic diagram showing HPLC components and the mobile phase flow (adapted from Chromacademy.com).

High-pressure pumps generate and meter a specified flow rate of mobile phase, typically millilitres per minute. Most of the systems, like the one used in this study, are equipped with an integrated degasser and two pumps that work in series in order to minimise pressure fluctuations in the systems due to the aspiration-delivery cycles. An injector introduces the sample into the continuously flowing mobile phase stream that carries the sample into the HPLC column. The column contains the chromatographic packing material (stationary phase) and, passing through the column, the different analytes contained in the sample get separated. The separation process results from the combined effects of rejection of analyte molecules by the solvent, and attraction of the analyte molecules by the stationary phase (Solvophobic theory, (Heron and Tchaplá, 1991)). Therefore in order to achieve satisfying separation, it is crucial to select the appropriate column, mobile phase and sample solvent carrier. For the analysis of BDE-209, a hydrophobic compound, a Reversed Phase Chromatography (RPC) set up was selected. Sample analyte elution from the column is retarded according to their affinity to hydrophobic support.

Based on studies found in literature (Ahn et al., 2005; Ghanem and Delmani, 2012), the RPC column selected for BDE-209 analysis is a ZORBAX Eclipse XDB-C18 Column; length: 150 mm, diameter: 4.6 mm, pore size: 5  $\mu\text{m}$  (Agilent Technologies, CA-USA). For mobile phase and sample solvent carrier, methanol and acetonitrile have been tested looking for the best combination in terms of amplitude of the signal and short retention time (RT). Peak areas

and retention times obtained for the four combinations tested are reported In Table 4.1. The best combination is methanol as mobile phase and acetonitrile as sample solvent.

Table 4.1: Retention time (RT) and peak area (mAU\*min) using methanol and acetonitrile as sample solvents and mobile phase for BDE-209 concentration of 10 µg/ml.

Mobile phase RT (min)	Sample solvent carrier	
	Methanol	Acetonitrile
Methanol (12.45)	6.76	16.78
Acetonitrile (14.83)	No peak detected in the detection range	

During the extraction method development, dispersive liquid liquid micro extraction (DLLME) was considered as extraction technique for water samples and the extraction solvent tetrachloroethane (C<sub>2</sub>H<sub>2</sub>Cl<sub>4</sub>) was tested as sample solvent using methanol as mobile phase. The retention time (12.29 min) and the peak area (16.98 mAU\*min) were comparable with the one obtained for acetonitrile, but the peak shape was presenting long front tail (see chromatogram in Appendix A). That could possibly happen because sample diluent retains the analyte so well to initially compete with the stationary phase of the column as explained in Figure 4.4. DLLME was discarded as extraction technique to avoid the use of dangerous and toxic compounds and because such concentrated samples (200 µl) was pointless due to the minimum injection volume required by the auto sampler of the instrument (500 µl). Therefore the combination methanol as mobile phase and acetonitrile as sample carrier solvent was adopted as the best option.

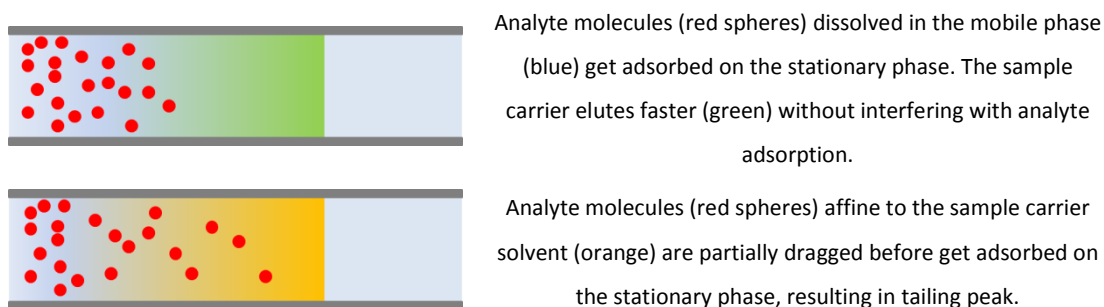


Figure 4.4: Sample solvent carrier effect on sample particles distribution and peak tail.

As the separated compound bands elute from the HPLC column, they enter the detector that is used to quantify the amount of analyte present in the bands. Different kinds of detectors can be connected to the liquid chromatography equipment, including



fluorescence detector, UV-vis spectroscopy detector and mass spectrometer detector (LC-MS). The HPLC instrument used for this study is equipped with a UV detector. LC-MS has the advantage to be more accurate and sensitive, nevertheless the vaporisation necessary for passing from the LC to the MS system present limitations. Three possible vaporisation processes have been developed: ESI (electro spray ionisation) APPI (atmospheric pressure photo ionisation) and APCI (Atmospheric pressure chemical ionisation). ESI and APCI processes are the most common, but are suitable only for charged compounds. APCI is the only one working for BDE-209 (Debrauwer et al., 2005). Unfortunately LC-MS instrument equipped with APCI system are not common and it has not been possible to find an available instrument. For what concern fluorescence no information has been found in literature of any method using fluorescence detector for PBDEs, therefore it is not sure the PBDEs are reacting with fluorescence. UV detector in contra is suitable, available and a solid detector.

In the UV detector used, the light source is a deuterium lamp able to produce light in the ultra violet wavelengths (190 nm - 670 nm). The light beam produced by the lamp is diffracted into the component wavelengths through a series of mirrors. A final mirror directs part of the light beam to the reference detector. The remaining light travels through the flow cell to the detector where the absorbance of the analyte is measured and processed. The degree of absorption depends on the sample molecule, its concentration, the light's path length in the sample, and the measurement wavelength as described by the definition of absorbance given by Lambert-Beer's Law Eq. 4.1.

$$A = \varepsilon cl = \log \left( \frac{I_r}{I_s} \right) - \log \left( \frac{I_{ro}}{I_{so}} \right) \quad \text{Eq. 4.1}$$

Absorbance is dimensionless, where:  $\varepsilon$  is the molar excitation coefficient of the analyte ( $\text{L mol}^{-1}\text{cm}^{-1}$ );  $c$  is the concentration (mol/L);  $l$  is the cell path length (cm);  $I_r$  is the reference beam intensity;  $I_s$  is the sample beam intensity;  $I_{ro}$  is the reference beam intensity with autozero and  $I_{so}$  is the sample beam intensity with autozero.

The wavelengths suggested by the literature for analysing BDE-209 are in the range of 220-400 nm (Ahn et al., 2005; Ghanem and Delmani, 2012; Guan et al., 2010). Different tests have been done in order to select the optimal wavelength on this particular instrument, and 226 nm has been found as the best wavelength in term of signal intensity.

As a final step, the HPLC detector connected to a computer reports for each peak in the chromatogram the absorbance as area of the peak. In order to transform that data in BDE-209 concentrations a calibration curve is required. The calibration curve has been calculated using 5 calibration points in the range 0.3-1.5 µg/ml plus the blank, and for each point, three measurements have been done. In Figure 4.5 and Table 4.2 are reported the calibration curve, the standard solutions concentration, the signal amplitude in term of average peak area and its standard deviation.

Table 4.2: Calibration points for BDE-209 measurement by HPLC. Each calibration point has been measured three times and the peak area reported is the average of the three measurements.

Standard solution concentration (µg/ml)	0.00	0.29	0.65	0.87	1.19	1.42
Peak area (mAU*min)	0.00	0.66	1.50	2.03	2.79	3.31
Peak standard deviation (n=3)	0.000	0.003	0.004	0.009	0.007	0.003

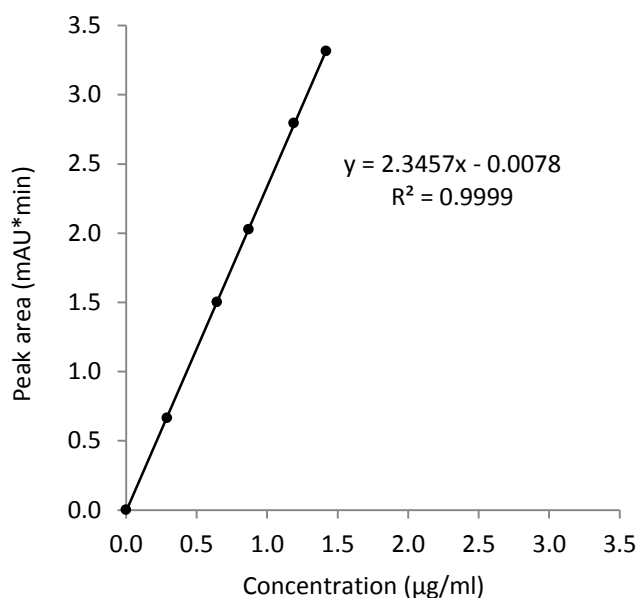


Figure 4.5: 6 points calibration curve for BDE-209 analysis on HPLC.

Frequently, the linearity of calibration curve is evaluated graphically by visually inspecting the plot of signal peak area as a function of analyte concentration. Because deviations from linearity are sometimes difficult to detect, an additional graphical procedure is here used. The deviation of the signal obtained for each calibration point from the regression line (residuals) is plotted versus the calibration concentration. For linear ranges, the residuals should be distributed between positive and negative values equally for all the different

concentrations. The less they differ from zero, the more the calibration is accurate. Figure 4.6 shows the graphical evaluation. The calibration curve results are linear in all the range tested.

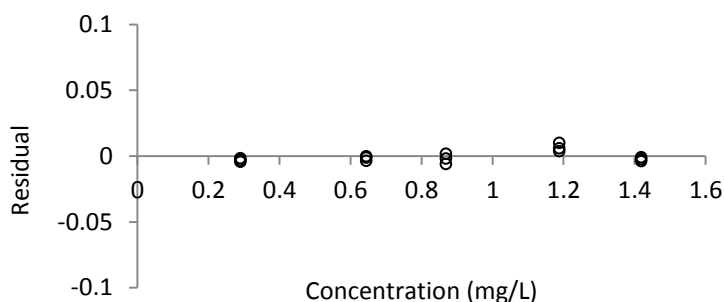


Figure 4.6: Graphical evaluation of calibration curve linearity: residual distribution through the calibration range.

The limit of detection (LOD) and limit of quantification (LOQ) of the instrument have been calculated using Equation 4.2 and 4.3.

$$\begin{cases} LOD = \frac{Ydl - Yb}{m} \\ Ydl = Yb + 3s \end{cases} \quad LOD = \frac{3s}{m} \quad \text{Eq. 4.2}$$

$$\begin{cases} LOQ = \frac{Yql - Yb}{m} \\ Yql = Yb + 10s \end{cases} \quad LOQ = \frac{10s}{m} \quad \text{Eq. 4.3}$$

Where:  $Ydl$  is the average of the signal detection limit,  $Yb$  is the average of the signal for blanks,  $m$  is the slope of the calibration curve for the corrected by the blank signal ( $Y_{\text{sample}} - Y_{\text{blank}}$ ) and  $s$  is the standard deviation for  $n=3$  repetition of the first calibration point ( $0.29 \mu\text{g/ml}$ ). The instrument detection and quantification limits are respectively:  $4 \mu\text{g/l}$  and  $14 \mu\text{g/l}$ . Values have been verified graphically observing the peak area produced at limit concentrations.

## 4.2 Pressurised Liquid Extraction (PLE)

Pressurised liquid extraction allows for liquid extraction of solid samples at high temperature by confining samples in cells capable to sustain high pressure to maintain the solvent liquids at temperatures above their boiling points (Richter et al., 1996). ASE 350

accelerated solvent extractor (Thermo Scientific, MA-USA) has been used to execute the extraction (Figure 4.7).

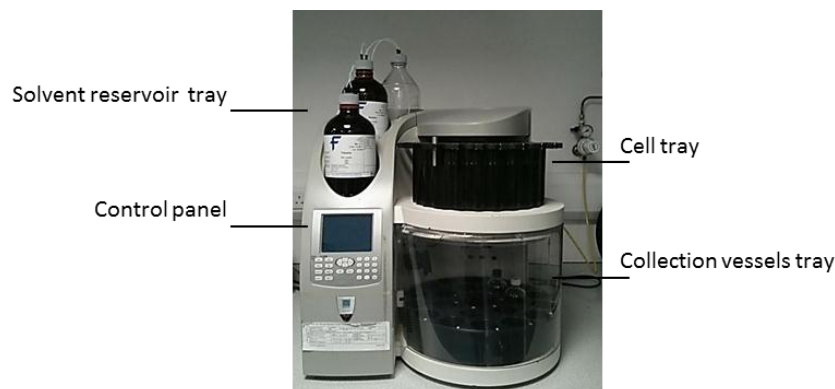
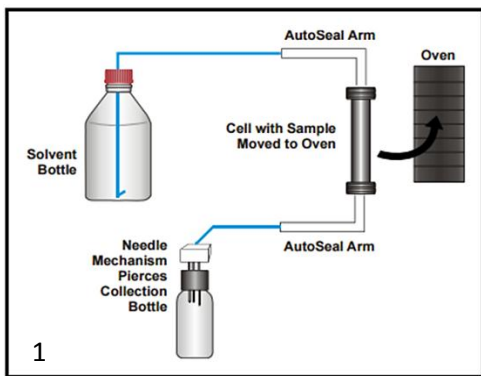


Figure 4.7: ASE 350 Thermo Scientific accelerator solvent extractor.

The cell design and associated fluid apparatus allow for operation of the extractions at elevated pressures (500 to 1500 psi) and repetition of several extraction cycles without removing samples from the extraction cells. A schematic representation of the extraction process is shown (Figure 4.8).

Through the selection of solvent extraction volume, number of static cycles, and temperature, it is possible to optimise the extraction process according to the samples characteristics and the target analyte. The rinse volume set up by the user is divided by the number of static cycles so that fresh solvent is present at the beginning of each static cycle. For a successful extraction, cell filling is crucial and specific adjustments may be required according to sample texture and humidity to avoid cell blockage. Cell filling procedures and the optimisation of the instrument set up for peat samples are described in Section 6.2.3.



1. Cell loading in the oven (room to 200 °C)
2. Cell filling with extraction solvents
3. Cell heating and static cycle
4. Cell rinsing with extraction solvents
5. Cell purging with inert gas (nitrogen)
6. Cell relief
7. Cell unloading

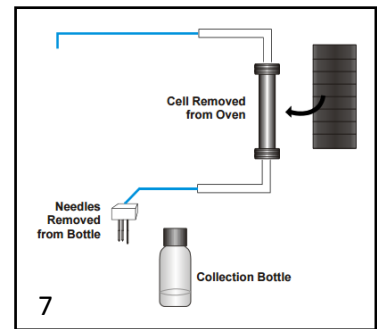
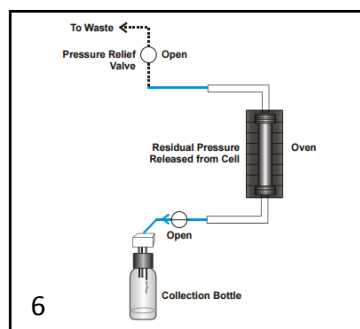
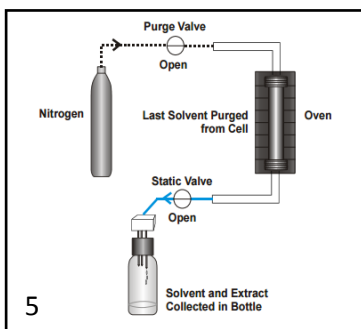
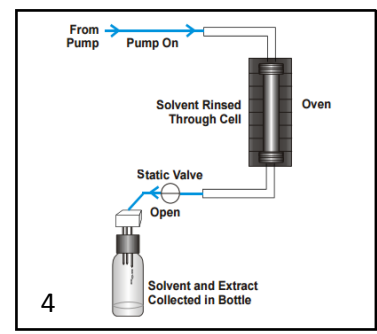
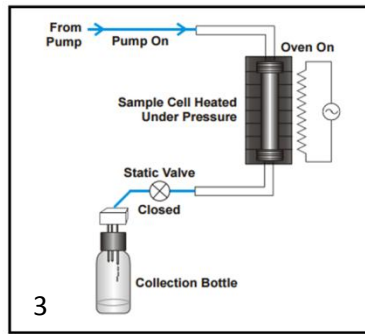
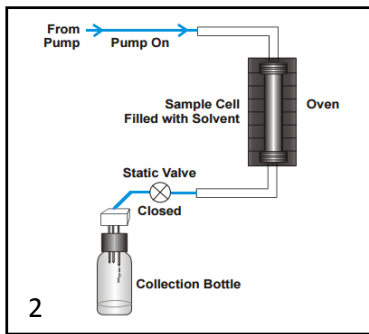


Figure 4.8: ASE Extraction process steps.

### 4.3 Microwave assisted extraction (MAE)

CEM MarsXpress Microwave Accelerated Reaction System (CEM Corporation, NC-USA) used in this study is shown in Figure 4.9. Solvent extraction efficiency is enhanced by increasing the temperature using microwave energy (0 - 1200 watts  $\pm 15\%$ ). Differently from PLE, solvents are not automatically introduced into the extraction tubes (Figure 4.8). They need to be manually transferred in the testing tubes and separated from samples after extraction. Multiple samples (up to 40) can be processed simultaneously.

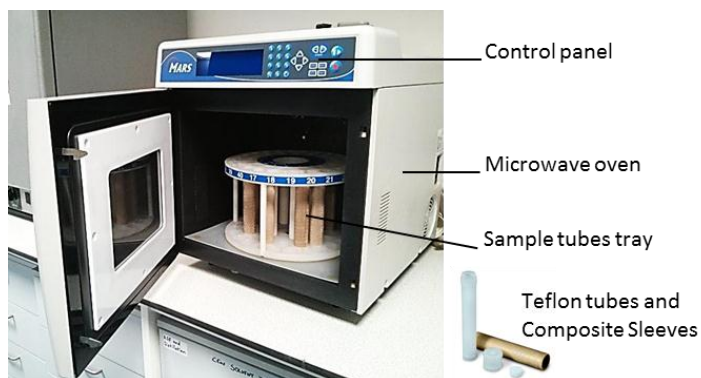


Figure 4.9: CEM MarsXpress Microwave Accelerated Reaction System and sample tubes.

#### 4.4 Sample concentration and solvent substitution

For sample concentration, BUCHI Syncore Polyvap (BUCHI, Flawil Switzerland) has been used. It allows concentrating samples by reducing analyte lost due to volatilisation and adherence to glass vials surfaces. The instrument is composed of a cooling system that keeps the bottoms of the vials cold to avoid total evaporation of solvent. At the same time, it cools the top part of the vial to create convective cell within it. On the external part of vials, solvent is cooled down and re-condensed on the glass surface bringing back part of analyte that could have remained on the glass when sample level was higher. In the centre of vials, a warmer passageway allows solvents to evaporate and to get sucked to the condenser. Working at low pressure (up to 1 mbar), the BUCHI Polyvap System is able to reach solvent boiling points at lower temperatures. In this way, losses and degradation of analytes are minimised and the solvent evaporation process is accelerated. All the components of the system are shown in Figure 4.10, and a schematic diagram showing components set-up and the cooling water loop is reported in Figure 4.11. Samples of different size can be processed. In this study, a 4 position rack for 250 ml samples and 12 position rack for 100 ml samples have been used.

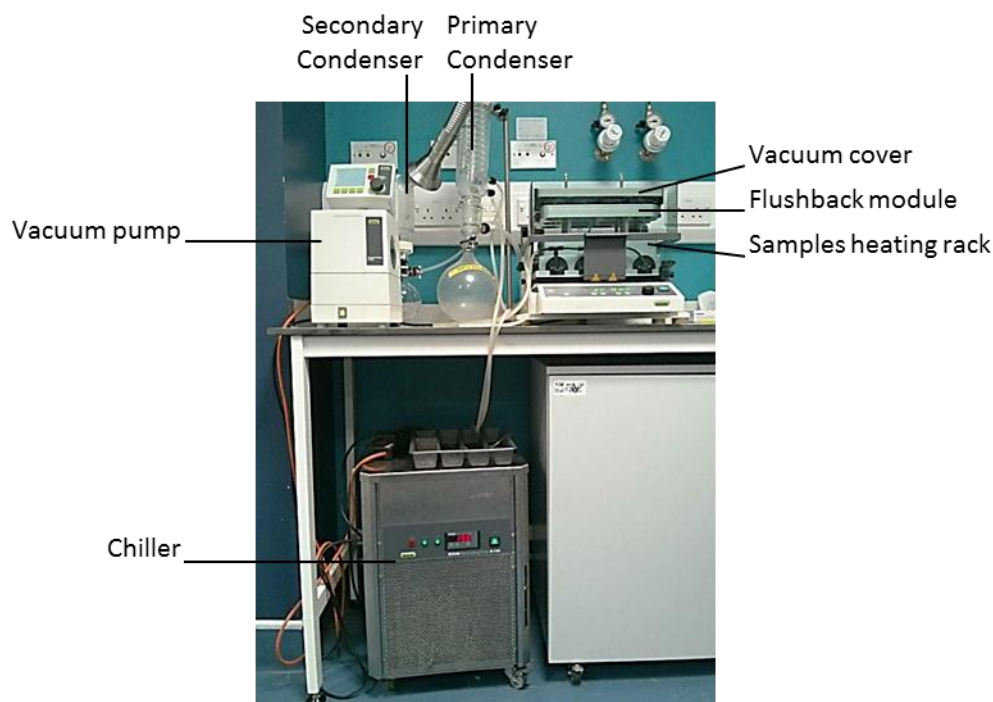


Figure 4.10: BUCHI Syncore Polyvap and its components.

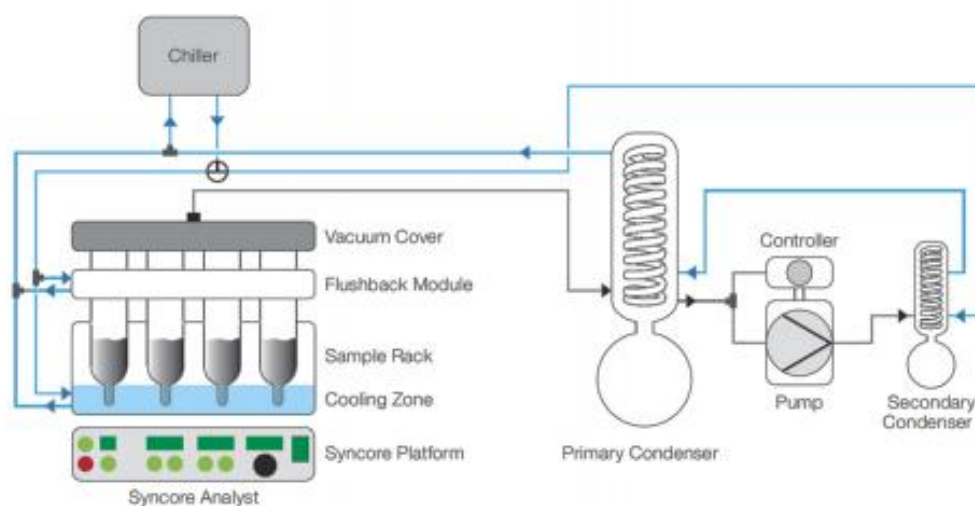


Figure 4.11: Schematic diagram showing BUCHI Syncore Polyvap components and the cooling water flow (adapted from BUCHI manual).

Pre-concentrated samples were evaporated under gentle nitrogen flow through TECHNE DB-3D Dry Block (Bibby Scientific, Staffordshire UK). Caution in the nitrogen flow set up is required to avoid turbulence in the sample that could facilitate analyte volatilisation. Sample vials are positioned in the instrument rack and nitrogen is delivered through steel needles (Figure 4.12).



Figure 4.12: TECHNE DB-3D Dry Block

#### 4.5 TOC combustion analyser

Analysis of Total Organic Carbon (TOC) was executed using a TOC Combustion Analyzer Apollo 9000 (Tekmar-Teledyne instrument, AZ USA) connected with 183 TOC Boat Sampler (Tekmar-Teledyne instrument, AZ USA) for solid sample analysis (Figure 4.13). Each sample is initially weighed into a platinum boat. The boat is introduced through the sample insert gate and manually advanced into the furnace by the magnet moving in the race tube. In the furnace, the sample is combusted at 800-1000 °C in a stream of oxygen. In that environment, all carbon within the sample is rapidly oxidized to CO<sub>2</sub>. Interfering reaction products (including sulphur oxides, halides, water and nitrous oxides) are removed by the post-combustion scrubbers.

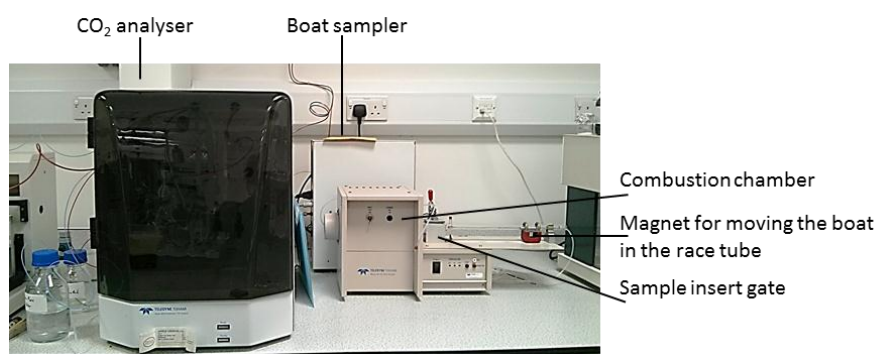


Figure 4.13: TOC Combustion Analyzer Apollo 9000 connected with 183 TOC Boat Sampler.

The CO<sub>2</sub> produced is then swept into the Apollo 9000 non dispersive (single beam) infrared detector, which uses infrared energy to measure the carbon dioxide flow. The instrument



returns that output signal as a voltage and a calibration curve is required for relating the signal to sample carbon content. Figure 4.14 shows the calibration curve built using five solutions of potassium hydrogen phthalate in diatomaceous earth. Three measurements have been repeated and data are reported as average  $\pm$  standard deviation.

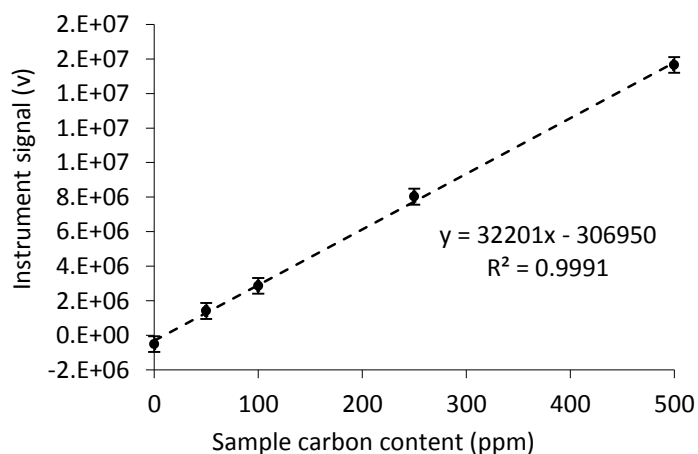


Figure 4.14: Calibration curve for TOC/TC measurement in solid sample.

#### 4.6 Laser diffraction particle size detector

Samples were analysed through Mastersizer 2000 equipped with disperser unit control Hydro 2000SM (Malvern, Worcestershire UK). As shown in Figure 4.15, it is composed of the optical bench that contains the laser source, the measurement chamber, the detectors, and an external dispenser unit with a stirring speed controller. Sample particles get dispersed in the dispenser unit in degassed Millipore water and pass through the measurement chamber. Here, the laser beam collides with particles producing diffracted beams that are detected on the other side of the optical bench. The detectors capture the scattering pattern produced by the field of particles. Using Mie theory, Mastersizer software predicts the size as equivalent spherical diameters of particles that created the pattern.

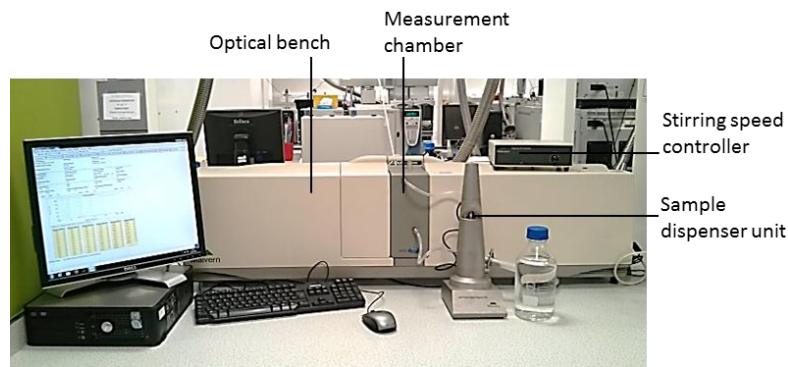


Figure 4.15: Laser diffraction particle size detector Mastersizer 2000 and the disperser unit control Hydro 2000SM.

## 4.7 Centrifugation

Centrifugation is a traditional technique for separating solid samples from water or other liquid solvents. It takes advantage of the centrifugal force generated by spinning samples to accelerate the sedimentation process. The centrifuge used in this study is a 5804R Eppendorf centrifuge (Figure 4.16). The sedimentation process at environmental conditions follows Stoke's Law reported in Equation 4.4. In centrifuge systems, gravity acceleration is artificially increased by a factor proportional to centrifugal force and therefore to the spinning speed.



Figure 4.16: Centrifuge Eppendorf 5804R.

$$V = \frac{2}{9} \frac{(\rho_p - \rho_m)}{\mu} g R^2 \quad \text{Eq. 4.4}$$

Where:  $V$  is the setting velocity (m/s),  $\rho_p$  is the particle density (Kg /m<sup>3</sup>),  $\rho_m$  is the fluid density (Kg /m<sup>3</sup>)  $\mu$  is water dynamic viscosity (kg /ms),  $g$  is the gravitational acceleration (m/s<sup>2</sup>), and  $R$  is the radius of particles (m). Implementing these factors in Equation 4.4 and resolving it for  $t$ , the time of sedimentation, it is obtained the equation suggested in ASTM standard (ASTM, 2001) for the calculation of the sedimentation time in seconds (Equation 4.5).

$$t = \frac{9}{2} \left[ \frac{3600}{4\pi^2 (rpm)^2} \right] \left[ \frac{\mu}{r_p^2 (\rho_p - \rho_m)} \right] \ln(R_b/R_t) \quad \text{Eq. 4.5}$$

Where:  $\rho_p$  is the particle density (g/cm<sup>3</sup>),  $\rho_m$  is water density (1 g/cm<sup>3</sup>)  $\mu$  is water dynamic viscosity (0.01 g / cms),  $g$  is the gravity acceleration (980 cm/s<sup>2</sup>),  $rpm$  is the spinning speed (revolutions per minutes),  $r_p$  is the particle radius (cm),  $R_b$  is the distance from centre centrifuge rotor to bottom of centrifuge tube (11.5 cm), and  $R_t$  is the distance from centre centrifuge rotor to top of centrifuge tube (3.5 cm).

Fixing the spinning speed at 2000 rpm, the time required for clay particles sedimentation is calculated. Considering the smallest particle diameter of 0.00003 cm and particle density of 2.65 g·cm<sup>-3</sup> in Eq. 4.5, the sedimentation time for the finest clay particle is about 14 minutes. Dissolved BDE-209 molecule by definition should not be affected by centrifugation. To be certain that the centrifugation process does not affect BDE-209 molecules, the sedimentation calculation is done considering BDE-209 molecules behaving like suspended particles of density 3.35 g·cm<sup>-3</sup> and radius 1.86·10<sup>-8</sup> (Hu et al., 2005b). The sedimentation time is about 6500 days. Therefore, even in the case that we consider BDE-209 molecules behave like suspended particles, the centrifugation time used for settling clay particles (20 minutes) is not enough long to affect BDE-209 molecules in suspension.

## 5 BDE-209 analysis in aqueous samples

### 5.1 Introduction

For monitoring the behaviour of BDE-209 in the environment it is fundamental to be able to measure it in two of the most important environmental compartments: water and soil. In relation to this study, analysis of water and soil samples are investigated for measuring BDE-209 mass in both phases involved in sorption and desorption experiments. The aim of this chapter is to select the most suitable technique to analyse BDE-209 in water samples. Different extraction methods have been tested on pure water, and the method with best recovery was optimised for extracting BDE-209 from the most complex matrix considered in this study: water after contact with peat. To contextualise the results obtained and justify the experimental set up selected, a summary of the operating principles and a review of its use for PBDE analysis in water samples is reported for each technique. The four techniques tested were liquid-liquid extraction (LLE), dispersive liquid-liquid micro extraction (DLLME), solid phase extraction (SPE), water evaporation and solvent substitution (WES).

### 5.2 Extraction methods

#### 5.2.1 Liquid-liquid extraction (LLE)

Liquid-Liquid Extraction (LLE) is a traditional technique for extraction and clean-up of liquid samples, and it is used in several standardised methods for analysis of organic pollutants in water (USEPA, 1996; BSI, 1997, 2005) It consists of selective transfer of chemicals from the aqueous sample to an extraction solvent that is temporarily mixed with it. In order to obtain an efficient and selective extraction, the extraction solvent should have the following characteristics. It must have a favourable distribution coefficient for the analyte of interest and an unfavourable distribution coefficient for other compounds dissolved in the sample. The solvent must be immiscible with the sample and have sufficient density difference with the sample matrix to ensure complete formation of two layers while avoiding the formation of emulsions. Finally, it must not chemically react with the analyte. LLE has been adopted for extracting BDE-28 and BDE-47 (tri- and tetra-BDE) in water samples using 2 mL of n-hexane per 10 mL of background solution. Recovery ranged between 94-115 % (Liu et al. 2010; Liu et al. 2011). A recovery of  $96 \pm 6\%$  was achieved for extraction of BDE-15 adding

200  $\mu\text{l}$  of trichloroethylene for 10 mL of water (Olshansky et al., 2011). No studies involving BDE-209 could be found in literature. In light of the consideration reported for lower brominated PBDEs, LLE was tested for the extraction of BDE-209 using dichloromethane, toluene, and n-hexane.

### 5.2.2 Dispersive liquid-liquid micro extraction (DLLME)

Dispersive liquid-liquid micro extraction (DLLME) is a variation of the more traditional liquid-liquid extraction. The principle is the same as LLE. A solvent with chemical affinity to the target analyte is mixed with the sample and then separated leaving in solution all the interference compounds more soluble in the sample matrix than in the solvent. Differently from LLE, DLLME works at micro-volume size. A dispersive solvent soluble in both the aqueous sample and extracting solvent is used to enhance the transfer of analyte from sample to the extracting solvent. Once dispersive and extracting solvents are injected in the water sample, a cloudy mixture is formed due to the tiny droplets of immiscible extracting solvent in the aqueous environment. Due to the high surface area of these extracting solvent droplets, analyte extraction is efficient and rapid. DLLME was introduced in 2006 (Rezaee et al., 2006) for simultaneous extraction and pre-concentration of organic analytes in aqueous matrices. Since then, new applications have been explored for the analysis of both organic and inorganic analytes. Reviews on the use and development of DLLME in analysis of organic analytes have been published by Herrera-Herrera et al. (2010), Saraji & Boroujeni (2013) and Zgoła-Grześkowiak & Grześkowiak (2011). So far, only two laboratories tested DLLME for BDE-209 analysis in water. A number of disperser and extracting solvents have been compared. Li et al. (2008) compared the recovery obtained with acetonitrile, acetone, methanol, and tetrahydrofuran as disperser solvents and dichloroethane, carbon disulphide, carbon tetrachloride and tetrachloroethane as extraction solvents; they concluded that the combination of acetonitrile (1ml) and tetrachloroethane (20  $\mu\text{l}$ ) gave the best recovery for BDE-209 in 5 ml spiked nanopure water (87%). Zhang et al. (2013) selected acetone (1 ml) and tetrachloroethylene (10  $\mu\text{l}$ ) as the best solvent combination and coupled DLLME with ultrasonic bath (2 minutes) to accelerate the formation of the cloudy solution. In these conditions, the recovery obtained for BDE-209 from a 5 ml water sample was about 75%. In this set of experiments, extraction tests were run trying to replicate the cited results using acetonitrile as disperser solvent and either tetrachloroethane or dichloromethane (DCM) as extracting solvent.

### 5.2.3 Solid phase extraction (SPE)

Solid phase extraction (SPE) is a traditional technique often used as an alternative to LLE. There are two approaches for SPE. In one, the analyte of interest is retained by the solid phase and matrix interferences are washed through. In the other, the analyte of interest is washed through and matrix interferences are retained. The first approach is referred to as reverse phase and it is the most common for extraction of hydrophobic compounds like PBDEs. In literature, few references are available for PBDE extraction by SPE and they are mainly for human and animal serum samples (Covaci & Voorspoels 2005; Keller et al. 2009; Lin et al. 2013; Thomsen et al. 2007; Zhang & Rhind 2011). Just one study has been published for PBDEs extraction from water, but it considers only up to hexa- brominated congeners (Barco-Bonilla et al., 2014). The selection of the cartridge is a crucial step in SPE extraction. In the cited studies, a number of approaches has been taken. Lin et al. (2013) used cartridge C18; Keller et al. (2009) and Thomsen et al. (2007) used Oasis HLB; and Zhang & Rhind (2011) used Strata-X. In the only study involving BDE-209, Covaci & Voorspoels (2005) suggested that Oasis HLB yielded a higher recovery in <sup>13</sup>C-BDE-209 extraction (64 ±17 %) than other three SPE cartridges (C18, Isolute Phenyl and Isolute Env+). In light of these considerations the cartridges adopted for this study was 200 mg/6 mL Oasis® HLB cartridge (Waters, Milford, MA, USA).

### 5.2.4 Water evaporation and substitution (WES)

Water evaporation and substitution (WES) is not strictly an extraction technique. WES consists of complete evaporation of the aqueous sample and re-dissolution into solvent. The method is particularly appropriate for BDE-209 analysis because it takes advantage of the low volatility of BDE-209 and minimises the loss of analyte caused by sample handling. Explicit references have not been found in literature to such a simple approach for BDE-209 analysis in water samples.

## 5.3 Experimental procedures

### 5.3.1 Materials

Decabromodiphenyl ether standard (98% purity) was purchased from Sigma-Aldrich (St. Louis, MO, USA). Working standard solutions of BDE-209 were prepared daily by dilution of

stock solution (10 mg/L BDE-209 in acetonitrile) using deionised water. All of the reagents used in these experiments (dichloromethane, toluene and hexane) were of analytical HPLC grade obtained from Fisher. Water was collected from the laboratory reverse osmosis deionizing system (RO180 El-Ion® twin-stage, SG)

### 5.3.2 LLE

Water solution (10 mL) containing 10 µg/L of BDE-209 was placed into a 25 mL screw-cap glass vial with PTFE cap septum. Extraction solvent (1 ml) was added by automatic pipette (Ergonomic high performance pipettor, VWR, Lutterworth-UK). Samples were agitated end-over-end at 300 rpm for two minutes and rested for five minutes. This step was repeated three times. The extraction solvent was removed with a glass Pasteur pipette and transferred to an HPLC vial where it was evaporated to dryness under nitrogen flow (TECHNE DB-3, Bibby Scientific Limited, Stone, UK) and reconstituted with acetonitrile (1 mL). Samples were analysed with HPLC following the procedure described in Section 3.1.2. In the first tests, complete recovery of the extraction solvent was not possible. because a thin layer of solvent remained on the meniscus at the interface with water. Thus, the second series of experiments was run using larger volumes of sample (25 mL) and solvent (2mL). In this way, a partial but known amount of the extraction solvent (1.5mL) was recovered for analysis.

### 5.3.3 DLLME

For DLLME, 250 mL of deionised water containing 5 µg/L of BDE-209 was pre-concentrated to a volume of 5 mL and placed into a 5 mL screw-PTFE cap glass test tube with conical bottom. The mixture of acetonitrile (1.5 mL) and tetrachloroethane or DCM (30 µl) was rapidly injected into the aqueous sample with a 1 mL glass syringe. The milky cloudy mixture (water/acetonitrile/tetrachloroethane or DCM) was centrifuged for 5 minutes at 3000 rpm. The sediment phase (tetrachloroethane or DCM) was removed using a micro-syringe and transferred to HPLC vial containing 1.5 mL of acetonitrile for analysis. 2 replicates were run for each combination of disperser and extracting solvents.

### 5.3.4 SPE

For SPE, BDE-209 aqueous solution (50 µg/L) was prepared diluting 250 µL of stock solution (10 mg/L in acetonitrile) in 50 ml of deionised water. SPE extraction procedure is divided in

four steps: cartridge pre-washing, conditioning, sample loading and elution. The system is composed by the loading cartridge at atmosphere pressure where washing solvent, sample or eluting solvent are loaded according to the specific running step. From the loading cartridge liquid are forced to pass through the SPE cartridge drop by drop at specific flow regulated by adjusting the vacuum level at the exit of the SPE cartridge. The procedure steps, solvent volume and flow are summarised in Table 5.1. The final 4 ml of acetonitrile was concentrated to 2 ml by gentle nitrogen flow and transferred to HPLC vial for analysis.

Table 5.1: Procedure of extraction with Oasis HBL cartridge.

Step	Process	Application	Flow (ml/min)	Time (min)
1	Prewash	2 mL methanol	1.5	1.3
2	Prewash	2 mL acetonitrile	1.5	1.3
3	Condition	3 mL methanol	1.5	1.3
4	Condition	3 mL water/methanol (19:1)	1.5	1.3
5	Load	50 mL water sample	0.5	100
6	Dry	2 minutes		2
7	Elute 1	4 mL Acetonitrile	0.5	8
8	Elute 2	4 mL Acetonitrile	0.5	8

### 5.3.5 WES

For WES, recovery tests were conducted on pure water. 200 mL of deionised water was spiked with 0.2 mL BDE-209 stock solution (5.4 mg/L). Samples were concentrated from 200 mL to 5 mL through BUCHI rotovapor system. BUCHI Syncore system description and specification are reported in section 3.4. Operational conditions are summarised in Tables 5.2 and 5.3 and the pressure profile is show in Figure 5.1. After concentration, samples were transferred to 30 mL screw cap glass vials. BUCHI vials were rinsed twice with 5 mL of acetone to ensure that no BDE-209 was left attached at the glass surface. Samples were transferred to the sample concentrator (TECHNE DB-3), where temperature of 45 °C and gentle nitrogen flow were applied. When water was totally evaporated, 2 mL of acetonitrile was added in the vials, samples were sonicated for 1 min and 1.5 mL of sample was filtered (0.20µm PTFE membrane, VWR, Leicestershire, UK) and transferred to HPLC vials to be analysed.



Table 5.2: Vacuum steps. BUCHI vacuum pump V-700

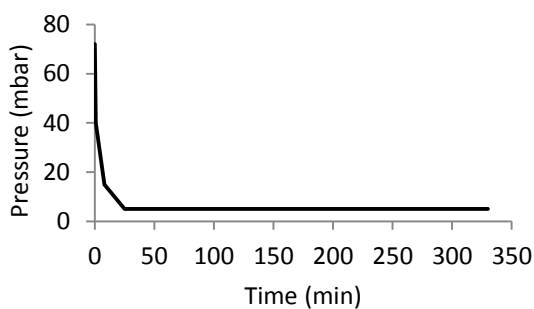


Figure 5.1: Vacuum operational profile. BUCHI vacuum pump V-700

Step	Start (mbar)	End (mbar)	Time (min)
1	72	40	1
2	40	15	7
3	15	5	17
4	5	5	305

Table 5.3: Operational parameters for BUCHI rack and cooling system.

Temperature of rack	42°C
Temperature of vacuum cover	50°C
Cooling temperature	- 10°C
Vortex speed	300 rpm

## 5.4 Results

### 5.4.1 LLE

All recovery values obtained for LLE extractions were below 20% (Table 5.4). The concentrations measured from some of the extractions with hexane and dichloromethane were below the instrumental LOD (4 µg/L). Toluene shows slightly better extraction recovery, higher than 10 % for both samples analysed. A possible reason of the toluene better extraction property might be that toluene contains itself an aromatic ring and it is smaller than the hexane aliphatic chain. This could make toluene more suitable than hexane for interaction with BDE-209 aromatic molecules. Dichloromethane instead presents the disadvantages that it is denser than water (density 1.33 g/mL at 20 °C) and its meniscus at the interface with water is wider than the ones of hexane or toluene. Thus it was more difficult to remove it completely from the vial. Since recovery values were lower than expected, an additional test was used to recognise if the reason was the inefficacy of the extraction or instead the loss of analyte during the steps of solvent evaporation and substitution with acetonitrile after the extraction. 25 mL of 100 µg/L BDE-209 solution in n-hexane was evaporated and re-dissolved in 1.5 mL of acetonitrile. Recovery values were

between 70 and 84 % (Table 5.5). Consequently, the extraction procedure was changed using larger sample and solvent volumes. The new approach facilitated the extraction procedure and allowed transferring just a partial but known amount of solvent. Nevertheless, most of the analyte (68-74%) was still lost during the process and recovery values (Table 5.6) were much lower than the ones reported in literature for other PBDEs. Opportunity for improvement is not excluded. Higher recovery values might be reached by optimising the LLE procedure, for example, by increasing the mixing time, changing the solvent volume, or assisting the process with an ultrasound bath.

Table 5.4: Recovery value for LLE extraction of BDE-209 from deionised water. Sample volume 10 mL, solvent volume 1 mL.

Extraction solvent	Measured concentration (µg/L)	Expected concentration (µg/L)	Recovery (%)
Hexane	8	100	8
Hexane	3	100	3
Toluene	13	100	13
Toluene	19	100	19
Dichloromethane	12	100	12
Dichloromethane	6	100	6

Table 5.5: BDE-209 recovery value for solvent substitution from hexane to acetonitrile. Hexane volume 25 mL, acetonitrile volume 1.5 mL.

Measured concentration (µg/mL)	Expected concentration (µg/mL)	Recovery (%)
1.40	1.67	84
1.18	1.67	71
1.32	1.67	79
1.17	1.67	70

Table 5.6: Recovery value for LLE extraction of BDE-209 from deionised water. Sample volume 25 mL, toluene volume 2 mL.

Extraction solvent	Measured concentration (µg/L)	Expected concentration (µg/L)	Recovery (%)
Toluene	40	125	34
Toluene	50	125	42

#### 5.4.2 DLLME

In the DLLME tests, the alternative extraction solvent DCM, was unsuccessful. Difficulties have been found collecting DCM from the bottom of the conical vial: it was not possible to draw a sufficient amount of solvent without mixing it with layer of acetonitrile. Extraction using acetonitrile (1.5 ml) as disperser solvent and tetrachloroethane (30 µl) as extraction solvent showed a recovery of 27-34 % (Table 5.7). The literature recoveries of 75-87% (Li et al., 2008b; Zhang et al., 2013) could not be reproduced, possibly because part of the analyte might get lost during the pre-concentration step. This step is necessary when working with low concentrations near to values expected from experiments and environmental samples. Results obtained for DLLME method in the cited in literature have been tested at very high concentrations 100 µg/L. Additionally, the advantage to reach high concentration factors by reducing the sample volume to 20 µl was eliminated because of the limitation imposed on the sample volume by the HPLC automatic injector. At least 1.5 mL of sample is required to run three injections.

Table 5.7: Recovery value for DLLME extraction of BDE-209 from deionised water. Different extraction solvents tested using 1.5 mL of acetonitrile as dispersive solvent.

Extraction solvent	Measured concentration (mg/L)	Expected concentration (mg/L)	Recovery (%)
Tetrachloroethane	0.28	0.83	34
Tetrachloroethane	0.22	0.83	27
Dichloromethane		Unsuccessful extraction	
Dichloromethane		Unsuccessful extraction	

### 5.4.3 SPE

In SPE, BDE-209 levels in the first and second elution steps were below detection limits (Table 5.8). No traces of BDE-209 were detected in the blank sample, assuring no contamination was occurring during the experiment.

Table 5.8: Recovery values for SPE extraction of BDE-209 from deionised water with Oasis HBL cartridge.

Extraction solvent	Measured concentration (mg/L)	Expected concentration (mg/L)	Recovery (%)
Sample Elute 1	0.01	1.25	0
Blank Elute 1	0.00	1.25	0
Sample Elute 2	0.01	1.25	0
Blank Elute 2	0.00	1.25	0

The SPE extraction of PBDEs is challenging and difficulties seem to increase with the degree of bromination. Failure in extracting the pentabrominated congener BDE-104 was reported (Keller et al., 2009). From a tribrominated congener (BDE-28) to a heptabrominated congener (BDE-183) recovered from human serum samples, the percentage of analyte recovered was halved (Zhang and Rhind, 2011). The absolute null result obtained in the experiment suggests that the set-up selected for extraction is not suitable for BDE-209. The reason might be the choice of acetonitrile as elution solvent, which could not be strong enough for catching the BDE-209 absorbed in cartridges.

No further attempts to improve the SPE process were done because of the long processing time required for loading drop by drop large volume of sample. The use of a higher flow during sample loading was excluded to ensure that the analyte had enough time to be absorbed and retained by the solid phase. Considering the volume of the cartridge (6 mL) and a flow of 0.5 mL/min, the contact time of sample and solid phase was 12 min. Based on the knowledge gained on BDE-209 adsorption and absorption processes and experience gained through the laboratory activity, a shorter contact time would be absolutely considered as an option and a stronger eluting solvent would be used to extract BDE-209 from the cartridge solid phase. A recently published study on SPE extraction of PBDEs from water confirms this idea (Barco-Bonilla et al., 2014). A 100 % recovery value was reached for lower brominated PBDEs congeners (from tetra- to hexa-BDE) using 10 mL/min flow rate and hexane/acetone (4:1) as elution solvent.

#### 5.4.4 WES

Recovery values obtained through WES with acetonitrile were satisfying. As data in Table 5.9 show, 97 % of recovery was reached with a relative standard deviation of 3%. At the same time, the method assures high concentration factor (100) and the use of solvent is minimised.

Table 5.9: Recovery value for WES extraction of BDE-209 from deionised water (200 mL), BDE-209 concentration 5.4 µg/L.

Measured concentration (mg/L)	Expected concentration (mg/L)	Recovery (%)
0.52	0.54	96
0.52	0.54	97
0.51	0.54	94

The complete procedure requires about 8 hours. Most of that time (6-7 hours) is required by automated steps (BUCHI and nitrogen flow) for which just periodic supervision is required. A possible further simplification of the method has been considered. Injecting the concentrated sample directly in the HPLC avoids the last step of acetonitrile substitution. Recovery was not calculated because a new calibration curve would have been required using water as sample carrier. However, the peak area of direct water injection was less than 2/3 of the one obtained after acetonitrile substitution. As a consequence, this further simplification has been discharged.

## 5.5 Comparison of the techniques

Recovery values obtained for BDE-209 extraction from deionised water under the conditions previously described are shown graphically in Figure 5.2. Literature suggests that better recovery could be achieved with some of the techniques tested, especially with SPE and DLLME. However, the high recovery and the simplicity of WES with acetonitrile make it the best choice for BDE-209 extraction. Moreover, from an environmental point of view, WES is the “greenest” method among methods explored. WES reduces drastically the volume of solvent in comparison with LLE. WES does not require the use of toxic chemicals and pollutants as DLLME does. Finally, WES does not produce solid waste for each extraction as SPE does.

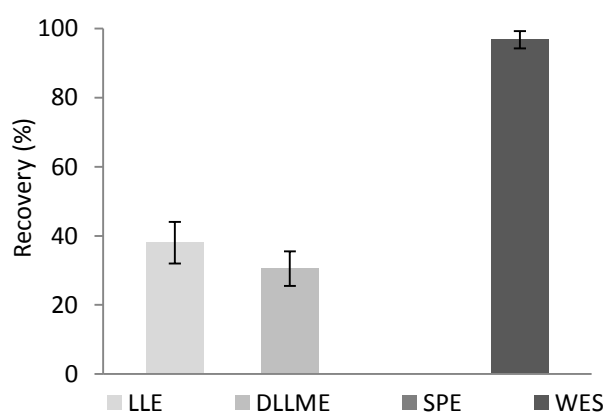


Figure 5.2: Comparison of BDE-209 recovery from deionised water using liquid-liquid extraction (LLE), dispersive liquid-liquid micro extraction (DLLME), solid phase extraction (SPE) and water evaporation plus substitution with acetonitrile (WES).

## **5.6 WES tested for extraction from more complex matrix using Chrysene as internal standard**

In order to evaluate the suitability of WES with acetonitrile for more complex matrices, the method was tested on deionised water with dissolved organic matter (DOM) that was created by mixing deionised water with peat for 24 hours (water-peat matrix). Subsequently the use of a surrogate has been investigated. Usually, PCB congeners or <sup>13</sup>C labelled congeners are used as surrogates for PBDEs (Allchin et al., 1999; Rhind et al., 2013) because these compounds have structure and properties similar to those of the analyte and thus mimics better its behaviour. PCB-209 like other chemical tested (naphthalene or triclosan) showed co-elution problems with BDE-209 peak, matrix interference peaks or solvent peaks. Chrysene elution time instead was compatible and avoided these problems (Illustrative chromatograms can be found in Appendix A). Thus, chrysene was the selected candidate to be investigated as possible internal standard.

### **5.6.1 Procedure**

To prepare the water with DOM, 0.5 g of peat oven dried at 105°C for 48 hour was weighed and added to 200 mL of deionised water. After 24 hours of mixing, peat was separated from water through vacuum filtration on glass fibre filters purchased from Sterlitech Corporation (90 mm diameter, 0.3 µm pore size, GF-75). The water fraction was transferred to BUCHI vials spiked with 0.2 mL of 5 mg/L BDE-209 solution and 1 ml of 110 mg/L chrysene solution in acetonitrile. Then samples underwent the same steps described in section 5.3.4 for deionised water samples.

### **5.6.2 Results**

Analysis of the water-peat matrix without BDE-209 excluded the presence of interferences. In the HPLC chromatogram, no peaks were eluting at the same retention time of BDE-209 (12.4 min), although other peaks were noted (Illustrative chromatogram in Appendix C). Recovery from the spiked water-peat matrix was 68 % with a standard deviation of 6 % and a relative standard deviation of 8% (Table 5.12). Each sample was measure three times on the HPLC and the relative standard deviation on the instrumental reading was always < 0.5 %. As expected, recovery values for the peat-water matrix were lower and more variable than those obtained on deionised water (Table 5.7).

As can be observed in Figure 5.3 (a), recovery of BDE-209 and chrysene underwent the same variation from sample to sample. The fluctuations around average value are comparable (Figure 5.3 (b)) and the proportion between chrysene and BDE-209 recoveries is consistent (Table 5.10). Results therefore show that chrysene is a suitable compound to be used as surrogate in WES extraction of BDE-209 from complex matrices like water in contact with peat soil.

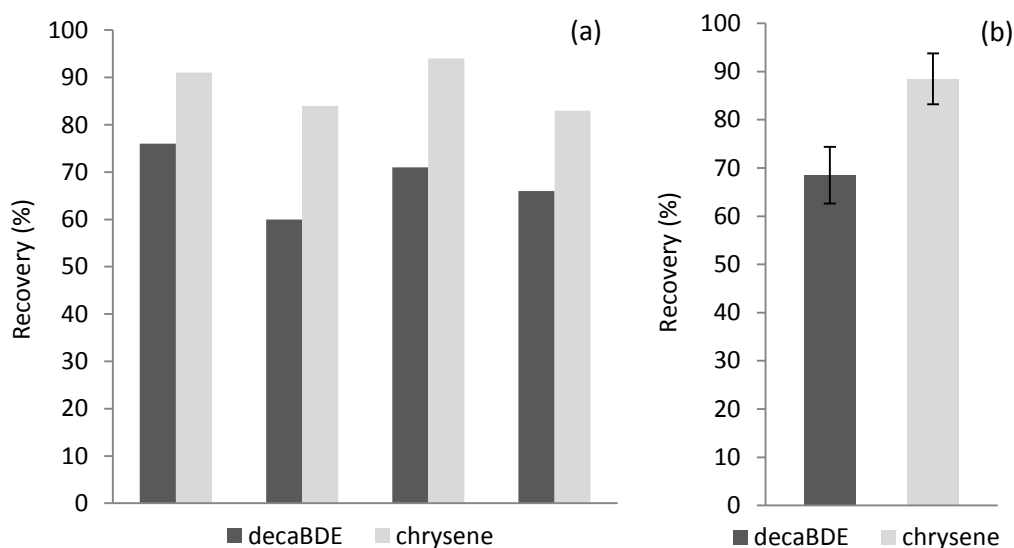


Figure 5.3: (a) WES recovery from peat-water matrix sample for BDE-209 (5.3 µg/L) and chrysene (550 µg/L.) (b) Average recovery and standard deviation for BDE-209 and chrysene recovery.

Table 5.10: Chrysene and BDE-209 spiking concentration and correspondent recovery values (%). Chrysene/BDE-209 recovery ratio is calculated. Average value and standard deviation are reported.

BDE-209 concentration (µg/l)	BDE-209 recovery (%)	chrysene concentration (µg/l)	chrysene recovery (%)	Recovery ratio
5.31	76	550	91	1.2
5.31	60	550	84	1.4
5.31	71	550	94	1.3
5.31	66	550	83	1.3
Average value	68	/	88	1.3
Standard deviation	5.9	/	5.3	0.1

## 5.7 Conclusion

The WES method with acetonitrile substitution has been found successful for BDE-209 analysis in both deionised water and water with DOM. Recovery values reached in the first case are on average  $97 \pm 3 \%$  and in the second case  $68 \pm 8 \%$ . Chrysene is an effective surrogate for BDE-209 and has been used to have a measure of BDE-209 extraction efficiency when water has been analysed after contact with peat (Chapter 7). Considering the HPLC limit of detection (LOD) of  $4 \mu\text{g/L}$  and the high concentration factor achievable through WES, the overall LOD of the water extraction analysis method is considerably low. For 200 mL samples the overall LOD results  $0.04\mu\text{g/L}$ .



## 6 BDE-209 analysis in soil samples

### 6.1 Introduction

As previously mentioned, sorption experiments are usually performed measuring the analyte which remain dissolved in water and using the mass balance equation to calculate the mass of analyte absorbed by the solid phase. This approach is accepted widely and standardised (e.g. ASTM E1195, 2001; OECD 106, 2000). Nevertheless, measuring directly the analyte absorbed by the solid matrix would avoid error due to loss of analyte through the experimental process. This observation is particularly important for highly hydrophobic compounds like BDE-209 for which the loss due to adherence to the glass surface or sorption on container surfaces and caps could be significant.

The aim of work presented in this chapter is to develop a method to analyse BDE-209 in peat and verify its suitability for the sorption experiment. Two common extraction techniques were tested for extracting BDE-209 from peat: microwave assisted extraction (MAE) and pressurised liquid extraction (PLE). Previous literature on PBDEs extraction through the two techniques is reviewed in the following sections and it provided the basis for the experimental design. A discussion of the results obtained for recovery and interferences coming from peat follow.

#### 6.1.1 Microwave assisted extraction (MAE)

The traditional technique for extraction of organic analytes from solid environmental samples is Soxhlet extraction, which usually requires large amount of solvent and more than 20 h to complete the extraction. Microwave assisted extraction (MAE) is a more recent technique based on the principle of increasing solvent extraction efficiency by increasing the extraction temperature. In this way, the volume of solvent used and the contact time required are significantly reduced.

MAE was first performed for pre-treatment of organic substances in 1986 (Ganzler et al., 1986) and analytical methods have been developed for extraction of persistent organic pollutants from solid samples: for instance polycyclic aromatic hydrocarbons, polychlorinated biphenyls and organochlorine pesticides from waste, soil, sediment, and

plants (Barriada-Pereira et al., 2003; Bartolomé et al., 2005; Düring and Gäth, 2000). Nevertheless, because of the recent interest in PBDEs, literature about MAE extraction of PBDEs is not extensive. A list of MAE methods developed for analysing PBDEs is presented in Table 6.1. Observing the MAE methods published in literature it seems that the use of a non-polar solvent (e.g. hexane or pentane) mixed with a polar solvent (e.g. isopropanol, acetone, methanol or dichloromethane) is a successful combination for extracting PBDEs. Possibly because the non-polar solvent is appropriate for extracting non-polar analytes and the polar solvent enhances the water solubility of the extraction mixture, allowing more capillary extraction in case drops of water are trapped in the micro-pores of the solid matrix.

Table 6.1: Literature review on application of MAE on extraction of PBDEs form solid samples.

Sample matrix	PBDEs congeners analysed	Recovery	Solvent (v:v)	Reference
Polymers from electronic equipment	deca-BDE	27 % 30 %	isopropanol:hexane (1:1) isopropanol:methanol (1:1)	(Vilaplana et al., 2008)
	mono- to deca-BDEs	73-75 % (mono-BDE) 95-98 % (di-BDE) 97-105 % (tri-BDE) 63-100 % (tetra-BDE) 60-80 % (penta- to hepta-BDE) 60-70 % (deca-BDE)	toluene:water (5:1) or hexane:water (5:1)	(Li et al., 2009)
	deca-BDE	30 %	isopropanol:hexane (1:1)	(Vilaplana et al., 2009)
Sewage sludge	tetra- to deca-BDEs	110 % (tetra-BDE) 105-110 % (penta-BDE) 100-103 % (hexa-BDE) 95 % (hepta-BDE) 105 % (deca-BDE)	hexane:acetone (3:1)	(Shin et al., 2007)
Dust	tetra- to hexa-BDEs	95 % (tetra-BDE) 94-107 % (penta-BDE) 89-104 % (hexa-BDE)	10%NaOH water:hexane (1:2)	(Regueiro et al., 2006)
Biological tissue	Tetra- and penta-BDEs	80-90 %	pentane:dichloromethane (1:1)	(Bayen et al., 2004)
Soil	tri- to hepta-BDEs	70-85 % (tri-BDE)** 60-95 % (tetra-BDE)** 85-95 % (penta-BDE)** 70-100 % (hexa-BDE)** 50-100 % (hepta-BDE)**	hexane:acetone (1:1)	(Wang et al., 2010)

\*\* Authors expressed recovery values only as percentage of the Soxhlet extraction recovery. No absolute recoveries were reported.

The only application on PBDEs extraction from soil samples does not include BDE-209 and recovery results are reported only in terms of relative recovery value normalised to the

compared Soxhlet extraction technique. However, one method for sewage sludge, the nearest analogue to peat and highly organic soils, does include BDE-209 (Shin et al., 2007). The extraction solvents used to extract BDE-209 is a mixture of hexane:acetone 3:1 resulting in a recovery of 105%. Considering that samples originating from sorption experiments will be water-saturated, the same solvent combination was tested on peat.

### 6.1.2 Pressurised liquid extraction (PLE)

Pressurised liquid extraction (PLE) often indicated also with the acronyms PSE (pressurized solvent extraction) or ASE (accelerated solvent extraction) is an automated technique for extraction of solid samples. Similarly to MAE, PLE works at elevated temperatures and pressures, achieving extraction in very short time (ca. 20 mins). From the physicochemical point of view, this is possible because higher temperatures increase the capacity of solvent to solubilise the analyte and diminish the solvent viscosity. As a result, the solvent can penetrate samples pores more easily. At the same time, higher pressure ensures that temperatures above the solvent boiling point can be reached without meeting with the problem of solvent gasification (Richter et al., 1996).

Since its invention, the use of PLE for extraction of organic compounds from environmental, food and biological samples increased considerably (Carabias-Martínez et al., 2005). PLE has been successfully applied specifically for extraction of several persistent organic pollutants like PCBs, chlorinated dioxins and furans, polycyclic aromatic hydrocarbons and organochlorine pesticides from sediments and soil samples (Antunes et al., 2008; Lang et al., 2005; Saim et al., 1997). But as Zhang et al. (2010) reported, literature about PBDEs extraction from soil is still limited. A list of PLE method for PBDEs extraction is listed in Table 6.2. Only two papers have been found for extraction from soil samples and five from sediment samples; of those, only three studies (1 soil and 2 sediment) include the BDE-209 congener. The considerations found in literature about the optimal PLE setup for extraction of PBDEs were taken into account for the selection of the PLE parameters.

Table 6.2: Literature review on PLE applied on PBDEs extraction form sediments and soil samples.

Solvent matrix	PBDEs congeners analysed	Recovery (%)	In cell clean-up	PLE method	Reference
River sediment reference material	mono- to octa-BDE	80-98 % (mono- & di-BDE) 71-102 % (tri-BDE ) 88-110 % (tetra- to hexa BDE) 104-116 % (hepta-BDE) 86-103 % (octa-BDE)	Forosil + silica gel	60 °C, 1500 psi, 1 cycle, acetone/hexane (1:1), 5 min static time, 20% flushing volume	(Park et al., 2009)
River sediment	mono- to hepta-BDE	22-41 % (mono-BDE) 46-82% (di-BDE) 53-82 % (tri- & tetra-BDE) 58-75 % (penta- & hexa-BDE) 46-53 % (hepta-BDE)	Alumina + copper	100 °C, 1500 psi, 2 cycles, hexane/dichloromethane (1:1), 10 min static time, 100% flushing volume	(de la Cal et al., 2003)
Coastal sediment	tri- to deca-BDE	Not reported	Alumina + copper	100 °C, 1500 psi, 2 cycles, hexane/dichloromethane (1:1), 10 min static time, 80-100% flushing volume	(Eljarrat et al., 2005)
Fish and river sediment	tri- to deca-BDE	Not reported	Alumina + copper	100 °C, 1500 psi, 2 cycles, hexane/dichloromethane (1:1), 10 min static time, 80-100% flushing volume	(Eljarrat et al., 2007)
River sediment	tri- to hexa-BDE	Not reported	Not applied	100 °C, 1500 psi, 1 cycles, hexane/dichloromethane (1:1), 10 min static time, 60% flushing volume	(Samara et al., 2006)
Soil (TOC 4.3%)	tetra- to deca-BDE	102 % (tetra-BDE) 104 % (penta-BDE) 94 % (hexa-BDE) 99 % ( hepta-BDE) 95 % (deca-BDE)	H <sub>2</sub> SO <sub>4</sub> acid silica	90 °C, 1500 psi, 3 cycles, hexane/dichloromethane (3:2), 4 min static time, 60% flushing volume	(Abdallah et al., 2013)
Non-calcareous clay-loamy top soil	tri- to hepta-BDE	102 % (tri- & tetra BDE) 99-103 % (penta-BDE) 86-92 % (hexa-BDE) 81 % (hepta-BDE)	Not applied	100 °C, 1500psi, 1 cycle, dichloromethane, 5 min static time	(Zhang et al., 2010)

## 6.2 Experimental procedure

### 6.2.1 Sample preparation

Extraction recovery was measured on spiked peat samples. Clean peat samples were spiked with a 9.5 or 5 mg/l solution of BDE-209 in acetonitrile and then extracted. The spiking method and the sample preparation technique were refined during the method development. Initially a fixed amount of peat were spiked, allowed to air dry for 24 hours to allow the solvent to evaporate and then sample were separated. Later, conditions more similar to the ones of real samples coming from the sorption experiment were reproduced. Thus peat was first mixed with deionised water and filtered, after that each sample was spiked and analysed still humid. Moreover cone and quartering techniques was implemented during sample preparation: from the original pot 3 kg of peat were isolated. From that approximately 175 gr of peat were isolated by a 4 steps cone and quartering and dried in oven (105 °C for 48 h). Finally 175 gr were separated again by cone and quartering to achieve the required amount for each batch. As the data of the next session will show, the standardisation of the sample preparation by cone and quartering and the spiking procedure are important steps to obtain consistent results working with such heterogeneous matrix like peat.

### 6.2.2 MAE

MAE extraction was performed in the MARS Express 5 Microwave reactor system (CEM Corp., North Carolina, USA). The oven was programmed for a temperature increase from room temperature to 130 °C over a 15 min period and then maintained for 20 min, while the pressure was monitored with a pre-set maximum of 150 psi. 0.5 g of peat were mixed directly in MARS Teflon tubes with 5 g of anhydrous Na<sub>2</sub>SO<sub>4</sub> to remove peat humidity, then 30 mL of the extraction mixture hexane:acetone (3:1) were added in the microwave vessels. All solvents were HPLC grade purchased by Thermo Fisher Scientific (Waltham, MA, USA). The extract was then filtered through 0.45 µm Teflon membrane, 5 mL of acetone were used to rinse the microwave tubes and filtered through the same syringe and membrane two times and following added to samples. Extraction was repeated at list in triplicate for each peat sample, a blank sample containing just anhydrous sodium sulphate Na<sub>2</sub>SO<sub>4</sub> and a

control sample containing clean peat were run every batch to check respectively for potential laboratory contamination and to measure the matrix interference.

### 6.2.3 PLE

Extractions were run using the Dionex ASE350 Accelerated Solvent Extractor (Thermo Fisher scientific, Waltham, Massachusetts, USA) using 10 mL stainless steel cells (Restek, Pennsylvania, USA). In most of PLE methods, temperature, pressure and static time were fixed at 100 °C, 1500 psi and 4-10 minutes, respectively, for two reasons.

Temperature and pressure values used (100 °C, 1500 psi) were the ones indicated as default settings by the instrument manufacturers, along with 5 min static time. Indeed, studies investigating the influence of those parameters on extraction efficiency reported that no significant improvement or even decreases in the extraction efficiency when higher temperature, higher pressure or longer extraction time were used (Abdallah et al., 2013; de la Cal et al., 2003; Park et al., 2009; Zhang et al., 2010).

Cells were filled from bottom to the top as it is schematised in figure 6.1: two cellulose filters were placed on the bottom to protect the ASE system ensuring no particles were migrating out of the cells; a first layer of DE was placed and gently compressed, when activated silica was used as sorbent 2 g (activated at 105 °C for 24 hours) were added in between the filters and the DE; thereafter sample was introduced and the remaining space filled with DE without any compression. The filling of the extraction cells is a delicate passage in the PLE extraction, and the following recommendations are suggested: do not over press the sample or the DE to avoid leaking problems; do not tightened too hard the cells caps to avoid they block after the extraction due to the high temperature and pressure reached during extraction.

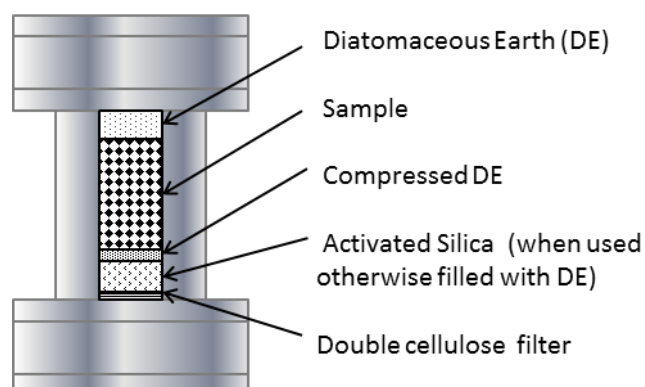


Figure 6.1: Packing of the PLE extraction cell.

The solvent flush percentage was kept at 100 % and 3 cycles were repeated considering the particularly challenging combination of the complex matrix and the lipophilicity of BDE-209, which is not expected to leave peat active sites easily. Three different combinations were investigated: 3 cycles of pure dichloromethane, 3 cycles of mixture hexane:acetone (3:1) and the combination of 2 cycles of hexane:acetone (3:1) plus 1 cycle toluene:acetone (3:1). Dichloromethane is an excellent extractor. Its affinity for hydrophobic compounds and at the same time its intermediate polarity makes it slightly more soluble in water than completely non-polar solvents like hexane, pentane or toluene. The combination of the hexane:acetone solved the problem of hexane immiscibility with the residual water in the sample avoiding the use of chlorinated solvents. The use of toluene, always mixed with acetone, has been explored due to the affinity to BDE-209 it showed in the LLE tests (Section 5.4.1). The three different solvents tested were associated to three different methods that will be from now on named ASE1 ASE2 ASE3 as it is shown in table 6.3.

Table 6.3: Extraction solvent used for PLE in the three methods tested on Dionex ASE350 extractor. All other parameters are the same: 100 °C, 1500 psi and 5 minutes static time, 3 cycles 100 % flush percentage.

Method name	Extraction solvent
ASE1	Dichloromethane, 3 cycles
ASE2	hexane:acetone (3:1), 3 cycles
ASE3	hexane:acetone (3:1), 2 cycles + toluene:acetone (3:1), 1 cycle

All solvents used were HPLC grade by Thermo Fisher Scientific (Waltham, MA, USA). ASE cells were rinse with methanol and acetone and dry in oven at 105 °C before each extraction. A blank sample containing DE was extracted with the same method use for sample extraction at the beginning and the end of each batch to have a control if any contamination from improper cell cleaning or the system. A rinse step was introduced before each sample to avoid sample to sample cross-contamination.

## 6.3 Results and discussion

### 6.3.1 Interference from peat extraction

Peat is a difficult matrix to analyse for organic compounds due to its high organic matter content and heterogeneous composition. The two extraction techniques (MAE and PLE) and three different solvent combinations were tested for BDE-209 extraction from peat. Several compounds were extracted along with BDE-209 from the matrix, including one interfering with BDE-209 analysis because it was eluting at the same retention time as BDE-209. The extraction techniques in combination with HPLC UV-detector were not selective enough to avoid the overlapping of matrix interference with the BDE-209 peak. Chromatograms in Figures 6.2 and 6.3 from clean peat samples extracted through MAE and PLE show the matrix interference peak eluting at 12.27 mins, which overlaps the BDE-209 peak at 12.45 mins.

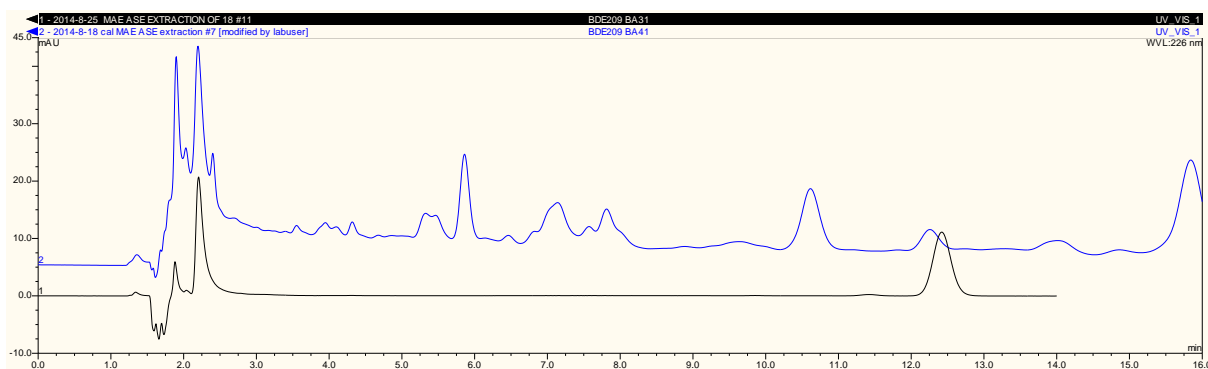


Figure 6.2: Chromatograms from clean peat sample (blue colour) and standard BDE-209 solution in acetonitrile 1.4 mg/L (black colour) extracted by MAE.

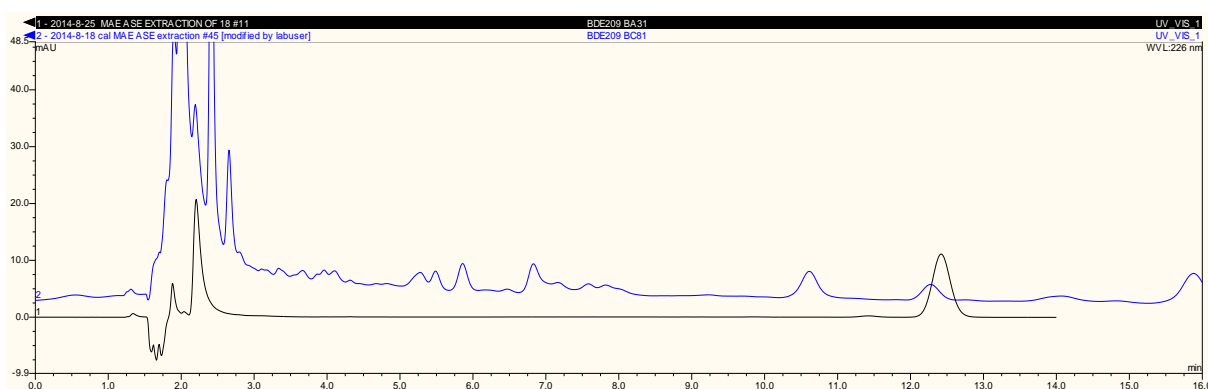


Figure 6.3: Chromatograms from clean peat sample (blue colour) and standard BDE-209 solution in acetonitrile 1.4 mg/L (black colour) extracted by PLE method ASE1.



When peat spiked with BDE-209 is analysed, the interference peak observed in clean peat samples is hidden in the BDE-209 peak (Figure 6.4). The presence of the interference peak hidden by the BDE-209 peak is indicated by two factors: the slight asymmetry of the BDE-209 peak and its early retention time with respect to the peak of BDE-209 in the standard solution. Indeed the BDE-209 peak from the standard solution (brown line) and the interference peak (black line) are symmetric. The BDE-209 peaks from the spiked peat (pink and blue line) instead present a tail on the right side because they are the result of the addition of two peaks shifted in time. Moreover, the retention time of BDE-209 peaks from spiked peat is intermediate between the retention time of the interference peak (12.27 mins) and the retention time of the BDE-209 peak from the standard solution (12.45 mins). Based on the comparison between 5 and 9.5mg/L initial spike, lower BDE-209 concentration in peat results in retention time shift towards the interference peak. The retention time is 12.42 mins for the high concentration sample (blue line) and 12.39 mins for the low concentration sample (pink line) (Figure 6.4).

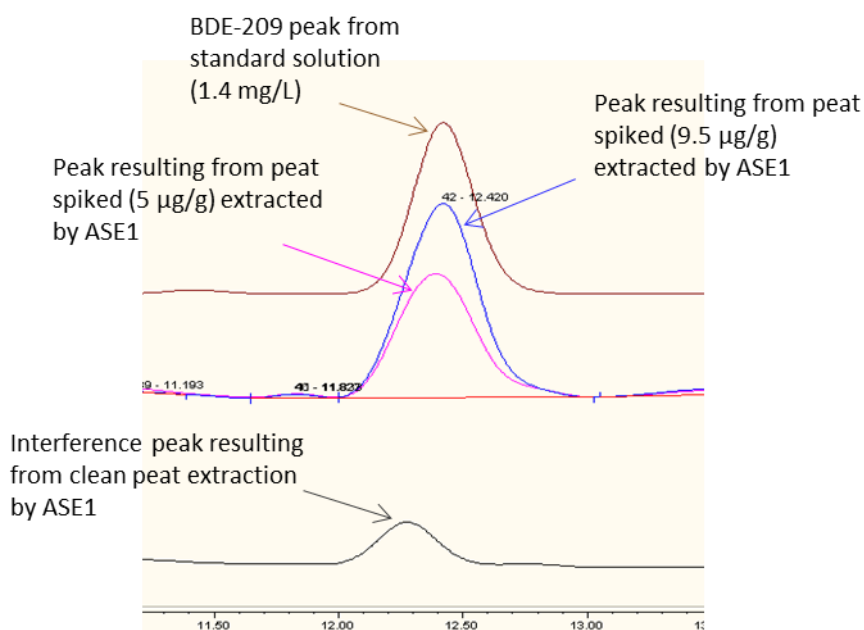


Figure 6.4: Zoomed chromatograms of BDE-209 acetonitrile standard solution 1.4 mg/L (brown line); spiked peat samples extracted with method ASE1 of PLE, concentrations 5 µg/g (pink line) 9.5 µg/g (blue line); clean peat sample extracted with method ASE1 PLE (black line)

HPLC reverse phase chromatography separates analytes mainly according to their hydrophobicity, the more the analyte is hydrophobic the later it will elute. The fact that the matrix peak coelutes with BDE-209 suggests that the interference compound has similar hydrophobicity and, thus, retention time to BDE-209. Therefore, standard clean up procedures that are based on solubility differences between interferences and analyte are not expected to be successful for this particular case. When in-cell clean up with activated silica gel has been tested for PLE extraction using method ASE3, the interference peak from clean peat samples was not significantly reduced: interference peak area expressed in apparent BDE-209 concentration was  $0.83 \pm 0.27 \mu\text{g/g}$  which is in the average of values obtained for extraction with method ASE3 without the silica layer  $0.95 \pm 0.25$  (figure 6.7). The use of acid silica gel for in cell clean-up has been found feasible for analysis of PBDEs in soil with a 4 % organic carbon content (TOC) (Abdallah et al., 2013) and may be worth exploring also for a high organic content matrices such as peat. This method is not feasible in stainless steel extraction cells and, instead, zirconium cells are required; applying acid silica gel clean up externally has not been explored because loss of BDE-209 during the additional sample handling steps is likely to eliminate the benefit gained by reducing the matrix interference peak. Therefore, the option of subtracting the interference from the BDE-209 signal as a blank subtraction has been considered.

Peat samples were spiked at low ( $5 \mu\text{g/g}$ ) and high concentration ( $9.5 \mu\text{g/g}$ ) and extracted with MAE, ASE1 and ASE2. For all the methods, if data without subtraction of the interference are considered, recovery values result higher in sample at low BDE-209 concentration and lower in the ones at higher BDE-209 concentration. Respectively recovery  $\pm$  the standard deviation for low and high concentration samples were  $101 \pm 9 \%$  and  $77 \pm 9 \%$  for ASE1,  $89 \pm 3 \%$  and  $67 \pm 6 \%$  for MAE and  $100 \pm 9 \%$  and  $85 \pm 3 \%$  for ASE2 (values indicated by the light grey column in figure 6.5 (a), (b) and (c)). Subtracting the interference instead, recovery values revealed that for neither of the methods the recovery depends on BDE-209 concentration and a constant value of recovery is measured despite the variation of the BDE-209 concentration:  $48 \pm 9 \%$   $48 \pm 9 \%$  for ASE1,  $55 \pm 3 \%$   $50 \pm 6 \%$  for MAE and  $70 \pm 9 \%$   $68 \pm 3 \%$  for ASE2 (values indicated by the dark grey columns in figure 6.4 (a), (b) and (c)). This suggests that both the recovery and the interference have a constant value and sensibly the interference has more significant effect on the measurement when samples at low concentration are considered. That supports the

feasibility of interference subtraction from the BDE-209 as in standard blank subtraction procedure. Number of repetitions for ASE extractions are limited at 2 because of the limited number of ASE cell available.

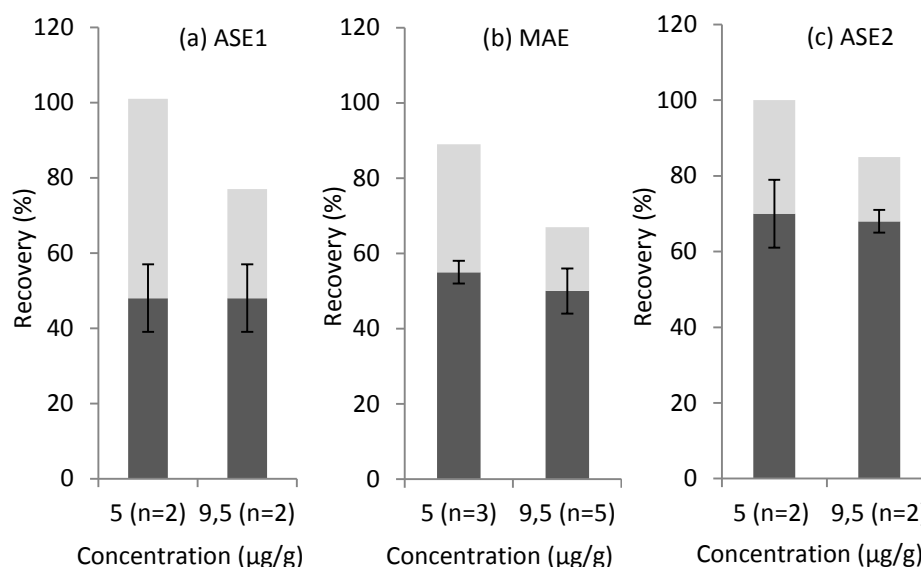


Figure 6.5: BDE-209 recovery from peat spiked at two concentrations 5 and 9.5 µg/g using different methods (a) ASE1 (b) MAE (c) ASE2 (n= number of repetition). Light grey columns indicate values calculated using the BDE-209 concentration measured as it is, values indicated by the dark grey columns are calculated after the subtraction of the interference.

### 6.3.2 Quantification of the interference peak in terms of apparent BDE-209 concentration

In attempt to establish an indicative value for the interference, several clean peat samples were extracted. Results in terms of apparent BDE-209 concentration are reported in figure 6.6. Data are separated by extraction method and batch of samples for evaluate both intra-batch and inter-batch variability of measurements. Before the adoption of the cone and quartering technique (batch 1,2 and 3), the variations within a single batch were smaller than the variations between batches. Variation from batch to batch (up to 60 %), irrespective of the technique (MAE or PLE) and extraction solvents used. In contrast, when repetitions of the same method were executed within the same batch (e.g. MAE method in batch 2 or ASE2 method in batch 3 and 4) variation was sensitively reduced. That suggested that the great variation of interference from batch to batch is probably due to the heterogeneous nature of peat. Indeed better homogenisation reached using cone and quartering (from batch 4 so on) consistently reduced the intra batch variability.

Focusing now on the results obtained in batches 1 and 2 (figure 6.6), MAE and PLE seems equivalent techniques in respect to the interference extraction and that main factor influencing the interference extraction is the extraction solvent. Indeed method ASE1 (extraction solvent: dichloromethane) extracted consistently 1.7 and 1.6 times the interference value detected with MAE (hexane:acetone 3:1). Instead using on PLE the same solvent used for MAE (method ASE2), the interference obtained was comparable to the one obtained with MAE (0.9 times) and considerably lower (0.6 times) than the one measured with method ASE1.

From a procedural point of view, PLE results advantageous because samples are automatically filtered in cell through the diatomaceous earth layer and this allows skipping the filtering passage after the extraction. On contrary samples from MAE extraction required an external filtration to separate the extraction solvent from the peat. Therefore PLE method was preferred to MAE and further attempts to improve the method have been done.

Considering now possible improvement on the extraction solvent used in PLE, a final method combining the use of hexane:acetone mixture for two cycle and toluene:acetone for the last cycle was tested (method ASE3). The introduction of method ASE3 reduced the interference extraction (figure 6.6) without losing in BDE-209 recovery (figure 6.9). The improvement gained with the method ASE3 in combination with the cone and quartering technique allowed to quantify the interference with acceptable variation from batch to batch. Based on the last three batches run with the method ASE3 (figure 6.6) the interference expressed in apparent BDE-209 concentration is equal to  $0.95 \pm 0.25 \mu\text{g/g}$ .

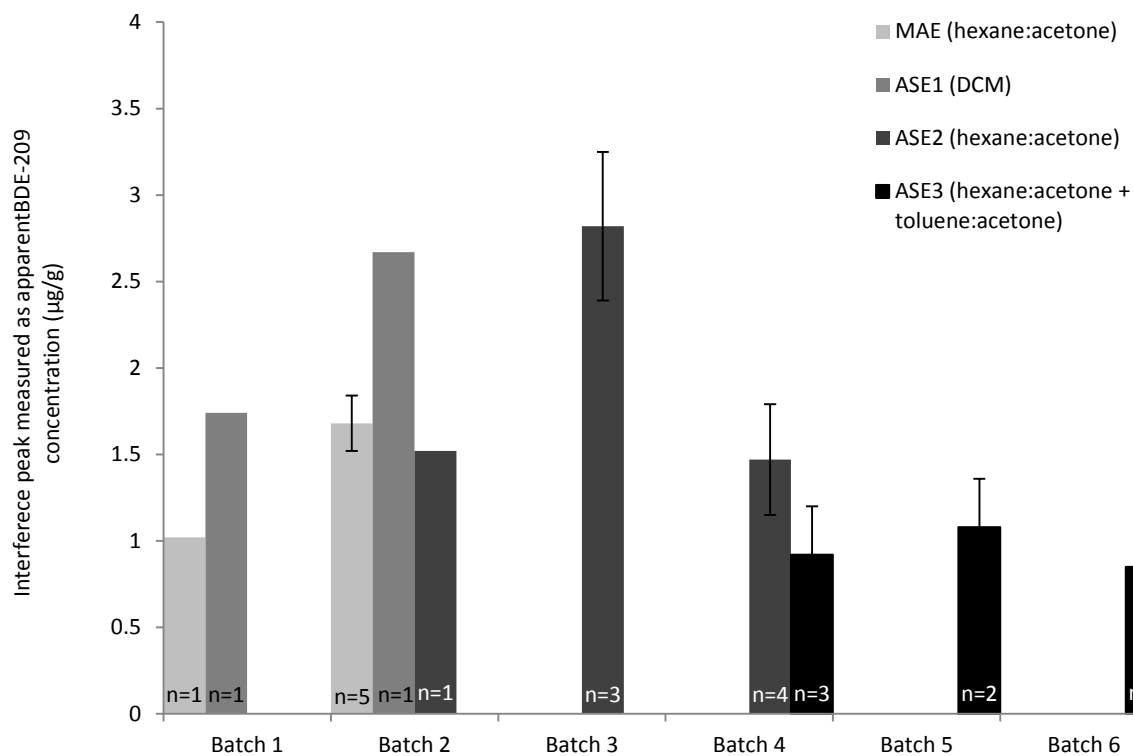


Figure 6.6: Matrix interference extracted from peat with the four methods tested expressed in apparent BDE-209 concentration (n=number of repetitions).

Values reported in Figure 6.6 are expressed in µg of apparent BDE-209 per g of peat in order to normalise interference to peat mass analysed. Figure 6.7 illustrates an apparent, positive linear correlation between the mass of peat and the mass of the interference compound. The maximal residual error between experimental data and the linear regression is  $\pm 0.2 \mu\text{g}$  (Figure 6.8) and the error does not seem to be dependent on the mass of peat analysed. Nevertheless the correlation coefficient ( $R^2=0.6$ ) is low, therefore in order to glean stronger conclusions on the linearity of the correlation, wider range of peat mass should be investigated. This kind of evaluation would be definitely important in case of environmental study of BDE-209 contamination on peat soil for avoiding overestimation of BDE-209 concentration. However it has been considered premature at the time the data were collected because the method were still not demonstrated feasible for the purposes of the study.

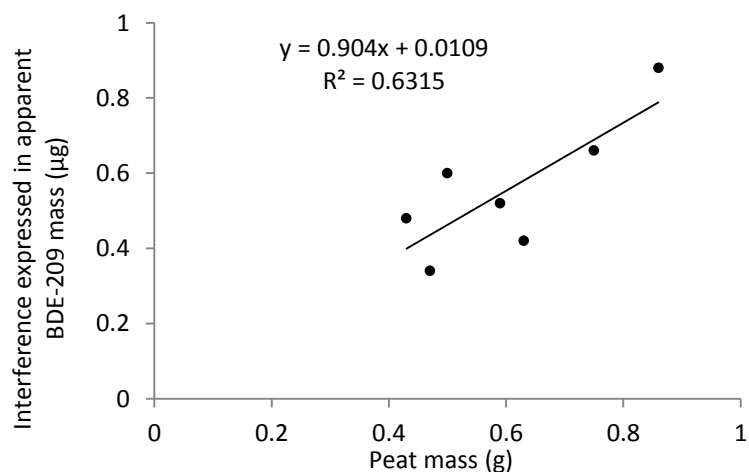


Figure 6.7: Correlation between the interference expressed in apparent mass of BDE-209 and the mass of peat analysed. Peat extracted with ASE 3method.

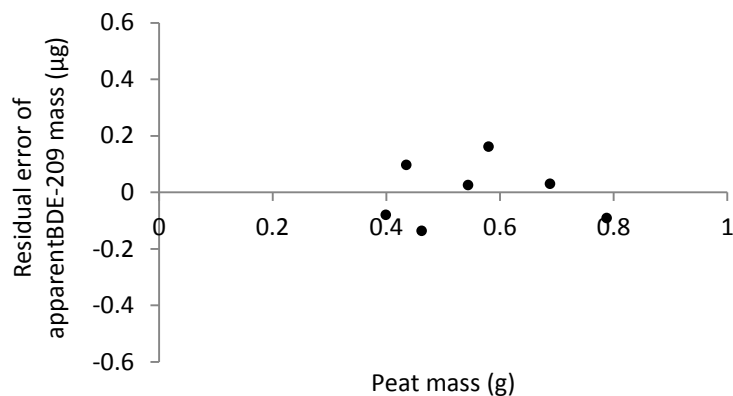


Figure 6.8: Plot of the residual error between experimental data and the linear interpolation for the apparent BDE-209 peak measured from peat extracted using ASE3 method.

### 6.3.3 Recovery values

BDE-209 recovery values change according to the extraction solvent and the extraction technique used. Figure 6.9 shows the recovery obtained for the different methods tested: dark grey column indicate the recovery after the interference subtraction; light grey columns indicate the effect of the interference on the recovery when it is not subtracted from the BDE-209 signal. Using the same extraction solvents (hexane:acetone), PLE appears to be more efficient than MAE: recovery is  $70 \pm 9 \%$  for ASE2 and  $55 \pm 5 \%$  was obtained with MAE. The use of dichloromethane in PLE extraction is not suggested because a reduction in recovery is observed ( $48 \pm 9 \%$ ) against an increase in the interference. The

introduction of a cycle of toluene:acetone instead is recommended as it improves the BDE-209 extraction to  $90 \pm 10 \%$  without increasing the interference extraction. Recovery from extractions of cells filled just with spiked diatomaceous earth (DE) and DE plus the glass fibre filter with method ASE3 were  $99 \pm 3 \%$  and  $101 \pm 2 \%$  respectively. Thus any loss due to sample handling during the analytical procedure has been excluded.

The final method suggested for BDE-209 analysis in peat soil is 2 cycles extraction with Hexane:acetone (3:1) followed by 1 cycle toluene:acetone (3:1).

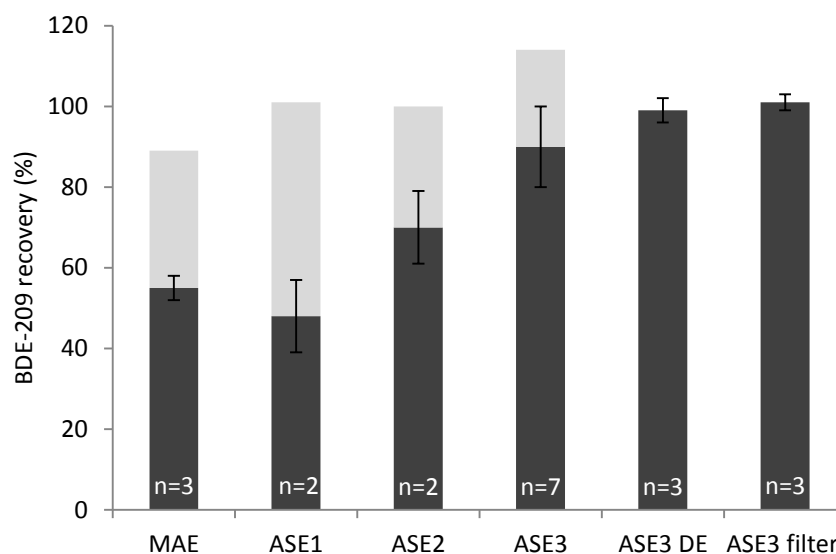


Figure 6.9: BDE-209 recovery from peat sample spiked at  $5 \mu\text{g/g}$  (dark grey columns) and interference influence (light grey column) for microwave assisted extraction (MAE) and different pressurised liquid extraction methods (ASE1, ASE2, ASE3). In sample ASE3 DE diatomaceous earth was spiked and ASE3 filter diatomaceous earth plus the glass fibre filter (n=number of repetitions).

### 6.3.4 Measurement uncertainty and limit of detection

The matrix interference value results not negligible and it has been quantified at  $0.95 \pm 0.25 \mu\text{g/g}$ . The range of applicability of the subtraction method needs now to be evaluated. According to error propagation theory, the standard deviation of a linear combination of two measurements A and B can be calculated from the standard deviation of the two measurements ( $\sigma_A$  and  $\sigma_B$ ) with Equation 6.1. In this case, the two measurements A and B are the BDE-209 and the interference concentrations, which are independent variables. Therefore the parameters a and b are both equal to one and the terms containing the covariance are null. Under this hypothesis, Equation 6.1 is simplified to Equation 6.2. Considering that the standard deviation of the two measurements are  $\pm 0.25 \mu\text{g/g}$  for the

interference and  $\pm 0.13 \mu\text{g/g}$  for the BDE-209, the error on the difference of the two measurements is equal to  $0.28 \mu\text{g/g}$ .

$$\sigma = \sqrt{a^2 \cdot \sigma_A^2 + b \cdot \sigma_B^2 + 2ab \cdot \sigma_{AB}} \quad \text{eq. 6.1}$$

$$\sigma = \sqrt{\sigma_A^2 + \sigma_B^2} \quad \text{eq. 6.2}$$

For calculating the method detection limit, the same approach used for the instrumental limit of detection (LOD) is used. The interference value becomes the new baseline noise and a value equal to  $3\sigma$  is added to the interference to identify the limit of detection. The  $\sigma$  chosen for the LOD calculation is the higher between the one of the interference ( $\pm 0.25 \mu\text{g/g}$ ) and the one of the BDE-209 measurement ( $\pm 0,13 \mu\text{g/g}$ ) and the one calculated for the difference ( $\pm 0.28 \mu\text{g/g}$ ). According to this calculation, the limit of detection of the method is  $1.8 \mu\text{g/g}$ . This limit needs now to be compared with the range of interest in the experiments. In regard to the peat sorption experiment, considering water samples of 200 mL and limitations imposed by the low solubility of BDE-209 in water, the mass of BDE-209 added in each sample is about 2-3  $\mu\text{g}$ . The amount of peat added in a single sample is 0.5 g. Therefore, the concentration expected to be measure in peat are between zero and 4-6  $\mu\text{g/g}$ . Being able to measure concentration in peat higher than  $1.8 \mu\text{g/g}$  would mean to lose 30-50% of the sorption data. Therefore the traditional approach of the measuring the analyte remained dissolved in water and infer from that the mass absorbed using the mass balance equation will be applied.

## 6.4 Conclusions

For the first time a method for BDE-209 extraction from high organic matter content soil has been developed. Recovery of 90 % has been achieved extracting peat with PLE (2 cycles of hexane:acetone followed by 1 cycle of toluene:acetone).

The study highlighted the presence of chemicals which interfere with the measure of BDE-209 by HPLC in peat. The interference peak from the peat matrix was quantified about  $0.95 \pm 0.25 \mu\text{g}$  per g of peat in terms of apparent BDE-209 concentration. Cone and quartering demonstrated to be a valid technique for reaching good homogenisation of peat samples up to 0.5 g.



The interference extraction resulted enhanced by the use of dichloromethane, therefore carefulness in the use of dichloromethane when working with soil reach in peat is suggested.

The presence of the interference limits the applicability of the method to sample containing BDE-209 at concentration higher than 1.8 µg/g. Due to this limitation and the restriction imposed by BDE-209 low solubility, the method is not suitable for being use in the sorption experiments. The method might be improved including in cell acid clean-up when the PLE instrument is equipped with zirconium cells. The method cloud be applied for extracting environmental soil samples, prior an evaluation of its efficiency on aged contaminated soil, as it is well recognised an increased difficulties in extracting HOC form aged samples compared to laboratory spiked ones (Loibner et al., 2015).

## **7 BDE-209 sorption on peat and kaolin**

### **7.1 Introduction**

The aim of this chapter is to investigate BDE-209 sorption in soil, in particular BDE-209 sorption on peat and kaolin are compared. Investigating sorption in batch for single matrixes separately makes the experimental conditions even more different from the one occurring during sorption on natural soil in the environment. The study therefore does not claim to mimic sorption in soil under environmental conditions. On the other hand, the approach simplifies the system conditions allowing for an easier observation of new factors involved in BDE-209 sorption in the single soil matrixes, like for instance the influence of the dissolved organic matter on the sorption process.

The two soil matrixes selected for this study have opposite characteristics. Peat is an organic matter rich soil formed by degradation of vegetal biomass. It gets formed through a biochemical process carried under the influence of aerobic micro-organisms in the surface layers of the vegetal deposits. It is a typical soil component in the topsoil of northern regions (European Soils Bureau Network, 2005) and covers more than 3 % of earth land surface (Clymo, 1987). Peat is a natural mix of variegated organic substances. Its heterogeneity makes peat a difficult but interesting substrate to investigate, because it contains a wide essay of the organic constituents commonly found in the soil organic fraction. Kaolin is a common component of the mineral soil fraction and between the clay minerals is the one with the simplest structure (shown in Appendix A). It does not show swelling properties like montmorillonite or bentonite therefore the adsorption of chemical is mainly due to interaction of chemicals on the mineral surface reducing at minimum the retention due to trapped water.

### **7.2 Methodology**

#### **7.2.1 Materials**

Decabromodiphenyl ether standard (98% purity) was purchased from Sigma-Aldrich (Gillingham, Dorset, UK). Spiking solutions of BDE-209 were prepared in acetonitrile by weighting the analyte on a microbalance (MC-5 microbalance, Sartorius, Epsom UK).

Concentrations were double checked by HPLC before each experiment with the same method used for samples analysis following resumed. Acetonitrile, acetone, methanol, and tetrahydrofuran were of analytical HPLC grade (Fisher Scientific UK Ltd, Leicestershire, LE11 5RG-UK). Deionised water was collected from the laboratory reverse osmosis deionizing system (RO180 El-Ion® twin-stage, SG, Germany).

### 7.2.2 Solid matrix Characterisation

Peat was purchased from Northern Peat & Moss Co (Peterhead, Aberdeenshire AB42 4JJ). It was extracted from a natural bog and the product was sent in its natural form without any additional manipulation. When received peat was sieved through 2 mm mesh and stored at 4 °C. Speswhite™ clay was purchased from IMERYS (IMERYS performance & filtration minerals, Par Cornwall, PL242SQ-UK). Speswhite is an ultrafine particle size kaolin from deposits in the South West of England. Characteristics of the two matrixes are summarised in Table 6.1. pH and electro conductivity (EC) of peat and kaolin were performed with a pH/conductivity meter (Mettler-Toledo S70-K SevenMulti, Toledo OH, USA) following standard procedures for measurements in soil samples (BSI, 1880, 2011a). Particle grading curves were generated through laser diffraction Mastersizer (Mastersizer 2000, Malvern, Worcestershire UK) equipped with disperser unit control (Hydro 2000SM). The particle size range is reported in Table 6.1, more detailed information about the sample preparation and the complete grading curve are reported in Appendix B. Organic matter content was measured by loss-on-ignition (ASTM, 1993; BSI, 2011b). Ignition temperature suggested in standard methods is  $450 \pm 25$  °C, but sometimes higher temperature (550 °C) are used (Badea et al., 2014). Here both temperatures (450, 550 °C) are tested after samples were oven-dried at 105 °C. For each temperature (105, 450, 550 °C) series of heating and measurement were repeated until the variation between two successive measurements were less or equal to 0.01 g. Data are reported in figure 6.1 as w/w percentage of the dry sample weight. Total organic carbon content (TOC) and total carbon (TC) reported in Table 7.1 were determined by a TOC combustion (800 °C) analyser APOLLO 9000 (Tekmar-Teledyne instrument, AZ USA) equipped with a boat sampler (Model 183 TOC Boat Sampler, Tekmar-Teledyne instrument, AZ USA) using 40 mg of sample pre-dried at 105 °C for 48 h.

Table 7.1: Peat and kaolin characterisation

Matrix	pH	EC ( $\mu\text{S}/\text{cm}$ )	Particles size (mm)	Water content (%)
Kaolin	$5.0 \pm 0.005$	$327 \pm 37$	0.0003-0.020	$0.9 \pm 0.2$
Peat	$3.4 \pm 0.01$	$718 \pm 4.6$	0.003-2	$22 \pm 1$

Matrix	SOM (%) 450 °C	SOM (%) 550 °C	TC (%)	TOC (%)
Kaolin	$0.9 \pm 0.3$	$12 \pm 0.5$	$0.04 \pm 0.001$	$0.02 \pm 0.001$
Peat	$93 \pm 1.4$	$93 \pm 1.2$	Out of range	Out of range

For TOC measurements, a pre-treatment with phosphoric acid was used to eliminate the inorganic carbon fraction in form of carbonates or bicarbonates: 40  $\mu\text{l}$  of phosphoric acid solution were added and sample heated into a 70 °C oven for 15 minutes before the analysis. More details on the procedure are reported in Appendix B.

Peat degree of humification has been visually evaluated according the Von Post Scale of Humification (Andriess, 1986). It was classified as slightly (H4) to moderately (H5) altered peat, which corresponds to a 20-40 % degree of decomposition. Coloration of water after contact with peat and filtration suggested variation in water properties (Figure 7.1) possibly caused by the released in water of the soluble organic fraction of peat. TOC measurements on water filtered (0.3  $\mu\text{m}$ ) after being mixed with peat for 5 days were accomplished (Figure 7.2). Approximately 347 mg of organic carbon are released in water per gram of peat mixed.



Figure 7.1: water mixed with peat after 0.3  $\mu\text{m}$  filtration; TOC 857mg/L (left) compared with pure water (right).

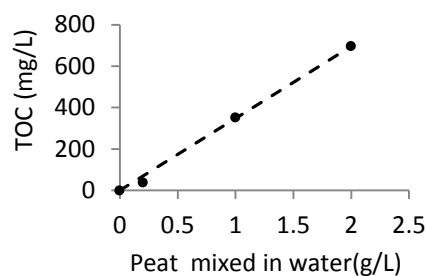


Figure 7.2: Total Organic Carbon (TOC) measured in water (200mL) after 5 days of contact with 0, 0.04, 0.2, 0.4 g of peat.

### 7.2.3 Experimental setup

Several experiments have been conducted for studying sorption kinetic and isotherm for BDE-209 sorption and desorption on peat and kaolin. In the following section the general procedures in common with all the experiments and in the following ones specific details for each single experiment are provided.

#### 7.2.3.1 General procedures

##### Control samples

Working with HOC, particular care needs to be given to possible loss of analyte on glass surfaces (Muwambaa et al., 2009). Therefore, in all the experiments, two kinds of control samples were prepared and analysed in parallel with samples: water control samples ( $S_W$ ) containing just water and BDE-209 and matrix control samples ( $S_M$ ) containing sorbent and water without BDE-209. The former were used to measure BDE-209 lost during the experiment due to sorption on material other than the sorbent (e.g. bottles caps and glass surfaces) while the latter were used to determine that no interferences from matrix or external contamination were present.

##### Sorbent/water ratio

The sorbent/water ratio adopted in other studies for investigating PBDEs kinetic sorption in soil (TOC in the range of 0.09-4.42) for PBDEs other than BDE-209 (BDE-15,-28,-47) are in the range 1:20-1:500 (Liu et al., 2010, 2011, 2012; Olshansky et al., 2011). Considering the high content of organic matter in peat (93%) and the higher hydrophobicity of BDE-209, the smallest soil-water ratio allowed by experimental limitation was selected. Preliminary

studies showed that cone and quartering is a suitable technique for preparing 0.5 g samples with acceptable homogeneity (Section 6.3). It was concluded that peat/water ratio of 1:400 guarantees manageable sample volume (200 mL) and sample homogeneity (0.5 g dry weight). Differently from peat, clay does not present homogeneity problems and it was possible to achieve smaller clay-water ratios directly in the centrifugation glass (50 mL) vials. The amount of kaolin added varies depending on the experiments; the kaolin/water ratio used is specified in the single experimental description.

#### Shaking and sorbent separation

Sample bottles sealed with PTFE screw cap were protected from UV radiation and shaken on either orbital shaker for bigger samples (Standard analog shaker, VWR International, Lutterworth, UK) or roller shaker (Roller mixer SRT1, Bibby-Stuart Scientific, Stone UK) for smaller ones. When the desired contact time was reached, water fraction was separated from the solid sorbent. Peat samples were vacuum filtered through 0.3  $\mu\text{m}$  glass fibre membrane filter on glass wool (GF-75-90mm, Sterlitech, Kent USA). Kaolin particles were separated by centrifugation (Centrifuge 5804R, Eppendorf, Stevenage, UK) at 2000 rpm for 20 minutes (equivalent acceleration 11.3 G). Filtration and centrifugation are commonly applied separation techniques. Centrifugation (Ahn et al., 2005; Liu et al., 2012, 2010; Olshansky et al., 2011) as well as filtration (Choi et al., 2009; Osako et al., 2004) have been previously used in experiments involving BDE-209 and other PBDEs. An experimental comparison of the two techniques is not possible because centrifugation has not been found effective on peat, and clay particles plug the filter making filtration unsuitable for kaolin samples. Nevertheless in literature a comparison of the effect of filtration and centrifugation for PCBs concentration in leachate samples from incineration residues has been found (Sakai et al., 2000). Filtration and centrifugation for the separation of particles < 0.45  $\mu\text{m}$  produced different results in terms of PCBs measured in the leachate: concentration in centrifuged samples were much higher than the one measured in filtered samples. The reason of the mismatch is the different efficiency of the separation techniques in retaining particles smaller than 0.3  $\mu\text{m}$ , on whom PCBs are adsorbed: centrifugation resulting less effective than filtration. In this study samples exposed to centrifugation (kaolin samples) do not contain particles smaller than 0.3  $\mu\text{m}$  (Appendix B) or if a small amount of fine particle is present it would be so small that ensures the effect observed in the cited study is not relevant in this case. As further precaution, conservative

centrifugation time has been adopted (Section 4.7) and, even if dissolved BDE-209 molecule by definition should not be affected by centrifugation, the possible effect of centrifugation on BDE-209 molecules has been estimated: considering if BDE-209 molecules behave like suspended particles with density  $3.35 \text{ g}\cdot\text{cm}^{-3}$  and radius  $1.86\cdot 10^{-8} \text{ cm}$  (Hu et al. 2005), the centrifugation time used for setting clay particles (20 minutes) should not affect BDE-209 molecules suspension, which has a sedimentation time of 6500 days (Section 4.7).

#### Solid phase extraction

An efficient extraction method for kaolin extraction was adapted from literature (Ahn et al., 2005). After removal of water, kaolin particles were re-suspended in 5 mL of tetrahydrofuran (THF):water (7:3) solution and shaken in incubator (MaxQ 5000, brand, Thermo Scientific, Renfrew, UK) for 24 h at 30 °C. Solid phase extraction for peat has not been found appropriate because of the presence of interfering compounds (see Chapter 6).

#### HPLC analysis

In preparation of HPLC analysis, water and THF:water solution were pre-concentrated (Syncore Polyvap, BUCHI, Flawil Switzerland), evaporated under gentle nitrogen flow (TECHNE DB-3D Dry Block, Bibby Scientific, Staffordshire UK), and redissolved in acetonitrile (2 mL). Samples were injected through  $0.2 \mu\text{m}$  PTFE syringe filter into amber HPLC vials and stored at 4 °C. BDE-209 concentration was analysed using methanol as mobile phase on reverse-phase HPLC (ZORBAX Eclipse XDB-C18,  $5 \mu\text{m}$ , 150 mm x 4.6 mm column on Thermo Scientific Dionex UltiMate 3000) with a deuterium lamp UV detector (226-nm wavelength) (Chapter 4). Preliminary studies (Chapter 5) showed recovery of  $97 \pm 3\%$  and  $68 \pm 8\%$  for pure water and water that has been in contact with peat, respectively. To better control the recovery, water samples in contact with peat were injected with 1 mL of chrysene solution ( $110 \mu\text{g}/\text{mL}$ ) before sample evaporation and measured BDE-209 concentration was corrected by chrysene recovery (Chapter 5). Samples from experiment run with water enriched with peat organic matter and kaolin were instead corrected by the average recovery value of 68 %.

#### Mass balance

For experiments in which peat was the sorbent matrix, only mass dissolved in water was directly measured. The mass of BDE-209 sorbed on peat ( $m_s$ ) was then calculated by mass balance, subtracting the final mass measured in water ( $m_w$ ) from the total initial mass ( $m_T$ ), as shown in equation 7.1:

$$m_s = m_T - m_w \quad \text{Eq. 7.1}$$

In experiments where kaolin was the sorbent matrix, mass adsorbed on particles ( $m_s$ ) was independently measured by extracting kaolin with THF-water solution. The mass balance equation was used as a control on total recovery, as shown in equations 6.2 and 6.3:

$$m_s = \text{THF extraction} \quad \text{Eq. 7.2}$$

$$m_T = m_w + m_s + m_g \quad \text{Eq. 7.3}$$

where  $m_T$  is the known BDE-209 mass initially dissolved in water,  $m_w$  is the BDE-209 mass measured in the water fraction, and  $m_g$  is the BDE-209 mass adsorbed on glass and cap surfaces on water control samples.

#### 7.2.3.2 Sorption kinetics of BDE-209 on peat and kaolin

The kinetic experiments were design in completely mixed batch reactors following the parallel method as described in the OECD guideline for adsorption/desorption experiments (OECD, 2000). Several parallel samples were prepared and the whole water fraction of each sample was analysed at different contact times. In this way, high concentrations factors were achieved, which ensured the BDE-209 to be above the instrument detection limit (4  $\mu\text{g/L}$ ). No salt was added to avoid possible salting out effect; the addition of NaCl in water solution has been shown to increase the escape of analyte from the water phase and the effect has a positive correlation with molecular volume and analyte hydrophobicity (Endo et al., 2012). In all experiments, deionised water was used to avoid complexities and ensure repeatability.

Using a micro syringe, 200  $\mu\text{L}$  of BDE-209 solution (14 mg/L) was added to 200 mL of water in peat samples and 50  $\mu\text{L}$  of BDE-209 solution (7.3 mg/L) was added to 50 mL of water in kaolin samples maintaining 0.1 % (v/v) acetonitrile concentration to minimise co-solvent effects (OECD, 2000). 0.1 g of Kaolin were added in water obtaining kaolin/water ratio of



1:500. Peat samples were analysed after 1, 4, 6, 11, 25, 36, 49, 55, 73, 145, 169, 193, 218, and 241 hours. Because of faster kinetics for kaolin, samples were analysed at 0.5, 1.5, 4, 18 and 24 hours contact time. Figure 7.3 illustrates the steps for samples processing in experiments run with peat and kaolin.

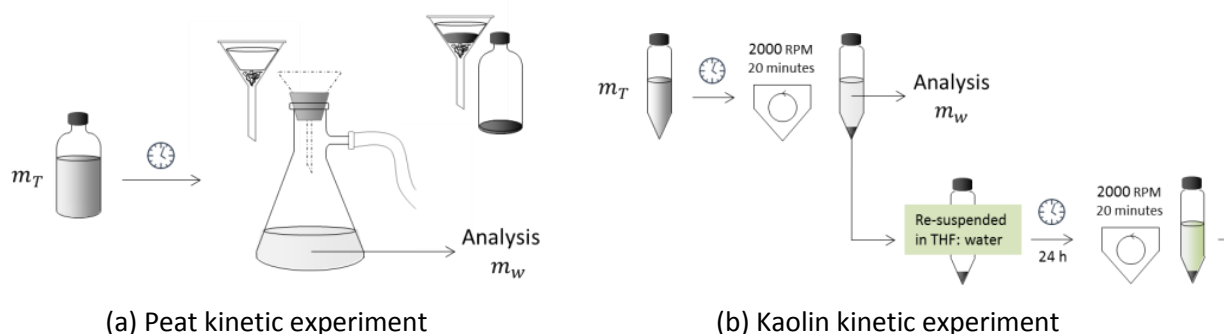


Figure 7.3: Schematic representation of samples processing step in kinetics experiments.

### 7.2.3.3 BDE-209 sorption isotherms on peat

Sorption isotherm was produced for BDE-209 sorption on peat under restricted experimental conditions. Due to limitations imposed by the low solubility of BDE-209, it was not possible to achieve initial concentrations varying in more than one order of magnitude (1.2, 2.3, 3.6, 6.9, 8.5 and 10.7  $\mu\text{g/L}$ ). Due to the small amount of BDE-209 in water and losses due to sorption to the glass, it has not been possible perform the isotherm experiment at equilibrium time (8-10 days). Results from the sorption kinetic shows indeed that starting from an initial concentration of 14  $\mu\text{g/L}$ , after 10 days less than 0.3  $\mu\text{g/L}$  remained dissolved in water. To ensure measurable concentrations even in samples with a starting concentration of 1.21  $\mu\text{g/L}$ , a shorter contact time of 5 days has been selected. The isotherm obtained is considered therefore a non-equilibrium isotherm. Two series of 6 samples were prepared, samples S containing peat and BDE-209 and water control samples ( $S_w$ ) containing just BDE-209. Sample processing is the same described above.

### 7.2.3.4 BDE-209 sorption and desorption from kaolin in non-equilibrium conditions

BDE-209 adsorption and desorption from kaolin has been tested measuring BDE-209 re-suspended in water after the sorption step following the procedure schematised in Figure 6.4. Through a micro syringe 50  $\mu\text{L}$  of BDE-209 solution (10.2  $\text{mg/L}$ ) were injected in 50 mL of pure water. Kaolin in the amount of 0.05, 0.1 or 0.5 g was added to obtain respectively clay/water ratios of 1/1000, 1/500, 1/100. After 2 minutes samples were centrifuged and

water fraction was directly analysed ( $m_w$ ). Kaolin was re-dissolved in deionised water, vigorously shaken to re-suspend kaolin particles, and agitated on the roller shaker for 2 minutes protected by light. After centrifugation, BDE-209 in the water phase was analysed to measure the mass of BDE-209 desorbed in water ( $m_d$ ). Finally kaolin was extracted with the THF:water (7:3) solution for measuring the BDE-209 mass remained adsorbed on clay ( $m_s$ ).

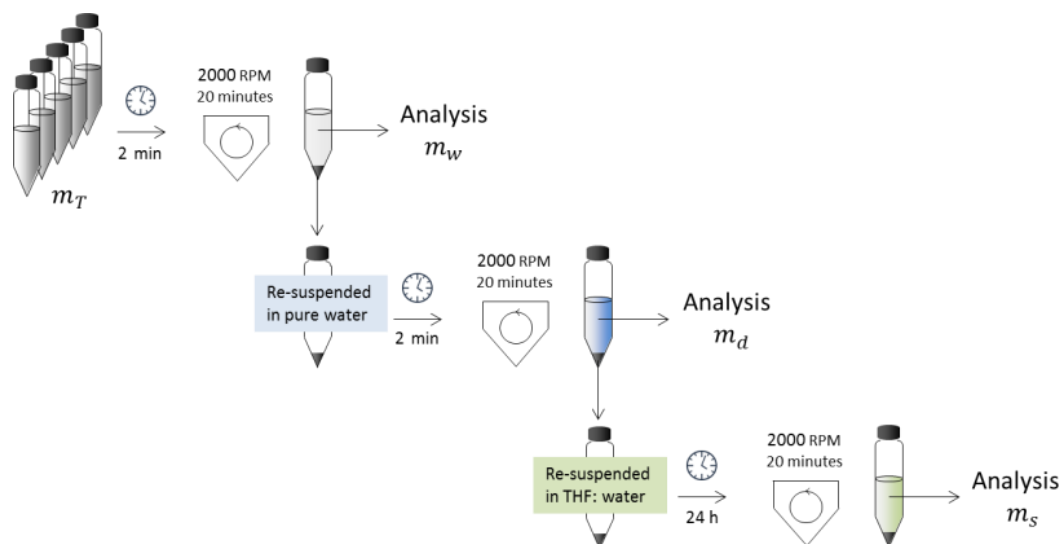


Figure 7.4: Schematic representation of samples processing steps in kaolin desorption experiments.

#### 7.2.3.5 Influence of DOM on BDE-209 sorption on kaolin

Water enriched with peat dissolved organic matter was prepared by adding 0.5g of peat (dry weight) to 200 mL of pure water and shaking for 5 days. The DOM enriched water was then filtered through a 0.3  $\mu\text{m}$  glass fibre filter following the same procedure as used for peat. The content of the bottles was finally mixed to obtain a matrix the most homogenous possible before transfer it in 50 mL tubes. Kaolin in the amount of 0.05, 0.1 or 0.5 g was added to obtain clay/water ratio of 1/1000, 1/500, or 1/100, respectively. After samples were shaken for 2 minutes, the kaolin suspension was transferred to new centrifugation tubes taking care to minimise the amount of clay particles remaining attached to the glass surface. The original tubes were extracted with THF:water solution to measure the BDE-209 mass that may remain attached to glass surfaces. Water and clay suspension transferred to the second tubes were centrifuged and water fraction was directly analysed for measuring BDE-209 mass dissolved. The clay fraction was re-suspended and extracted with the THF:water (7:3) to measure the mass adsorbed by kaolin ( $m_s$ ). The procedure is illustrated

in the scheme in Figure 6.5. The experiment was repeated two times: one using water spiked with 50  $\mu\text{l}$  of BDE-209 solution (10.4 mg/L) as the liquid phase and the other using DOM enriched water spiked with 50  $\mu\text{l}$  of BDE-209 solution (7.2 mg/L).

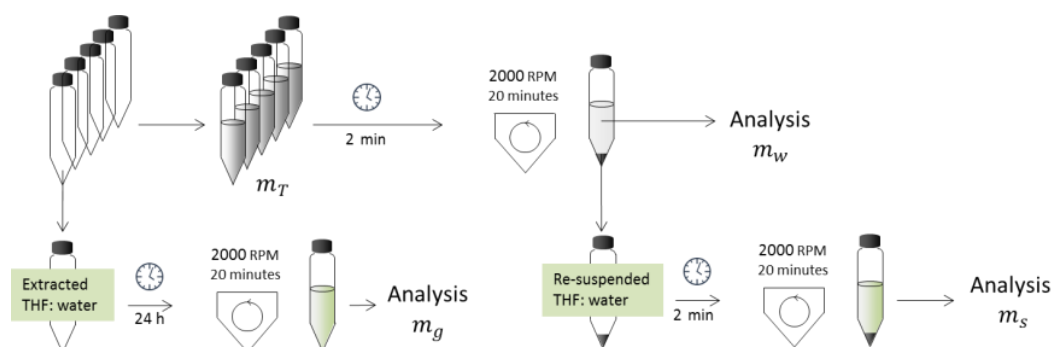


Figure 7.5: Schematic representation of samples processing steps in experiments for DOM influence on kaolin sorption.

## 7.3 Results and discussion

### 7.3.1 Sorption kinetics of BDE-209 on peat

Analysis on the peat control samples  $S_M$  showed that the dissolvable fraction of peat organic matter is not interfering with BDE-209 measurement and no contamination during the experiment was occurring. Measurement of dissolved BDE-209 in water control samples  $S_W$  and samples  $S$  are shown in Figure 7.6 (a). After the first hour, the mass dissolved in water from samples decreased to 1.54  $\mu\text{g}$ , which represent the 55% of the initial mass added in the system (2.78  $\mu\text{g}$ ). A similar drop (40%) is observed also in water control samples  $S_W$ . The loss of analyte due to sorption on container walls is a known problem when working with strongly hydrophobic compounds and the use of glass and PTFE is not a sufficient countermeasure to undergo this problem (Muwambaa et al., 2009). Loss of analyte may be avoided by rinse the container surface with a mix of organic solvent and water. Tests run during the extraction method development (Chapter 5) demonstrated that rinsing with acetone is an efficient solution and it allowed reaching high recovery values. Nevertheless, there are steps during sample preparation in which washing the glass surface could cause a partial extraction of BDE-209 from peat particles (e.g. during transferring of samples from the bottle to the filtering apparatus and during the filtering process itself). Therefore water control samples became an essential reference for the data analysis that follows.

After the initial drop, BDE-209 mass dissolved in water ( $m_w$ ) in samples (S) follows an exponential profile

$$m_w(t) = 1.40e^{-0.011t} \quad \text{Eq. 7.4}$$

and BDE-209 mass dissolved in water ( $m_w$ ) in water control samples ( $S_w$ ) a logarithmic curve (Figure 7.6 (a))

$$m_w(t) = 1.66 - 0.12\ln(t) \quad \text{Eq. 7.5}$$

Linearization of experimental data shows that they are well represented by equation 7.4 and 7.5: for water control samples,  $m_w$  is plotted with the natural logarithm of time (Figure 7.6 (b)); for samples containing peat, the natural logarithm of BDE-209 mass dissolved in water ( $m_w$ ) divided by the initial mass added in the system is plotted in time (Figure 7.6 (c)).

The fact that BDE-209 mass dissolved in water control samples is not constant indicates that even the sorption of BDE-209 on container surfaces is not instantaneous, but it follows its own kinetics. It is possible to speculate that a fast sorption to all available surfaces (glass surfaces and PTFE cap septa) might be related with the fast loss happening in the first hour corresponding to 40 % of total initial mass, followed by a slow diffusion of the BDE-209 through the polymer responsible for an additional loss of 18 % of the initial mass. More investigation would be required to confirm this interpretation. However the sorption on container walls observed in water control samples is likely happening in some proportion also in samples S containing peat and there is no way to experimentally uncouple the two phenomena. The proportion at which the sorption on container surfaces influences data obtained for samples S is not known, indeed in presence of peat suspended in water a competition is established between the container surfaces and peat, therefore the amount of BDE-209 adsorbed on the container surfaces could be lower than the one measured in absence of peat. That complicates the application of the mass balance equation for the determination of  $m_s$  sorbed on peat, and two extreme scenarios are considered: a) in presence of peat suspended in water, BDE-209 molecules can reach peat easier than the container surface and get attracted on the lipophilic particles ignoring the container surfaces. Therefore the kinetic profile observed for samples (S) (Figure 7.1) represents exactly the net absorption on peat particles; b) even in presence of peat the amount of

BDE-209 adsorbed on the container surfaces does not change. In this second case, the BDE-209 mass sorbed by container surfaces in water control samples should be subtracted from the BDE-209 mass sorbed by peat to obtain the net sorption profile.

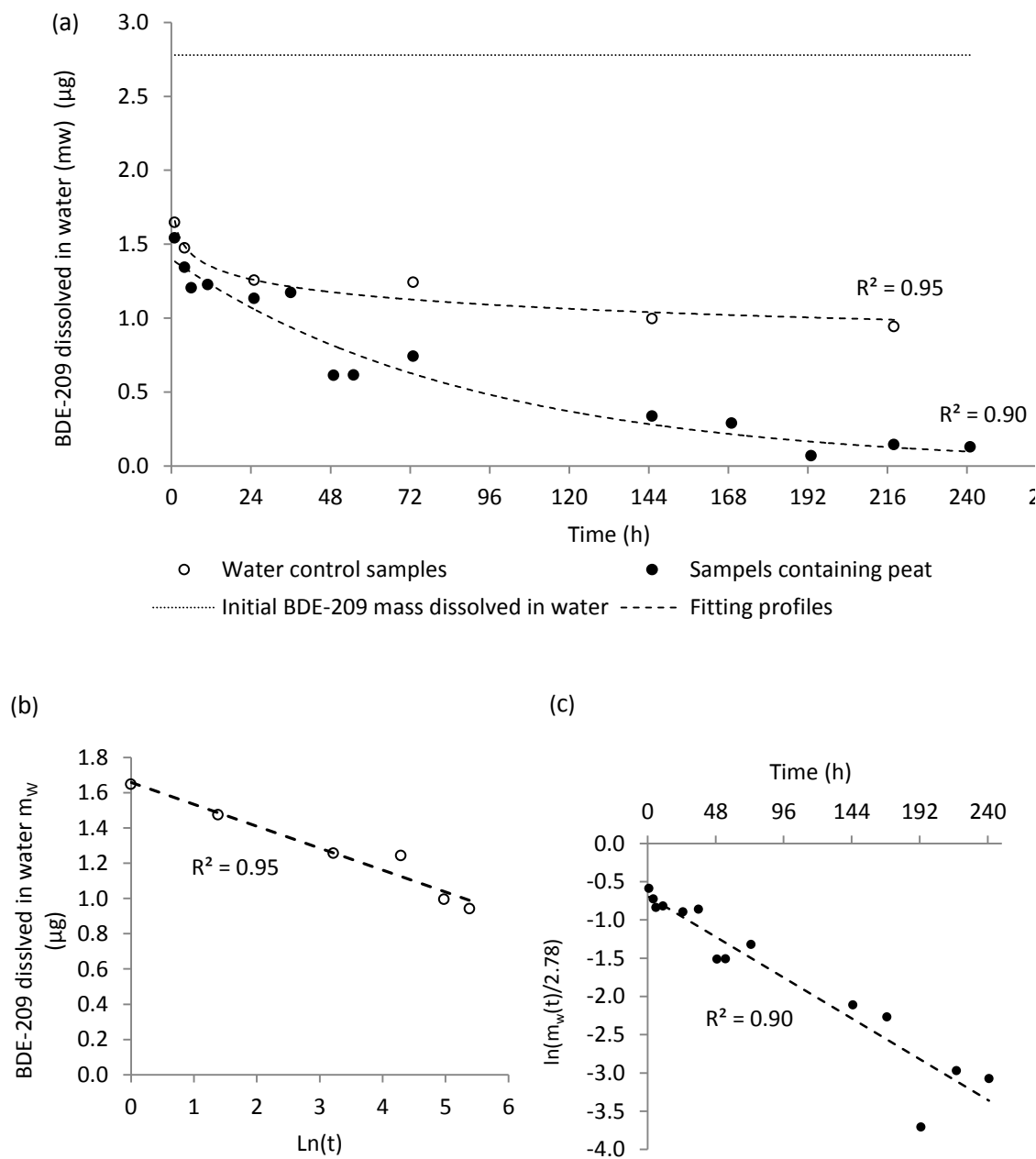


Figure 7.6: Panel (a): BDE-209 measured in water ( $m_w$ ) from samples (S) containing peat (full points) and water control samples (empty points). The initial mass dissolved in water is reported (dashed line). Dotted lines are the fitting profiles described in Equation 6.4 and 6.5 respectively, statistic correlation factor is reported in graph ( $R^2$ ). Panel (b): BDE-209 mass measured in water control samples plotted with the natural logarithm of time fitting the linear profile, ( $R^2$ ) statistic correlation reported. Panel (c): Natural logarithm of BDE-209 ( $m_w$ ) divided by the initial mass added in the system plotted in time fitting the linear profile, ( $R^2$ ) statistic correlation reported.

The calculated profile for the net mass absorbed by peat follows the power law in Equation 7.6. Subtracting net mass absorbed by peat here calculated from the initial mass  $m_T$  the kinetic profile shown in Figure 7.7 for the second scenario considered is obtained.

$$m_s = 0.08t^{0.41}$$

Eq.7.6

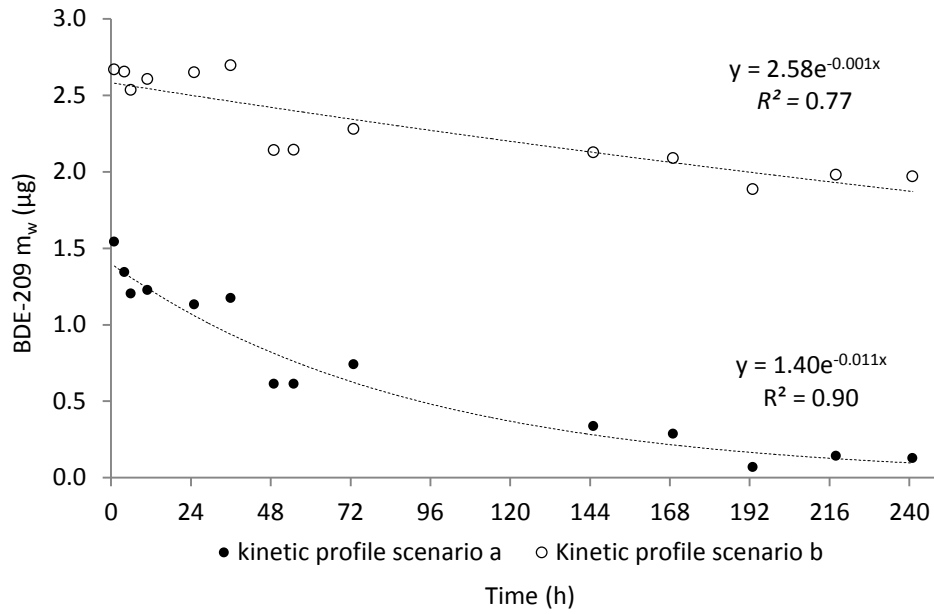


Figure 7.7: Kinetic profile obtained by plotting BDE-209 mass dissolved in water with time under the two scenarios considered: uncorrected profile (full points), profile corrected by subtraction of the mass sorbed on container surfaces in control samples (empty points). The dotted lines represent the fitting profiles; equations and statistic correlation ( $R^2$ ) are reported.

The kinetic profile uncorrected has been already commented in Figure 7.6 and it is well fitted with a first order kinetic profile. While in the case of the profile obtained after the subtraction of BDE-209 mass adsorbed on the surfaces of control samples, data are fitted by an extremely slow first order kinetic, one order of magnitude slower. It is worth to notice that the starting points of the two curves in Figure 7.7 are different merely because of the different way in which the initial drop is taken in consideration: in the case of the profile corrected by the sorption on control samples it has been subtracted from the initial value, in the other case not.

Values obtained for the kinetic profile indicate that sorption of BDE-209 on peat particles is slow. A comparison with data obtained for lower brominated PBDEs (citation Liu 2010) is useful because it gives the order of magnitude of the sorption rate constant so far observed

for PBDEs. Nevertheless it needs to be carefully evaluated because of the differences in the soil tested, the higher hydrophobicity of BDE-209 and the problem of mass losses, all factors that strongly influence the final results. Said that, kinetic rate constant here obtained (0.01 and 0.001) would fit with the slow compartment (0.01-0.04) of the first order kinetic model proposed by Liu and co-worker for lower brominated PBDEs and it would ascribe peat in the slow sorption organic matter domain of the DRM model.

In regard to the nature of BDE-209 mechanisms of interaction with peat particles, one of the most likely ways is the  $\pi$ - $\pi$  interaction between the aromatic rings of BDE-209 and organic matter (Nuerla et al., 2013; Olshansky et al., 2011). In relation to this aspect, the humification grade of peat influences the number of active sites available for interaction, as humic matter has been found less aromatic than mixed bulk SOM (Olshansky et al., 2011).

### 7.3.2 BDE-209 sorption isotherm on peat

Results from the partitioning of BDE-209 between peat and water at different concentrations are reported in Figure 7.8. Concentrations in peat cleansed by the mass adsorbed on the bottle surfaces are plotted versus concentrations measured in water after 5 days. Coherently with BDE-209 high hydrophobicity the partition is completely in favour of peat and the amount remained dissolved in water is small and concentrations vary in a narrow range (0.04-0.7  $\mu\text{g/L}$ ). The range is actually so small that it is impossible to distinguish if data are following a linear, Freundlich ( $n > 1$ ) or simply all BDE-209 is taken up and these data reflect experimental fluctuations. To our knowledge, experimental values of BDE-209  $K_d$  coefficient have never been reported. From the experimental limitations encountered and the results obtained at 5 days contact time, it is possible to conclude that the measurement of a sorption isotherm at equilibrium conditions (for  $K_d$  calculation) is even more unworkable.

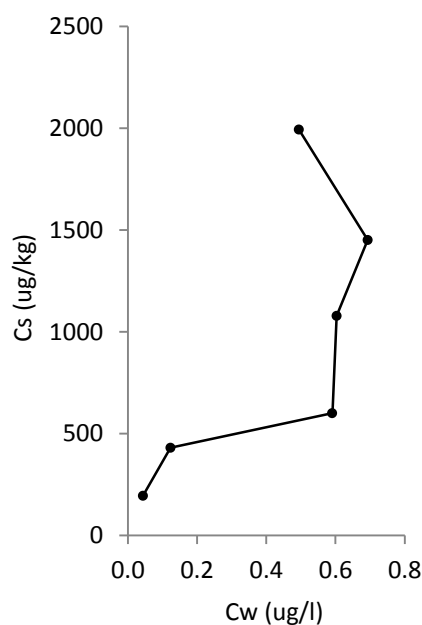


Figure 7.8: BDE-209 sorption isotherm for samples with initial concentration in water of 1.2, 2.3, 3.6, 6.9, 8.5 and 10.7 µg/L.  $C_w$  and  $C_s$  are BDE-209 concentration in water and peat after 5 days contact time.

### 7.3.3 BDE-209 sorption kinetic on clay

During analysis of matrix control samples, no traces of BDE-209 or co-eluting substances were detected, indicating that no interferences are coming from clay. In panel (a) of Figure 7.9 results from water control samples are reported. On average, 0.08 µg of BDE-209, which represents 23% of the initial mass, was adsorbed to container surfaces and this value seems to be constant with increasing contact time. BDE-209 in the water fraction ( $m_w$ ) presents a constant profile in time with an average value of 0.30 µg which correspond to 82 % of the initial BDE-209 mass added in samples. The two series of data independently measured, show overall complementary profiles and mass balance is respected: their sum results on average is 0.38 µg which correspond to 105 % of the total BDE-209 mass initially added in the system ( $m_T$ ). Profiles of BDE-209 mass dissolved in water and adsorbed in samples containing kaolin (Panel (a)) are significantly different from the ones observed in control samples (Panel (b)): in the first 4 hours BDE-209 is rapidly sorbed from water on clay particles reaching an equilibrium plateau when 80 % of total BDE-209 is sorbed. As with peat sorption, glass adsorption observed in control samples may not be the same in presence of clay particles. Constant BDE-209 adsorbed on glass and container surfaces simplifies the interpretation of the adsorption profile on clay. Subtracting a constant value, whether it is exactly the same measured for the clay control samples or a fraction of this



measurement, will not modify the kinetic profile observed. Thus, it is in any case reasonable to conclude that the adsorption equilibrium is reached after 4 hours contact time.

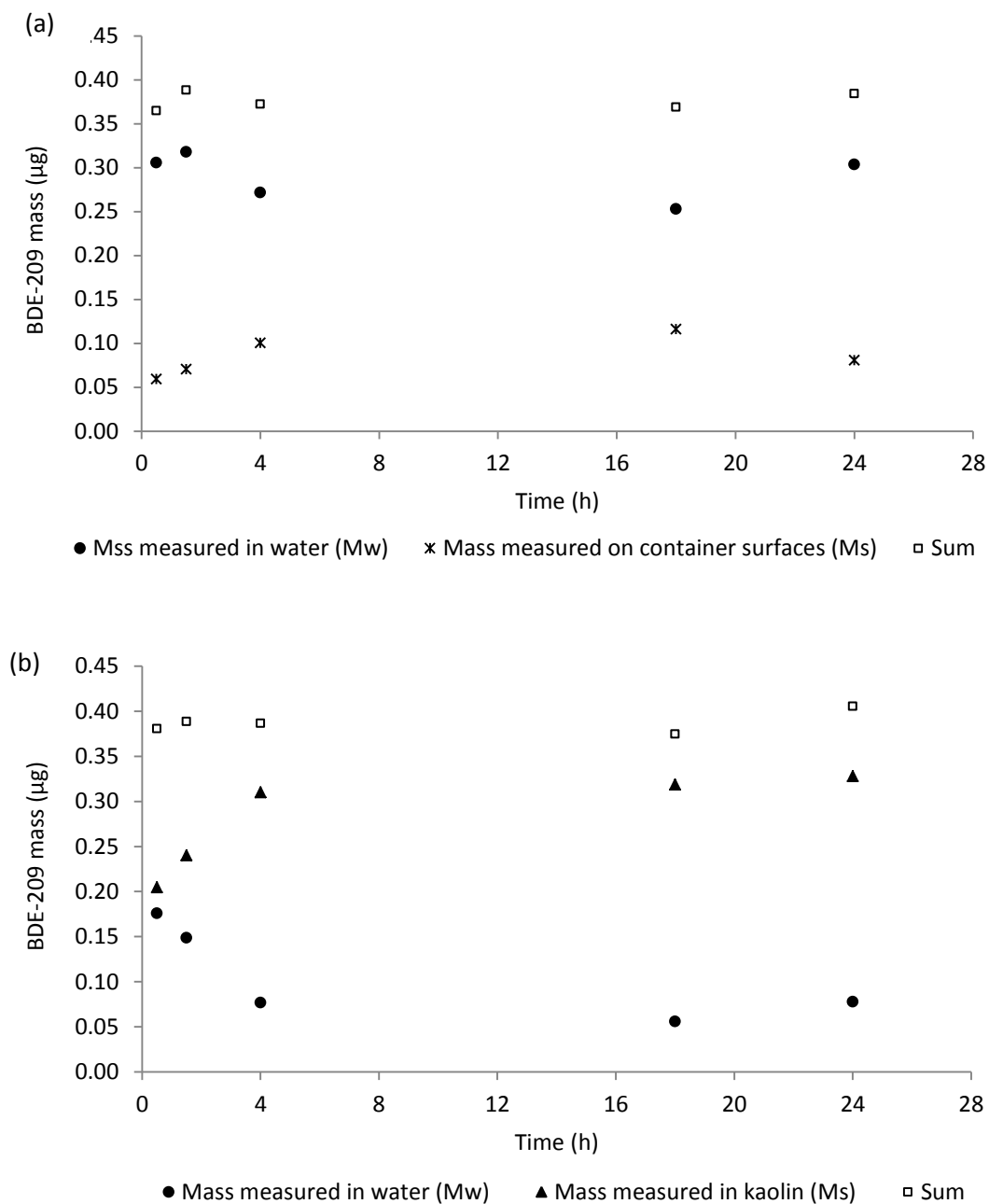


Figure 7.9: Panel (a): BDE-209 mass measured in water ( $m_w$ ), sorbed by container surfaces ( $m_s$ ) and the calculated sum in water control samples. Initial BDE-209 mass in water 0.36 µg. Panel (b): BDE-209 mass measured in water ( $m_w$ ), sorbed on kaolin ( $m_s$ ) and the calculated sum in samples containing 0.1 g of kaolin. Initial BDE-209 mass in water 0.36 µg.

The kinetic profile is well fitted (statistical correlation  $R^2 = 0.99$ ) by the first order kinetic profile in Equation 7.7. The kinetic profile obtained for kaolin is faster than the one observed for peat, nevertheless the kinetic rate constant it is still smaller in comparison of the fast rate constant reported for the fast compartment in the study on lower brominated compounds, 0.24 compared to 0.62-1.68 (citation Liu 2010), it is actually in between the slow and the fast sorption rate constant proposed by Liu and co-workers.

$$m_w = 0.205 \cdot e^{-0.243t} \quad \text{Eq. 7.7}$$

The nature of the interaction between BDE-209 molecules and kaolin particles is not completely understood. Considering BDE-209 functional groups and kaolin structure reported, it is possible to speculate that it could involve induced-dipole/dipole interaction between the aromatic rings and the hydroxyl groups on kaolin surface. Indeed a similar behaviour has been reported for benzene and silica interaction (Schwarzenbach et al., 1993b) and adsorption by donation of  $\pi$  electron of aromatic compounds has been reported on clay (Kowalska et al., 1994). Furthermore the interaction could be facilitated by the fact that, despite BDE-209 has a small global dipole moment (0.635 Debye) due to its symmetrical structure, BDE-209 is more susceptible to be polarised than other PBDEs congeners (Hu et al., 2005a). The second functional group in the BDE-209 molecule which could interact with the hydroxyl groups of kaolin is the ethereal oxygen, but BDE-209 conformation does not seem to facilitate the access of the oxygen atom to the active sites on clay particles. Indeed, studies investigating the bonding angle and the torsional angles between the two aromatic rings identify for BDE-209 a twist conformation (Hu et al. 2005) similar to the one showed in Figure 7.10 modelled for BDE-209 adsorbed on graphene surface (Ding et al. 2014). In light of these considerations, the nature of the interaction of BDE-209 with clay might not be much different from the one with aromatic organic molecules contained in peat. Nevertheless, in order to capture the ultimate nature of the interaction of BDE-209 with kaolin a study involving stereochemistry considerations and the electrostatic potential map of BDE-209 would be required.

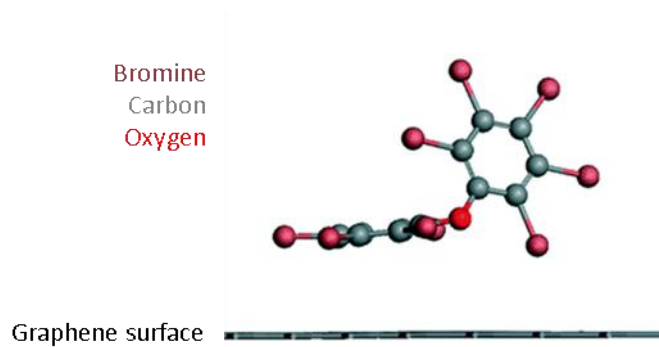


Figure 7.10: BDE-209 molecule conformation when adsorbed on graphene surface modelled through density functional theory (DFT) and molecular dynamic (MD). Adapted from (Ding et al., 2014).

### 7.3.4 Comparison of the two kinetics

Kaolin and peat sorption kinetics presented in the previous sections (Figure 7.9 and 7.6) show that partitioning equilibrium is reached faster by kaolin than peat. To overcome differences in the experimental set up and obtain a direct comparison, the mass sorbed is normalised to the sorbent mass added in the system ( $\mu\text{g/g}$ ) (Figure 7.11). The direct comparison confirms that clay uptake is faster than peat one. Therefore in situation of short contact time where there is no time for the equilibrium to be achieved (e.g. ground water infiltration under high water flow or storm-related soil erosion events (Schwarzenbach et al. 1993)), kaolin contribution to the sorption process of BDE-209 and possibly other HOCs is important. Describing the partitioning of BDE-209 based only on  $K_{OW}$  or  $K_{OM}$  would drive to the wrong conclusion that a soil poor in organic matter is not able to retain BDE-209 and possibly other PBDEs.

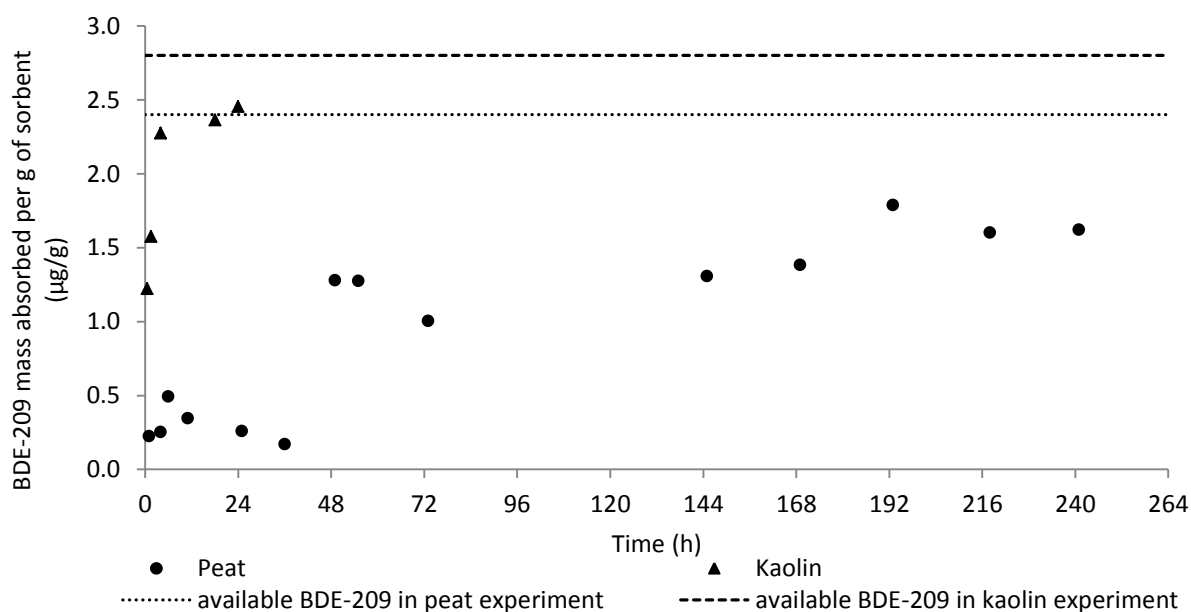


Figure 7.11: Sorption profile for peat (points) and kaolin (triangle) derived from the kinetic experiments discussed in Figure 6.6 and 6.9 respectively. Data are here normalised to the mass of sorbent. Dotted and dashed lines indicate the initial BDE-209 mass dissolved in water normalised to the mass of sorbent respectively for peat and kaolin.

PBDEs retention was observed in soils with low organic matter from the Tibetan plateau. The Tibetan plateau is the highest plateau in the world also called “the third pole” because of its unique meteorological and geographical characteristics. In the central part, the organic carbon content of soil is low (<0.9 %) and the area is affected by high precipitation due to the air masses coming from the Indian subcontinent. PBDEs show strong correlation with clay content (illite, kaolinite, and chlorite) and weaker correlation with organic matter or grain size (Yuan et al., 2012). At sufficiently low quantities of organic matter, the large surface area of clays minerals may compete with SOM for PBDE sorption. The environmental relevance of BDE-209 adsorption on clay minerals becomes even more important because kaolinite and montmorillonite have been shown to enhance BDE-209 photodegradation as a result of the electron-donating ability of clay minerals during irradiation (Ahn et al., 2005; An et al., 2008). Degradation patterns observed by Ahn and An might justify the kind of relationship observed for PBDEs with clay minerals on the Tibetan plateau: positive correlation of tetra-, penta-, and hexa-brominated congeners and negative for PBDEs outside this range (Yuan et al., 2012).

A second confirmation on the fact that sorption on kaolin particles might be faster than the on peat ones can be found in the sorption models described in Section 3.2. Both the

Sorption Related Pore Diffusion (SRPD) model and Distributed Reactivity Model (DRM) capture this dichotomy. In the SRPD model, the main retarding factor is the interaction between the analyte and the internal pore walls, which is irrelevant for kaolin. Loose particles were suspended in water and the particles themselves are characterised by no porosity and high specific surface area ( $14 \text{ m}^2/\text{g}$ ). Therefore, kaolin adsorption is expected to be faster than peat. The DRM ascribes the reason for the delay in sorption of hydrophobic compounds in soil and sediments to the presence of a condensed soil organic matter domain. In the case of pure clay with 0 % organic matter, the slow sorption domain is completely absent and the sorption rate depends entirely on the mineral domain, which is the domain characterised by the faster sorption rate.

Nevertheless SRPD, DRM, and Polanyi-based models all focus on the sorbent characteristics. They focus on retarding factors on analyte diffusion due to sorbent media characteristics while neglecting possible changes in the liquid phase properties. In all models, water is assumed to be an inert medium with constant solubility. If suspended organic matter is released in water, this assumption may no longer be true. Instead, water solubility of PBDEs and other compounds may be enhanced by DOM. PBDEs have been demonstrated to interact with DOM (Nuerla et al., 2013) and DOM has been demonstrated to change the equilibrium partitioning between water and soil for PBDEs (W. Wang et al., 2011). Re-imagining the kinetics as a succession of temporary equilibrium conditions the presence of DOM may give a new and alternative explanation to the slower sorption rate of observed for BDE-209 in peat and generally for HOC into soil organic matter. Other observations support this hypothesis. For example, PCBs and PBDEs adsorption and desorption from PDMS (polydimethylsiloxane) fibres were observed to be strongly influenced by the presence of humic acid (Ter Laak et al., 2009).

### 7.3.5 BDE-209 sorption and desorption from kaolin in non-equilibrium conditions

BDE-209 sorption and desorption from kaolin in non-equilibrium conditions is here investigated. BDE-209 mass dissolved in water ( $m_w$ ) after 2 minutes contact time for different kaolin/water ratios (Figure 7.12) showed that BDE-209 adsorption on kaolin was related to the amount of kaolin in water. Samples have been prepared as dilution serie for clay starting from highest clay:water ratio (1:4) until the ratio at which the BDE-209

remained dissolved in water was comparable with the one obtained in the control sample (1:1000). Samples were prepared in group of three with the one characterised by the highest clay:water ratio overlapping with the smallest ratio of the previous group. The relevance of the result is the serie rather than the individual data point. Therefore a single measure per point has been considered sufficient. Moreover the standard deviation observed for the control sample (included in each group of samples) and for clay:water ratio repeated in the three groups are reported to give an indication of the variability of the result obtained.

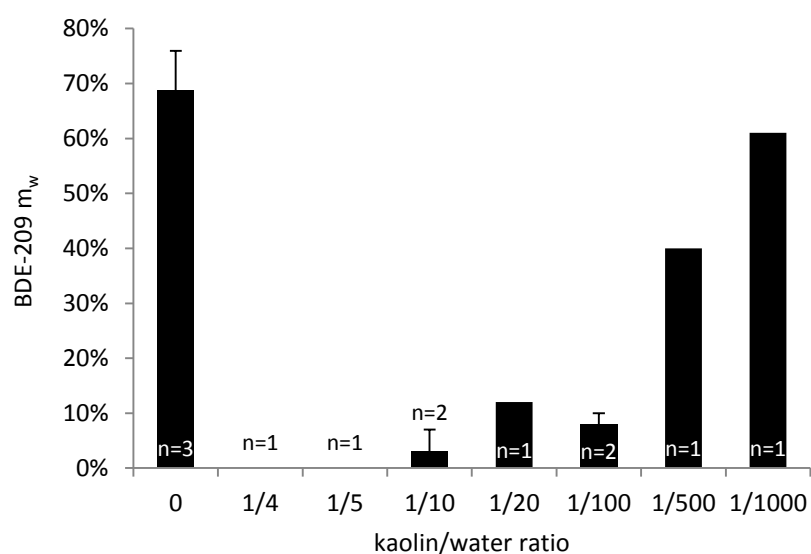


Figure 7.12: BDE-209 mass dissolved in water after 2 minutes contact time with kaolin for decreasing kaolin/water ratio (n=number of repetitions).

If the fraction of BDE-209 adsorbed on clay from pure water is positively related with the amount of clay suspended in water, desorption does not show the same pattern. Results from the desorption experiment (Figure 7.13) show that BDE-209 desorbed in water  $m_d$  in the first two minutes is a small part of  $m_T$  (1-7 %) and it does not depend on the clay/water ratio.

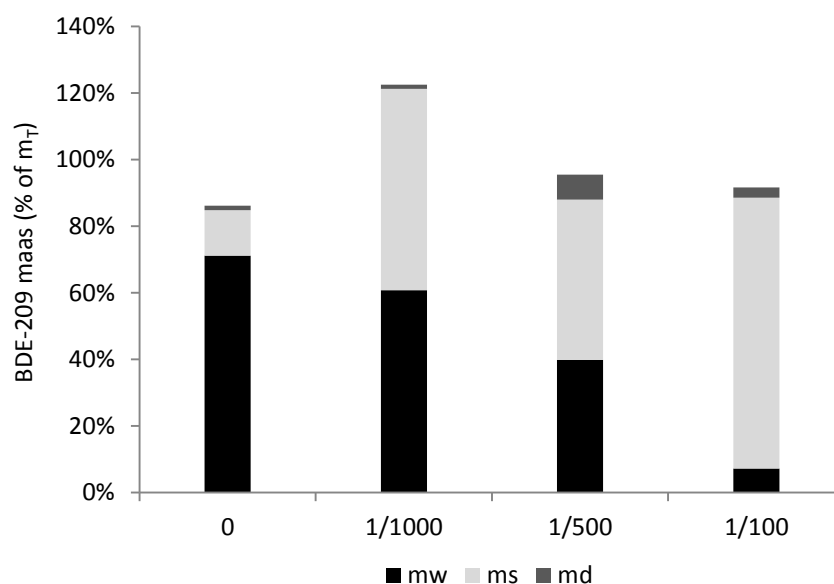


Figure 7.13: BDE-209 mass measured in water ( $m_w$ ) and in kaolin ( $m_s$ ) expressed as percentage of the total mass added ( $m_T$ ) after two minutes contact time. BDE-209 desorbed from kaolin in fresh deionised water after a second period of 2 minutes contact time ( $m_d$ ) for increasing kaolin/water ratio.

The result is consistent with previous studies where no BDE-209 was observed to desorb from kaolinite, montmorillonite, sediments, or aluminium hydroxide in water after 24 hours (Ahn et al., 2005), which suggests that BDE-209 adsorption on clay is characterised by strong hysteresis. This quick sorption and strong hysteresis of BDE-209 on kaolin particles highlight the importance of kaolin sorption in non-equilibrium conditions.

### 7.3.6 Influence of dissolved organic matter (DOM) on BDE-209 sorption on kaolin

The hypothesis of dissolved organic matter (DOM) influencing BDE-209 sorption process by enhancing the solubility of BDE-209 was tested for kaolin in a follow-up experiment.

The ratio between BDE-209 sorbed mass and dissolved mass in pure water increases 10 times (from 0.6 to 1.4 and 7.2), proportionally to the 10x increase of clay/water ratio (from 1/1000 to 1/500 and 1/100) (Figure 6.14a). When DOM-enriched water was used as the liquid phase instead of pure water, BDE-209 sorption to kaolin decreased (Figure 7.14b) and sorbed mass does not depend on the amount of clay dissolved in water. Instead, the ratio between mass sorbed and mass remaining dissolved in DOM-enriched water is constant of approximately 0.5. DOM in water is competing with clay in BDE-209 partitioning and DOM capacity to retain BDE-209 dominates the partitioning process.

The nature of the interaction of BDE-209 with DOM released in water by peat is not clear. Further investigation is required to identify the nature of DOM (fine particles, dissolved molecules, or both) and consequently the nature of the interaction. Lately PBDEs have been found to interact with a common component of soil dissolvable organic matter, Leonardite humic acid, through  $\pi$ - $\pi$  interaction (Nuerla et al., 2013).

Nevertheless the result clearly shows that the sorption of BDE-209 is strongly influenced by the presence of the DOM in non-equilibrium conditions. The tendency of PBDEs to complex with the dissolved organic carbon released by soil in water has been found already responsible for deviations in the measurement of equilibrium partitioning coefficient (W. Wang et al., 2011), and for enhancing PBDEs desorption from polymeric materials (Ter Laak et al., 2009). Besides that, leachability of PCBs from soil has been found increasing with pH and the correlated increases in the content organic carbon in the leachate (Badea et al., 2014). All these evidences encourage further investigation for proving if the presence of dissolved organic matter in water could affect not only the equilibrium condition and therefore the partitioning of BDE-209 between soil and water, but also the kinetic of the process itself. Therefore if it could be a factor, so far ignored, responsible for the slower kinetics observed for the sorption HOC on soil reach in organic matter.

$M_s$  in the water control sample (kaolin/water ratio=0), essentially a second measurement of the BDE-209 mass adsorbed to the glass, showed a small increase in pure water (Figure 7.14b), suggesting that the fraction of BDE-209 retained on the glass when water is poured out vigorously was less than the one remained attached after centrifugation. This highlight that mechanical forces could affect BDE-209 adsorption on glasses surfaces therefore particular attention is required for keeping all the experimental procedure as constant as possible in order to obtain consistent results. Anyway the increased loss on the glass should not affect the observed trends and the consideration emerging from their comparison.

The total recovery of samples from experiment with DOM enriched water is about 110 % except for the water control sample in which about 20 % of the mass added was lost. When pure water is used, the sum of the three fractions exceeds the initial mass added of about 20-25 % for all samples. Being confident that no contamination is coming from water and clay because of the null results obtained for control samples containing just kaolin and



water, the excess is possibly due to some imprecisions during samples extraction that has been persistently repeated.

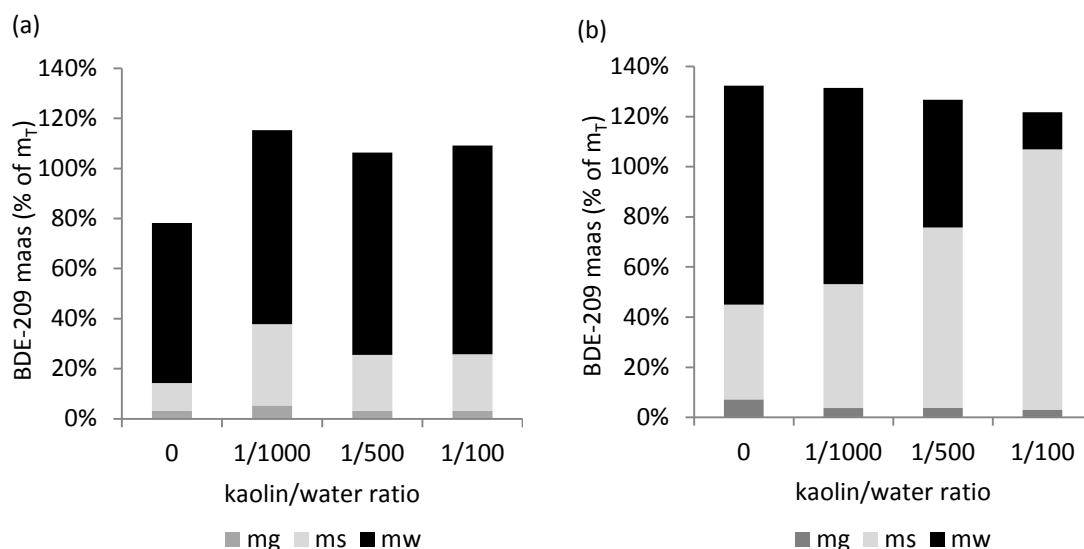


Figure 7.14: BDE-209 dissolved in water ( $m_w$ ), adsorbed on kaolin ( $m_s$ ) and adsorbed on glass surface (mg) expressed as percentage of the total mass added ( $m_T$ ) from both experiments run with (a) DOM enriched water and (b) pure water for increasing kaolin/water ratio.

## 7.4 Conclusions

For the first time the challenging topic of sorption and desorption behaviour of BDE-209 have been here investigated. Results shows that an experimental calculation of partitioning coefficient through isotherm curves is not possible for BDE-209, because of experimental limitation imposed by BDE-209 low solubility. Instead, sorption kinetic profiles for BDE-209 on peat and kaolin have been successfully measured.

The approach chosen of studying soil matrixes separately demonstrated to be successful in characterising the sorption process of the single matrix and therefore in identifying which could be the contributions of the different matrixes in the sorption process into soil. That allowed for identifying an important factor, otherwise hardly recognisable, influencing the equilibrium partitioning and sorption kinetic of HOC: the dissolved organic carbon released by soil organic matter into water. This have an important consequence on BDE-209 mobility, as the presence of dissolved organic matter released by peat facilitate BDE-209 transportation in water by enhancing BDE-209 solubility. These results provide insight into

the unexplained mobility observed for PBDEs (Chapter 2.1): BDE-209 may be washed away with DOM from soil with high organic matter content like peat.

BDE-209 sorption on peat particles is particularly slow and the sorption kaolin particles is instead much faster. This along with the strong hysteresis shown by kaolin highlights the important role kaolin, and generally clay particles might play in the retention of BDE-209 at non-equilibrium conditions. Even if sorption capacity it is expected to be greater for peat than kaolin, peat sorption ability might be irrelevant compared to the one of kaolin when contact time between water and soil particle is short (less than 4 hours).

The overall picture produced by this study highlights that equilibrium partitioning coefficient is not always comprehensive for the description of environmental behaviour of pollutants. Indeed, modelled  $K_d$  values for BDE-209 based on BDE-209 physico-chemical properties would suggest that BDE-209 should be mostly sorbed and retained by organic matter fraction of soil (like peat) rather than mineral particles. Here instead results show that sorption by kaolin is much more important in non-equilibrium conditions and the presence of peat enhances BDE-209 solubility in water.

Finally the effects of peat dissolved organic matter and kaolin hysteresis on BDE-209 sorption are fundamentals for the evaluation of BDE-209 bioavailability in soil. Bioavailability is a crucial aspect for designing bioremediation strategies, like for instance the one explored in the next chapter.

## 8 Pleurotus Ostreatus tolerance to BDE-209

### 8.1 Introduction

After investigating BDE-209 physico-chemical properties and behaviour in soil, the attention is here addressed to investigate a novel bioaugmentation technique for soil remediation. Evidence on the ability of *P. ostreatus* to degrade several recalcitrant pollutants along with the non-specific nature of its enzymes and the large availability of mycelia make *P. ostreatus* a possible candidate for remediation of soil contaminated by BDE-209. However, no studies are reported on the use of *P. ostreatus* for degradation of BDE-209. In this study some tests have been done to optimise *P. ostreatus* cultivation, test the fungus tolerance to BDE-209, and identify the effects of soil composition on mycelia development.

### 8.2 Materials and method

Decabromodiphenyl ether standard (98% purity) was purchased from Sigma-Aldrich (Gillingham, Dorset, UK). All of the reagents (acetonitrile, acetone and methanol) were of analytical HPLC grade obtained from Fisher Scientific (Leicestershire, LE11 5RG-UK). Deionised water was collected from the laboratory reverse osmosis deionizing system (RO180 El-Ion® twin-stage, SG). Wheat grains colonised with *P. ostreatus* mycelia (spawn) and oak straw were purchased from local suppliers (Oyster mushroom grain spawn, Ann Miller's Mushrooms Ltd., Aberdeenshire-Scotland)(William Alexander & Son Dripps mill, Glasgow-Scotland). Nutrient Agar (N-agar) and Malt Extract Yeast Agar (MEYA) were purchased from Oxoid (Oxoid Ltd, Altrincham, UK)

#### 8.2.1 *Pleurotus Ostreatus* spawn cultivation on straw: parameter optimisation

A large number of agricultural, forest and agro industrial by-products can be used for growing oyster mushrooms as long as they are rich in cellulose, lignin and hemicellulose (Esser and Hofrichter, 2010). The substrate selected for this study was oak straw. Cultivation productivity under different conditions was evaluated after 20 days of incubation by visual examination of mycelia development.

Oak straw was soaked overnight to be prewashed and wet. Drained soak water was then sterilised. Steam, chemical, and autoclave sterilisation processes were tested to identify the one promoting mycelia development avoiding at the same time the formation of mould. For steam pasteurisation, straw was left two hours under steam flow from water at 80°C and allowed to cool for few minutes. For chemical sterilisation, straw was immersed in a hydrogen peroxide solution at 0.3% in volume for 2 minutes and then drained. For autoclave pasteurization, straw was pasteurised at 105°C for 18 minutes at pressure of 220 kPa and then cooled for 1 hour in the autoclave.

Sterilised straw was transferred to 10 3L polyethylene cultivation bags. 4 of them were prepared by adding 500 gr of humid straw and the others 6 were prepared by adding 800 gr to determine if the culture size may influence mycelia development. Finally, *P. ostreatus* spawns were added to humid straw in in proportion of 1:30 (w:w) according to supplier indication (1:30-1:15) and literature examples (Esser and Hofrichter, 2010).

Bags containing the inoculated straw were closed and preserved protected by light. During mycelia development, *Pleurotus* species tolerate high level of CO<sub>2</sub> (20-22 %). Therefore no precautions are required for controlling the CO<sub>2</sub> level. Optimal temperatures for *P. ostreatus* species lie between 25-28 °C, mycelia can develop at 10-30 °C, although mycelia can develop even at 10-30 °C (Esser and Hofrichter, 2010). Available temperatures in laboratory rooms were 18 °C or 23 °C. Both conditions were tested.

*Pleurotus Ostreatus* during the fruiting period requires low temperature (10-20 °C), high relative humidity (70-80 %), CO<sub>2</sub> level less than 0.6% and light. Once mycelium fully colonised the straw, all bags were transferred to 18 °C. Cuts of a few centimetres were made in the polyethylene bags to enable ventilation. Light protection was removed. Water spraying was done daily to maintain high relative humidity.

### 8.2.2 *Pleurotus ostreatus* BDE-209 tolerance test on straw

*P. ostreatus* spawns were cultivated on contaminated straw to verify the fungi tolerance to BDE-209 when growing on a favourable substrate. Cultivation conditions previously identified as optimal for mycelia development were applied: autoclave pasteurisation of

straw, and temperature of 20-22 °C. Spawn:straw ratio was increased to 1:12.5 to enhance mycelia colonisation. 250 gr of pasteurised straw were spiked with 50 mL of BDE-209 solution in acetone to obtain 10 µg/kg, 100 µg/kg and 1000 µg/kg BDE-209 concentration in wet straw. Control cultures were prepared on straw containing acetone but no BDE-209. Each sample was prepared in triplicate and the mycelia development was observed for 10 months.

### 8.2.3 *Pleurotus ostreatus* isolation and cultivation on petri disks

To have more accurate measure of mycelia development in presence of BDE-209, *P. ostreatus* was cultivated on agar disks. Cultivation was performed starting from the original spawn and inoculating part of the mycelia previously developed on straw on two different media. Standard N-agar was prepared adding 2.8 gr of powder per 100 mL of pure water. Malt extract yeast agar (MEYA), a substrate richer in nutrients, was prepared by adding 0.2 gr of yeast and 5 gr of malt extract in 100 mL of pure water. The presence of a bacteria coexisting and growing with the fungi on petri dish culture was observed. Therefore antibiotic and antifungal were applied on disks before inoculation to isolate *P. ostreatus* from coexisting bacteria. Antibiotic solution was prepared dissolving 1 mg of Chloramphenicol in 20 mL of water:methanol solution (1:1) to obtain a concentration of 50 µg/mL. 10 mL of cycloheximide antifungal solution (25 µg/mL) were prepared in pure water. Both antibiotic and antifungal solutions were sterilised by filtering through 0.2 µm PTFE membrane. Either 2 mL or 1 mL per 100 mL of N-agar and MEYA, respectively, were applied on petri dishes before fungi inoculation. To observe the microorganism tolerance to BDE-209 in successful cultivations, slices of Agar spiked with BDE-209 were alternated with control slices containing methanol within in a 20cm diameter glass petri dish. To prepare the contaminated agar, 50 mL of BDE-209 solution in methanol at 10 mg/L was added to 200 mL of agar to obtain a concentration of 2.5 µg/mL. Control slices were prepared adding to the agar the same amount of methanol without BDE-209.

### 8.2.4 Growing on soil

*P. ostreatus* spawns were added to soil at a ratio of 1:30 w/w (spawn:dry soil). Cultures were prepared in beakers covered with parafilm to preserve humidity. Two kind of soil were tested: a loamy-sand soil collected from field in Scotland highlands and a commercial horticultural soil, whose properties are described in Table 8.1. For two months they were

incubated protected by light at 20-22 °C. During that period the mycelia development on spawn and into soil has been observed.

Table 8.1: Properties of soil tested for *P. ostreatus* mycelia colonisation. Measure repeated in triplicate, average value reported  $\pm$  standard deviation.

	OM (%)	pH	EC ( $\mu$ S/cm)	Sand (%)	Silt (%)	Clay (%)	Humidity (%)
Loamy sand	2.8 $\pm$ 0.1	4.1 $\pm$ 0.1	31 $\pm$ 5	80 $\pm$ 0.2	16.2 $\pm$ 0.2	3.0 $\pm$ 0.1	11.3
Horticultural soil	17.3 $\pm$ 0.9	7.4 $\pm$ 0.0	732 $\pm$ 16	70.9 $\pm$ 1.1	19.2 $\pm$ 1.3	9.9 $\pm$ 0.3	38.2

## 8.3 Results and Discussion

### 8.3.1 *Pleurotus Ostreatus* spawn cultivation on straw: parameters optimisation

Cultures prepared under different conditions were classified in three categories according to the mycelia development after 20 days from inoculation: (i) no development apart from initial spawns; (ii) partial colonisation of the straw; and (iii) well-developed mycelia with full colonisation of the straw (Table 8.2). Incubation temperature and the amount of straw per bag do not seem to affect the mycelia development. Chemical and steam sterilisation of straw not always create favourable conditions for mycelia to develop. Autoclave pasteurisation creates the best condition for mycelia developing although mould was present in some cultures. In Figure 8.1, examples of mycelia development for the three categories are shown. Autoclave was chosen as sterilisation technique for further experiments. Fruit body formation was induced in all cultures free from mould. In Figure 8.2, fruit body development timing is captured.

Table 8.2: *P. ostreatus* mycelia development after 20 days on straw for the different condition tested.

Sterilisation process	Cultivation conditions		Mould formation	Mycelia development after 20 days of incubation
	Incubation temperature (°C)	Straw amount (gr)		
Chemical	18	800	No	Mycelia did not develop or develop only on spawns
Chemical	23	800	No	Mycelia did not develop or develop only on spawns
Autoclave	18	500	Yes	Mycelia partially colonised straw
Autoclave	18	800	No	Mycelia well develop and fully colonised straw
Autoclave	23	500	No	Mycelia well develop and fully colonised straw
Autoclave	23	800	Yes	Mycelia well develop and fully colonised straw
Steam	18	500	No	Mycelia partially colonised straw

Steam	18	800	No	Mycelia well develop and fully colonised straw
Steam	23	500	No	Mycelia did not develop or develop only on spawns
Steam	23	800	No	Mycelia did not develop or develop only on spawns



Figure 8.1: Examples for the three categories defined for evaluating the mycelia development on straw.



Figure 8.2: Fruits growing on straw in laboratory conditions.

### 8.3.2 *Pleurotus ostreatus* BDE-209 tolerance test on straw

After 8 months, even the higher contaminated straw was fully colonised by mycelia (Figure 8.3). Mycelia development was inhibited by the presence of acetone. It took 3 months for the mycelia to develop on control sample instead of the 20 days observed when clean straw was inoculated. The presence of BDE-209 caused an additional delay in mycelia development, as straw spiked with BDE-209 at different concentrations (0, 10, 100 and 1000 µg/kg) showed different mycelia developing rates. Growing rate seemed to decrease for increasing contamination level (Table 8.3). In several samples (the ones labelled with X in Table 8.3) mould grew on straw along with the fungus *P. ostreatus*. For the porpoise of the experiment these samples were not useful, because the presence of mould made impossible to observe tolerance *P.ostreatus*. Nevertheless the presence of mould is a spark

for future work and new interesting questions: is the presence on mould and the simultaneous presence of different microorganisms enhancing *P.ostreatus* tolerance and its degradation ability? Along with this point an additional step in future work will be the development of a method for straw extraction and analysis before and after the colonisation by *P.ostreatus* and/or mould.

Table 8.3: *P. ostreatus* mycelia development on contaminated straw. (X) indicates mould formation.

BDE-209 (µg/kg)	10 weeks	3 months	6 months	8 months
Control	X	X	X	X
	X	X	X	X
	colonising straw	straw colonised	straw decomposition	Straw decomposition
10	X	X	X	X
	colonising straw	1/2 bag straw colonised	straw colonised	Straw decomposition
	colonising straw	straw colonised	straw decomposition	Straw decomposition
100	X	X	X	X
	half mouldy	X	X	X
	spawn	colonising straw	straw colonised	Straw decomposition
1000	X	X	X	X
	X	X	X	X
	spawn	colonising straw	colonising straw	straw colonised

Straw spiked with BDE-209 (1000 µg/kg) after 8 months



Figure 8.3: *P. ostreatus* mycelia developed on straw containing 1000 µg/kg of BDE-209 after 8 months from inoculation.

### 8.3.3 *Pleurotus ostreatus* isolation and cultivation on petri disks

Direct inoculation of spawns on N-agar did not result in successful *P. ostreatus* mycelia development. Instead a filamentous microorganism was growing. Transfer to a dishes containing antibiotic or antimycotic agents showed it to be a bacteria (Figure 8.4). Most



likely it is a soil bacterium that coexists with *P. ostreatus* on spawns, possibly *Bacillus mycoides* (Figure 8.5).

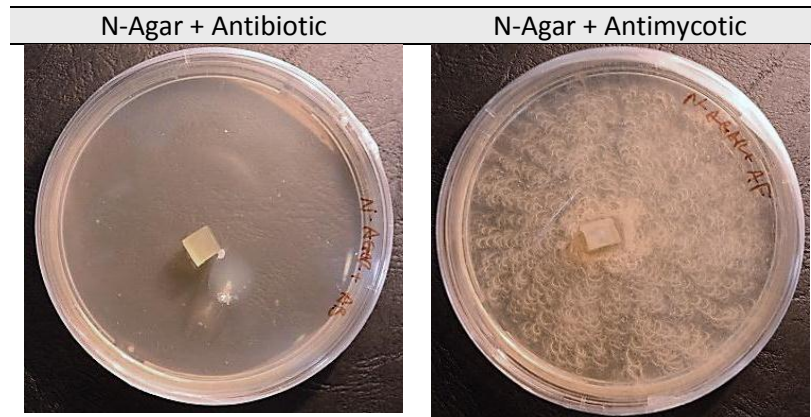


Figure 8.4: Filamentous microorganism developed from *P. ostreatus* spawn inoculated on N-agar enriched with antibiotic (left) or antimycotic.

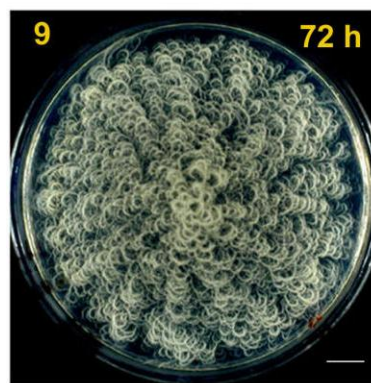


Figure 8.5: Picture of *Bacillus mycoides* isolated from soil. Adapted from (Di Franco et al., 2002).

When the soil bacterium was transferred on N-agar containing BDE-209, it developed mostly on the slices without BDE-209 and avoiding the slices containing BDE-209 at concentration of 2.5  $\mu\text{g}/\text{mL}$  (Figure 8.6). The presence of methanol on the slices free from BDE-209 does not seem to inhibit the bacteria growth. Nevertheless, the bacteria geometry appeared modified: filaments lost their spiral geometry and developed more linearly.

*P. ostreatus* was successfully growing when a portion of mycelia, previously developed on the straw, was inoculated into MEYA (Figure 8.7). Successively, pieces of the mycelia cultivated on MEYA were then transferred to new cultures containing antibiotic, antimycotic or neither of the two to verify the possible coexistence of the bacterium in the

culture. As it is shown in Figure 8.8, the colony growing on MEYA seems composed by both fungi (*P. ostreatus*) and bacterium. Indeed *P. ostreatus* developed on MEYA enriched with antibiotic and a bacterium grew on the MEYA enriched with antimycotic.

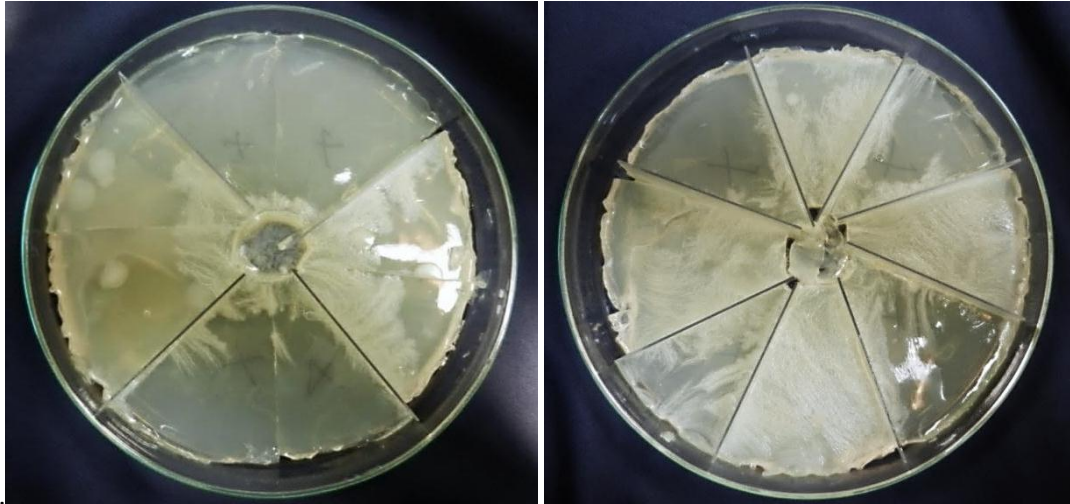


Figure 8.6: Soil bacterium development on N-agar after 4 days: slices labelled with “X” are the part in which N-agar contains BDE-209; unlabelled slices are the ones containing only methanol.

The morphology of the bacterium colony developing on MEYA is different from the one observed on the N-agar culture. The morphology of some of the colony mutants derived from a *B. mycoides* strain (Figure 8.9) present similarity with the colony observed in the MEYA culture. Therefore it is not excluded the bacterium observed on MEYA culture is the same developing from the spawns on N-agar dish. Nevertheless, further investigation including bacterium DNA identification would be necessary to verify it.



Figure 8.7: *P. ostreatus* mycelia developed on MEYA culture after 1 month from inoculation.

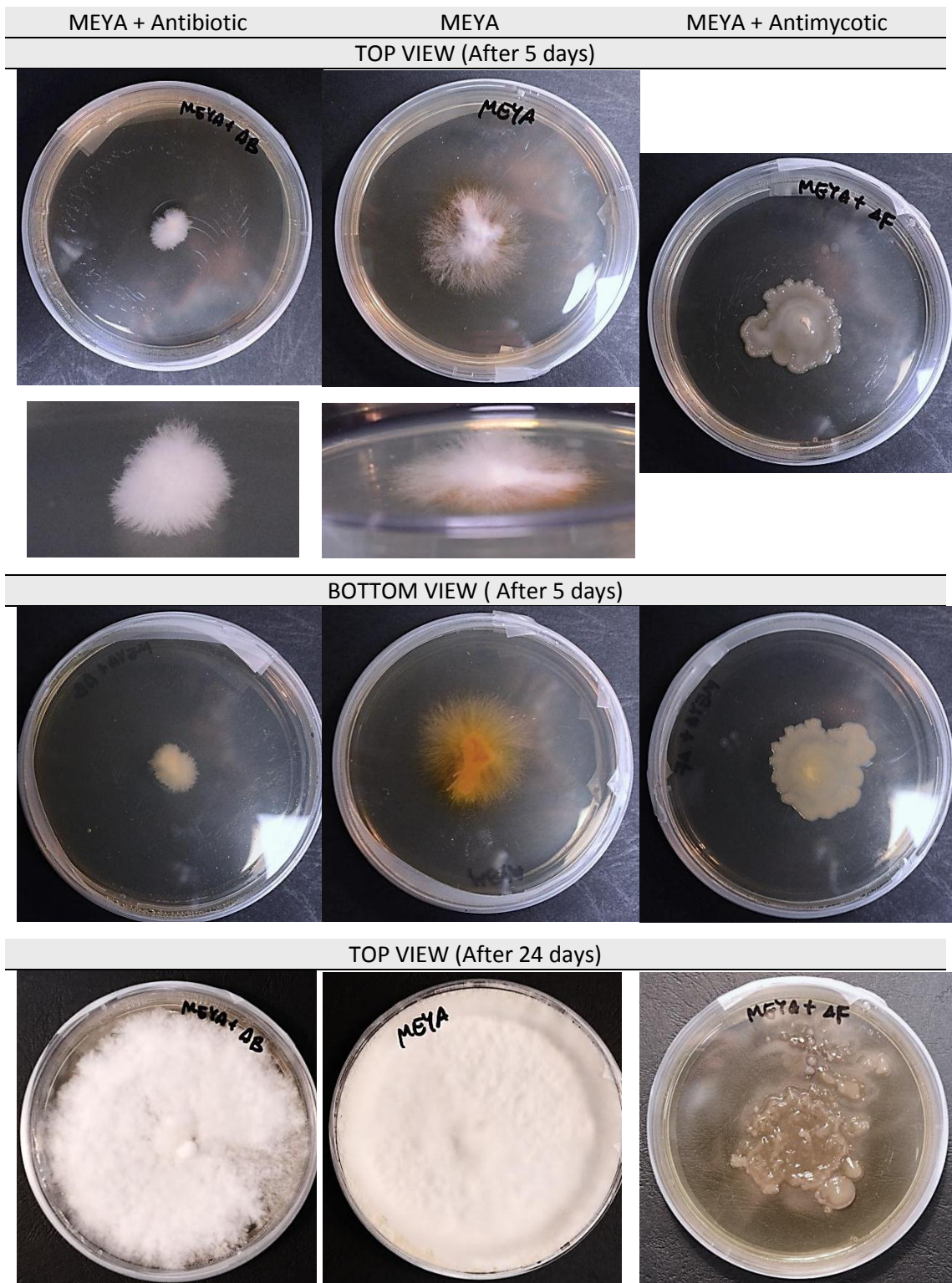


Figure 8.8: Fungus and bacterium colonies growing on MEYA culture enriched with antibiotic or antimycotic inoculated with a portion of *P. ostreatus* mycelia collected from straw.



Figure 8.9: Colony mutants derived from SIN96 *B. mycooides* strain on agar medium. Adapted from (Di Franco et al., 2002).

The cultivation of *P. ostreatus* on substrate spiked with BDE-209 was not successful. Fungi, which is a much more structured microorganism, seems to suffer from the presence of solvent in the growing media. Several tests have been performed to verify the tolerance of *P. ostreatus* to the solvents acetone, acetonitrile and methanol. Some mycelia development was obtained by keeping dishes open to air in a sterilised laminar flow hood at least 10 hours to allow solvent to evaporate before inoculation with *P. ostreatus* mycelia. With this step, it was difficult to avoid contamination by mould or other microorganisms from the surrounding environment. Moreover, increasing evaporation time results in a decrease of the MEYA humidity and, consequently, inhospitable conditions for mycelia development. A better system allowing solvent evaporation avoiding at the same time dish contamination could be set up by pumping sterilised air into the dish. This option deserve further investigation and it is ascribed in the following up works of this research.

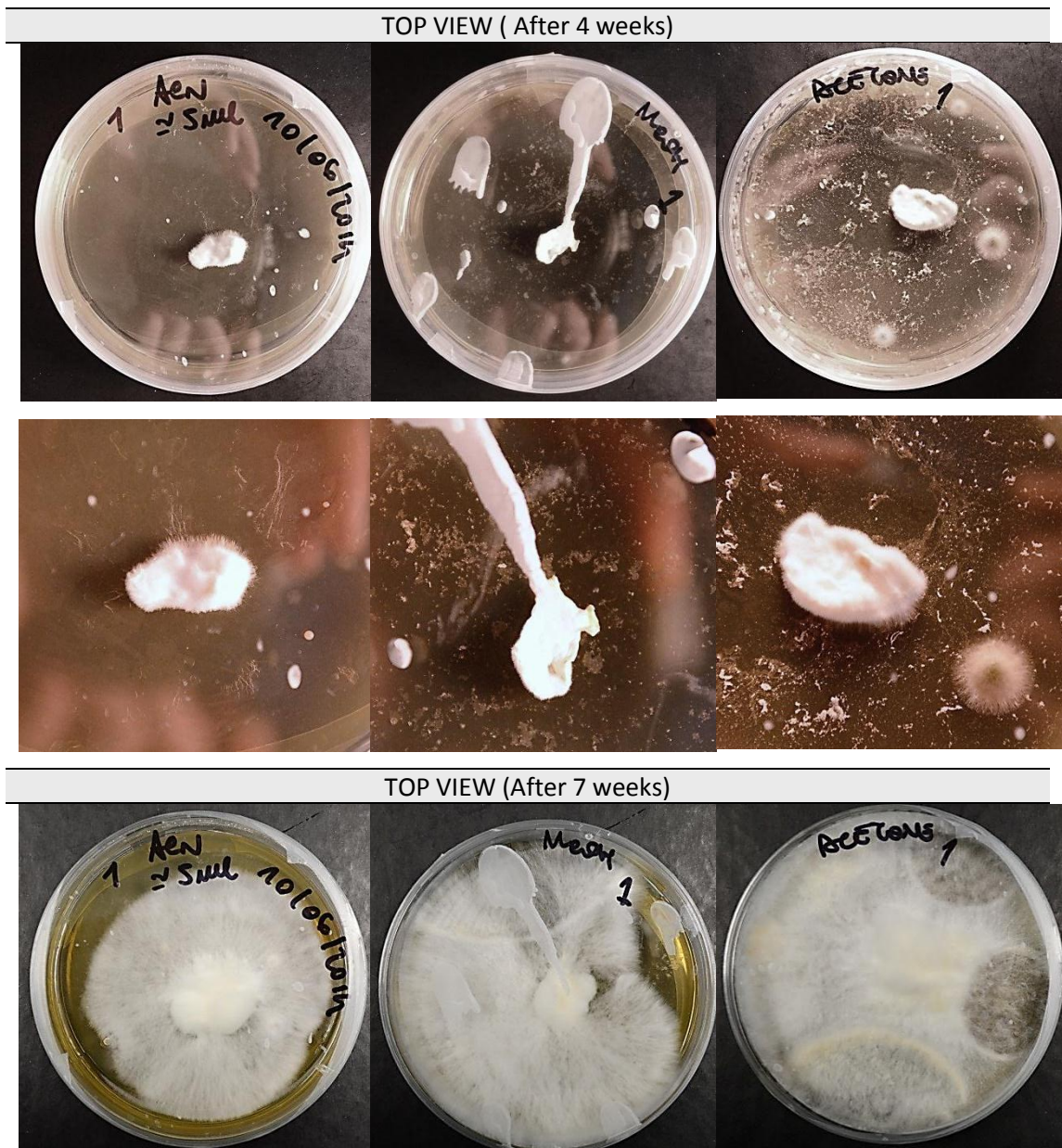


Figure 8.10: *P.ostreatus* mycelium developing after being transferred on MEYA disk sprinkled with different organic solvents (acetonitrile, methanol or acetone).

Comparing mycelia development obtained for culture on MEYA at 24 days (Figure 8.8) with the culture on MEYA sprinkled with organic solvents after 4 and 7 weeks (Figure 8.10) shows that addition of solvent generally retards mycelia development. Solvent delaying of mycelia development is greater in acetonitrile then methanol and acetone. Contamination by other microorganism on acetone dish was more diffuse. A second growing test on MEYA

spiked with methanol (Figure 8.11) confirmed difficulties in keeping the media clean after the period of solvent evaporation.

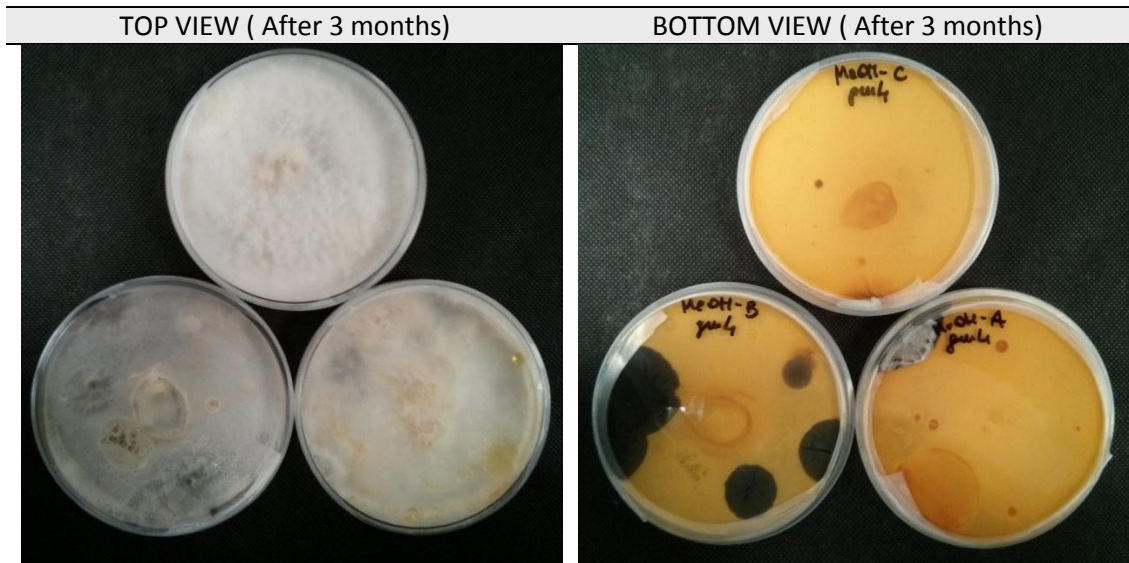


Figure 8.11: *P.ostreatus* mycelium developing after being transferred on MEYA disk sprinkled with methanol after 3 months.

#### 8.3.4 Growing on soil

In both loamy sand and commercial horticultural soils, after few days, *P. ostreatus* mycelium developed on spawns and after two weeks it started exploring the surrounding soil creating connection between spawns. On a long term, horticultural soil seems to provide a better support for mycelia growth. After two months, when the original source nutrient was completely consumed the mycelium was more developed in horticultural soil than in loamy sand culture (Figure 8.12). Experiment confirmed that high organic matter content, basic pH and higher humidity are preferable to induce mycelia growth into soil. This is consistent with the fact that *P. ostreatus* slightly decreases pH during the laccase activity (Hestbjerg et al., 2003). Moreover the experiment suggests that the amount of original substrate for inoculation should be enough for supporting the mycelia development in the earlier stage, but at the same time it should not be overestimated, because a limited carbon source is crucial for inducing mycelia development into soil.

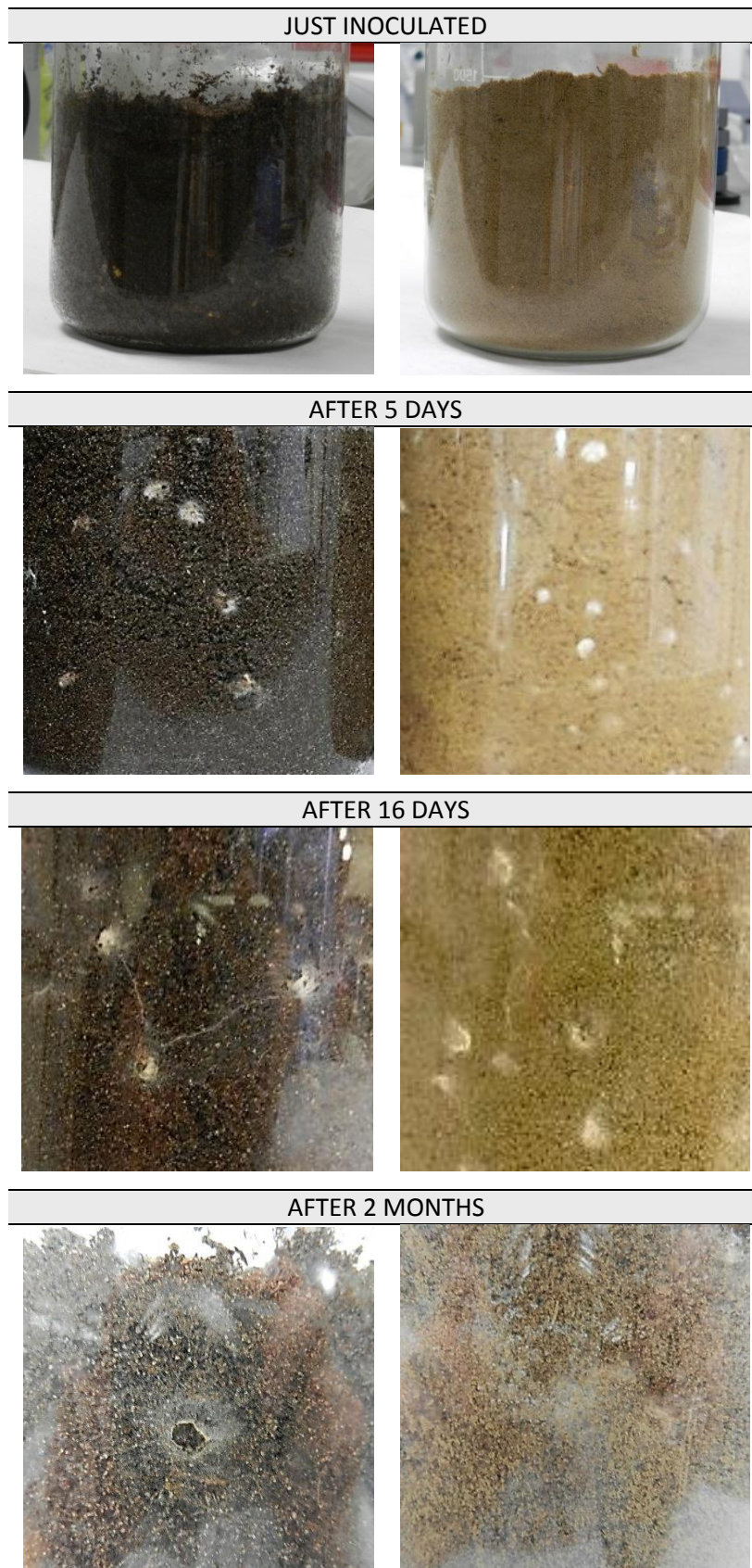


Figure 8.12: *P. ostreatus* mycelia development from spawns into the two soil tested.

## 8.4 Conclusions

Cultivation of *P. ostreatus* on contaminated straw provides the first prove of its tolerance to BDE-209. *P. ostreatus* mycelium was able to develop even in presence of high concentration of BDE-209 (1 mg/kg) despite mycelia growth was considerably retarded by the presence of acetone and BDE-209: instead of 20 days, 3 to 6 months were required to obtain complete colonisation of straw depending on BDE-209 concentration. Further investigation is required to evaluate if the mycelia development is accompanied by an effective BDE-209 degradation and by the production and activity of laccase and other enzymes possibly involved in the biodegradation of BDE-209.

The coexistence of bacteria with *P.ostreatus* mycelia on straw has been observed, it is not clear if, and in case at which extent, the synergic interaction of the fungus with the bacterium is supporting the fungus development on straw containing BDE-209. Future work to clarify this point would open a new and interesting research branch.



## **9 Conclusion and future work**

The goal of this research was to gain a better understanding on some of the aspects influencing BDE-209 mobility and biodegradation in soil. This goal has been achieved through the development of original analytical techniques and experimental approaches. In this final chapter, key findings and future research opportunities are discussed and novel aspects of the research are highlighted.

In the thesis's body any aspect considered of value for the scientific community from experimental details to more theoretical observations and negative results have been included and commented. Such details are often excluded from data available on articles published on peer review journal, but are useful for progression in the research.

### **9.1 Key findings**

Some of the findings achieved with this research are conclusive and open new perspectives on the sorption and mobility issues (Chapter 7). Others remain at the stage of preliminary testing, providing a valid starting point for further investigation in the field of BDE-209 bioremediation (Chapter 8). Others results have been preparatory to the achievement of these findings (Chapters 5 and 6). In the following sections, key findings relevant to these three aspects are summarised.

#### **9.1.1 BDE-209 sorption on mineral and organic matter matrices**

Prior this work, no data were available on BDE-209 partitioning and sorption kinetics. For the first time, BDE-209 sorption kinetics have been successfully measured and results presented in chapter 7 will be published on a peer review journal. The choice to study separately kaolin as an example of the mineral domain, and peat for the organic component of soil allowed for direct comparison of the sorption kinetics in the two domains. Sorption kinetics are much faster in kaolin than peat (4 hours compared to more than 10 days). This is in line with what is reported in literature for PBDEs other than BDE-209 and theoretical models describing sorption of hydrophobic organic compounds (HOC). The fast kinetics and strong hysteresis characterising BDE-209 adsorption on kaolin provides important insight into BDE-209 adsorption during non-equilibrium phenomena in

conditions where organic matter is particularly low or completely absent (e.g. bedrock aquifers, high mountains). Dissolved organic matter in water competes with mineral solid particles, acting in favour of BDE-209 dissolution in water. In the conditions tested, dissolved organic matter (DOM) rules the fate of BDE-209 limiting considerably the adsorption on kaolin particles. These results overturn the role that organic matter plays on BDE-209 sorption and mobility when it is in the form of DOM and it opens interesting questions on more general aspects. For instance, DOM could be an alternative reason for the slow sorption kinetics measured in peat and unexpected BDE-209 mobility in soil. In a soil rich in organic matter, DOM could enhance BDE-209 dissolution in water, slowing down the sorption process and promoting BDE-209 transport. Finally, results presented in this thesis show that experimental measurement of a BDE-209 partitioning coefficient in soil is not achievable due to the limitation of BDE-209 solubility in water.

### 9.1.2 Measure of BDE-209 from environmental samples and experimental limitations

Experience developed during the thesis suggests that to achieve reliable BDE-209 measurement, particular attention needs to be given to sample handling during experimental design. Contact between samples and containers should be minimised. Container surfaces should be rinsed with organic solvent when it is compatible with the experimental scope. Experimental design should be done in manner to have controls on losses that are impossible to avoid. It has been thanks to these considerations that a successful method for BDE-209 extraction from water has been developed: water evaporation and solvent substitution (WES). This method achieved  $97 \pm 3\%$  and  $86 \pm 3\%$  recoveries of BDE-209 from deionised water and water after contact with peat, respectively. In case direct control on recovery is required, chrysene was demonstrated as a suitable surrogate. In comparison to liquid-liquid extraction (LLE), dispersive liquid-liquid micro extraction (DLLME), and solid phase extraction (SPE), WES minimises the use of solvent and cost of analysis. These aspects make WES method even more competitive than other methods, demonstrating that the easiest option is not necessarily less valuable than more refined and elaborate techniques.

For the extraction of BDE-209 from peat soil, pressurised liquid extraction (PLE) and microwave assisted extraction (MAE) were compared. Extraction efficiency seems more

influenced by the extraction solvent than the technique. PLE is preferred because it presents the advantage that solvent separation is completely automated and no additional sample filtration is required. Regardless of the extraction technique, when dealing with peat, sample preparation through cone and quartering is strongly recommended and the presence of interferences that could be misinterpreted for BDE-209 peak is here advised. Interference peaks have been extracted by both MAE and PLE. In particular, the interference extraction through PLE is solvent dependent. It is enhanced when dichloromethane is used. Therefore the use of dichloromethane, usually adopted for its high extraction power, should be avoided when working with peat and other organic-rich soils.

### 9.1.3 BDE-209 biodegradation

In regards to BDE-209 biodegradation, the research focused on the exploration of a possible remediation technique rather than studying the naturally occurring biodegradation processes. Nevertheless sorption processes strictly influences biodegradation of chemicals. Therefore results produced in Chapter 7 studying BDE-209 sorption on dissolved organic matter and kaolin are useful when investigating BDE-209 bioavailability in soil.

In this work, for the first time, *P. ostreatus* tolerance to BDE-209 has been tested. *P. ostreatus* mycelium are capable of growing on straw in the presence of concentrations of 1000 µg/kg BDE-209, although mycelia growth is slowed by the presence of an organic solvent and BDE-209. The observed delay in mycelia development of 3-6 months is certainly an aspect to be considered for the evaluation of the remediation technique.

## 9.2 Future research opportunities

Results obtained through the research here presented open new questions that constitute interesting research opportunities. Several points of interest on BDE-209 sorption, mobility and degradation are worth follow up studies.

The fact that kaolin adsorbs BDE-209 much faster than peat highlights the importance of kaolin and other mineral solids in fast non-equilibrium processes. Nevertheless, the contributions of mineral solids in equilibrium conditions and BDE-209 soil storage capacity remain unclear. In order to answer this question, it would be interesting to compare peat and kaolin sorption capacities as well as other forms of organic matter and mineral solids.

Experiments in this thesis show that small amounts of dissolved organic matter can have significant impacts on retention in the aqueous phase. Nevertheless it is unclear to what extent kaolin and, generally, the mineral domain contribution is worthy of consideration when organic matter is also present in soil. Studying sorption kinetics on sorbents prepared as combinations of mineral and organic matter mixed in different proportions would allow for evaluation of the limit on organic matter content at which the mineral contribution is still worth of consideration.

Further, the study of DOM effects on sorption processes on other matrixes is worth investigating. In particular, it is interesting to evaluate at which extent the effects of DOM released by soil organic matter (SOM) is effecting the SOM sorption process itself. It could indeed represent an alternative justification to slow sorption kinetic of HOC on solid organic matter.

Because soil is inherently heterogeneous, systematic evaluation should continue in highly controlled conditions with increasing complexity before advancing to the investigation of whole soils. For example, the question of DOM effects on SOM could be investigated by studying the sorption kinetics and capacity of alternative organic matrixes (e.g. activated carbon) in presence of peat DOM. Varying the DOM concentration in water could identify the limit at which DOM action dominates over other matrix sorption processes. A combination of batch and column experiments would be useful to evaluate the speculative hypothesis that DOM effectively enhances BDE-209 mobility in soil. Finally, because BDE-209 is a highly hydrophobic pollutant and an extreme case, in order to have a comparison with other contaminants, further work would include other PBDEs and different HOCs such as PCBs and PAHs.

Although the analytical methods developed in this thesis are consistent and repeatable, there is scope for improvement, particularly the extraction method from soil. For BDE-209 analysis in peat, the problem of interference should be solved so that direct extraction is possible for analysis of environmental soil samples and future sorption experiments. The implementation of in-cell acid clean up in tungsten cells has the potential to solve the

interference problem with the additional advantage of avoiding additional handling steps that risk loss of analyte.

In relation to the issue of BDE-209 degradation and remediation by *P. ostreatus*, the next step would be to investigate if mycelia development on contaminated straw is accompanied by BDE-209 degradation. This could be achieved by analysis of enzyme activity in colonised straw and measurement of BDE-209 and potential degradation products. If degradation and mineralisation of BDE-209 are demonstrated, this could represent an opportunity for development of myco-remediation.

The coexistence of a bacterium with *P. ostreatus* mycelium has been detected. Further research is required to identify this bacterium and investigate if it plays any role in relation to *P. ostreatus* tolerance to BDE-209 or its degradation ability. Moreover, because *P. ostreatus* is an edible fungus, the potential transfer of BDE-209 or its degradation products from the straw through the mycelia to fruiting bodies should be investigated. In addition to the critical aspect of possible direct human exposure to organic pollutants through the food chain. This study would be interesting for the additional purposes of myco-remediation and pollution monitoring. Further fungi species may be worth investigating as well.

Based on the results presented, this thesis advises on the importance of evaluating the implications of DOM-enhanced solubility for HOCs and investigating the possible effects it could have on their mobility. DOM is a new and important factor to study for its contribution in slowing down sorption kinetic for HOCs. Extension of bioaugmentation remediation via fungi shows promise in the potential for uptake and remediation of BDE-209 and the other PBDEs.

## REFERENCES

- Abbasi, G., Buser, A.M., Soehl, A., Murray, M.W., Diamond, M.L., 2015. Stocks and flows of PBDEs in products from use to waste in the U.S. and Canada from 1970 to 2020. *Environ. Sci. Technol.* 49, 1521–8. doi:10.1021/es504007v
- Abdallah, M.A.-E., Drage, D., Harrad, S., 2013. A one-step extraction/clean-up method for determination of PCBs, PBDEs and HBCDs in environmental solid matrices. *Environ. Sci. Process. Impacts* 15, 2279–87. doi:10.1039/c3em00395g
- Ahn, M.-Y., Filley, T.R., Jafvert, C.T., Nies, L., Hua, I., Bezares-Cruz, J., 2005. Photodegradation of Decabromodiphenyl Ether Adsorbed onto Clay Minerals, Metal Oxides, and Sediment. *Environ. Sci. Technol.* 40, 215–220. doi:10.1021/es051415t
- Allchin, C.R., Law, R.J., Morris, S., 1999. Polybrominated diphenylethers in sediments and biota downstream of potential sources in the UK. *Environ. Pollut.* 105, 197–207. doi:http://dx.doi.org/10.1016/S0269-7491(98)00219-X
- An, T., Chen, J., Li, G., Ding, X., Sheng, G., Fu, J., Mai, B., O’Shea, K.E., 2008. Characterization and the photocatalytic activity of TiO<sub>2</sub> immobilized hydrophobic montmorillonite photocatalysts: Degradation of decabromodiphenyl ether (BDE 209). *Catal. Today* 139, 69–76. doi:http://dx.doi.org/10.1016/j.cattod.2008.08.024
- Andriessse, J.P., 1986. Nature and Management of Tropical Peat Soils, Issue 59, in: *FAO Soils Bulletin* 59. Rome, p. 47.
- Antunes, P., Viana, P., Vinhas, T., Capelo, J.L., Rivera, J., Gaspar, E.M.S.M., 2008. Optimization of pressurized liquid extraction (PLE) of dioxin-furans and dioxin-like PCBs from environmental samples. *Talanta* 75, 916–25. doi:10.1016/j.talanta.2007.12.042
- ASTM, 2001. E1195 - Standard Test Method for Determining a Sorption Constant (K<sub>oc</sub>) for an Organic Chemical in Soil and Sediments. *Astm E1195* 1, 1–8. doi:10.1520/E1195-01R08.1
- ASTM, 1993. ASTM D 2974-87 Standard Test Methods for Moisture, Ash, and Organic Matter of Peat and Other Organic Soils. *Usga Green Sect. Rec.* 31–33. doi:10.1520/D2974-07A.2
- Aveyard, R., Haydon, D.A., 1973. 5.13 The Polanyi potential theory of adsorption, in: *An Introduction to the Principles of Surface Chemistry*. pp. 166–167.
- Babrauskas, V., 1983. Upholstered Furniture Heat Release Rates: Measurements and

- Estimation. *J. Fire Sci.* 1, 9–32. doi:10.1177/073490418300100103
- Babrauskas, V., Arlene, B., Rebecca, D., Linda, B., 2011. Flame retardants in furniture foam: benefit and risks. *Fire Saf. Sci. tenth Int. Symp.* 265–278. doi:DOI: 10.3801/IAFSS.FSS.10-265
- Babrauskas, V., Harris, R.H., Gann, R.G., Levin, B.C., Lee, B.T., Richard, P.D., Paabo, M., Twilly, W., Yocklavich, M.F., Clark, H.F., 1988. Fire hazard comparison of fire-retarded and non-fire-retarded products.
- Babrauskas, V., Lucas, D., Eisenberg, D., Singla, V., Dedeo, M., Blum, A., 2012. Flame retardants in building insulation: a case for re-evaluating building codes. *Build. Res. Inf.* 40, 738–755. doi:10.1080/09613218.2012.744533
- Badea, S.-L., Mustafa, M., Lundstedt, S., Tysklind, M., 2014. Leachability and desorption of PCBs from soil and their dependency on pH and dissolved organic matter. *Sci. Total Environ.* 499, 220–227. doi:http://dx.doi.org/10.1016/j.scitotenv.2014.08.031
- Baldrian, P., Gabriel, J., 2002. Copper and cadmium increase laccase activity in *Pleurotus ostreatus*. *FEMS Microbiol. Lett.* 206, 69–74. doi:10.1111/j.1574-6968.2002.tb10988.x
- Barco-Bonilla, N., Plaza-Bolaños, P., Tarifa, N.M.V., Romero-González, R., Martínez Vidal, J.L., Frenich, A.G., 2014. Highly sensitive determination of polybrominated diphenyl ethers in surface water by GC coupled to high-resolution MS according to the EU Water Directive 2008/105/EC. *J. Sep. Sci.* 37, 69–76. doi:10.1002/jssc.201300757
- Barr, D.P., Aust, S.D., 1994. Mechanisms white rot fungi use to degradate pollutants. *Environ. Sci. Technol.* 28, 78A.
- Barriada-Pereira, M., Concha-Graña, E., González-Castro, M., Muniategui-Lorenzo, S., López-Mahía, P., Prada-Rodríguez, D., Fernández-Fernández, E., 2003. Microwave-assisted extraction versus Soxhlet extraction in the analysis of 21 organochlorine pesticides in plants. *J. Chromatogr. A* 1008, 115–122. doi:10.1016/S0021-9673(03)01061-6
- Bartolomé, L., Cortazar, E., Raposo, J.C., Usobiaga, A., Zuloaga, O., Etxebarria, N., Fernández, L.A., 2005. Simultaneous microwave-assisted extraction of polycyclic aromatic hydrocarbons, polychlorinated biphenyls, phthalate esters and nonylphenols in sediments. *J. Chromatogr. A* 1068, 229–236. doi:10.1016/j.chroma.2005.02.003
- Bartrons, M., Grimalt, J.O., Catalan, J., 2011. Altitudinal distributions of BDE-209 and other polybromodiphenyl ethers in high mountain lakes. *Environ. Pollut.* 159, 1816–1822. doi:http://dx.doi.org/10.1016/j.envpol.2011.03.027

- Bayen, S., Lee, H.K., Obbard, J.P., 2004. Determination of polybrominated diphenyl ethers in marine biological tissues using microwave-assisted extraction. *J. Chromatogr. A* 1035, 291–294. doi:10.1016/j.chroma.2004.02.055
- Bezalel, Hadar, Y., 1997. Enzymatic Mechanisms Involved in Phenanthrene Degradation by the White Rot Fungus *Pleurotus ostreatus* 63, 2495–2501.
- Bezalel, Hadar, Y., Cerniglia, C.E., 1996. Mineralization of Polycyclic Aromatic Hydrocarbons by the White Rot Fungus *Pleurotus ostreatus* 62, 292–295.
- Boon, J.P., Lewis, W.E., Tjoen-A-Choy, M.R., Allchin, C.R., Law, R.J., de Boer, J., ten Hallers-Tjabbes, C.C., Zegers, B.N., 2002. Levels of Polybrominated Diphenyl Ether (PBDE) Flame Retardants in Animals Representing Different Trophic Levels of the North Sea Food Web. *Environ. Sci. Technol.* 36, 4025–4032. doi:10.1021/es0158298
- BSEF, (Bromine Science and Environmental Forum), 2016. <http://www.bsef.com> [WWW Document].
- BSEF, (Bromine Science and Environmental Forum), 2006. Applications of Deca-BDE. Fact Sheet Washington, 2006.
- BSI, (British Standard Institute), 2011a. Determination of pH. *Br. Stand. Inst. Soil Improv. Grow. media*.
- BSI, (British Standard Institute), 2011b. Determination of organic matter content and ash. *Br. Stand. Inst. Soil Improv. Grow. media*.
- BSI, (British Standard Institute), 2005. Determination of polycyclic aromatic hydrocarbons ( PAH ). *Br. Stand. Inst. Water Qual. Stand. Water Qual.* 3.
- BSI, (British Standard Institute), 1997. Determination of certain organochlorine insecticides , polychlorinated biphenyls and chlorobenzenes - Gas chromatographic method after liquid-liquid extraction. *Br. Stand. Inst. water Qual. Stand.*
- BSI, (British Standard Institute), 1880. Determination of the specific electrical conductivity. *Br. Stand. Inst. soil Qual. Stand.*
- Bumpust, J. a, Austt, S.D., 2008. Biodegradation of DDT [ 1 , 1 , 1-Trichloro-2 , 2-Bis ( 4-Chlorophenyl ) Ethane ] by the White Rot Fungus *Phanerochaete chrysosporium*. *Society* 53, 2001–2008.
- Buser, 1986. Polybrominated Dibenzofurans and Dibenze-p-dioxins: Thermal reactino Products of Polybrominated Diphenyl Ethers Flame Retardants. *Environ. Sci. Technol.* 20, 404–408.
- Callahan, P., Hawthorne, M., 2012. Chemical in the crib. *Chicago Trib.*



- Callahan, P., Roe, S., 2012a. Big tobacco wins fire marshals as allies in flame retardant push. Chicago Trib.
- Callahan, P., Roe, S., 2012b. Fear fans flames for chemical makers. Chicago Trib.
- Callahan, P., Roe, S., 2012c. Flame retardant: the role of big tobacco. Chicago Trib.
- Carabias-Martínez, R., Rodríguez-Gonzalo, E., Revilla-Ruiz, P., Hernández-Méndez, J., 2005. Pressurized liquid extraction in the analysis of food and biological samples. *J. Chromatogr. A* 1089, 1–17. doi:10.1016/j.chroma.2005.06.072
- Chen, Y., Li, J., Liu, L., Zhao, N., 2012. Polybrominated diphenyl ethers fate in China: a review with an emphasis on environmental contamination levels, human exposure and regulation. *J. Environ. Manage.* 113, 22–30. doi:10.1016/j.jenvman.2012.08.003
- Chiou, C.T., Malcolm, R.L., Brinton, T.I., Kile, D.E., 1986. Water solubility enhancement of some organic pollutants and pesticides by dissolved humic and fulvic acids. *Environ. Sci. Technol.* 20, 502–508. doi:10.1021/es00147a010
- Choi, K.-I., Lee, S.-H., Osako, M., 2009. Leaching of brominated flame retardants from TV housing plastics in the presence of dissolved humic matter. *Chemosphere* 74, 460–466. doi:http://dx.doi.org/10.1016/j.chemosphere.2008.08.030
- Chou, H.-L., Chang, Y.-T., Liao, Y.-F., Lin, C.-H., 2013. Biodegradation of decabromodiphenyl ether (BDE-209) by bacterial mixed cultures in a soil/water system. *Int. Biodeterior. Biodegradation* 85, 671–682. doi:10.1016/j.ibiod.2013.05.006
- Cincinelli, A., Martellini, T., Misuri, L., Lanciotti, E., Sweetman, A., Laschi, S., Palchetti, I., 2012. PBDEs in Italian sewage sludge and environmental risk of using sewage sludge for land application. *Environ. Pollut.* 161, 229–34. doi:10.1016/j.envpol.2011.11.001
- Clymo, R.S., 1987. Peatland ecology. *Sci. Prog. Oxford*, 71 593–614. 593–614.
- Covaci, A., Harrad, S., Abdallah, M.A.E., Ali, N., Law, R.J., Herzke, D., de Wit, C.A., 2011. Novel brominated flame retardants: A review of their analysis, environmental fate and behaviour. *Environ. Int.* 37, 532–556. doi:http://dx.doi.org/10.1016/j.envint.2010.11.007
- Covaci, A., Voorspoels, S., 2005. Optimization of the determination of polybrominated diphenyl ethers in human serum using solid-phase extraction and gas chromatography-electron capture negative ionization mass spectrometry. *J. Chromatogr. B* 827, 216–223. doi:http://dx.doi.org/10.1016/j.jchromb.2005.09.020
- Covaci, A., Voorspoels, S., Ramos, L., Neels, H., Blust, R., 2007. Recent developments in the analysis of brominated flame retardants and brominated natural compounds. *J.*

- Chromatogr. A 1153, 145–171. doi:http://dx.doi.org/10.1016/j.chroma.2006.11.060
- Crittenden, J.C., Sanongraj, S., Bulloch, J.L., Hand, D.W., Rogers, T.N., Speth, T.F., Ulmer, M., 1999. Correlation of Aqueous-Phase 33, 2926–2933.
- de la Cal, A., Eljarrat, E., Barceló, D., 2003. Determination of 39 polybrominated diphenyl ether congeners in sediment samples using fast selective pressurized liquid extraction and purification. J. Chromatogr. A 1021, 165–173. doi:http://dx.doi.org/10.1016/j.chroma.2003.09.023
- de Wit, C.A., 2002. An overview of brominated flame retardants in the environment. Chemosphere 46, 583–624. doi:http://dx.doi.org/10.1016/S0045-6535(01)00225-9
- de Wit, C.A., Herzke, D., Vorkamp, K., 2010. Brominated flame retardants in the Arctic environment — trends and new candidates. Sci. Total Environ. 408, 2885–2918. doi:http://dx.doi.org/10.1016/j.scitotenv.2009.08.037
- Debrauwer, L., Riu, A., Jouahri, M., Rathahao, E., Jouanin, I., Antignac, J.-P., Cariou, R., Le Bizec, B., Zalko, D., 2005. Probing new approaches using atmospheric pressure photo ionization for the analysis of brominated flame retardants and their related degradation products by liquid chromatography–mass spectrometry. J. Chromatogr. A 1082, 98–109. doi:http://dx.doi.org/10.1016/j.chroma.2005.04.060
- Deng, D., Guo, J., Sun, G., Chen, X., Qiu, M., Xu, M., 2011. Aerobic debromination of deca-BDE: Isolation and characterization of an indigenous isolate from a PBDE contaminated sediment. Int. Biodeterior. Biodegradation 65, 465–469. doi:10.1016/j.ibiod.2011.01.008
- Di Franco, C., Beccari, E., Santini, T., Pisaneschi, G., Tecce, G., 2002. Colony shape as a genetic trait in the pattern-forming *Bacillus mycoides*. BMC Microbiol. 2, 1–15. doi:10.1186/1471-2180-2-33
- Ding, N., Chen, X., Wu, C.-M.L., 2014. Interactions between polybrominated diphenyl ethers and graphene surface: a DFT and MD investigation. Environ. Sci. Nano 1, 55–63. doi:10.1039/C3EN00037K
- Drori, Y., Aizenshtat, Z., Chefetz, B., 2008. Sorption of organic compounds to humin from soils irrigated with reclaimed wastewater. Geoderma 145, 98–106. doi:10.1016/j.geoderma.2008.02.012
- Du, W., Ji, R., Sun, Y., Zhu, J., Wu, J., Guo, H., 2013. Fate and Ecological Effects of Decabromodiphenyl Ether in a Field Lysimeter. Environ. Sci. Technol. 47, 9167–9174. doi:10.1021/es400730p

- Dubinin, M.M., 1960. The Potential Theory of Adsorption of Gases and Vapors for Adsorbents with Energetically Nonuniform Surfaces. *Chem. Rev.* 60, 235–241. doi:10.1021/cr60204a006
- Dubinin, M.M., Astakhov, V.A., 1971. Development of concepts of the volume filling of micropores in the adsorption of gases and vapors by microporous adsorbents - Communication 4. Differential heats and entropies of adsorption. *Bull. Acad. Sci. USSR Div. Chem. Sci.* 20, 17–22. doi:10.1007/BF00849310
- Dumler, R., Lenoir, D., Thoma, H., Hutzinger, O., 1990. Thermal formation of polybrominated dibenzofurans and dioxins from decabromodiphenyl ether flame retardant: Influence of antimony(III) oxide and the polymer matrix. *Chemosphere* 20, 1867–1873. doi:http://dx.doi.org/10.1016/0045-6535(90)90354-V
- Dumler, R., Thoma, H., Lenoir, D., Hutzinger, O., 1989a. PBDF and PBDD from the combustion of bromine containing flame retarded polymers: A survey. *Chemosphere* 19, 2023–2031. doi:http://dx.doi.org/10.1016/0045-6535(89)90025-8
- Dumler, R., Thoma, H., Lenoir, D., Hutzinger, O., 1989b. Thermal formation of polybrominated dibenzodioxins (PBDD) and dibenzofurans (PBDF) from bromine containing flame retardants. *Chemosphere* 19, 305–308. doi:http://dx.doi.org/10.1016/0045-6535(89)90328-7
- Durán, N., Esposito, E., 2000. Potential applications of oxidative enzymes and phenoloxidase-like compounds in wastewater and soil treatment: A review. *Appl. Catal. B Environ.* 28, 83–99. doi:10.1016/S0926-3373(00)00168-5
- Düring, R.-A., Gäth, S., 2000. Microwave assisted methodology for the determination of organic pollutants in organic municipal wastes and soils: extraction of polychlorinated biphenyls using heat transformer disks. *Fresenius. J. Anal. Chem.* 368, 684–688. doi:10.1007/s002160000559
- Eggen, T., 1999. Application of fungal substrate from commercial mushroom production — *Pleurotus ostreatus* — for bioremediation of creosote contaminated soil. *Int. Biodeterior. Biodegradation* 44, 117–126. doi:http://dx.doi.org/10.1016/S0964-8305(99)00073-6
- Eljarrat, E., Barceló, D., 2004. Sample handling and analysis of brominated flame retardants in soil and sludge samples. *TrAC Trends Anal. Chem.* 23, 727–736. doi:http://dx.doi.org/10.1016/j.trac.2004.07.009
- Eljarrat, E., De La Cal, A., Larrazabal, D., Fabrellas, B., Fernandez-Alba, A.R., Borrull, F.,

- Marce, R.M., Barcelo, D., 2005. Occurrence of polybrominated diphenylethers, polychlorinated dibenzo-p-dioxins, dibenzofurans and biphenyls in coastal sediments from Spain. *Environ. Pollut.* 136, 493–501. doi:10.1016/j.envpol.2004.12.005
- Eljarrat, E., Labandeira, A., Marsh, G., Raldúa, D., Barceló, D., 2007. Decabrominated diphenyl ether in river fish and sediment samples collected downstream an industrial park. *Chemosphere* 69, 1278–86. doi:10.1016/j.chemosphere.2007.05.052
- Emsley, A., Lim, L., Stevens, G., Williams, P., 2005. International Fire Statistics and the Potential Benefits of Fire Counter-Measures Executive Summary UK Fire Statistics Update. Univ. Surrey Polym. Res. Cent. Rep.
- Endo, S., Pfennigsdorff, A., Goss, K.-U., 2012. Salting-Out Effect in Aqueous NaCl Solutions: Trends with Size and Polarity of Solute Molecules. *Environ. Sci. Technol.* 46, 1496–1503. doi:10.1021/es203183z
- Environment Canada, 2006. Canadian Environmental Protection Act 1999.
- Esser, K., Hofrichter, M., 2010. The Mycota. A Comprehensive Treatise on Fungi as Experimental Systems for Basic and Applied Research.
- European commission, 2003. European union risk assessment report. Diphenyl ether octabromo derivate. Brussels.
- European commission, 2001. European union risk assessment report. Diphenyl ether pentabromo derivate. Brussels.
- European Soils Bureau Network, 2005. Soil Atlas of Europe. doi:LB-37-01-744-EN-C
- Field, J.A., de Jong, E., Feijoo Costa, G., de Bont, J.A.M., 1992. Biodegradation of polycyclic aromatic hydrocarbons by new isolated of white-rot fungi. *Appl. Environ. Microbiol.* 58, 2219–2226.
- Fromme, H., Körner, W., Shahin, N., Wanner, A., Albrecht, M., Boehmer, S., Parlar, H., Mayer, R., Liebl, B., Bolte, G., 2009. Human exposure to polybrominated diphenyl ethers (PBDE), as evidenced by data from a duplicate diet study, indoor air, house dust, and biomonitoring in Germany. *Environ. Int.* 35, 1125–1135. doi:10.1016/j.envint.2009.07.003
- Gandhi, N., Bhavsar, S.P., Gewurtz, S.B., Tomy, G.T., 2011. Can biotransformation of BDE-209 in lake trout cause bioaccumulation of more toxic, lower-brominated PBDEs (BDE-47, -99) over the long term? *Environ. Int.* 37, 170–7. doi:10.1016/j.envint.2010.08.013
- Ganzler, K., Salgó, A., Valkó, K., 1986. Microwave extraction. *J. Chromatogr. A* 371, 299–306. doi:10.1016/S0021-9673(01)94714-4

- Gao, S., Hong, J., Yu, Z., Wang, J., Yang, G., Sheng, G., Fu, J., 2011. Polybrominated diphenyl ethers in surface soils from e-waste recycling areas and industrial areas in South China: Concentration levels, congener profile, and inventory. *Environ. Toxicol. Chem.* 30, 2688–2696. doi:10.1002/etc.668
- Gascon, M., Fort, M., Martínez, D., Carsin, A.-E., Forns, J., Grimalt, J.O., Santa Marina, L., Lertxundi, N., Sunyer, J., Vrijheid, M., 2012. Polybrominated diphenyl ethers (PBDEs) in breast milk and neuropsychological development in infants. *Environ. Health Perspect.* 120, 1760–5. doi:10.1289/ehp.1205266
- Gerecke, A.C., Giger, W., Hartmann, P.C., Heeb, N. V., Kohler, H.P.E., Schmid, P., Zennegg, M., Kohler, M., 2006. Anaerobic degradation of brominated flame retardants in sewage sludge. *Chemosphere* 64, 311–317. doi:10.1016/j.chemosphere.2005.12.016
- Gerecke, A.C., Hartmann, P.C., Heeb, N. V., Kohler, H.-P.E., Giger, W., Schmid, P., Zennegg, M., Kohler, M., 2005. Anaerobic Degradation of Decabromodiphenyl Ether. *Environ. Sci. Technol.* 39, 1078–1083. doi:10.1021/es048634j
- Ghanem, R., Delmani, F.-A., 2012. Kinetics of thermal and photolytic degradation of decabromodiphenyl ether (BDE 209) in backcoated textile samples. *J. Anal. Appl. Pyrolysis* 98, 79–85. doi:http://dx.doi.org/10.1016/j.jaap.2012.09.001
- Guan, G., Chen, L., Peng, S., 2010. Solubility of Decabromodiphenyl Ether in Different Solvents at (283.0 to 323.0) K. *J. Chem. Eng. Data* 55, 5294–5296. doi:10.1021/je100316k
- Guo, W., Holden, A., Smith, S.C., Gephart, R., Petreas, M., Park, J.-S., 2015. PBDE levels in breast milk are decreasing in California. *Chemosphere.* doi:10.1016/j.chemosphere.2015.11.032
- Hale, R.C., Alae, M., Manchester-Neesvig, J.B., Stapleton, H.M., Ikonou, M.G., 2003. Polybrominated diphenyl ether flame retardants in the North American environment. *Environ. Int.* 29, 771–779. doi:10.1016/S0160-4120(03)00113-2
- Hale, R.C., La Guardia, M.J., Harvey, E.P., Mainor, T.M., Duff, W.H., Gaylor, M.O., 2001. Polybrominated Diphenyl Ether Flame Retardants in Virginia Freshwater Fishes (USA). *Environ. Sci. Technol.* 35, 4585–4591. doi:10.1021/es010845q
- Hardy, M., 2002. A comparison of the properties of the major commercial PBDPO/PBDE product to those of major PBB and PCB products. *Chemosphere* 46, 717–728. doi:10.1016/S0045-6535(01)00236-3
- Hawthorne, M., 2012a. Chemical industry lobbyists keep stronger oversight plan at bay.

Chicago Trib.

Hawthorne, M., 2012b. Toxic roulette. Chicago Trib.

He, J., Robrock, K.R., Alvarez-Cohen, L., 2006. Microbial reductive debromination of polybrominated diphenyl ethers (PBDEs). *Environ. Sci. Technol.* 40, 4429–4434. doi:10.1021/es052508d

Heron, S., Tchaplá, A., 1991. Description of retention mechanism by solvophobic theory. *J. Chromatogr. A* 556, 219–234. doi:10.1016/S0021-9673(01)96223-5

Herrera-Herrera, A. V., Asensio-Ramos, M., Hernández-Borges, J., Rodríguez-Delgado, M. Ángel, 2010. Dispersive liquid-liquid microextraction for determination of organic analytes. *TrAC - Trends Anal. Chem.* 29, 728–751. doi:10.1016/j.trac.2010.03.016

Hestbjerg, H., Willumsen, P.A., Christensen, M., Andersen, O., Jacobsen, C.S., 2003. Bioaugmentation of tar-contaminated soils under field conditions using *Pleurotus ostreatus* refuse from commercial mushroom production. *Environ. Toxicol. Chem.* 22, 692–698. doi:10.1002/etc.5620220402

Hu, J., Eriksson, L., Bergman, Å., Jakobsson, E., Kolehmainen, E., Knuutinen, J., Suontamo, R., Wei, X., 2005a. Molecular orbital studies on brominated diphenyl ethers. Part II—reactivity and quantitative structure–activity (property) relationships. *Chemosphere* 59, 1043–1057. doi:http://dx.doi.org/10.1016/j.chemosphere.2004.11.029

Hu, J., Eriksson, L., Bergman, Å., Kolehmainen, E., Knuutinen, J., Suontamo, R., Wei, X., 2005b. Molecular orbital studies on brominated diphenyl ethers. Part I—conformational properties. *Chemosphere* 59, 1033–1041. doi:http://dx.doi.org/10.1016/j.chemosphere.2004.11.028

Huang, H., Zhang, S., Christie, P., Wang, S., Xie, M., 2009. Behavior of Decabromodiphenyl Ether (BDE-209) in the Soil–Plant System: Uptake, Translocation, and Metabolism in Plants and Dissipation in Soil. *Environ. Sci. Technol.* 44, 663–667. doi:10.1021/es901860r

Huang, W., Schlautman, M.A., Weber, W.J., 1996. A Distributed Reactivity Model for Sorption by Soils and Sediments. 5. The Influence of Near-Surface Characteristics in Mineral Domains. *Environ. Sci. Technol.* 30, 2993–3000. doi:10.1021/es960029w

Hutzinger, O., Dumler, R., Lenoir, D., Teufel, C., Thoma, H., 1989. PBDD and PBDF from brominated flame retardants: Combustion equipment, analytical methodology and synthesis of standards. *Chemosphere* 18, 1235–1242. doi:http://dx.doi.org/10.1016/0045-6535(89)90260-9

- INCHEM, I.P. on Ch.S. (IPCS), 1994. Environmental health criteria 162: Polybrominated diphenyl ethers. <http://www.inchem.org/documents/ehc/ehc/ehc162.htm>.
- Jaward, F.M., Farrar, N.J., Harner, T., Sweetman, A.J., Jones, K.C., 2003. Passive Air Sampling of PCBs, PBDEs, and Organochlorine Pesticides Across Europe. *Environ. Sci. Technol.* 38, 34–41. doi:10.1021/es034705n
- Keller, J., Swarthout, R., Carlson, B.R., Yordy, J., Guichard, A., Schantz, M., Kucklick, J., 2009. Comparison of five extraction methods for measuring PCBs, PBDEs, organochlorine pesticides, and lipid content in serum. *Anal. Bioanal. Chem.* 393, 747–760. doi:10.1007/s00216-008-2453-6
- Kelly, B.C., Ikonomou, M.G., Blair, J.D., Morin, A.E., Gobas, F.A.P.C., 2007. Food Web-Specific Biomagnification of Persistent Organic Pollutants. *Science* (80-. ). 317, 236–239.
- Kemmlin, S., Herzke, D., Law, R.J., 2009. Brominated flame retardants in the European chemicals policy of REACH—Regulation and determination in materials. *J. Chromatogr. A* 1216, 320–333. doi:http://dx.doi.org/10.1016/j.chroma.2008.05.085
- Kim, Y.-M., Nam, I.-H., Murugesan, K., Schmidt, S., Crowley, D.E., Chang, Y.-S., 2007. Biodegradation of diphenyl ether and transformation of selected brominated congeners by *Sphingomonas* sp. PH-07. *Appl. Microbiol. Biotechnol.* 77, 187–194. doi:10.1007/s00253-007-1129-z
- Kirchgeorg, T., Dreyer, A., Gabrieli, J., Kehrwald, N., Sigl, M., Schwikowski, M., Boutron, C., Gambaro, A., Barbante, C., Ebinghaus, R., 2013. Temporal variations of perfluoroalkyl substances and polybrominated diphenyl ethers in alpine snow. *Environ. Pollut.* 178, 367–74. doi:10.1016/j.envpol.2013.03.043
- Kowalska, M., Güler, H., Cocke, D.L., 1994. Interactions of clay minerals with organic pollutants. *Sci. Total Environ.* 141, 223–240. doi:http://dx.doi.org/10.1016/0048-9697(94)90030-2
- Kubátová, A., Erbanová, P., Eichlerová, I., Homolka, L., Nerud, F., Šašek, V., 2001. PCB congener selective biodegradation by the white rot fungus *Pleurotus ostreatus* in contaminated soil. *Chemosphere* 43, 207–215. doi:10.1016/S0045-6535(00)00154-5
- Lang, Y., Cao, Z., Nie, X., 2005. Extraction of organochlorine pesticides in sediments using Soxhlet, ultrasonic and accelerated solvent extraction techniques. *J. Ocean Univ. China* 4, 173–176. doi:10.1007/s11802-005-0012-8

- Langford, K.H., Scrimshaw, M.D., Birkett, J.W., Lester, J.N., 2005. The partitioning of alkylphenolic surfactants and polybrominated diphenyl ether flame retardants in activated sludge batch tests. *Chemosphere* 61, 1221–1230. doi:<http://dx.doi.org/10.1016/j.chemosphere.2005.04.043>
- Laoutid, F., Bonnaud, L., Alexandre, M., Lopez-Cuesta, J.-M., Dubois, P., 2009. New prospects in flame retardant polymer materials: From fundamentals to nanocomposites. *Mater. Sci. Eng. R Reports* 63, 100–125. doi:[10.1016/j.mser.2008.09.002](http://dx.doi.org/10.1016/j.mser.2008.09.002)
- Lau, K.L., Tsang, Y.Y., Chiu, S.W., 2003. Use of spent mushroom compost to bioremediate PAH-contaminated samples. *Chemosphere* 52, 1539–1546. doi:[http://dx.doi.org/10.1016/S0045-6535\(03\)00493-4](http://dx.doi.org/10.1016/S0045-6535(03)00493-4)
- Leal, J.F., Esteves, V.I., Santos, E.B.H., 2013. BDE-209: Kinetic Studies and Effect of Humic Substances on Photodegradation in Water. *Environ. Sci. Technol.* 47, 14010–14017. doi:[10.1021/es4035254](http://dx.doi.org/10.1021/es4035254)
- LeBoeuf, E.J., Weber, W.J., 1997. A Distributed Reactivity Model for Sorption by Soils and Sediments. 8. Sorbent Organic Domains: Discovery of a Humic Acid Glass Transition and an Argument for a Polymer-Based Model. *Environ. Sci. Technol.* 31, 1697–1702. doi:[10.1021/es960626i](http://dx.doi.org/10.1021/es960626i)
- Lee, L.K., He, J., 2010. Reductive debromination of polybrominated diphenyl ethers by anaerobic bacteria from soils and sediments. *Appl. Environ. Microbiol.* 76, 794–802. doi:[10.1128/AEM.01872-09](http://dx.doi.org/10.1128/AEM.01872-09)
- Lee, S., Gan, J., Liu, W.P., Anderson, M.A., 2003. Evaluation of K<sub>d</sub> Underestimation Using Solid Phase Microextraction. *Environ. Sci. Technol.* 37, 5597–5602. doi:[10.1021/es0344563](http://dx.doi.org/10.1021/es0344563)
- Leung, A.O.W., Luksemburg, W.J., Wong, A.S., Wong, M.H., 2007. Spatial Distribution of Polybrominated Diphenyl Ethers and Polychlorinated Dibenzo-p-dioxins and Dibenzofurans in Soil and Combusted Residue at Guiyu, an Electronic Waste Recycling Site in Southeast China. *Environ. Sci. Technol.* 41, 2730–2737. doi:[10.1021/es0625935](http://dx.doi.org/10.1021/es0625935)
- Levchik, S. V., 2006. Introduction to Flame Retardancy and Polymer Flammability, in: *Flame Retardant Polymer Nanocomposites*. John Wiley & Sons, Inc., pp. 1–29. doi:[10.1002/9780470109038.ch1](http://dx.doi.org/10.1002/9780470109038.ch1)
- Levison, J., Novakowski, K., Reiner, E., Kolic, T., 2012. Potential of groundwater contamination by polybrominated diphenyl ethers (PBDEs) in a sensitive bedrock



- aquifer (Canada). *Hydrogeol. J.* 20, 401–412. doi:10.1007/s10040-011-0813-3
- Li, Y., Hu, J., Liu, X., Fu, L., Zhang, X., Wang, X., 2008a. Dispersive liquid–liquid microextraction followed by reversed phase HPLC for the determination of decabrominated diphenyl ether in natural water. *J. Sep. Sci.* 31, 2371–2376. doi:10.1002/jssc.200800112
- Li, Y., Niu, S., Hai, R., Li, M., 2015. Concentrations and distribution of polybrominated diphenyl ethers (PBDEs) in soils and plants from a Deca-BDE manufacturing factory in China. *Environ. Sci. Pollut. Res.* 22, 1133–1143. doi:10.1007/s11356-014-3214-z
- Li, Y., Wang, T., Hashi, Y., Li, H., Lin, J.-M., 2009. Determination of brominated flame retardants in electrical and electronic equipments with microwave-assisted extraction and gas chromatography-mass spectrometry. *Talanta* 78, 1429–35. doi:10.1016/j.talanta.2009.02.046
- Li, Y., Wei, G., Hu, J., Liu, X., Zhao, X., Wang, X., 2008b. Dispersive liquid–liquid microextraction followed by reversed phase-high performance liquid chromatography for the determination of polybrominated diphenyl ethers at trace levels in landfill leachate and environmental water samples. *Anal. Chim. Acta* 615, 96–103. doi:http://dx.doi.org/10.1016/j.aca.2008.03.038
- Lin, Y., Pessah, I.N., Puschner, B., 2013. Simultaneous determination of polybrominated diphenyl ethers and polychlorinated biphenyls by gas chromatography-tandem mass spectrometry in human serum and plasma. *Talanta* 113, 41–8. doi:10.1016/j.talanta.2013.04.001
- Linares, V., Bellés, M., Domingo, J.L., 2015. Human exposure to PBDE and critical evaluation of health hazards. *Arch. Toxicol.* 89, 335–356. doi:10.1007/s00204-015-1457-1
- Liu, W., Cheng, F., Li, W., Xing, B., Tao, S., 2012. Desorption behaviors of BDE-28 and BDE-47 from natural soils with different organic carbon contents. *Environ. Pollut.* 163, 235–242. doi:http://dx.doi.org/10.1016/j.envpol.2011.12.043
- Liu, W., Li, W., Hu, J., Ling, X., Xing, B., Chen, J., Tao, S., 2010. Sorption kinetic characteristics of polybrominated diphenyl ethers on natural soils. *Environ. Pollut.* 158, 2815–2820. doi:http://dx.doi.org/10.1016/j.envpol.2010.06.021
- Liu, W., Li, W., Xing, B., Chen, J., Tao, S., 2011. Sorption isotherms of brominated diphenyl ethers on natural soils with different organic carbon fractions. *Environ. Pollut.* 159, 2355–2358. doi:http://dx.doi.org/10.1016/j.envpol.2011.06.032
- Loibner, A., Scherr, K.E., Edelmann, E., Humel, S., Kopp, D., Mayer, P., 2015. Canaged spiked

- soils reflect bioaccessibility of native PAHs in historically contaminated soil?, in: AquaConSoil Copenhagen 2015- Sustainable Use and Management of Soil, Sediment and Water Resources. p. 79.
- Lu, M., Zhang, Z.-Z., Wu, X.-J., Xu, Y.-X., Su, X.-L., Zhang, M., Wang, J.-X., 2013. Biodegradation of decabromodiphenyl ether (BDE-209) by a metal resistant strain, *Bacillus cereus* JP12. *Bioresour. Technol.* 149, 8–15. doi:10.1016/j.biortech.2013.09.040
- MacGregor, J.A., Nixon, W.B., 1997. Decabromodiphenyl oxide (DBDPO): determination of n-octanol/water partition coefficient.
- Machado, K.M.G., Matheus, D.R., Rosim Monteiro, R.T., Ramos Bononi, V.L., 2005. Biodegradation of pentachlorophenol by tropical basidiomycetes in soils contaminated with industrial residues. *World J. Microbiol. Biotechnol.* 21, 297–301. doi:10.1007/s11274-004-3693-z
- Mackay, D., 1979. Finding fugacity feasible. *Environ. Sci. Technol.* 13, 1218–1223.
- Manes, M., Hofer, L.J.E., 1969. Application of the Polanyi adsorption potential theory to adsorption from solution on activated carbon. *J. Phys. Chem.* 73, 584–590. doi:10.1021/j100723a018
- McGinley, P.M., Katz, L.E., Weber, W.J., 1993. A distributed reactivity model for sorption by soils and sediments. 2. Multicomponent systems and competitive effects. *Environ. Sci. Technol.* 27, 1524–1531. doi:10.1021/es00045a006
- Möller, A., Xie, Z., Sturm, R., Ebinghaus, R., 2011. Polybrominated diphenyl ethers (PBDEs) and alternative brominated flame retardants in air and seawater of the European Arctic. *Environ. Pollut.* 159, 1577–83. doi:10.1016/j.envpol.2011.02.054
- Mueller, K.E., Mueller-Spitz, S.R., Henry, H.F., Vonderheide, A.P., Soman, R.S., Kinkle, B.K., Shann, J.R., 2006. Fate of Pentabrominated Diphenyl Ethers in Soil: Abiotic Sorption, Plant Uptake, and the Impact of Interspecific Plant Interactions. *Environ. Sci. Technol.* 40, 6662–6667. doi:10.1021/es060776l
- Muwambaa, A., Nkedi-Kizza, P., Rhuea, R.D., Keaffaberb, J.J., 2009. Use of Mixed Solvent Systems to Eliminate Sorption of Strongly Hydrophobic Organic Chemicals on Container Walls. *J. Environ. Qual.* 38, 1170–6.
- Nuerla, A., Qiao, X., Li, J., Zhao, D., Yang, X., Xie, Q., Chen, J., 2013. Effects of substituent position on the interactions between PBDEs/PCBs and DOM. *Chinese Sci. Bull.* 58, 884–889. doi:10.1007/s11434-012-5464-9

- Nyholm, J.R., Lundberg, C., Andersson, P.L., 2010. Biodegradation kinetics of selected brominated flame retardants in aerobic and anaerobic soil. *Environ. Pollut.* 158, 2235–40. doi:10.1016/j.envpol.2010.02.010
- OECD, 2000. Adsorption - Desorption Using a Batch Equilibrium Method. *Oecd Guidel. Test. Chem.* 1–44. doi:10.1787/9789264069602-en
- Olshansky, Y., Polubesova, T., Vetter, W., Chefetz, B., 2011. Sorption–desorption behavior of polybrominated diphenyl ethers in soils. *Environ. Pollut.* 159, 2375–2379. doi:http://dx.doi.org/10.1016/j.envpol.2011.07.003
- Osako, M., Kim, Y.J., Sakai, S.I., 2004. Leaching of brominated flame retardants in leachate from landfills in Japan. *Chemosphere* 57, 1571–1579. doi:10.1016/j.chemosphere.2004.08.076
- Pallerla, S., Chambers, R.P., 1998. Reactor development for biodegradation of pentachlorophenol. *Catal. Today* 40, 103–111. doi:10.1016/S0920-5861(97)00128-4
- Palm, A., Cousins, I.T., Mackay, D., Tysklind, M., Metcalfe, C., Alaei, M., 2002. Assessing the environmental fate of chemicals of emerging concern: a case study of the polybrominated diphenyl ethers. *Environ. Pollut.* 117, 195–213. doi:http://dx.doi.org/10.1016/S0269-7491(01)00276-7
- Pan, B., Zhang, H., 2014. Reconstruction of Adsorption Potential in Polanyi-Based Models and Application to Various Adsorbents. *Environ. Sci. Technol.* 48, 6772–6779. doi:10.1021/es501393v
- Pan, B., Zhang, H., 2012. A Modified Polanyi-based Model for Mechanistic Understanding of Adsorption of Phenolic Compounds onto Polymeric Adsorbents. *Environ. Sci. Technol.* 46, 6806–6814. doi:10.1021/es300951g
- Park, H.-M., Hong, S.-M., Agustin-Camacho, M.R., Dirwono, W., Lee, K.-B., 2009. Pressurized Liquid Extraction for the Simultaneous Analysis of Polychlorinated Biphenyls and Polybrominated Diphenyl Ethers from Soil by GC-TOF-MS Detection. *J. Chromatogr. Sci.* 47, 681–688. doi:10.1093/chromsci/47.8.681
- Pignatello, J.J., Xing, B., 1995. Mechanisms of Slow Sorption of Organic Chemicals to Natural Particles. *Environ. Sci. Technol.* 30, 1–11. doi:10.1021/es940683g
- Pointing, S., 2001. Feasibility of bioremediation by white-rot fungi. *Appl. Microbiol. Biotechnol.* 57, 20–33. doi:10.1007/s002530100745
- Qiu, M., Chen, X., Deng, D., Guo, J., Sun, G., Mai, B., Xu, M., 2011. Effects of electron donors on anaerobic microbial debromination of polybrominated diphenyl ethers (PBDEs).

- Biodegradation 23, 351–361. doi:10.1007/s10532-011-9514-9
- Rayne, S., Ikononou, M.G., Whale, M.D., 2003. Anaerobic microbial and photochemical degradation of 4,4'-dibromodiphenyl ether. *Water Res.* 37, 551–560. doi:10.1016/S0043-1354(02)00311-1
- Regueiro, J., Llompart, M., García-Jares, C., Cela, R., 2006. Determination of polybrominated diphenyl ethers in domestic dust by microwave-assisted solvent extraction and gas chromatography-tandem mass spectrometry. *J. Chromatogr. A* 1137, 1–7. doi:10.1016/j.chroma.2006.09.080
- Renner, R., 2000. Increasing levels of flame retardants found in North American environment. *Environ. Sci. Technol.* 34, 452A–453A. doi:10.1021/es003482n
- Rezaee, M., Assadi, Y., Milani Hosseini, M.-R., Aghaee, E., Ahmadi, F., Berijani, S., 2006. Determination of organic compounds in water using dispersive liquid-liquid microextraction. *J. Chromatogr. A* 1116, 1–9. doi:10.1016/j.chroma.2006.03.007
- Rhind, S.M., Kyle, C.E., Kerr, C., Osprey, M., Zhang, Z.L., Duff, E.I., Lilly, A., Nolan, A., Hudson, G., Towers, W., Bell, J., Coull, M., McKenzie, C., 2013. Concentrations and geographic distribution of selected organic pollutants in Scottish surface soils. *Environ. Pollut.* 182, 15–27. doi:http://dx.doi.org/10.1016/j.envpol.2013.06.041
- Richter, B.E., Jones, B.A., Ezzell, J.L., Porter, N.L., Avdalovic, N., Pohl, C., 1996. Accelerated Solvent Extraction: A Technique for Sample Preparation. *Anal. Chem.* 68, 1033–1039. doi:10.1021/ac9508199
- Robrock, K.R., Korytar, P., Alvarez-Cohen, L., 2008. Pathways for the anaerobic microbial debromination of polybrominated diphenyl ethers. *Environ. Sci. Technol.* 42, 2845–2852. doi:10.1021/es0720917
- Roe, S., 2012. Doubts cast on new research touted by fire-retardant lobby. *Chicago Trib.*
- Roe, S., Callahan, P., 2012. Distorting science. *Chicago Trib.*
- Saim, N., Dean, J.R., Abdullah, M.P., Zakaria, Z., 1997. Extraction of polycyclic aromatic hydrocarbons from contaminated soil using Soxhlet extraction, pressurised and atmospheric microwave-assisted extraction, supercritical fluid extraction and accelerated solvent extraction. *J. Chromatogr. A* 791, 361–366. doi:10.1016/S0021-9673(97)00768-1
- Sakai, S., Urano, S., Takatsuki, H., 2000. Leaching behavior of PCBs and PCDDs / DFs from some waste materials. *Waste Manag.* 20.
- Sakai, S., Watanabe, J., Honda, Y., Takatsuki, H., Aoki, I., Futamatsu, M., Shiozaki, K., 2001.

- Combustion of brominated flame retardants and behavior of its byproducts. *Chemosphere* 42, 519–531. doi:[http://dx.doi.org/10.1016/S0045-6535\(00\)00224-1](http://dx.doi.org/10.1016/S0045-6535(00)00224-1)
- Samara, F., Tsai, C.W., Aga, D.S., 2006. Determination of potential sources of PCBs and PBDEs in sediments of the Niagara River. *Environ. Pollut.* 139, 489–97. doi:10.1016/j.envpol.2005.06.001
- Saraji, M., Boroujeni, M., 2013. Recent developments in dispersive liquid–liquid microextraction. *Anal. Bioanal. Chem.* 1–40. doi:10.1007/s00216-013-7467-z
- Schwarzenbach, R.P., 1993. Quantifying the relative abundance of dissolved and sorbed species: the solid-water distribution ratio  $K_d$ , in: *Environmental Organic Chemistry*. First Edition. pp. 258–276.
- Schwarzenbach, R.P., Gschwend, P.M., Imboden, D.M., 1993a. The organic matter-water partitioning coefficient,  $K_{ow}$ , in: *Environmental Organic Chemistry*. First Edition. pp. 272–275.
- Schwarzenbach, R.P., Gschwend, P.M., Imboden, D.M., 1993b. Sorption kinetics, in: *Environmental Organic Chemistry*. First Edition. pp. 328–330. doi:10.1007/s13398-014-0173-7.2
- SEC, U.S. and E.C., 2014. United States Securities and Exchange Commission.
- Sellström, U., de Wit, C.A., Lundgren, N., Tysklind, M., 2005. Effect of Sewage-Sludge Application on Concentrations of Higher-Brominated Diphenyl Ethers in Soils and Earthworms. *Environ. Sci. Technol.* 39, 9064–9070. doi:10.1021/es051190m
- Shaw, S.D., Blum, A., Weber, R., Kannan, K., Rich, D., Lucas, D., Koshland, C.P., Dobraca, D., Hanson, S., Birnbaum, L.S., 2010. Halogenated flame retardants: do the fire safety benefits justify the risks? *Rev. Environ. Health* 25, 261–305. doi:10.1515/REVEH.2010.25.4.261
- Shi, G., Yin, H., Ye, J., Peng, H., Li, J., Luo, C., 2013. Effect of cadmium ion on biodegradation of decabromodiphenyl ether (BDE-209) by *Pseudomonas aeruginosa*. *J. Hazard. Mater.* 263 Pt 2, 711–7. doi:10.1016/j.jhazmat.2013.10.035
- Shih, Y., Wang, C.-K., 2009. Photolytic degradation of polybromodiphenyl ethers under UV-lamp and solar irradiations. *J. Hazard. Mater.* 165, 34–38. doi:<http://dx.doi.org/10.1016/j.jhazmat.2008.09.103>
- Shin, M., Svoboda, M.L., Falletta, P., 2007. Microwave-assisted extraction (MAE) for the determination of polybrominated diphenylethers (PBDEs) in sewage sludge. *Anal. Bioanal. Chem.* 387, 2923–2929. doi:10.1007/s00216-007-1168-4

- Siddiqi, M.A., Laessig, R.H., Reed, K.D., 2003. Polybrominated Diphenyl Ethers (PBDEs): New Pollutants—Old Diseases. *Clin. Med. Res.* 1, 281–290. doi:10.3121/cmr.1.4.281
- Söderström, G., Marklund, S., 2002. PBCDD and PBCDF from Incineration of Waste-Containing Brominated Flame Retardants. *Environ. Sci. Technol.* 36, 1959–1964. doi:10.1021/es010135k
- Söderström, G., Sellström, U., de Wit, C.A., Tysklind, M., 2003. Photolytic Debromination of Decabromodiphenyl Ether (BDE 209). *Environ. Sci. Technol.* 38, 127–132. doi:10.1021/es034682c
- Stahl, J.A., Aust, S.D., 1995. Biodegradation of 2,4,6-trinitrotoluene by the white rot fungus *Phanerochaete chrysosporium*. *Biodegrad. Nitroaromatic Compd.* 54, 117–133.
- Stapleton, H.M., 2006. Instrumental methods and challenges in quantifying polybrominated diphenyl ethers in environmental extracts: A review. *Anal. Bioanal. Chem.* 386, 807–817. doi:10.1007/s00216-006-0400-y
- Steffen, K.T., Tuomela, M., 2010. Fungal soil bioremediation: development toward large scale application, in: Hofrichter, M. (Ed.), *The Mycota*. Springer-Verlag Berlin Heidelberg, pp. 451–467.
- Stenzel, A., Goss, K.-U., Endo, S., 2013. Determination of Polyparameter Linear Free Energy Relationship (pp-LFER) Substance Descriptors for Established and Alternative Flame Retardants. *Environ. Sci. Technol.* 47, 1399–1406. doi:10.1021/es304780a
- Stenzel, J., Markley, B., 1997. Decabromodiphenyl oxide (DBDPO): determination of n-octanol/water partitioning coefficient.
- Stockholm Convention, 2013. SC-6/13: Listing of hexabromocyclododecane.
- Stockholm Convention, 2009. SC-4/13: Listing of hexabromobiphenyl.
- Talley, T., 1995. Annual AFMA Flammability Conference, in: *Small Open Flame Tests and Cigarette Ignition Tests*. p. Phases 1&2, UFAC.
- Ter Laak, T.L., van Eijkeren, J.C.H., Busser, F.J.M., van Leeuwen, H.P., Hermens, J.L.M., 2009. Facilitated Transport of Polychlorinated Biphenyls and Polybrominated Diphenyl Ethers by Dissolved Organic Matter. *Environ. Sci. Technol.* 43, 1379–1385. doi:10.1021/es802403v
- Thoma, H., Hauschulz, G., Knorr, E., Hutzinger, O., 1987. Polybrominated dibenzofurans (PBDF) and dibenzodioxins (PBDD) from the pyrolysis of neat brominated diphenylethers, biphenyls and plastic mixtures of these compounds. *Chemosphere* 16, 277–285. doi:http://dx.doi.org/10.1016/0045-6535(87)90132-9

- Thoma, H., Hutzinger, O., 1989. Pyrolysis and GC/MS-analysis of brominated flame retardants in on-line operation. *Chemosphere* 18, 1047–1050. doi:[http://dx.doi.org/10.1016/0045-6535\(89\)90234-8](http://dx.doi.org/10.1016/0045-6535(89)90234-8)
- Thomsen, C., Liane, V.H., Becher, G., 2007. Automated solid-phase extraction for the determination of polybrominated diphenyl ethers and polychlorinated biphenyls in serum—application on archived Norwegian samples from 1977 to 2003. *J. Chromatogr. B* 846, 252–263. doi:<http://dx.doi.org/10.1016/j.jchromb.2006.09.011>
- Tlili, K., Labadie, P., Alliot, F., Bourges, C., Desportes, A., Chevreuril, M., 2012. Polybrominated Diphenyl Ether Dynamics in Ambient Air and Atmospheric Bulk/Wet Deposition in Downtown Paris (France). *Water, Air, Soil Pollut.* 223, 1543–1553. doi:10.1007/s11270-011-0963-x
- Tokarz, J.A., Ahn, M.Y., Leng, J., Filley, T.R., Nies, L., 2008. Reductive debromination of polybrominated diphenyl ethers in anaerobic sediment and a biomimetic system. *Environ. Sci. Technol.* 42, 1157–1164. doi:10.1021/es071989t
- Tortella, G.R., Diez, M.C., Durán, N., 2005. Fungal Diversity and Use in Decomposition of Environmental Pollutants. *Crit. Rev. Microbiol.* 31, 197–212. doi:10.1080/10408410500304066
- Uhnáková, B., Petříčková, A., Biedermann, D., Homolka, L., Vejvoda, V., Bednár, P., Papoušková, B., Sulc, M., Martínková, L., 2009. Biodegradation of brominated aromatics by cultures and laccase of *Trametes versicolor*. *Chemosphere* 76, 826–832. doi:10.1016/j.chemosphere.2009.04.016
- UNEP, S.C., 2013. Decabromodiphenyl ether proposal 2013 2, 1–20.
- UNEP, S.C. on P.O.P., 2009a. Listing of hexabromodiphenyl ether and heptabromodiphenyl ether 3–4.
- UNEP, S.C. on P.O.P., 2009b. Listing of tetrabromodiphenyl ether and pentabromodiphenyl ether 17–18.
- USEPA, (USA Environmental Protection Agency), 2016. <http://www.epa.gov/opptintr/existingchemicals/pubs/actionplans/deccadbe.html> [WWW Document].
- USEPA, (USA Environmental Protection Agency), 1996. Method 3510C: Separatory Funnel Liquid-Liquid Extraction. *Test Methods Eval. Solid Waste, Phys. Methods. Environ. Prot. Agency* 1–8.
- VECAP, 2014. Annual Report 2014.

- Vilaplana, F., Karlsson, P., Ribes-Greus, A., Ivarsson, P., Karlsson, S., 2008. Analysis of brominated flame retardants in styrenic polymers: Comparison of the extraction efficiency of ultrasonication, microwave-assisted extraction and pressurised liquid extraction. *J. Chromatogr. A* 1196–119, 139–146. doi:<http://dx.doi.org/10.1016/j.chroma.2008.05.001>
- Vilaplana, F., Ribes-Greus, A., Karlsson, S., 2009. Microwave-assisted extraction for qualitative and quantitative determination of brominated flame retardants in styrenic plastic fractions from waste electrical and electronic equipment (WEEE). *Talanta* 78, 33–9. doi:[10.1016/j.talanta.2008.10.038](http://dx.doi.org/10.1016/j.talanta.2008.10.038)
- Vitali, V.M.V., Machado, K.M.G., Andrea, M.M. De, Bononi, V.L.R., 2006. Screening mitosporic fungi for organochlorides degradation. *Brazilian J. Microbiol.* 37, 256–261. doi:[10.1590/S1517-83822006000300012](http://dx.doi.org/10.1590/S1517-83822006000300012)
- Vonderheide, A.P., Mueller, K.E., Meija, J., Welsh, G.L., 2008. Polybrominated diphenyl ethers: causes for concern and knowledge gaps regarding environmental distribution, fate and toxicity. *Sci. Total Environ.* 400, 425–36. doi:[10.1016/j.scitotenv.2008.05.003](http://dx.doi.org/10.1016/j.scitotenv.2008.05.003)
- Wang, P., Zhang, Q., Wang, Y., Wang, T., Li, X., Ding, L., Jiang, G., 2010. Evaluation of Soxhlet extraction, accelerated solvent extraction and microwave-assisted extraction for the determination of polychlorinated biphenyls and polybrominated diphenyl ethers in soil and fish samples. *Anal. Chim. Acta* 663, 43–48. doi:<http://dx.doi.org/10.1016/j.aca.2010.01.035>
- Wang, S., Zhang, S., Huang, H., Christie, P., 2011a. Behavior of decabromodiphenyl ether (BDE-209) in soil: Effects of rhizosphere and mycorrhizal colonization of ryegrass roots. *Environ. Pollut.* 159, 749–753. doi:<http://dx.doi.org/10.1016/j.envpol.2010.11.035>
- Wang, S., Zhang, S., Huang, H., Zhao, M., Lv, J., 2011b. Uptake, translocation and metabolism of polybrominated diphenyl ethers (PBDEs) and polychlorinated biphenyls (PCBs) in maize (*Zea mays* L.). *Chemosphere* 85, 379–385. doi:<http://dx.doi.org/10.1016/j.chemosphere.2011.07.002>
- Wang, W., Delgado-Moreno, L., Ye, Q., Gan, J., 2011. Improved Measurements of Partition Coefficients for Polybrominated Diphenyl Ethers. *Environ. Sci. Technol.* 45, 1521–1527. doi:[10.1021/es103087a](http://dx.doi.org/10.1021/es103087a)
- Wang, X., Sheng, J., Gong, P., Xue, Y., Yao, T., Jones, K.C., 2012. Persistent organic pollutants in the Tibetan surface soil: spatial distribution, air-soil exchange and implications for



- global cycling. *Environ. Pollut.* 170, 145–51. doi:10.1016/j.envpol.2012.06.012
- Wania, F., Dugani, C.B., 2003. Assessing the long-range transport potential of polybrominated diphenyl ethers: A comparison of four multimedia models. *Environ. Toxicol. Chem.* 22, 1252–1261. doi:10.1002/etc.5620220610
- Watanabe, I., Tatsukawa, R., 1987. Formation of brominated dibenzofurans from the photolysis of flame retardant decabromobiphenyl ether in hexane solution by UV and sun light. *Bull. Environ. Contam. Toxicol.* 39, 953–959. doi:10.1007/BF01689584
- Weber, W.J., McGinley, P.M., Katz, L.E., 1992. A distributed reactivity model for sorption by soils and sediments. 1. Conceptual basis and equilibrium assessments. *Environ. Sci. Technol.* 26, 1955–1962. doi:10.1021/es00034a012
- Wei, H., Zou, Y., Li, A., Christensen, E.R., Rockne, K.J., 2013. Photolytic debromination pathway of polybrominated diphenyl ethers in hexane by sunlight. *Environ. Pollut.* 174, 194–200. doi:http://dx.doi.org/10.1016/j.envpol.2012.11.035
- White, G.F., Russell, N.J., Tidswell, E.C., 1996. Bacterial scission of ether bonds. *Microbiol. Rev.* 60, 216–232.
- WHO, 1994. Environmental health criteria no. 162.
- Wong, A., Lei, Y.D., Alaei, M., Wania, F., 2001. Vapor Pressures of the Polybrominated Diphenyl Ethers. *J. Chem. Eng. Data* 46, 239–242. doi:10.1021/je0002181
- Wu, S.C., Gschwend, P.M., 1986. Sorption kinetics of hydrophobic organic compounds to natural sediments and soils. *Environ. Sci. Technol.* 20, 717–725. doi:10.1021/es00149a011
- Xia, G., Ball, W.P., 2000. Polanyi-Based Models for the Competitive Sorption of Low-Polarity Organic Contaminants on a Natural Sorbent. *Environ. Sci. Technol.* 34, 1246–1253. doi:10.1021/es9812453
- Xia, G., Ball, W.P., 1999. Adsorption-Partitioning Uptake of Nine Low-Polarity Organic Chemicals on a Natural Sorbent. *Environ. Sci. Technol.* 33, 262–269. doi:10.1021/es980581g
- Xu, G., Wang, J., 2014. Biodegradation of decabromodiphenyl ether (BDE-209) by white-rot fungus *Phlebia lindtneri*. *Chemosphere* 110, 70–7. doi:10.1016/j.chemosphere.2014.03.052
- Yang, Z.Z., Li, Y.F., Hou, Y.X., Liang, H.Y., Qin, Z.F., Fu, S., 2010. Vertical Distribution of Polybrominated Diphenyl Ethers (PBDEs) in Soil Cores Taken from a Typical Electronic Waste Polluted Area in South China. *Bull. Environ. Contam. Toxicol.* 84, 260–263.

doi:10.1007/s00128-009-9924-0

- Yen, J.H., Liao, W.C., Chen, W.C., Wang, Y.S., 2009. Interaction of polybrominated diphenyl ethers (PBDEs) with anaerobic mixed bacterial cultures isolated from river sediment. *J. Hazard. Mater.* 165, 518–524. doi:10.1016/j.jhazmat.2008.10.007
- Yogui, G.T., Sericano, J.L., Montone, R.C., 2011. Accumulation of semivolatile organic compounds in Antarctic vegetation: A case study of polybrominated diphenyl ethers. *Sci. Total Environ.* 409, 3902–3908. doi:http://dx.doi.org/10.1016/j.scitotenv.2011.06.010
- Young, T.M., Weber, W.J.J., 1995. A Distributed Reactivity Model for Sorption by Soils and Sediments. 3. Effects of Diagenetic Processes on Sorption Energetics. *Environ. Sci. Technol.* 29, 92–97. doi:10.1021/es00001a011
- Yuan, G.-L., Xie, W., Che, X.-C., Han, P., Liu, C., Wang, G.-H., 2012. The fractional patterns of polybrominated diphenyl ethers in the soil of the central Tibetan Plateau, China: The influence of soil components. *Environ. Pollut.* 170, 183–189. doi:http://dx.doi.org/10.1016/j.envpol.2012.07.011
- Yue, C., Li, L.Y., 2013. Filling the gap: Estimating physicochemical properties of the full array of polybrominated diphenyl ethers (PBDEs). *Environ. Pollut.* 180, 312–323. doi:http://dx.doi.org/10.1016/j.envpol.2013.05.029
- Zgoła-Grzeškowiak, A., Grzeškowiak, T., 2011. Dispersive liquid-liquid microextraction. *TrAC Trends Anal. Chem.* 30, 1382–1399. doi:http://dx.doi.org/10.1016/j.trac.2011.04.014
- Zhang, Q., Liang, T., Guan, L., 2013. Ultrasound-assisted dispersive liquid–liquid microextraction combined with gas chromatography–mass spectrometry in negative chemical ionization mode for the determination of polybrominated diphenyl ethers in water. *J. Sep. Sci.* 36, 1263–1269. doi:10.1002/jssc.201201049
- Zhang, Z., Rhind, S.M., 2011. Optimized determination of polybrominated diphenyl ethers and polychlorinated biphenyls in sheep serum by solid-phase extraction–gas chromatography–mass spectrometry. *Talanta* 84, 487–493. doi:http://dx.doi.org/10.1016/j.talanta.2011.01.042
- Zhang, Z., Shanmugam, M., Rhind, S., 2010. PLE and GC–MS Determination of Polybrominated Diphenyl Ethers in Soils. *Chromatographia* 72, 535–543. doi:10.1365/s10337-010-1693-8
- Zhou, J., Jiang, W., Ding, J., Zhang, X., Gao, S., 2007. Effect of Tween 80 and  $\beta$ -cyclodextrin on degradation of decabromodiphenyl ether (BDE-209) by White Rot Fungi.

doi:<http://dx.doi.org/10.1016/j.chemosphere.2007.06.036>

Zihms, S.G., 2013. Smouldering and Thermal Remediation Effects on Properties and Behaviour of Porous Media Stephanie Gabriele Zihms Submitted for the degree of Doctor of Philosophy University of Strathclyde Department of Civil & Environmental Engineering August 2013 Declara. Strathclyde University.

## Appendix A

In this appendix are reported chromatograms to whom is referred in Section 4.1 and 5.6

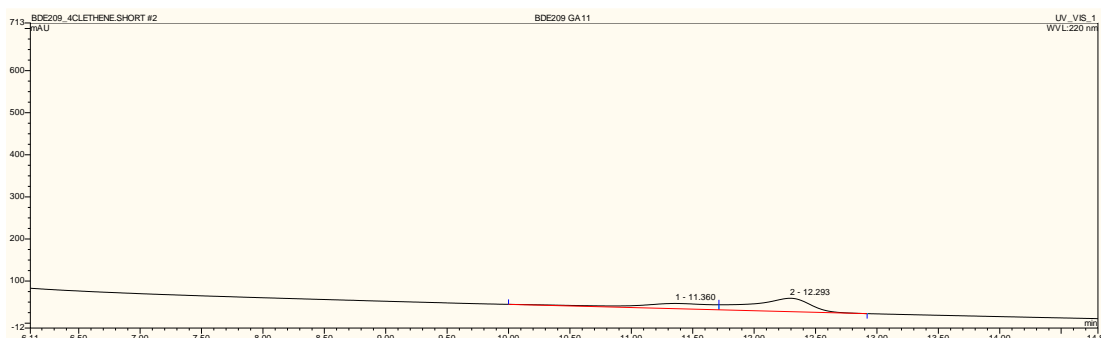


Figure A.1: Chromatogram obtained from analysis of BDE-209 in tetrachloroethene (10 mg/L) in HPLC reverse phase system using methanol as mobile phase.

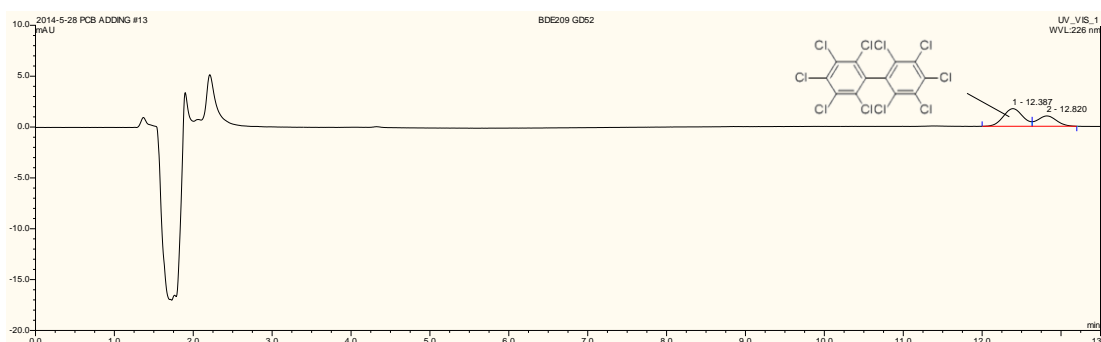


Figure A.2: Chromatogram obtained from analysis of BDE-209 (0.25 µg/ml) and PCB-209 (0.1 µg/ml) in acetone using HPLC reverse phase system and methanol as mobile phase (0.8 ml/min).

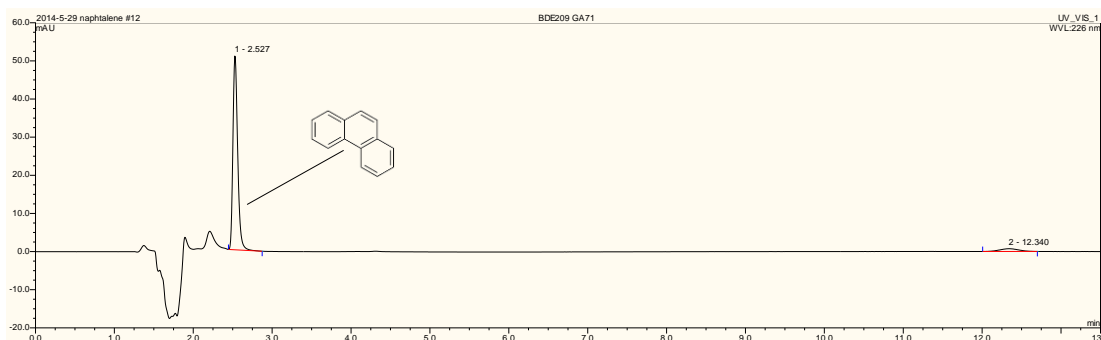


Figure A.3: Chromatogram obtained from analysis of BDE-209 (0.1 µg/ml) and Naphthalene (1.1 µg/ml) in acetone using HPLC reverse phase system and methanol as mobile phase (0.8 ml/min).

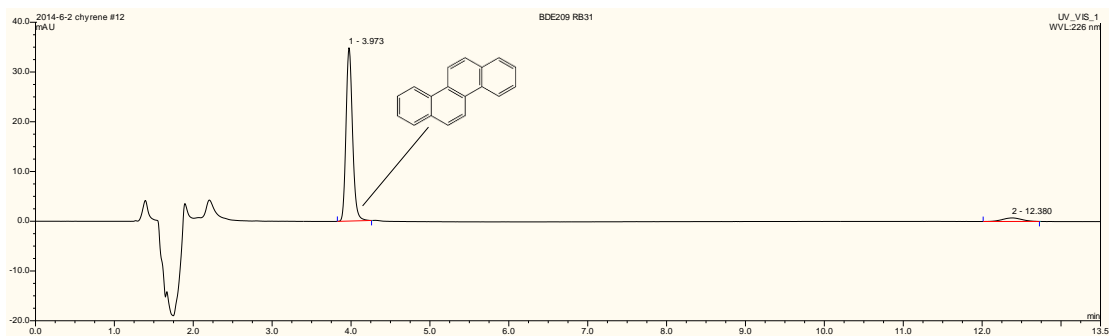


Figure A.4: Chromatogram obtained from analysis of BDE-209 (0.1 µg/ml) and Chrysene (1.1 µg/ml) in acetone using HPLC reverse phase system and methanol as mobile phase (0.8 ml/min).

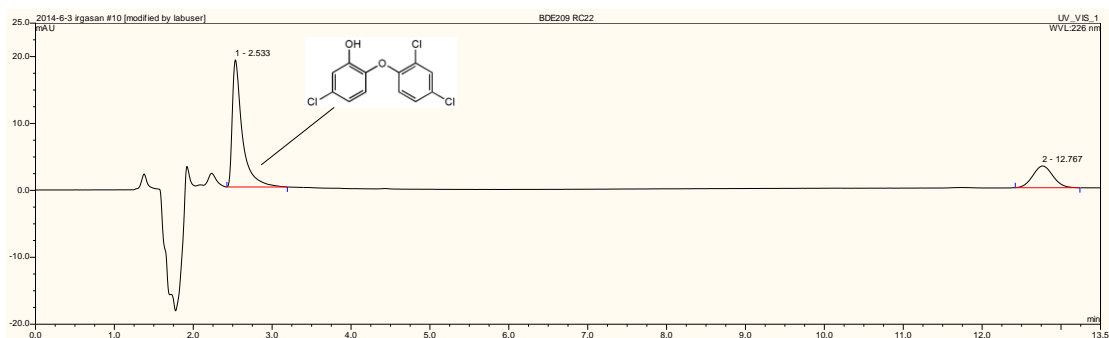


Figure A.5: Chromatogram obtained from analysis of BDE-209 (0.1 µg/ml) and Triclosan (1.1 µg/ml) in acetone using HPLC reverse phase system and methanol as mobile phase (0.8 ml/min).

## Appendix B

In this appendix clay minerals structure are reported and the exhaustive procedures followed for matrixes characterisation (briefly summarised in Section 7.2.2) are described. Besides kaolin and peat, sand samples have been analysed and results are here reported because they has been helpful in the interpretation of some results obtained for kaolin (e.g. organic matter content). Moreover it is a common component of soil and it is not excluded that in future work the kinetic of adsorption of BDE-209 on sand could be investigated.

### Matrixes characterisation-Methodology

#### pH and electrical conductivity measurement

2 grams of clay or peat (dry weight) were placed in a 15 mL plastic centrifuge tube with 10 mL of deionised water collected form the laboratory's reverse osmosis system (*RO180 El-Ion*<sup>®</sup> twin-stage, SG). Samples were shaken end-over-end for two hours. PH readings were taken while samples were still in suspension, whereas EC readings were executed after filtering samples through a 20 ml plastic syringe fitted with 0.45 µm filters (MCE-10460031, Fisher scientific, Waltham MA, USA). In this way, three samples for each matrix were measured. Results are reported in the following section as average values ± standard deviation.

#### Organic matter content

For performing measurements by LOI method 2.5 g of clay and 3 g of peat were weighted, placed in ceramic basin and heated at 105 °C then 450 °C and finally at 550 °C. The following measurements were taken: weight of basins ( $W_b$ ) weight of basins and content ( $W_a$ ), weight of basin and content after heating at 105 °C ( $W_{105}$ ), weight of basins and content after heating at 450 °C ( $W_{450}$ ) and weight of basin and content after heating at 550 °C ( $W_{550}$ ). Weight measurements were taken through a 0.0001 g precision balance after letting basins and contents cool down at room temperature in a desiccator. For each temperature tested (105, 450, 550 °C) series of heating and measurement were repeated until the variation between two successive measurements were less or equal to 0.01 g. Water content was then calculated as a percentage by mass with Equation B.1, organic matter content at 450 °C and 550 °C respectively with equation B.2 and B.3 and expressed as a percentage by mass of the dried samples.

$$\text{Water content (\%)} = \frac{W_{105} - W_a}{W_a - W_b} \times 100 \quad \text{Eq. B.1}$$

$$\text{Organic matter content at 450 °C (\%)} = \frac{W_{450} - W_{105}}{W_a - W_b} \times 100 \quad \text{Eq. A.2}$$

$$\text{Organic matter content at 550 °C (\%)} = \frac{W_{550} - W_{105}}{W_a - W_b} \times 100 \quad \text{Eq. A.3}$$

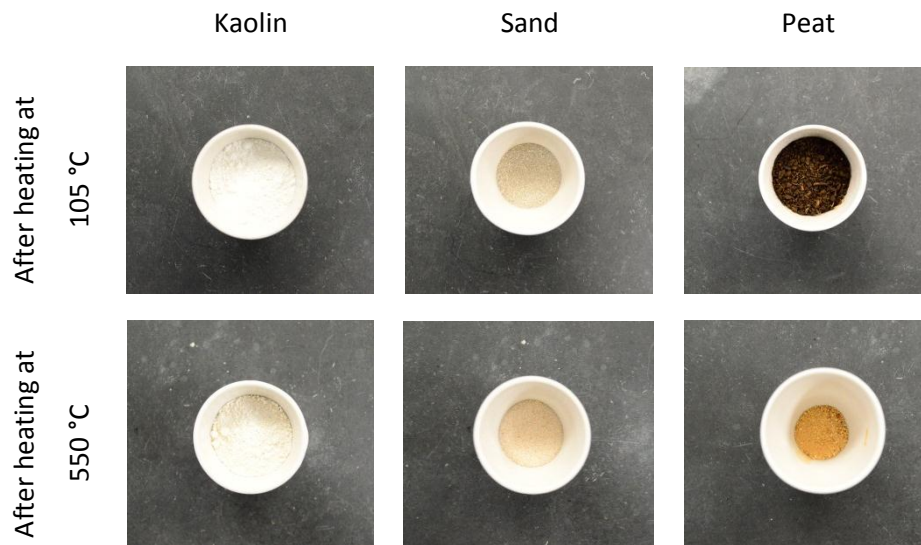


Figure B.1: Kaolin, sand and peat samples after water evaporation (heating at 105 °C) and after organic matter loss (heating at 550 °C).

Subsequently, because an unexpected high value was recorded for organic matter in clay, results have been verified by TOC Combustion Analyser. Differently from the LOI method, TOC analyser measure the CO<sub>2</sub> produced during sample combustion giving a direct measure of the total carbon content of samples. TOC combustion analyser APOLLO 9000 (Tekmar-Teledyne instrument, AZ USA) equipped with a boat sampler (Model 183 TOC Boat Sampler, Tekmar-Teledyne instrument, AZ USA) was calibrated as shown in section X.Y.Z using five solutions of potassium hydrogen phthalate in diatomaceous earth.

#### Particles size distribution

Samples grading curves were generated through a laser diffraction instrument (Mastersizer 2000, Malvern, Worcestershire UK) equipped with disperser unit control (Hydro 2000SM).

The instrument exploits laser diffraction properties for determination of particle size distribution. Samples were added in the disperser unit previously filled with degassed Millipore water. The disperser unit by stirring the water keeps particles suspended and delivers them to the optical bench. Preliminary tests have been conducted to optimise particles dispersion by varying the stirring speed and the sample delivery to the disperser unit (dry or wet). For clay and sand the main factor affecting measurements is the stirring speed: low speed causes the loss of smaller particles. In the case of peat instead, sample delivery plays the major role: bigger particles were lost when peat was delivered dry instead of wet into the disperser chamber. The methods finally used to obtain the particle size distribution are reported in table 6.1. The amount of sample delivered is in the range of few milligrams and it varies from sample to sample according to signal/noise ratio indications given in real time by the software.

Table B.1: Parameters used for analysis of sand, clay and peat on Malvern Mastersizer.

Sample	Stirring speed (rpm)	Sample delivery
Sand	2000	dispersed in water
Clay	2000	dispersed in water
Peat	1000	humid/wet

## Matrixes characterisation-Results

pH and EC results are reported in Figure B.2. According to expectations peat is characterised by the lowest pH (3.4) and the highest electric conductivity (718  $\mu\text{S}/\text{cm}$ ). Clay has intermediate values pH is 5.0 and the electrical conductivity is half of peat one (327  $\mu\text{S}/\text{cm}$ ). Sand is expected to be inert in water, and as expected pH measure in sand (6.1) does not deviate from the pH measured in deionised water used for preparing the samples (6.0). Electrical conductivity (155  $\mu\text{S}/\text{cm}$ ) instead results higher than the one measured in deionised water 4  $\mu\text{S}/\text{cm}$ , possibly due to some impurity.

Table B.2: pH and electrical conductivity measures. Average reading on three samples  $\pm$  standard deviation.

	pH	EC ( $\mu\text{S}/\text{cm}$ )
Sand	6.1 $\pm$ 0.03	155 $\pm$ 45
Kaolin	5.0 $\pm$ 0.005	327 $\pm$ 37
Peat	3.4 $\pm$ 0.01	718 $\pm$ 4.6

Organic matter and water contents measured by LOI are reported in Table B.3. Peat results composed for the 93% by organic matter and no differences between the measure at 450



and 550 °C is observed. Variation in temperature does not affect either measure of sand organic content which results negligible. Unexpectedly values measured in clay addresses traces of organic matter when measured at 450 °C (0.9 %) and 12 % organic matter content at 550 °C. Results from the analysis done through TOC analyser reported in Table B.4 conduce to different and more sensible conclusions. Indeed in both clay and sand the organic content is less 0.05%. Higher values obtained by LOI are possibly caused by degradation of clay minerals. Indeed at high temperature (450 °C) kaolin can lose part of the molecular water still present after treatment at 105 °C and perhaps some of the hydroxyl groups; at 550 °C kaolin undergoes degradation of its structure (Zihms, 2013). To measure organic matter content of soil by LOI at 550 °C therefore cause a sensitive overestimation in presence of kaolin. The error is less important, and for most application negligible, when a temperature of 450 °C is adopted (proximally 1 %). In case of peat instead LOI results the most appropriate method for two reasons: the small sample size of TOC analyse are not suitable for such heterogeneous material and the carbon concentration was too high for TOC analyser even after dilution with diatomaceous earth.

Table B.3: Water content measured through sample exsiccation at 105 °C, and organic matter content measured by loss on ignition at 450 and 550°C.

	Water content (%)	Organic matter content at 450 °C (%)	Organic matter content at 550 °C (%)
Sand	0 ± 0.1	0.1 ± 0.1	0.2 ± 0.1
Clay	0.9 ± 0.2	0.9 ± 0.3	12 ± 0.5
Peat	22 ± 1	93 ± 1.4	93 ± 1.2

Table B.4: Total carbon and Total organic carbon measured by total combustion at 800°C and CO<sub>2</sub> analysis.

	Total carbon (%)	Total organic carbon (%)
Sand	0.01 ± 0.006	0.01 ± 0.007
Clay	0.04 ± 0.001	0.02 ± 0.001
Peat	Out of range	Out of range

Grading curves obtained for sand, kaolin and peat are reported in Figure B.2, B.3 and B.4. Sand curve is tight and more than 90 % of particles are included between diameters 0.2-0.5 mm. Results satisfyingly overlap supplier specifications which indicates 90 % of particles to have a diameter between 0.2-0.3 mm. Kaolin has more spread grading curve (Figure B.3)

indeed particles equivalent spherical diameter is between 0.3-15  $\mu\text{m}$ , this is in accordance with supplier specification which indicates particle diameter between 0.3-10  $\mu\text{m}$  and a surface area of 14  $\text{m}^2/\text{g}$ . Grading curve of peat is the most spread, particles diameter varies from 3  $\mu\text{m}$  to 2 mm (Figure B.4).

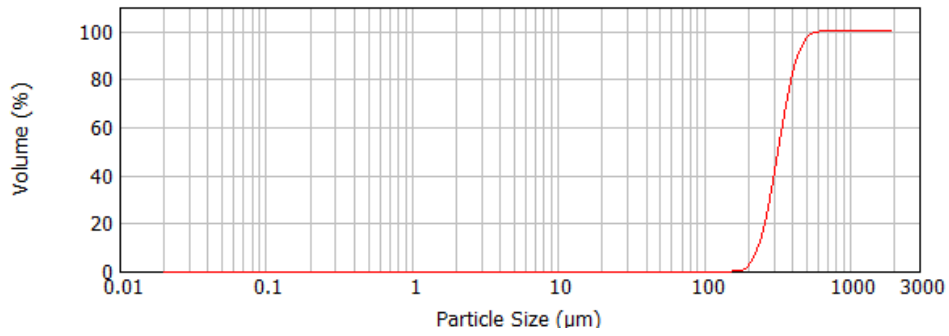


Figure B.2: Cumulative distribution curve of sand particles size expressed as equivalent spherical diameter ( $\mu\text{m}$ ).

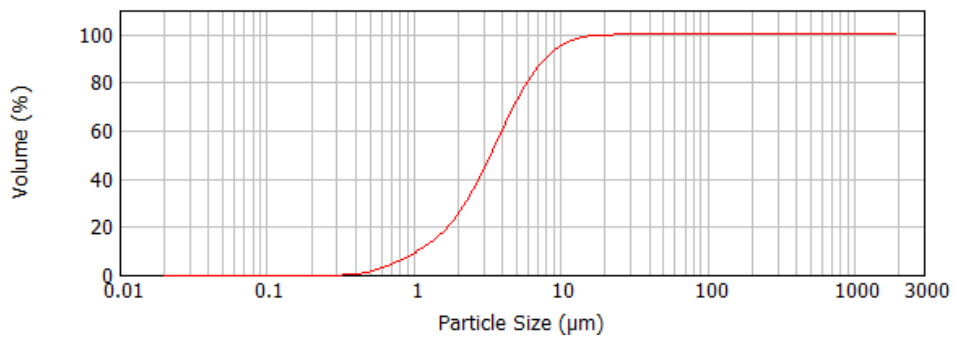


Figure B.3: Cumulative distribution curve of clay particles size expressed as equivalent spherical diameter ( $\mu\text{m}$ ).

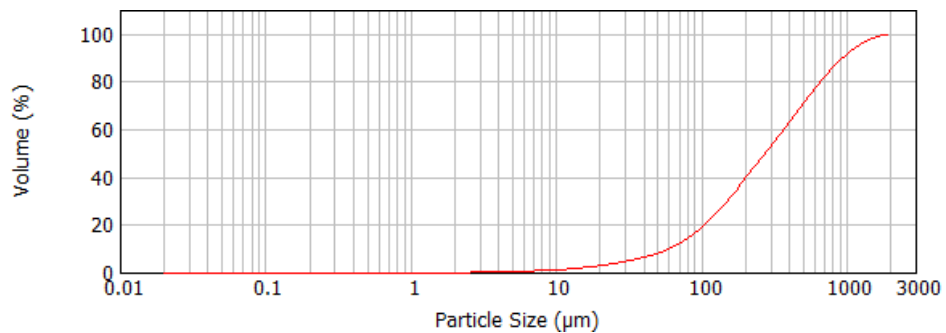


Figure B.4: Cumulative distribution curve of peat particles size expressed as equivalent spherical diameter ( $\mu\text{m}$ ).

## Clay structure

Clay minerals are silicates and their basic structural units consist of a silica tetrahedron and alumina octahedron schematically represented in Figure B.5.

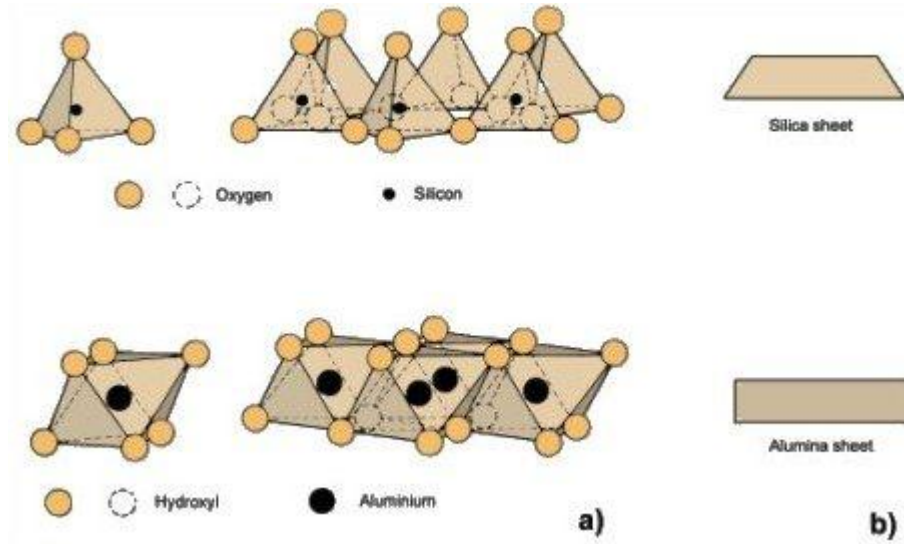


Figure B.5: Basic units of clay minerals and the silica and alumina sheets (from Mitchell, 1993)

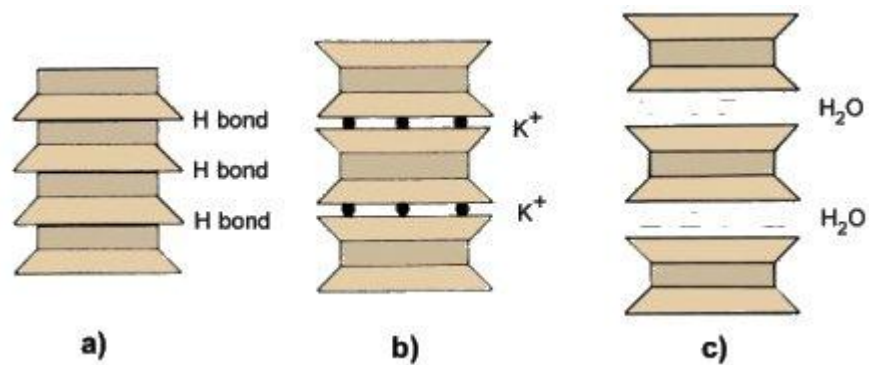


Figure B.6: Structure of the main clay minerals: (a) kaolinite, (b) illite and (c) montmorillonite, based on combined sheets (from Craig, 1990).

## References

- Mitchell, J.K., 1993. Fundamentals of Soil Behavior (chapter 3), 2nd edition, John Wiley & Sons.
- Craig, R.F., 1987. Soil Mechanics. Chapman & Hall.

## Appendix C

In this appendix as illustrative example, some of the chromatograms obtained from the extractions of water from samples analysed from kaolin and peat experiments are reported. Chromatograms from water control samples ( $S_W$ : water + BDE-209), matrix control samples ( $S_M$ : water + kaolin or peat) can be compared to the one obtained from samples containing water + BDE-209 + kaolin or peat. For kaolin samples are reported also chromatogram obtained from the analysis of tetrahydrophuran:water solution used to extract kaolin and measure BDE-209 adsorbed on kaolin.

### Kaolin sorption experiment: water analysis

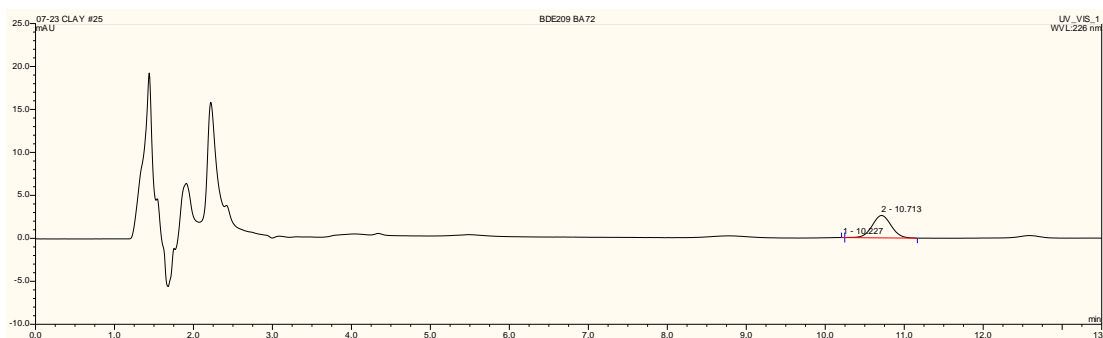


Figure C.1: Chromatogram obtained from water control sample ( $S_W$ ) containing 50 ml of water + 0.5 g of kaolin.

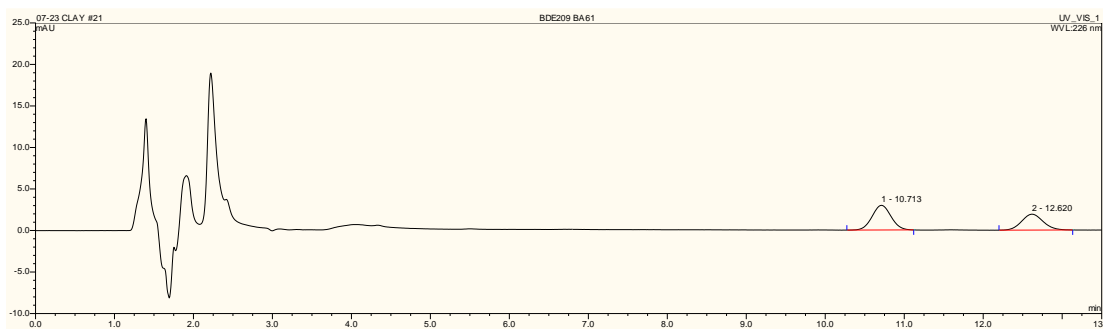


Figure C.2: Chromatogram obtained from matrix control sample ( $S_M$ ) containing 50 ml of water + BDE-209.

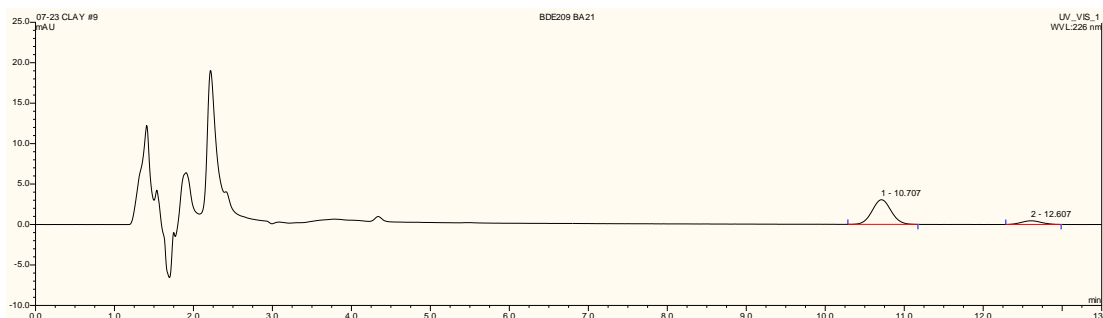


Figure C.3: Chromatogram obtained from sample (S) containing 50 ml of water + 0.5 g of kaolin+ BDE-209.

### Peat kinetic experiment: water analysis

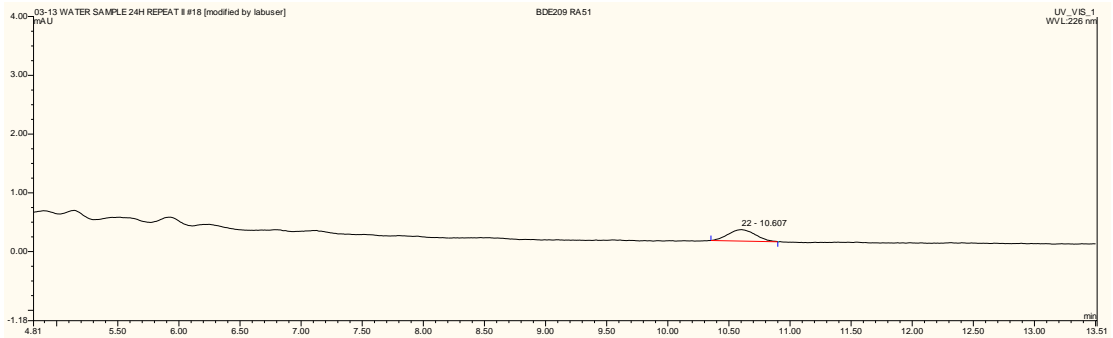


Figure C.4: Chromatogram obtained from matrix control sample ( $S_M$ ) containing 200 ml of water + 0.5 g of kaolin.

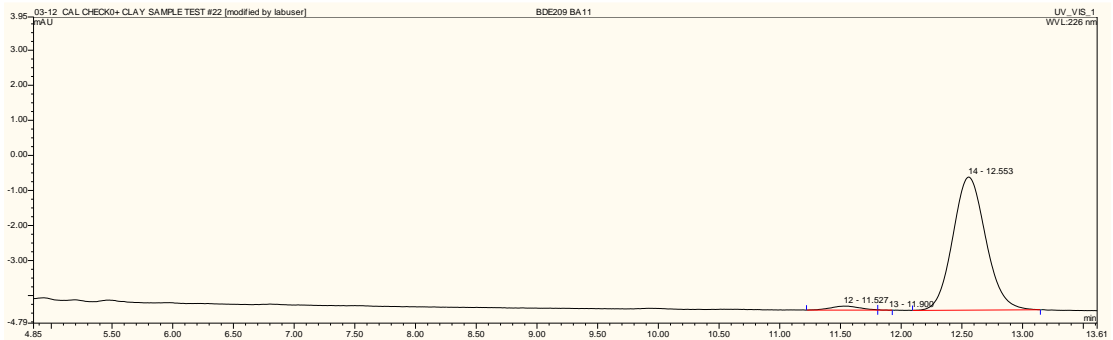


Figure C.5: Chromatogram obtained from water control sample ( $S_W$ ) containing 200 ml of water + BDE-209

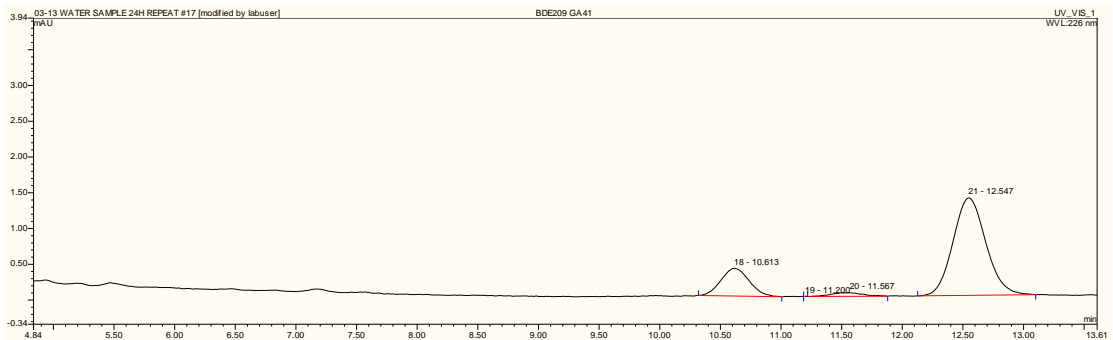


Figure C.6: Chromatogram obtained from sample (S) containing 200 ml of water + 0.5 g of peat + BDE-209.

## Kaolin sorption experiment: tetrahydrofuran:water solution analysis

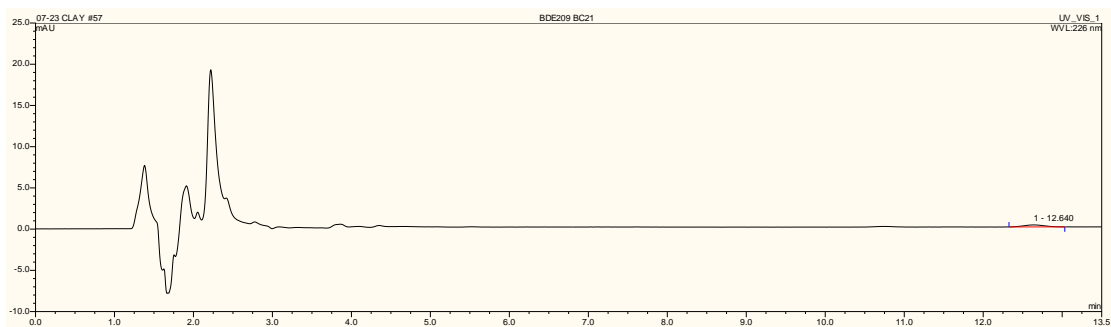


Figure C.7: Chromatogram obtained from water control sample ( $S_W$ ) containing 50 ml of water + 0.5 g of kaolin.

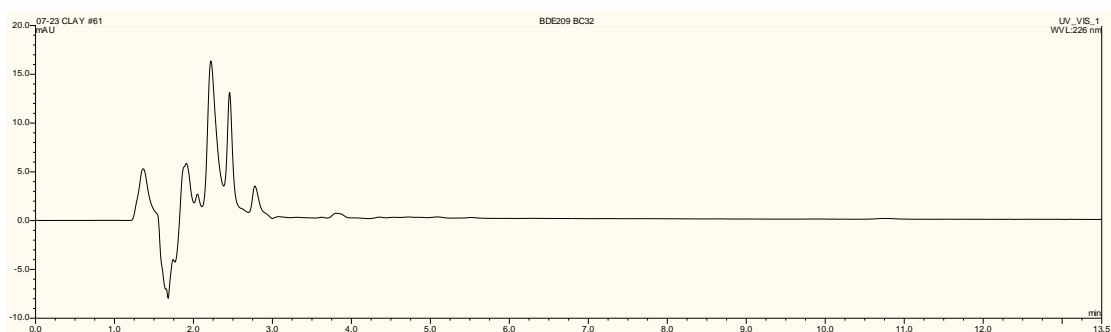


Figure C.8: Chromatogram obtained from matrix control sample ( $S_M$ ) containing 50 ml of water + BDE-209.

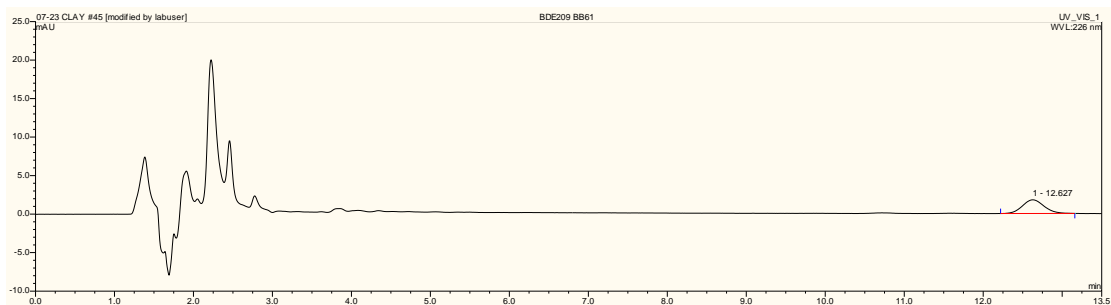


Figure C.9: Chromatogram obtained from sample (S) containing 50 ml of water + 0.5 g of kaolin+ BDE-209.